Applying Mobile Boundary Water Surface Profile Models To Coarse-Bedded Bridge Crossings

by

Mark Clayton Browning

A dissertation submitted in partial fulfillment
of the requirements for the degree of

Doctor of Philosophy
University of Washington
2001
Department of Civil and Environmental Engineering

UMI Number: 3036447

UMI

ProQuest Information and Learning Company
300 North Zeeb Road
P.O. Box 1346
Ann Arbor, MI 48106-1346

Doctoral Dissertation

Signature Mark C. Browning

Date 11/15/01

University of Washington
Graduate School

This is to certify that I have examined this copy of a doctoral dissertation by

Mark Clayton Browning

and have found that it is complete and satisfactory in all respects, and that any and all revisions required by the final examining committee have been made.

Chair of Supervisory Committee:

Catherine M. Petroff

Reading Committee:

Brian W. Mar

Richard N. Palmer

Catherine M. Petroff

Date: 11/15/01

University of Washington

Abstract

Applying Mobile Boundary Water Surface Profile Models To Coarse-Bedded Bridge Crossings

Mark Clayton Browning

Chairperson of the Supervisory Committee:
Research Scientist, Affiliate Assistant Professor
Catherine M. Petroff
Department of Civil and Environmental Engineering

This thesis presents general processes for applying mobile boundary models at coarse-bedded bridge crossings. To develop these processes, the research uses a series of case studies involving highway bridges that span coarse-bedded rivers (gravel, cobble beds). From the case studies, the thesis presents seven tables and charts describing the overall processes and criteria for applying mobile boundary models at coarse-bedded bridge crossings. These include the preferred physical attributes for using a mobile boundary model at a bridge site, the required fixed boundary analysis, an evaluation of the dominating morphological feature at the crossing (e.g., bridge opening), a mobile boundary model cost analysis, and the requirements for performing a mobile boundary analysis. The presented mobile boundary analysis also includes recommended values for various operational parameters. These parameters include time step, active layer thickness, sediment transport equation, and stream bed gradation.

The research shows that mobile boundary models will produce lower bridge backwater elevations (water surface profiles) than those that fixed boundary models produce. This occurs when the bridge opening dominates the hydraulics at the crossing. To test for bridge dominance, the Froude value, F_u, upstream of the bridge site should not exceed the

Froude value, F_b, at the bridge site.

The research also shows that values of hydraulic parameters (e.g., bridge scour) from fixed boundary models are useful in obtaining a broad estimate of the reduction in backwater that a mobile boundary model might produce. The statistical relationship between fixed boundary hydraulic values and mobile boundary backwater elevations, however, is weak. This relationship, nevertheless, is qualitatively strong enough to indicate when to use a mobile boundary model.

Finally, the research uses additional selected case studies to evaluate the water surface profile accuracy of mobile boundary models versus fixed boundary models. These case studies show that the mobile boundary model will produce a more accurate water surface profile than a fixed boundary model. However, in some instances the added accuracy of a mobile model may not produce backwater curves with more practical use than a fixed model in the hydraulic design of a bridge.

TABLE OF CONTENTS

LIST OF FIGURES

Number Page

LIST OF TABLES

LIST OF SYMBOLS

A = flow area for complete cross-section

A_i = flow area for cross-section subdivision

A_d = volume of sediment deposition per unit length

A_L = factor applied to D(NF) or the representative grain size for determining the active layer thickness of the stream bed

A_s = area of scour

A_{SM} = area of scour at bridge section for mobile boundary condition

A_{SR} = area of scour at bridge section for rigid boundary condition

A_{ss} = volume of sediment in suspension at the cross-section per unit length

A_y = statistical parameter for Yang's log-linear regression equation for total sediment concentration

a = flow area for cross-section subdivision

a_y = log-linear regression coefficient for Yang's sediment transport equations

B = statistical parameter for log-linear equation

B' = roughness function

B_y = statistical parameter for Yang's log-linear regression equation for total sediment concentration

b = bridge flow width

b_y = log-linear regression coefficient for Yang's sediment transport equations

C = Chezy roughness coefficient

C_L = expansion or contraction loss coefficient

C_t = total sediment concentration of bed material transported as bed load and suspended load

C_{tg} = total sediment concentration of gravel bed material transported as bed load and suspended load

D = flow depth

D(NF) = geometric mean of the maximum gradation size

d = particle diameter (i.e., d_{50} = % passing by weight)

d_m = representative grain size

dt = time step for flood hydrograph

EC = engineering design costs

F_b = Froude number for bridge section

F_u = Froude number for upstream backwater section

FBM = fixed or rigid boundary model

g = acceleration of gravity

H = difference in water surface elevation of two stream cross-sections

h = energy head losses

h_1^* = total backwater or rise above normal stage at section 1 (Figures 2.7 and 2.8)

h_{1M}^* = backwater depth for the mobile model

h_{1R}^* = backwater depth for the rigid model

h_e = energy head losses

i = cross-section index

L = discharge weighted reach length; distance between cross-section

L_{ch} = reach length for main channel

L_{lob} = reach length for left flood plain or over bank

L_{rob} = reach length for right flood plain or over bank

K = total cross-section conveyance

K^* = total backwater coefficient

K_b = backwater coefficient based upon bridge opening ratio

K_p = pier shape coefficient

k_i = conveyance for cross-section subdivision

k_s = equivalent roughness

M = bridge opening ratio

MBM = mobile boundary model

MPM = Meyer-Peter and Müller (1948) sediment transport method

n = Manning's roughness coefficient

n_s = volume of sediment in a unit bed layer

NSIZE = the number of size fractions of sediment

P = wetted perimeter

Q = volume of water per unit time; or flood event for a given return interval (i.e., Q_{100} = 100-year flood).

Q_b = flow in portion of channel within projected length of bridge at upstream backwater section

Q_s = volumetric sediment discharge

Q_{sin} = sediment inflow

Q_{sout} = sediment outflow

Q_{100} = total discharge for 100-year flood

$\overline{Q_{ch}}$ = arithmetic average flows at the ends of the reach for the main channel

$\overline{Q_{lob}}$ = arithmetic average flows at the ends of the reach for the left flood plain or over bank

$\overline{Q_{rob}}$ = arithmetic average flows at the ends of the reach for the right flood plain or over bank

q_s = lateral sediment inflow

R = hydraulic radius for complete cross-section

R_i = hydraulic radius for cross-section subdivision

$R_{p/m}$ = ratio of predicted to modeled h_{1M}^*/h_{1R}^*

S = energy slope

SB = stream bed elevation at a given time (i.e., SB 0 HR = stream bed elevation at 0 hours)

SBC = potential savings in bridge costs

SP_d = unit stream power (Eq. 2-18, velocity times energy slope) for reach located downstream from the bridge section

SP_u = unit stream power for reach located upstream from the bridge section

STA = stream cross-section station (i.e., STA 3670 = the stream cross-section at station 3670)

S_0 = bed slope

$\overline{S_f}$ = average friction slope

t = time

U_* = shear velocity

V = cross-section averaged water velocity

V_{cr} = velocity at incipient motion

W = flow width

WSEL = water surface elevation

WSM = mobile boundary water surface elevation at a given time (i.e., WSM 15 HR = water surface elevation for mobile model at 15 hours)

WSR = rigid boundary water surface elevation at a given time (i.e., WSR 15 HR = water surface elevation for rigid model at 15 hours)

X = distance along the stream channel

X_P = predicted h_{1M}^*/h_{1R}^* from Figure 4.1

x = stream-wise coordinate; or incremental distance along the channel

Y = depth of water at a given cross-section

Y_M = modeled h_{1M}^*/h_{1R}^* from Equation 4-1 and Figure 4.3

y = flow depth

$\bar{y}$ = mean depth of flow under bridge

y_c = critical flow depth

y_n = normal flow depth

Z = elevation of the main channel invert

α = velocity weighted coefficient (kinetic energy coefficient)

α_o = ratio of obstructed area to total unobstructed area

ν = kinematic viscosity

τ_b = shear stress for bridge section

τ_{cr} = critical shear stress for bridge section

ψ = mathematical coefficients for particle drag, lift, and friction

ω = particle fall velocity

ω_v = ratio of velocity head to depth downstream from the bridge

ACKNOWLEDGMENTS

I appreciate the advice, time, and effort of my supervisory committee consisting of Brian Mar, Richard Palmer, Catherine Petroff, and Richard Sternberg in the development of my thesis. I am especially grateful for the support I received from Catherine Petroff. She gave me numerous comments and considerable advice in the preparation of this document. Also, a special thanks to Brian Mar for his general guidance in completing my doctoral work. Finally, I would like to thank Albert Molinas, Colorado State University, for his input on sedimentation processes in rivers; my wife, Mary Ann, for her patience and support; and the Federal Highway Administration for its financial support of my doctoral studies at the University of Washington.

CHAPTER 1: INTRODUCTION

1.1 Background

Engineers use water surface profiles to set bridge elevations and lengths, determine roadway profiles, evaluate regulatory limits (i.e., ordinary high water, increases in flood elevations), and predict environmental impacts related to human activities (USACE, 1986; AASHTO, 1999). They also use the water surface profile information to compute bridge scour, road bank stability, and develop stream rehabilitation measures (FHWA, 1995). Water surface profile analysis provides the expected water surface elevations, depths, velocities, and other hydraulic parameters used in hydraulic engineering design.

Hydraulic engineers often use fixed boundary models for computing water surface profiles. These models compute the profile of a flood wave as it passes adjacent to a road or through a bridge opening. The model assumes that no changes occur to the boundaries (i.e., stream bed, side slopes) (AASHTO, 1999).

An alternate model is a mobile boundary model (Molinas, 1994). This type of model allows for adjustments to flow boundaries as the flood wave passes through the study area. The model simulates the scour and deposition processes that occur during a flood event. Because this model type generally requires more input data and a higher level of analytical skills, hydraulic engineers have not commonly used it for analyzing river systems. In certain instances, the mobile model may compute significantly different water surface elevations compared to the fixed model (Molinas, 1998).

1.2 Research Objectives

This thesis starts with the underlying assumption that mobile boundary models will provide a more accurate water surface profile than a fixed or rigid boundary model. Another assumption associates a more accurate profile with a more efficient and cost-effective hydraulic design. To test these assumptions, the following research focuses on the hydraulic design of highway bridges that span coarse-bedded streams (gravel, cobble beds).

Given the above, the following research has four primary objectives. First, the research tests the idea that mobile boundary models will produce lower water surface elevations upstream from a bridge (bridge backwater elevations) as compared to the fixed boundary model if the bridge dominates the local hydraulic and morphologic characteristics. It is assumed that a mobile model that produces lower bridge backwater elevations compared to a fixed model will allow for a more cost-effective bridge design.

Second, the research tests the assumption that certain fixed boundary, hydraulic parameters can be used to estimate the mobile bridge backwater elevations. The engineer could possibly predict the reduction in bridge backwater elevations for the mobile boundary conditions without having to use the mobile boundary model. This approach is similar to using fixed boundary hydraulic parameters to predict scour at bridge crossings. Assuming a reasonable accuracy in the predicted backwater reductions, the engineer could produce more cost-effective bridge designs while minimizing hydraulic modeling time and costs.

Third, the thesis presents a cost-based method for when and how to use a mobile model at coarse-bedded bridge crossings. Although mobile models may produce more accurate profiles, it may not always be cost-effective to employ these models in the hydraulic design of bridges. Furthermore, how the engineer uses these models could affect the bridge backwater elevations and, thus, the hydraulic bridge design.

Fourth, the research evaluates the assumption that mobile boundary models will produce more accurate water surface profiles than fixed boundary models. While the mobile model may consistently produce lower bridge backwater elevations compared to the fixed boundary model, this does not necessarily translate into a more accurate water surface profile. The presented research, thus, closes with a comparison of the computed fixed and mobile boundary water surface profiles to field-verified water surface profiles.

Collectively, the presented thesis based upon the above research objectives should lead to more cost-effective highway bridge designs.

1.3 Research Scope

To meet the defined objectives, the research uses a series of case studies. Including this introductory chapter, this research thesis consists of seven chapters that discuss and apply the findings from the studied cases. The following briefly summarizes the content of each thesis chapter.

Chapter 1 discusses the research background, objectives, and scope. It also presents the research methods, limits of the proposed research methods, and compares the proposed research with past research as it relates to mobile boundary models. Overall, Chapter 1 provides a summary of the objectives, methods, and limits of the proposed research and its potential findings.

Chapter 2 provides the research information applied in the thesis development. This information includes the general selection criteria and attributes for the case studies. It also includes data requirements, computer model descriptions and differences, stream types, and hydraulic/sediment variables.

Chapter 3 presents the five case studies used in the research. The case studies cover four stream systems located in California, Washington and Wyoming. For each case, the chapter presents the hydraulic, sediment, and bridge design information unique to each study location and stream system. This chapter contains the core information for testing and meeting the defined research objectives.

Chapter 4 provides a sensitivity analysis of the input variables used in the Chapter 3 case studies. The sensitivity analysis tests both physical and operational variables. This chapter also tests for statistical relationships between various hydraulic/sediment variables and bridge backwater values. This section primarily focuses on the assumption that a certain combination of fixed boundary hydraulic values will provide a reasonable estimate of actual mobile-bed, bridge backwater values.

Chapter 5 provides a method for applying mobile boundary models at bridge crossings. Using the case studies from Chapter 3, this chapter discusses when and how to apply mobile models. The chapter presents a cost-based approach to applying these models. Using information from the literature and the sensitivity analysis from Chapter 4, it also provides guidance for selecting the physical and operational parameters used in mobile models.

Chapter 6 presents two test cases for the findings presented in the previous chapters. Using the Cispus River in Washington and the Snake River in Idaho, this chapter compares the modeled results of the fixed and mobile models to actual 100-year flood elevations at a coarse-bedded bridge crossing. For the given research constraints and assumptions, it provides a test of the underlying assumption that mobile models will provide more accurate bridge backwater elevations than fixed boundary models. It also quantifies the extent of those differences.

Chapter 7 summarizes the research findings from the previous chapters. It also discusses research goals not met and further data needs for improving the results. The chapter furthermore discusses the limitations of this type of research.

1.4 Research Methods

Using the collected data and computer models discussed in Chapter 2, Chapter 3 presents five cases that consist of developing water surface profiles for a variety of bridge lengths. The bridge length represents the allowed stream width of the bridge opening. Each case typically analyzes the water surface profiles for six to seven bridge lengths. The research for each study area contains the following two steps:

First, the analysis consists of developing fixed boundary water surface profiles for each bridge length. The study uses the Federal Highway Administration's (FHWA) computer model BRI-STARS (Molinas, 1994). For this part, the model needs stream cross-sections, flood peak data (i.e., 100-year event), and boundary roughness values. As a comparison, the research also uses US Army Corps of Engineers' (USACE) computer models HEC-2 (USACE, 1990) and HEC-RAS (USACE, 1998) to develop fixed boundary profiles.

Second, each case consists of developing a mobile boundary water surface profile for each bridge length. Again, each case uses the computer model BRI-STARS. For this part, the model uses the data from the fixed boundary model plus the complete flood hydrograph and sediment data. The sediment data uses a field-collected particle size distribution and an assumed active layer thickness.

For the bridge hydraulics, each case uses the methods presented in FHWA's

"Hydraulics of Bridge Waterways" (Bradley, 1978). The BRI-STARS model accommodates the bridge losses computed from the methods presented in this publication. The expected bridge losses mainly derive from the constriction that the bridge opening imposes upon the natural stream geometry.

After completing the mobile/fixed profiles for all five cases, the research includes a sensitivity analysis for selected physical and operational parameters. The physical parameters include active layer thickness and sediment size distribution. The operational factors include the selection of sediment transport equations and time-step intervals. Active layer thickness, sediment size distribution, sediment transport equations, and time-step intervals represent parameters that only apply to the mobile models.

The sensitivity analysis measures the relative change in the mobile backwater value relative to the change of each individual variable. For example, increasing the active layer thickness by 100% could result in a decrease of the mobile backwater value of 25%. For the active layer thickness, the relative response becomes 0.25 (relative change in mobile backwater times the inverse of the relative change in the isolated variable). This approach assumes that all other variables remain constant (Bierman, Bonini, and Hausman, 1986).

The research also includes a statistical analysis (i.e., statistical regression) between various hydraulic/sediment variables (independent) and bridge backwater values (dependent). For each case, the analysis consists of selecting the hydraulic properties and related groups (dimensionless groups) for comparison to the mobile/fixed backwater values (Fischer, List, Koh, Imberger, and Brooks, 1979). As stated in Section 2.3, the research assumes that the fluid and sediment traits remain fairly constant within the study area. This leaves the hydraulic properties and related dimensionless groups as the main variables for analyzing the differences in the mobile/fixed backwater profiles. Most sediment transport methods use some combination of flow depth, velocity, hydraulic radius, energy slope and/or discharge to compute the rate of sediment transport (i.e., volume per unit time). Typical groups include such values as unit stream power (velocity times slope), shear stress (specific weight times hydraulic radius times slope), and stream power (shear stress times velocity).

Each selected bridge length exerts some influence on the hydraulic traits as the flood wave passes through the study reach. For example, a selected bridge length may cause slower velocities and increased flow depths upstream of the bridge site compared to higher velocities and shallower depths through the bridge opening itself. The relative changes in hydraulic properties will ultimately cause changes in the stream bed boundary of the study reach. This should then lead to differences in the computed backwater values for mobile versus fixed boundary models.

The analysis for each study site should expose those hydraulic variables and groups having the strongest correlation and the most sensitivity relative to the mobile/fixed backwater values. While this approach may not lead to an exhaustive evaluation of all possible hydraulic properties, it should render an analysis of those properties and groups most commonly used in the development of bridge water surface profiles.

Using the sensitivity analysis and statistical relationships discussed in Chapter 4, Chapter 5 presents a comprehensive method for selecting when and how to use the mobile boundary model at coarse-bedded bridge crossings. This approach includes a cost analysis to determine the economic viability of employing a mobile boundary model at a bridge site.

For example, the mobile model generally requires more time and information to compute the bridge backwater curve than that required for the fixed boundary model. For the additional time and information, the mobile model should produce a more accurate profile than the typical fixed boundary profile. This in turn should produce a more cost effective design (i.e., shorter bridge length). The mobile model should produce an expected savings in bridge costs exceeding the additional model costs. If this is the case, then the user employs the mobile model in the hydraulic analysis of the bridge crossing. The savings in bridge costs normally includes the initial capital costs (i.e., bridge construction) and the associated economic risks (i.e., bridge maintenance).

Chapter 6 presents two test cases to compare the accuracy of the mobile model profile to the fixed model profile. The procedure is similar to that used for the first five cases. In addition to the usual field-collected data, each case also uses surveyed, high water marks from a 1996 flood. The test cases compare the high water marks to the computed profiles using BRI-STARS (fixed and mobile), HEC-RAS (fixed), HEC-6 (fixed and mobile)

(USACE, 1993), and FESWMS (2-D fixed) (FHWA, 1989).

1.5 Limits of Proposed Research Methods

The research presented in the following chapters does have limits related to the above research objectives. These limits come mainly in the form of water surface profile accuracy and verification (see section 2.6) and using a case approach to test some of the proposed research assumptions. The following discusses each of those research limitations.

1.5.1 Water Surface Profile Accuracy and Verification

Water surface profile accuracy derives from technique applicability and computational and data estimation errors (USACE, 1986). Each aspect of developing a water surface profile (i.e., data collection, parameter estimation, calibration of results) normally lies in the subjective experience of the modeler. There is generally limited field data for calibrating the accuracy of these models.

For example, there are rarely accurate field-based, high water marks in the desired profile location that the modeler can calibrate to a given design flood (AASHTO, 1999). Instead, the collected field data is typically the very same data that the model uses to produce a profile (i.e., topographic data, sediment samples). The engineer "calibrates" the selected model through dimensional adjustments of simplified geometric elements and empirical hydraulic coefficients so that modeled flow events approximate those occurring in nature (Cunge, Holly, and Verwey, 1980). Actual comparisons between the computed profile and those occurring in nature are normally based upon visual observations. These observations rely heavily upon such physical features as limited and approximate high water marks, changes in stream side vegetation, stream bed deposits, and variations in the stream morphology.

For the above reasons, much of the presented research in this thesis focuses on the modeling differences and profile results between mobile and fixed boundary models. Despite the subjectiveness of the model analysis, the modeler does have numerous references to supplement his or her past engineering experience. The FHWA, the US Army

Corps of Engineers (USACE), the US Geological Survey (USGS), and many state and local government agencies provide considerable literature on computer modeling of water surface profiles (i.e., AASHTO, 1999; USACE, 1998; FHWA, 1995; Molinas, 1996). Assuming proper use of the referenced materials, a modeler should be able to produce a modeled water surface profile resembling that found in nature at a bridge crossing.

1.5.2 The Case Approach

As discussed above, the proposed research relies heavily on a few selected case studies. The research, thus, uses carefully selected cases that collectively provide a broad range of hydraulic, hydrologic, morphologic, and sediment-based stream conditions. Section 2.2 presents the case attributes and a brief justification for the importance of each attribute in the selected cases. Chapters 3 and 6 also present the general reasons for selecting the specific cases and their associated bridge lengths.

Although the research employs great care in selecting the cases, the limited number of cases does potentially constrain the findings from the studies. There are numerous classes of streams that bridges may cross (Rosgen, 1996). Limiting the case studies to coarse beds (gravel, cobble) with the attributes described in Chapter 2 eliminates several stream types. The small number of cases analyzed in this thesis, also, limits the data for testing the selected research objectives (i.e., estimating mobile backwater values from fixed boundary parameters). Similar to the water surface profile analysis, there is, furthermore, a certain amount of subjectiveness to the case selection and the use of the cases in the proposed research objectives.

The coarse bed limitation and the proposed research attributes used in selecting the specific cases are, nevertheless, not so restrictive as to trivialize the findings and conclusions presented in this thesis. Coarse bed streams generally exist in steep terrain throughout the United States and the world (Jarrett, 1990; Habibi, 1994; Haschenburger, 1994). The hydraulic, hydrologic, morphologic, and sediment traits found in Chapter 2 represent a broad range of stream conditions (Rosgen, 1996). The presented stream conditions have attributes typical in the application of both fixed and mobile boundary computer models. Similar to the water surface profile applications, the research relies heavily on the referenced materials to reduce the subjectiveness of the case approach (i.e., Molinas, 2000; USACE, 1998; USACE, 1993).

1.6 Past Research Versus the Proposed Research

Historically, engineers have used mobile or sediment-based models for such applications as assessing sedimentation of reservoir systems, the impacts of gravel operations on natural river systems, and dredging plans for navigational purposes (Molinas, 2000; USACE, 1993). There is documentation on the potential influences of sedimentation processes at bridge crossings (FHWA, 1995; Mansfield, 1988; FHWA 1990). There is, however, very little in the literature assessing these processes or on applying mobile/sediment models at such crossings.

1.6.1 Past Studies

Most studies have focused on water surface profile errors for fixed boundary model systems. For example, the USACE (1986) evaluated model input errors and their effect upon the modeled water surface profile generated with the computer program HEC-2. The input parameters included such items as survey data and methods, Manning's roughness, and computational steps. In a different study, the USACE (1998) compared water profile differences between HEC-2 and the more recent computer program HEC-RAS as it relates to their computational style for hydraulic conveyance. Conclusions from these studies are summarized in Sections 2.6.1 and 2.6.2.

Other similar studies have used a combination of field measurements and computational values to compare bridge backwater values among various computer models or methods. For example, Kaatz and James (1997) used field measured water surface profiles and computed natural profiles to determine a "measured" backwater. Kaatz and James (1997) then compared this value to the computed backwater values for HEC-2, WSPRO, and the modified Bradley method. FHWA (1986) has also documented similar studies using HEC-2, WSPRO, and E431 to compare the modeled water surface profiles to field observed water surface profiles. Conclusions from these studies are summarized in Section 2.6.1.

For mobile or sediment transport models, the research has focused primarily on comparing various differences in the sediment transport equations versus actual measured rates of transport (Gomez and Church, 1989; Nakato, 1990). This is a logical approach since errors in sediment transport rates will lead to errors in the computed boundary or bed of the model. This ultimately may lead to errors in the computed water surface profile. Conclusions from these studies are summarized in Section 2.6.3.

Other mobile model studies have relied upon changes in the stream morphology to evaluate the accuracy of the model computations. For example, Chang (1994) used measured changes in stream morphology to compare the accuracy of various sediment transport formulas. He evaluated such sediment transport formulas as Meyer-Peter and Müller, Yang, Parker, and Engelund-Hanson. Based upon field measurements, the Yang and Parker formulas replicated the changes in stream morphology more accurately than the Meyer-Peter and Müller and Engelund-Hanson formulas in that particular study.

1.6.2 Comparison of Past Research to the Proposed

It is quite clear that the proposed research differs from past research because it focuses on a subject - applying mobile models at bridge crossings - with little research history. However, there are similarities between the research methods employed in this dissertation and those used for researching fixed boundary models. For example, the proposed research relies heavily upon model-computed water surface profiles and their relative differences to meet most of the research objectives (i.e., fixed model profile versus mobile model profile).

Similar to past field-related case studies, this thesis also uses limited high water marks and field observations to evaluate the accuracy of the model results. The proposed research, furthermore, uses sensitivity analysis to evaluate the impact of various physical and operational parameters on the computed water surface profile. Finally, this thesis uses the case approach that several past studies have commonly employed in evaluating water surface profile computations (i.e., FHWA, 1986; Kaatz and James, 1997).

Besides the focus on the mobile boundary analysis at bridge crossings, there is one other unique aspect of the proposed research. It generally takes a holistic approach in the presented case studies. In most hydraulic and sedimentation studies, the research focuses on particular parameters (Manning's roughness, sediment transport equation, etc.). The water surface profile, in particular for a mobile boundary situation, is the product of many physical and computational parameters. Many of these parameters are inter-related. For example, the stream hydraulics (depth, velocity, etc.) is a product of the stream boundary (morphology, sediment size, etc.) and the boundary is a product of the stream hydraulics. Depending upon the time scale, hydraulic and sedimentation parameters can be either a cause or an effect (Chang, 1998). Thus, it is neither easy to predict the results (the profile) for the given parameters nor to evaluate completely their particular influence on the computed results.

Despite the potential complexities, the presented research in this thesis should enhance the understanding of mobile boundary models. As stated in the research objectives, it should lead to more cost effective hydraulic bridge designs. Collectively, the following chapters present case studies and implementation processes ("when to", "how to") that do not exist in the current literature. The presented thesis, thus, should greatly improve the future application and study of mobile boundary models at bridge crossings.

CHAPTER 2: CASE CRITERIA, ATTRIBUTES, DATA, AND MODELS

2.1 Overview

In five sections, this chapter describes the case criteria, attributes, data, and models used for developing the thesis. Section 2.2 presents the case selection criteria and process. Section 2.3 describes the attributes of the case studies contained in Chapters 3 and 6. Section 2.4 describes the collected data for the research methods used in Chapters 3, 4, 5, and 6. Section 2.5 presents the analytical tools employed in the selected computer models. The final section, Section 2.6, discusses computer model accuracy and differences.

2.2 Case Selection Criteria and Process

Chapters 3 and 6 present cases selected using the following criteria:

- Case Attributes - These attributes represent the original physical criteria for selecting the presented case studies. They fall into four basic categories: stream hydraulics, hydrology and morphology, sediment traits, and bridge hydraulics. Section 2.3 provides a detailed discussion of each category.
- Collected data - The required data needed for each case study include stream cross-sections, stream gage flows, sedimentation properties, and boundary roughness values. Section 2.4 presents more detailed information on each data collection item.
- Bridge lengths - For the Chapter 3 cases, each case had to have the potential to generate at least six discernible bridge lengths or openings. This criterion insures at least 30 data "points" for the statistical analysis presented in Chapter 4. Each bridge length must have a Froude number ≤ 1 and a bridge opening ratio ≥ 0.50 (see Section 4.2). This insures that excessive contraction or choking does not occur at the selected bridge site. It also insures general compliance with the bridge hydraulics constraints of Section 2.3 (i.e., subcritical to critical flow).
- High water marks and major flood events - For the Chapter 6 cases, each case requires high water marks for a major flood event. This criterion insures a field-

verified water surface profile. The research compares the modeled (rigid, mobile) profile to the field-verified profile. The comparison should determine which model type produces the more accurate water surface profile during a major flood event such as a 100-year flood.

As stated in Section 1.5.2, the research uses selected cases that collectively provide a broad range of hydraulic, hydrologic, morphologic, and sediment-based stream conditions. The selected cases derive from a review of the literature and discussions with various Federal, State, and local highway officials. The literature reviews and discussions focus on finding bridge sites meeting the above criteria.

2.3 Case Attributes

The case studies presented in Chapters 3 and 6 possess certain general attributes in common. These attributes fall into four basic categories: stream hydraulics, stream hydrology and morphology, sediment traits, and bridge hydraulics. The following is a brief summary of the characteristics for each category. The first three categories apply only to the natural stream properties (no bridge influences). Table 2.1 presents a summary of the following case attributes.

For the stream hydraulics, the natural stream flow primarily consists of gradually varied, subcritical flow conditions. The flow mainly occurs in a one-dimensional manner (i.e., along the stream thalweg). These conditions are typically analyzed using HEC-2 (USACE, 1990), WSPRO (Shearman, 1990), HEC-RAS (USACE, 1998), BRI-STARS (Molinas, 1994), and other commonly used water surface profile models. These models can analyze some supercritical flow conditions, however, subcritical flow conditions, generally lead to more predictable water surface profiles (Morris and Wiggert, 1972). Most streams, furthermore, typically function in subcritical flow when energy slopes do not exceed about 3% (Jarrett, 1984).

The stream hydrology is characterized by the 100-year flood event. Most engineers use the 100-year or comparable flood to comply with government flood plain regulations and bridge design methods (AASHTO, 1999). For the selected case studies, the expected peak of the 100-year flood wave ranges from 2500 cubic feet per second (cfs) to 75,000 cfs. Generally, a crossing with a 100-year flood wave of 2500 cfs typically requires a bridge to pass the flood peak without significant damage(i.e., a hydraulic-caused structural failure). For this thesis, a bridge is defined as any structure with a minimum span and minimum vertical clearance of 20 feet and 10 feet, respectively. The 75,000 cfs represents a somewhat arbitrary upper 100-year flood limit. Streams that have 100-year flood peaks larger than this value present difficulties in collecting accurate data on sediment traits, stream geometry, and flow data (i.e., flood hydrographs).

The stream morphology consists of a main channel with flood plains. The main channel and flood plains generally have uniform widths and slopes. Most methods for computing bridge water surface profiles derive from the superposition of a bridge upon a fairly uniform channel and overbank geometry. The more uniform the geometry, the more likely that the selected computer model will accurately predict the 100-year water surface profile (Morris and Wiggert, 1972).

The stream slopes in the case studies range from 0.1% to 3%. Streams with this range of slopes generally have gravel beds with subcritical flow conditions (Jarrett, 1984; Rosgen, 1996). As stated above, these traits represent favorable conditions for the conducted research. The selected channel and flood plains mostly have distinct boundaries (i.e., changes in vegetation, sediment). This allows for more easily defined values within the stream geometry such as roughness, sediment sizes, and flow distribution. The selected streams sites, furthermore, tend toward long-term stability (i.e., neither aggrading or degrading). This also should insure that the proposed bridges exert the primary influence on the local stream morphology.

Using Rosgen's (1996) stream classification system, the research focuses on B3, C4, D4, DA4, E4, and F4 stream types. These streams typically have gravel beds with some silt, sand, and cobbles. These streams also have low to moderately, sinuous flow patterns with slightly to moderately entrenched channels.

For the sediment properties, the stream bed sediment sizes range from very fine gravels (2 mm) to large cobbles (256 mm). For gravel beds, the individual particle size normally dominates the boundary roughness values. Bed form (i.e., dunes, ripples), thus, should not significantly influence the boundary roughness. Similarly, the stream beds consist of fairly uniform or armored beds with a predominant sediment size. This improves prediction of roughness values and also possibly improves prediction of sediment transport rates.

The sediment inflow and outflow normally have comparable values for the given study areas. This insures that excessive deposition or scour will not occur in the study area. Excessive deposition or scour may cause a significant change in bed elevation. This could alter the water surface elevation without any influence from the bridge crossing.

For a typical bridge site, the study reach length is less than one-half mile. For the selected study areas, the research assumes that the fluid and sediment properties remain fairly constant. These properties include viscosity, specific weights, particle sizes and distribution, and temperature.

For the 100-year flood, the stream bed shear stresses typically exceed the critical shear stresses of the boundary or bed particles. This simply means that sediment movement will occur during the given flood events. For 100-year flood events, this is a reasonable assumption.

In terms of the bridge hydraulics, the bridge opening, piers, skew, and eccentricity represent the main factors affecting the bridge water surface profile. For most cases, the bridge opening is the most influential profile factor. To insure the dominance of the opening on the water surface profile, the selected bridge crossings normally have good alignment with the natural stream flow (i.e., negligible skew and eccentricity). Some of the selected sites have piers within the opening. The piers, however, have little influence on the computed water surface profiles.

The flow through the bridge opening consists of critical to subcritical flow. This insures that energy-based methods will properly predict the profile through the bridge opening. The research avoids hydraulic jumps and other abrupt hydraulic features that may require momentum-based methods for solving the water surface profile (USACE, 1998) at the bridge.

The selected sites have bridge lengths where the bridge opening should dominate the water surface profile at the stream crossing. The bridge opening, thus, should cause enough scour at the crossing to reduce the mobile boundary upstream backwater compared to the fixed boundary model.

2.4 Collected Data

Chapter 3 presents five case studies. The cases include the Nisqually River and Skagit River in Washington, two locations in the Stony Creek stream system in California, and the Gibbon River in Wyoming. Chapter 6 presents the Cispus River in Washington and the Snake River in Idaho as test case studies to verify the conclusions from Chapter 3 and to evaluate fixed and mobile bed model accuracy.

For each case study, the collected data includes stream cross-sections, stream gage flows, sediment properties, and boundary roughness values. The stream cross-sections either consist of numerous sections taken upstream and downstream of the bridge or a representative cross-section taken near the bridge site. The cross-sections come from collected field data of the main channel and the adjacent flood plains.

For stream gage flows, all the data derive from US Geological Survey (USGS) gaging stations. Most bridge sites have nearby stations. For most cases, the 100-year flood hydrograph comes from USGS gage data and USGS regression equations.

The sediment data primarily consists of field-collected, stream bed gradations and physical observations. Each study relies upon pebble counts for the bed gradations. Using field observations, aerial photographs, and USGS topographic maps, the cases consist of bridge sites lying in areas of sediment transport equilibrium (sediment inflow equals sediment outflow).

Similarly, boundary roughness values for each case come from field and aerial observations. Generally, the main channel has one roughness value (i.e., Manning's n) based upon the collected stream bed gradations. The flood plains have another value based upon the vegetation types (i.e., grasses, trees).

2.5 Computer Models and Analysis

As stated earlier, the case studies primarily use BRI-STARS (Bridge Stream Tube Model for Alluvial River Simulation Model) (Molinas, 1994) and HEC-2 (USACE, 1990) or HEC-RAS (USACE, 1998) for the water surface profile computations. Dr. Albert Molinas, Hydrau-Tech Inc., developed BRI-STARS under the National Cooperative Highway Research Program (NCHRP) for FHWA and the American Association of State Highway and Transportation Officials (AASHTO). The USACE's Hydrologic Engineering Center developed the HEC programs. The following briefly discusses the similarities in the BRI-STARS and HEC models. Chapter 6 briefly discusses the HEC-6 and FESWMS models used in the Cispus and Snake cases.

2.5.1 Fixed Boundary Approach

BRI-STARS and HEC-2 or HEC-RAS will compute water surface elevations for a fixed boundary condition. For this condition, both model types assume that the channel geometry does not change with time. Both models use the standard step method to compute a water surface profile for a given discharge. The standard step method is a well-known approach for solving a one-dimensional energy equation (Chow, 1959; Morris and Wiggert, 1972) in the case of gradually varied flow.

Assuming subcritical flow, the models begin with a given water surface elevation at the most downstream cross-section. Using the energy, continuity, and Manning's equations, the models solve for the water surface elevation at the next upstream cross-section. The friction slope and expansion/contraction head losses represent the differences in the two water surface elevations (Figure 2.1). The following presents the basic standard step equations. The information below is taken from the HEC-2 user manual (USACE, 1990) and the HEC-RAS hydraulic reference manual (USACE, 1998). Here the subscript 1 refers to downstream conditions and the subscript 2 refers to upstream conditions (Figure 2.1).

$$Y_2 + Z_2 + \frac{\alpha_2 V_2^2}{2g} = Y_1 + Z_1 + \frac{\alpha_1 V_1^2}{2g} + h_e \qquad (2\text{-}1)$$

$$h_e = L\overline{S_f} + C_L \left| \frac{\alpha_2 V_2^2}{2g} - \frac{\alpha_1 V_1^2}{2g} \right| \tag{2-2}$$

Where: Y_1, Y_2 = depth of water at downstream (1) and upstream (2) cross-sections, feet (ft)

Z_1, Z_2 = elevation of the main channel invert, ft.

V_1, V_2 = average flow velocities, feet per second, fps

α_1,α_2 = weighted coefficients for nonuniform cross-section, velocity distribution(kinetic energy coefficient)

g = acceleration of gravity, ft/s^2

h_e = energy head losses, ft

L = discharge weighted reach length, ft

$\overline{S_f}$ = average friction slope between sections, ft/ft

C_L = expansion or contraction loss coefficient

The discharge weighted reach length, L, and average friction slope, $\overline{S_f}$, are defined as follows.

$$L = \frac{L_{lob}\overline{Q_{lob}} + L_{ch}\overline{Q_{ch}} + L_{rob}\overline{Q_{rob}}}{\overline{Q_{lob}} + \overline{Q_{ch}} + \overline{Q_{rob}}} \tag{2-3}$$

Where: L_{lob}, L_{ch}, L_{rob} = reach lengths for flow in the left flood plain, main channel, and right flood plain, respectively, ft

$\overline{Q_{lob}}$, $\overline{Q_{ch}}$, $\overline{Q_{rob}}$ = arithmetic average of flows at the ends of the reach for the left flood plain, main channel, and right flood plain, respectively, cubic feet per second (cfs)

$$\overline{S_f} = \left(\frac{Q_1 + Q_2}{K_1 + K_2} \right)^2 \tag{2-4}$$

$$K = \sum_{i=1}^{n} k_i \tag{2-5}$$

$$k_i = \frac{1.486}{n} A_i R_i^{\frac{2}{3}} \text{(in English units)} \tag{2-6}$$

Where: k_i = conveyance for subdivision, cfs

n = Manning's "n" for subdivision

A_i = flow area for subdivision, ft^2

R_i = hydraulic radius for subdivision(area (A_i) divided by wetted perimeter(P_i)), ft

Figure 2.2 presents the typical incremental areas, k_i, for computing the total conveyance, K, for a given stream cross-section.

The model works well for flow that is gradually varied, steady, and one-dimensional. The flow should also have energy slopes less than 10% (USACE, 1990). For flood peaks, the modeler assumes that an observer follows the peak of the flood wave as it passes through the given stream cross-sections. This becomes the water surface profile for the given flood peak. The stream cross-sections also should have limited variability in elevation and width. Finally, subcritical flow conditions with flood waves of small amplitude should provide the most predictable energy losses for this approach. If the modeled situation meets these conditions, both the BRI-STARS and HEC models should provide accurate water surface profiles for fixed boundary flood peaks.

The HEC programs use a discharge-weighted reach length (Eq. 2-3) to compute friction losses. The modeler subdivides each stream cross-section into a main channel and two adjacent flood plains. The modeler also enters the distance between each upstream and downstream channel and flood plain section (3 distances). The HEC programs compute an effective length using the weighted average of the given channel/flood plain distances and their respective section discharges.

BRI-STARS permits only one distance between stream cross-sections. To allow for unequal distances between flood plains and channels (i.e., for meandering streams), the modeler should enter estimated loss coefficients. The modeler should also artificially increase or decrease the flood plain roughness values to compensate for unequal lengths.

BRI-STARS permits the modeler to select the Manning's, Chezy, or Darcy-Weisbach equation for computing friction losses between the channel cross-sections. The HEC programs limit the modeler to the Manning's equation. It does, however, permit an equivalent roughness, k_s, conversion to a Manning's n, roughness value. In this sense, HEC programs permit changes in friction factor with water surface elevation similar to the Chezy equation. The following is the Chezy equation and the k_s conversion to Manning's n.

$$C = 32.6 \log_{10}\left(12.2\frac{R}{k_s}\right) \tag{2-7}$$

Where: C = Chezy roughness coefficient

R = hydraulic radius, ft

k_s = equivalent roughness, ft

$$n = \frac{1.486 R^{1/6}}{32.6 \log_{10}\left(12.2\frac{R}{k_s}\right)} \tag{2-8}$$

2.5.2 Mobile Boundary Approach

The HEC-2/HEC-RAS models limit themselves to fixed boundary water surface profiles. BRI-STARS has the following mobile boundary features. The mobile model primarily consists of four analytical steps.

For step one, BRI-STARS, as previously discussed, will compute the water surface profile for a given discharge, channel geometry, boundary roughness, and respective energy losses. The modeler specifies a certain number of stream tubes for the selected study reach. BRI-STARS uses the number of tubes to subdivide the channel cross-sections. BRI-STARS then computes the hydraulic traits (depth, velocity) for each tube of each channel section. The modeler may specify a certain percentage of the discharge for each tube. The modeler also may distribute the flow uniformly among the selected stream tubes. Typically, the modeler will select three to five tubes for the study area (Figure 2.3).

Under step two, the modeler will generally enter a series of discrete discharges at a specified interval (Figure 2.4). BRI-STARS will compute the sediment discharge for each tube of each channel section. The sediment discharge is a function of the computed hydraulic traits, the selected sediment transport formula (i.e., Yang, Meyer-Müller), and the specified sediment distribution.

For the third step, BRI-STARS computes the total sediment load for each tube of each channel section. If the incoming sediment load exceeds the outgoing sediment load, then deposition will occur within the tube at the specified channel section. Conversely, scour will occur when the outgoing sediment load exceeds the incoming sediment load. BRI-STARS uses the following sediment continuity equation for this analysis (Molinas, 1994).

$$\frac{\partial Q_s}{\partial x} + n_s \frac{\partial A_d}{\partial t} + \frac{\partial A_{ss}}{\partial t} - q_s = 0 \qquad (2\text{-}9)$$

Where: n_s = volume of sediment in a unit bed layer volume = 0.6

A_d = volume of sediment deposition per unit length, ft^3/ft

A_{ss} = volume of sediment in suspension at the cross-section per unit length, ft^3/ft

Q_s = volumetric sediment discharge, cfs

q_s = lateral sediment inflow, cfs/ft

Assuming steady state conditions during each time step, the change in velocity is zero. Similarly, none of the parameters in the sediment transport function are allowed to change during the time step. The change in the average suspended sediment volume, A_{ss}, is thus zero since it is a function of location and velocity. Assuming $q_s \approx 0$,

$$\frac{\partial Q_s}{\partial t} = 0 \quad \text{or} \quad \frac{\partial Q_s}{\partial x} = \frac{dQ_s}{dx} \qquad (2\text{-}10)$$

The sediment continuity equation is then as follows.

$$n_s \frac{\partial A_d}{\partial t} + \frac{dQ_s}{dx} = 0. \qquad (2\text{-}11)$$

In discrete form, the terms below can be substituted into equation 2-11.

$$n_s \frac{\partial A_d}{\partial t} = \frac{n_s(2P_i + P_{i+1} + P_{i-1})\,\Delta Z_i}{4\Delta t} \tag{2-12}$$

$$\frac{dQ_s}{dx} = \frac{Q_{si} - Q_{si-1}}{\dfrac{\Delta x_i + \Delta x_{i-1}}{2}}. \tag{2-13}$$

Where: P = wetted perimeter, ft

Z = bed elevation above a certain datum, ft

i = cross-section index

Finally, in the fourth step, BRI-STARS uniformly spreads the scour and deposition over the tube length and width. From this approach, it computes the vertical change in the tube/section elevation (i.e., decrease in elevation for scour). Before proceeding to the next discharge, BRI-STARS adjusts the elevations for each tube/section throughout the study area. Combining equations 2-11, 2-12, and 2-13, equation 2-14 represents the change in bed elevation (Figure 2.5).

$$\Delta Z_i = \frac{8\Delta t(Q_{si} - Q_{si-1})}{n(\Delta x_i + \Delta x_{i-1})(2P_i + P_{i-1} + P_{i+1})} \tag{2-14}$$

For a given stream tube, equation 2-15 presents the total change in bed elevation at station i during a time step, Δt.

$$\Delta Z_i = \sum_{k=1}^{NSIZE} \Delta Z_{ik} \tag{2-15}$$

Where: NSIZE = the number of size fractions of sediment.

BRI-STARS repeats steps one through four for each specified discharge. The model uses a sequential or uncoupled approach to solve the mobile version of the water surface profile of the study area. Figure 2.6 presents the general approach for this iterative process.

BRI-STARS also will adjust the channel section width. It uses a minimum stream power approach to decide whether to adjust the vertical or lateral part of the selected stream tube. For the case studies, the analysis did not include this minimizing features (i.e., channel widening). Instead the analysis assumed that all section changes occurred in the vertical direction.

2.5.3 Bridge Waterways Analysis

Both HEC-2/HEC-RAS and BRI-STARS present different options for computing water surface profiles at bridge crossings. For most situations, HEC-2 (USACE, 1990) uses the following approach.

Typically, the user can adjust the expansion and contraction coefficients at a bridge crossing. For example, since the abutments generally constrict the stream channel, the increased coefficients should reflect the increased energy losses attributable to the bridge abutments.

For bridges with piers, HEC-2 computes the momentum relationships through the bridge opening. Using these relationships, the model determines the class of non-pressure flow through the opening (subcritical, critical, or supercritical). For subcritical flow, HEC-2 uses Yarnell's equation to compute the energy losses from the downstream bridge section to the upstream bridge section. Yarnell's equation is as follows.

$$H_3 = 2K_p\,(K_p + 10\omega_v - 0.6)\,(\alpha_o + 15\alpha_o^4)\,\frac{V_3^2}{2g} \tag{2-16}$$

Where: H_3 = drop in water surface elevation from upstream to downstream sides of the bridge, ft

K_p = pier shape coefficient

ω_v = ratio of velocity head to depth downstream from the bridge

α_o = obstructed area/total unobstructed area

V_3 = velocity downstream from the bridge, fps

For pressure flow and flow over the bridge, the model uses orifice and weir equations. These equations provide the water surface elevations through the bridge using the increased loss coefficients with the standard step method (Eq. 2-1). When piers exist, the model will use Yarnell's equation for subcritical flow through the bridge opening (Eq. 2-16).

HEC-RAS (USACE, 1998) uses similar bridge waterways methods to those described for HEC-2. HEC-RAS does allow additional computational options. For example, HEC-RAS also has FHWA's WSPRO as an option for analyzing bridge waterways under low flow conditions. WSPRO uses an empirical discharge coefficient for the bridge based upon the contracted opening method (USGS, 1953; USGS, 1968). The case studies (Chapter 6), however, that employed HEC-RAS and HEC-2 use only the energy equation. To compensate for the bridge, these models simply increase the expansion and contraction coefficients used in equations 2-1 and 2-2.

BRI-STARS allows the user to select different approaches for solving water surface computations through the bridge crossing. For the selected case studies, the model uses a single loss coefficient applied at the bridge cross-section to reflect all the losses through the opening. The single loss coefficient derives from the "Hydraulics of Bridge Waterways", HDS No. 1, by FHWA, dated March 1978 (Bradley, 1978).

BRI-STARS sums the losses between the bridge and the next upstream cross-section. These losses include friction, constriction, and the above bridge opening losses. The model adds these head losses to the water surface elevation at the bridge opening to get the water surface elevation upstream from the bridge crossing.

Figure 2.7 presents the plan, section, and profile views for a typical bridge water surface profile. Figure 2.8 presents the possible types of flow through a bridge opening. For the case studies, Type I and IIA flows generally occur in the models. Figure 2.9 presents the base curves for computing the opening loss coefficient.

The loss or backwater coefficient consists of an opening, pier, eccentricity, and skew coefficient (Eg. 2-17). The user sums the value of each bridge-related coefficient to derive the complete backwater coefficient for the bridge. The bridge backwater loss is then the product of the backwater coefficient and the bridge section velocity head.

$$h_1^* = K^* \alpha_2 \frac{V_{n2}^2}{2g} \qquad (2\text{-}17)$$

Where: h_1^* = Total backwater or rise above normal stage at section 1(Figures 2.7 and 2.8), ft

K^* = Total backwater coefficient for subcritical flow

= Opening + pier + eccentricity + skew loss coefficients

α_2 = Velocity head coefficient for the constriction (for nonuniform cross-section, velocity distribution)

V_{n2}= Average velocity in the constriction, fps

The opening loss coefficient is a function of the abutment type (i.e., spill-through, vertical) and opening ratio. The opening ratio is the ratio of the flow in the portion of the upstream channel within the projected bridge length to the total flow through the opening. The smaller the opening ratio the greater the loss coefficient for the selected bridge opening (Figure 2.9).

The pier coefficient is primarily a function of the pier type and width. For example, circular piers will typically have lower loss coefficients than square-nosed piers. The opening ratio also will influence the pier loss coefficient. The pier loss coefficient decreases as the opening ratio decreases.

The eccentricity coefficient is a function of the flow in the over banks and the opening ratio. If the approaching flow to the bridge is extremely asymmetrical, then this coefficient will increase the computed backwater. For example, if one approaching overbank transports less than 20% of the flow relative to the other over bank, then the eccentricity coefficient could cause a measurable increase in the total backwater coefficient.

The skew coefficient is a function of the alignment of the bridge to the approaching flow. The opening ratio also influences the skew coefficient. For a given opening ratio, the skew coefficient increases as the skew angle increases. The skew angle is the angle between the center line of the flow and a line perpendicular to the bridge opening.

HDS No.1 (Bradley, 1978) presents the figures for computing the pier, eccentricity, and skew coefficients. For the case studies, the open ratio represented the primary value for computing the bridge backwater coefficient, K^*. In general, bridges that have well-aligned approaches and do not significantly constrict the flow should produce very little backwater.

Well-aligned approaches are symmetrical to the flow and should also have small skew angles to the approaching flow.

2.5.4 Sedimeat Transport Analysis

BRI-STARS allows the user to select from several sediment transport equations. For example, the user may select sediment discharge equations developed by Yang (1973, 1984), Meyer-Peter and Müller (1948), Ackers and White (1973), and Engelund and Hanson (1967). It also allows the user to enter a regression equation for the sediment discharge.

According to the literature, there is no one universal sediment transport equation (Gomez and Church, 1989; Nakato, 1990). Yang's (1984) research has shown that his gravel transport equation may provide a more accurate estimate of the sediment discharges for natural gravel rivers than other methods. The case studies use his sediment transport equation for gravel.

Yang's (1984) equation computes the total gravel concentration as a function of unit stream power (velocity times slope). Yang (1984) starts with the following basic unit stream power equation.

$$\frac{dY}{dt} = \frac{dY}{dX}\frac{dX}{dt} = SV = VS \qquad (2\text{-}18)$$

Where: V = average water velocity, fps

S = energy slope, ft/ft

Y = elevation above datum, ft

X = distance along the stream channel, ft

t = time, s

Since Y also represents potential energy, the above equation defines the unit stream power as the time rate of potential energy expenditure per unit weight of water. Using his studies of stream morphology, Yang (1973) concluded that the following log-linear equation effectively defined the relationship between unit stream power and total sediment concentration, C_t. C_t is the total sediment concentration of stream bed material transported as bed load and suspended load. C_t is in parts per million by weight.

$$\log C_t = A_y + B_y \log(VS - V_{cr}S) \tag{2-19}$$

$V_{cr}S$ represents the critical unit stream power to set the sediment in motion. A_y and B_y represent log-linear, statistical regression parameters. Yang (1973) expresses V_{cr} in the dimensionless form shown in equation 2-20.

$$V_{cr}/\omega = \left(\frac{5.75\,[\log(D/d) - 1]}{B'} + 1 \right) \sqrt{\frac{\psi_1 \psi_2 \psi_3}{\psi_2 + \psi_3}} \tag{2-20}$$

ω is the particle fall velocity. B' is a roughness function. ψ_1, ψ_2, and ψ_3 are coefficients for particle drag, lift, and friction, respectively. Using theoretical concepts on boundary layers, surface roughness, and numerous sets of independently collected data, Yang (1973) presented the following equations for smooth (Eq. 2-21) and rough (Eq. 2-22) boundary flow conditions, respectively.

$$V_{cr}/\omega = \frac{2.5}{\log(U_* d/\nu) - 0.06} + 0.66, \quad 0 < (U_* d/\nu) < 70 \tag{2-21}$$

$$V_{cr}/\omega = 2.05, \qquad 70 \le (U_* d/\nu) \tag{2-22}$$

Here, U_* is the shear velocity, d is the particle diameter, and ν is the kinematic viscosity of the water.

Yang uses dimensionless relationships to present a general form of equation 2-19. He defines total sediment concentration as a function of three dimensionless ratios. The first ratio is unit stream power to particle fall velocity or dimensionless unit stream power. With this ratio, he further includes a dimensionless minimum unit stream power ratio. This ratio is the critical unit stream power as defined above divided by the particle fall velocity. The difference in the dimensionless unit stream power and the minimum unit stream power ratio is the effective dimensionless unit stream power. This is the portion of the unit stream power responsible for transporting the sediment concentration.

The second of the three ratios is shear velocity to fall velocity. The third and last ratio is the Reynold's number based upon particle fall velocity and diameter. The following shows Yang's (1973) use of these dimensionless ratios to develop his sediment concentration equations.

$$C_t = \Phi\left(\frac{VS}{\omega} - \frac{V_{cr}S}{\omega}, \frac{U_*}{\omega}, \frac{\omega d}{\nu} \right) \tag{2-23}$$

Based upon more than 1000 sets of laboratory and field data, Yang (1973) presented equation 2-19 in the following dimensionless form.

$$\log C_t = I + J \log\left(\frac{VS}{\omega} - \frac{V_{cr}S}{\omega} \right) \tag{2-24}$$

Where:

$$I = a_{y1} + a_{y2}\log\left(\frac{\omega d}{\nu} \right) + a_{y3}\log\left(\frac{U_*}{\omega} \right) \tag{2-25}$$

$$J = b_{y1} + b_{y2}\log\left(\frac{\omega d}{\nu} \right) + b_{y3}\log\left(\frac{U_*}{\omega} \right) \tag{2-26}$$

a_y and b_y are log-linear, statistical regression coefficients.

For gravel beds, Yang (1984) used multiple regression analysis on numerous data sets of gravel concentrations to solve the coefficients in equations 2-25 and 2-26. From this statistical analysis, Yang (1984) presented the following transport equation for gravel stream beds.

$$\log C_{tg} = 6.681 - 0.633 \log \frac{\omega d}{\nu} - 4.816 \log \frac{U_*}{\omega}$$
$$+ \left(2.784 - 0.305 \log \frac{\omega d}{\nu} - 0.282 \log \frac{U_*}{\omega} \right) \log\left(\frac{VS}{\omega} - \frac{V_{cr}S}{\omega} \right) \tag{2-27}$$

C_{tg} is the total sediment concentration of gravel bed material transported as bed load and suspended load. C_{tg} is in parts per million by weight. Equation 2-27 represents the core sediment concentration equation for determining the changes in the channel boundary of the stream sections.

For the sensitivity analysis, Chapter 4 uses the Parker (1990) (Parker, Klingeman, and McLeon, 1982) and Meyer-Peter and Müller (1948) methods for computing sediment loads. This chapter discusses their effect on the case results and also briefly presents the application requirements for the Parker (1990) and Meyer-Peter and Müller (1948) methods.

2.6 Model Accuracy and Differences

This section discusses the expected accuracy for modeling water surface profiles. It also discusses potential computational differences between the various models that the research uses in the case studies. Finally, this section discusses the accuracy of sediment transport equations typically used in mobile boundary studies.

2.6.1 Model Accuracy - Fixed Boundary Models

The USACE (1986) and USACE (1994) present minimum standard deviations for one dimensional subcritical, gradually-varied flow, and rigid boundary conveyance of the one-percent chance discharge (100-year flood). The standard deviations derive from the study and analysis of 98 natural stream data sets. They represent the expected difference in the computed water surface profile and the actual profile of a natural stream. These differences are, thus, the elevation differences in the two profiles.

For stream cross-sections based upon field surveys, the USACE presents minimum standard deviations ranging from 0.3 feet to 1.3 feet. The lower 0.3 foot value applies for good, reliable Manning's n or roughness values. The higher 1.3 foot value applies to poor reliability in estimating the natural stream Manning's roughness. A middle value of 0.7 feet would apply for a fair estimation of Manning's roughness. If the computer profile has a Manning's value based upon highly reliable field calibration data (i.e., stream gage validation, high water marks, other field observations), then the lower standard deviation values apply. Conversely, poor or limited field calibration data leads to larger standard deviations in the computed water surface profile. Also, the standard deviations may increase with an increase in the stream complexity or analysis.

FHWA (1986) presented six study sites with water surface comparisons between the computed profile (i.e., HEC-2, WSPRO) and the observed profile elevations. The FHWA study generated elevation difference between the computed and observed profiles ranging from zero feet to more than two feet for a given stream section. All study sites had bridges with flows ranging from 1,500 cfs to 16,000 cfs. The study sites were on streams in Alabama, Louisiana, and Mississippi.

2.6.2 Model Differences - Fixed Boundary Models

Besides differences between the computed and observed profile elevation differences, relatively minor differences in computational methods may lead to measurable differences in the computed profiles of different models. For example, the USACE (1998) compared HEC-2 and HEC-RAS conveyance computation methods and their effect on the computed water surface profile. They used the 100-year flood (1% chance event) and 2048 cross-section locations for the comparisons. For the two conveyance methods, 47.5% of the cross-sections had computed water surface elevations within 0.10 feet of each other. Similarly, 71% of the cross-sections had computed elevation differences within 0.20 feet, 94.4% were within 0.40 feet, and 99.4% were within 1.0 feet. The HEC-RAS approach generally produced a lower water surface profile. There is no field data, however, to support one approach as more accurate than the other approach (USACE 1998). Thus, there is a need for field-observed water surface profiles for comparing the accuracy of computed water surface profiles.

2.6.3 Sediment Transport Accuracy

Gomez and Church (1989) evaluated 12 bed load transport equations for gravel bed streams. They used both river and flume data in their analysis. No one formula performed consistently well. They did recommend stream power-based equations because these equations lend themselves to easier scale corrections (i.e., flume vs. natural channel conditions). They evaluated the various sediment equations by comparing the calculated sediment transport rate to the observed rate (C/O). The results varied widely. For example, nearly every equation had mean C/O ratios greater than 2 for at least one or more of the base data sets.

Similarly, Nakato (1990) found the computed sediment transport values differed greatly from measured values using several commonly used sediment transport equations (i.e., Meyer-Peter and Müller, Yang, Ackers-White). The study focused on the Sacramento River in California. The stream bed materials consisted of fine sands to coarse gravels. Generally, the computed sediment transport values (i.e., tons/day) differed from the measured values by more than a factor of 2. Sometimes the computed values were much greater than the measured values, sometimes they were much less.

2.6.4 Summary on Computer Model Accuracy

As stated in Section 1.6, there is minimal research on applying mobile boundary models at bridge crossings. There is, thus, little information on their accuracy or on the effect of modeling differences (i.e., conveyance approaches) in applying these models. Furthermore, the "engine" of the mobile models, the sediment transport formula, may generate large errors relative to the actual sediment transported in natural streams.

The studies discussed in this section, however, should alert the user to the potential elevation differences on the order of a foot or more between the computed and observed water surface profiles. Although Sections 2.6.1 and 2.6.2 focus on rigid boundary models, the user should expect similar or even possibly greater errors for mobile models. This is evident from the increased complexity of a mobile model and the potentially large inaccuracies of the associated sediment transport formula.

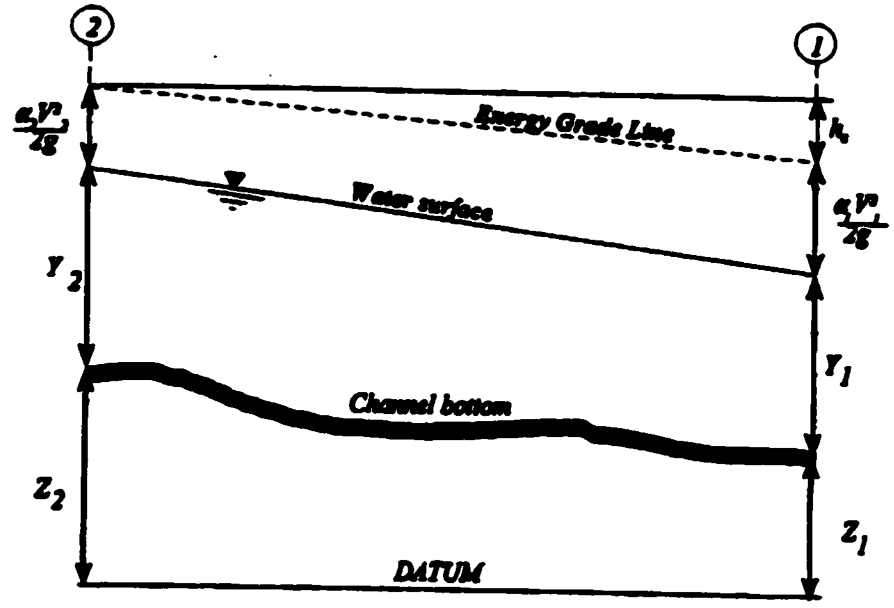

Figure 2.1 Representative energy equation terms (USACE, 1998)

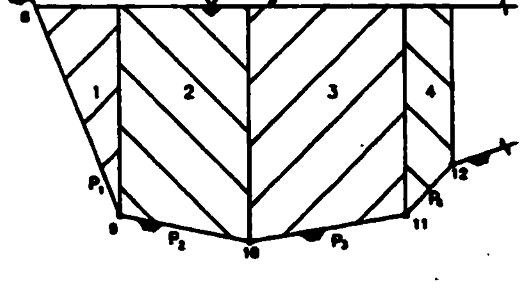

Figure 2.2 Incremental flow areas (USACE, 1990)

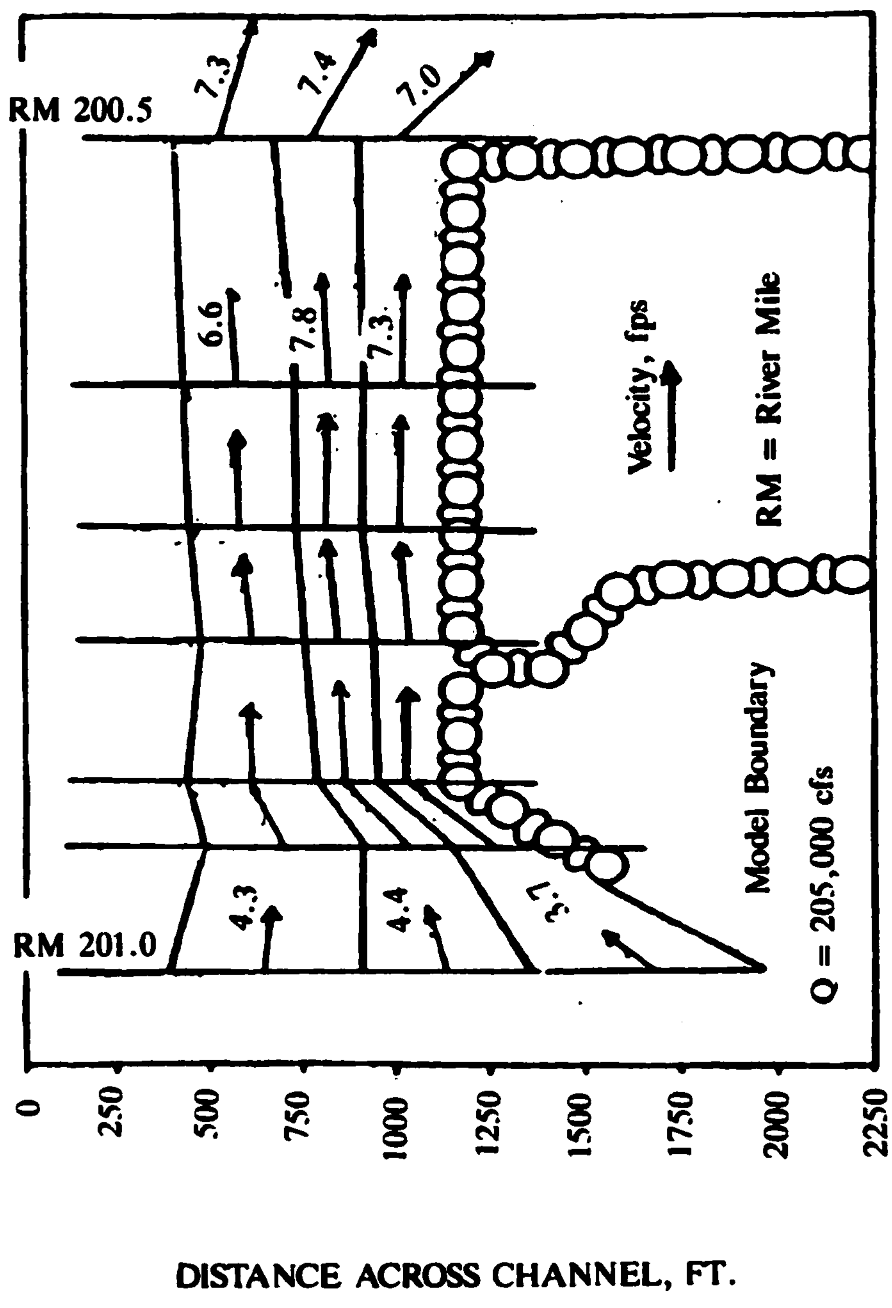

Figure 2.3 Planimetric stream tubes (Molinas, 1994)

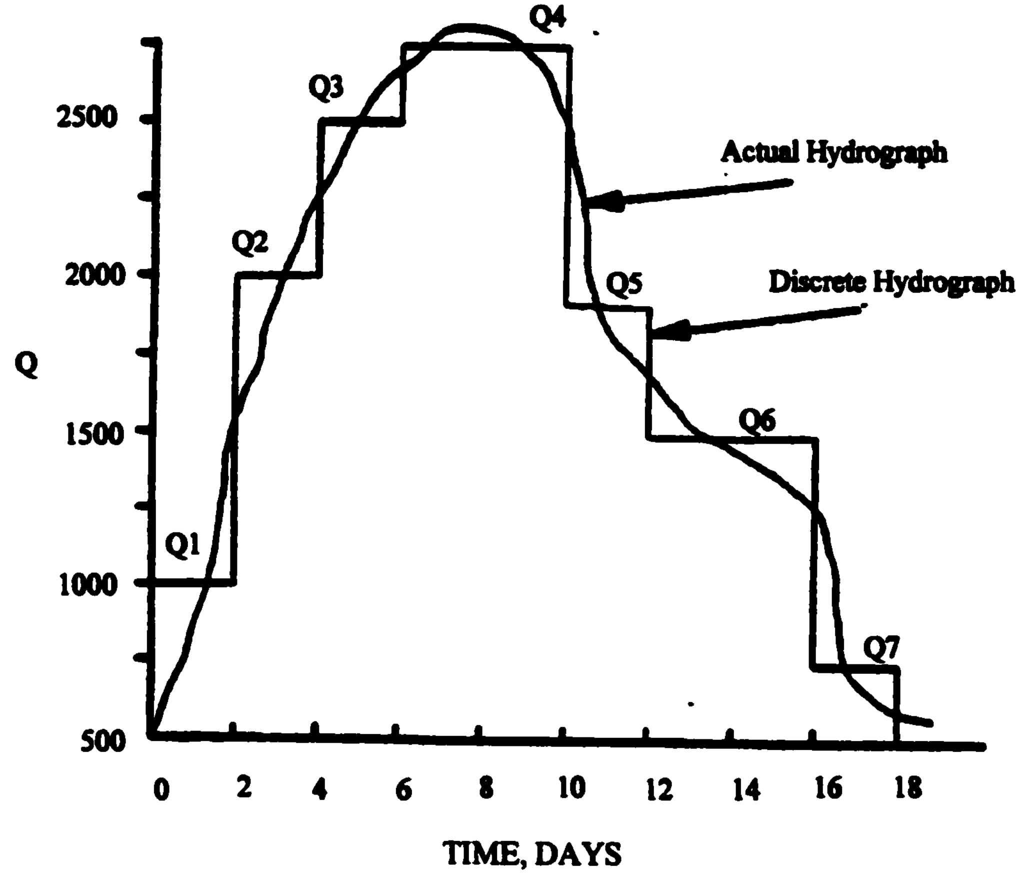

Figure 2.4 Discrete discharge hydrograph (Molinas, 1994)

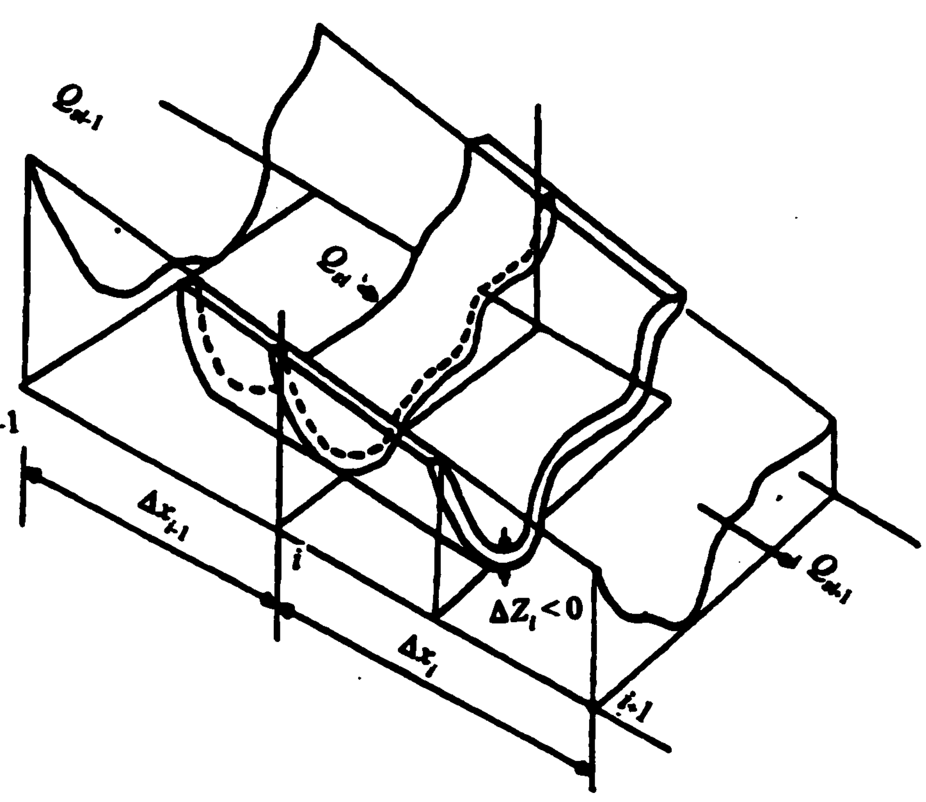

Figure 2.5 Reach variables (Molinas, 1994)

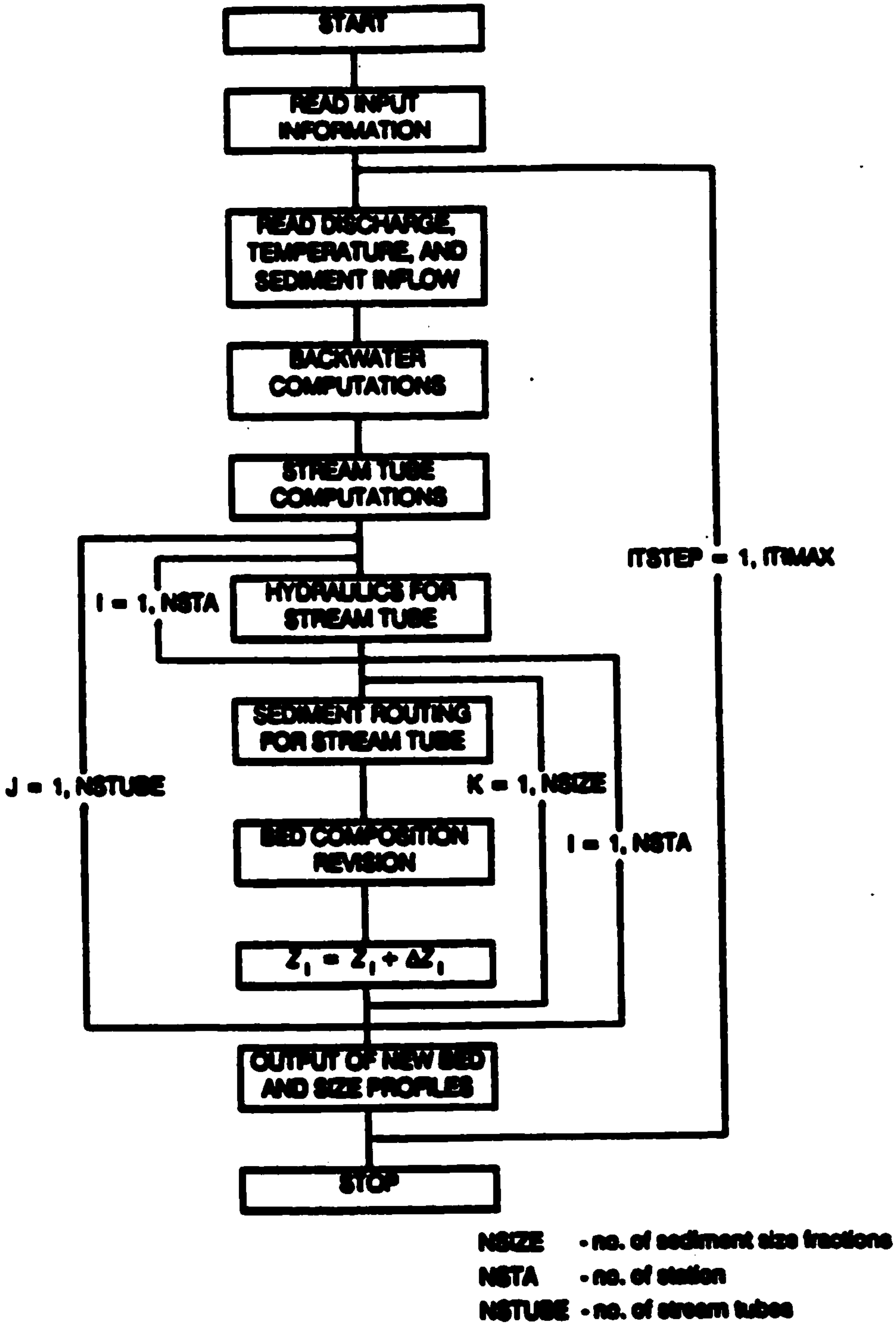

Figure 2.6 BRI-STARS flow chart (Molinas, 1994)

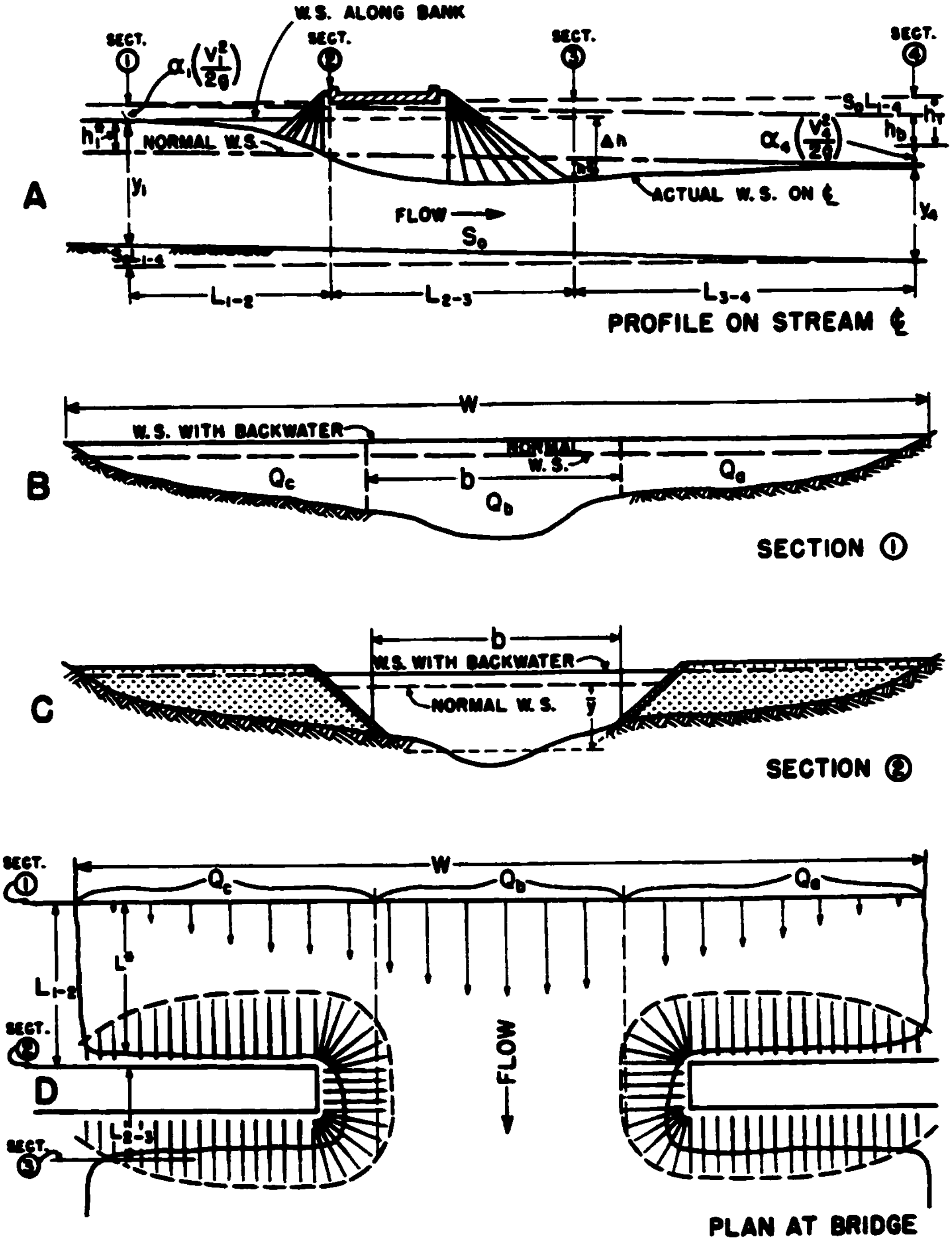

Figure 2.7 Typical bridge crossing (Bradley, 1978)

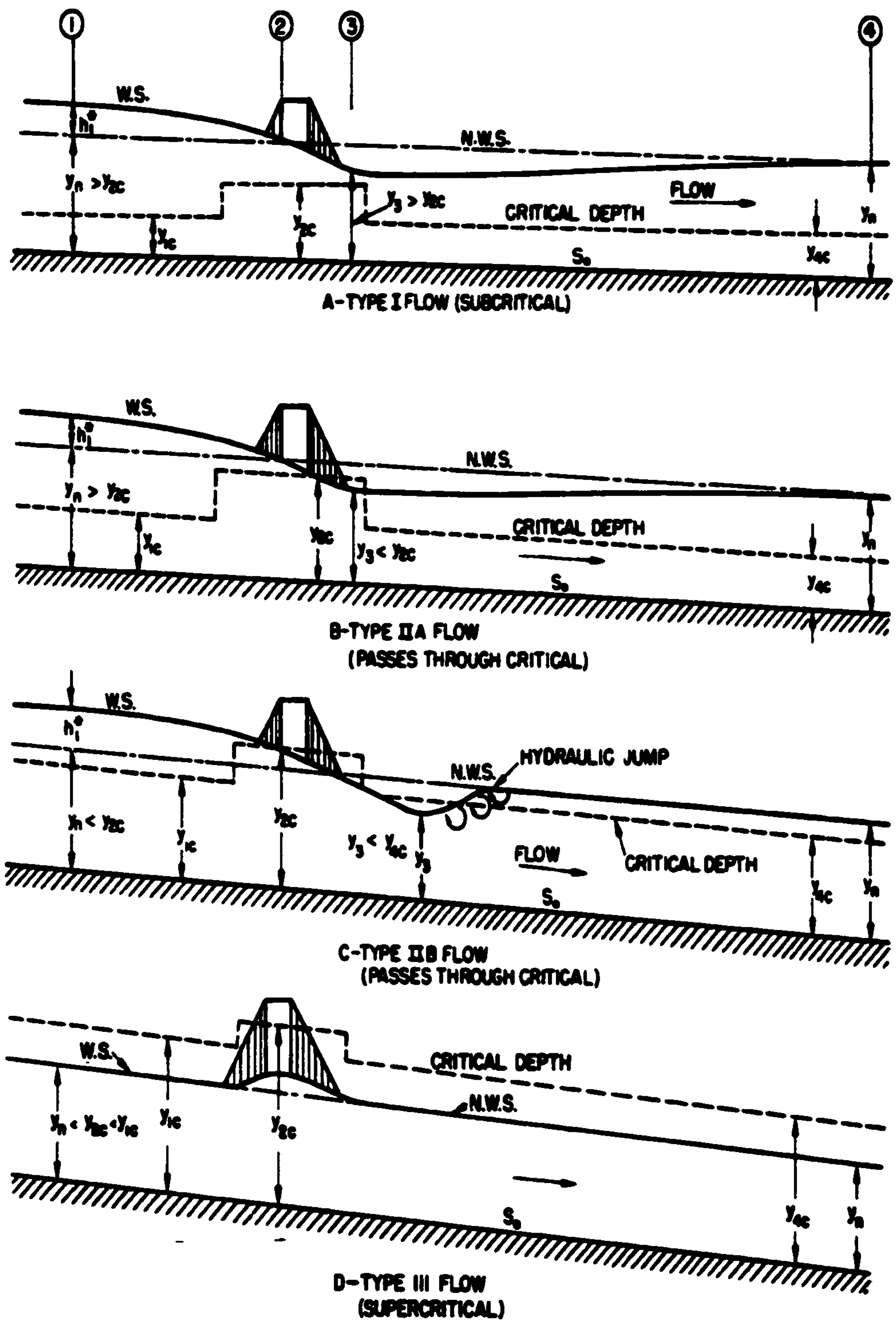

Figure 2.8 Typical bridge flow types (Bradley, 1978)

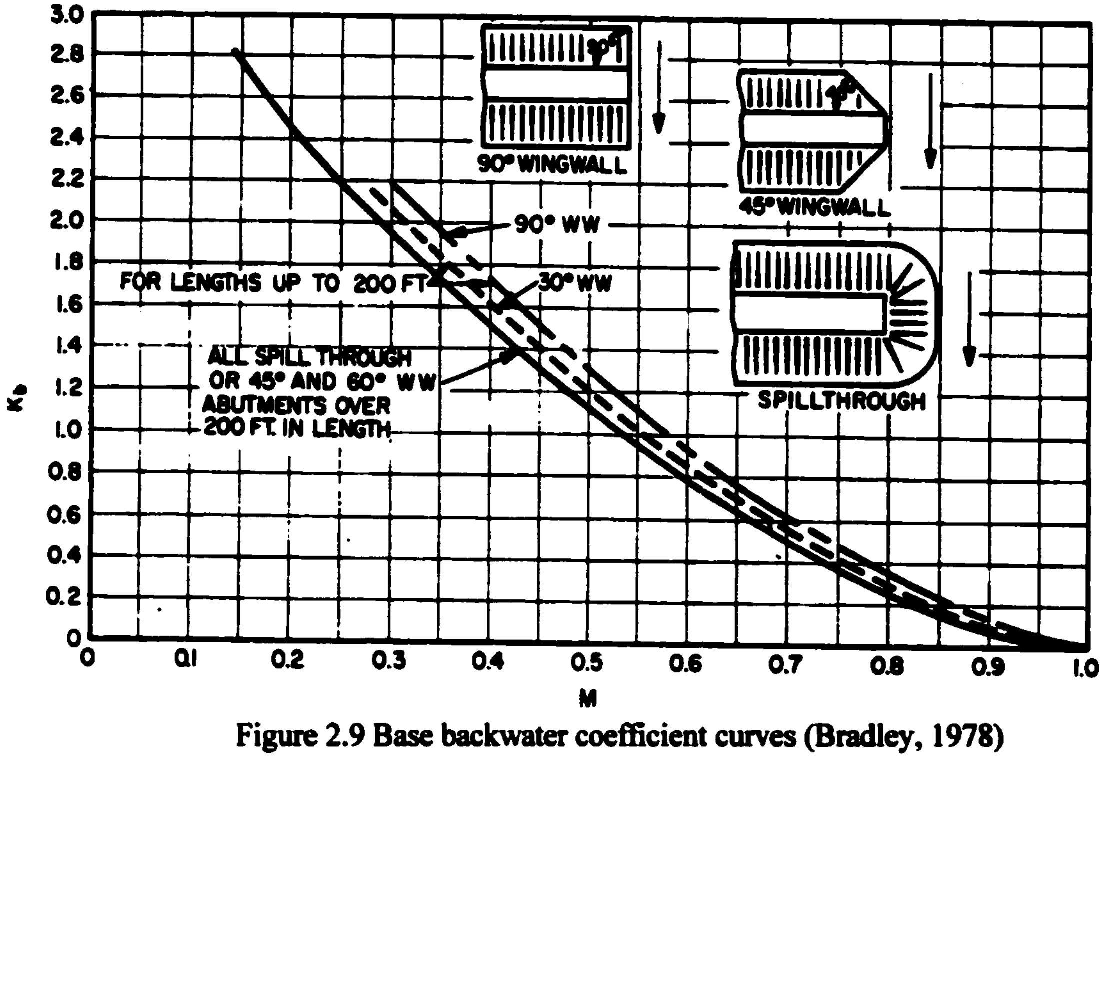

Figure 2.9 Base backwater coefficient curves (Bradley, 1978)

Table 2.1 Case attributes

Category	Sub Category	Attribute
Stream Hydraulics	Flow Type	Gradually-varied flow, subcritical, one-dimensional
Stream Hydrology and Morphology	Flow Rate	2500 to 75,000 cfs
	Flow Duration	Approximately two days
	Channel Configuration	Single channel with over banks
	Rosgen Classification	B3, C4, D4, DA4, E4, F4
	Stream Slopes	0.1% to 3%
Sediment Traits	Particle Size	2 mm to 256 mm
	Sediment Flux	Inflow ≈ outflows
	Sediment Properties	Viscosity, specific weight, particle sizes and distribution, and temperature are constant
	Particle Motion	Bed shear > critical shear
Bridge Hydraulics	Geometry	Minimal skew or eccentricity, bridge well-aligned with flow
	Piers	With and without piers; piers have negligible influence on stream flow
	Flow in Opening	Subcritical to critical
	Bridge Lengths	Selected so that fixed back water curve is generally ≥ mobile back water curve (i.e., bridge opening dominates the back water curve).

CHAPTER 3: CASE STUDIES

3.1 Overview

This chapter presents the five case studies for the three primary research objectives discussed in Chapter 1. In particular, this chapter tests the hypothesis that mobile models will produce lower water surface elevations upstream from a bridge as compared to the fixed boundary model if the bridge dominates the local hydraulic and morphologic characteristics. For testing this hypothesis, Sections 3.2, 3.3, 3.4, 3.5, and 3.6 present the Nisqually, the Skagit, the Stony Creek #1, the Stony Creek #2, and Gibbon case studies, respectively. Section 3.7 discusses the conclusions from the case studies.

The Chapter 3 case studies also provide the hydraulic information for testing the assumption that a certain combination of fixed boundary hydraulic values will provide a reasonable estimate of actual mobile-bed, bridge backwater values (Chapter 4). Chapter 3, furthermore, provides the hydraulic and morphologic characteristics that a bridge crossing should have when applying the mobile boundary models according to the processes described in Chapter 5.

To aid the reader, Tables 3.1 and 3.2 present morphological traits and hydraulic values of the selected case studies. These tables present the natural characteristics (without bridge influences) that each stream system exhibits for a given set of hydrologic conditions (i.e., the 100-year flood). The tables show that the following case studies represent a wide range of hydraulic and morphological conditions for coarse bed rivers.

Unless otherwise stated, the author of this thesis implemented the computer models used in the following case studies.

3.2 Nisqually River

The Nisqually River is the subject of the first case study. As described below, the USGS has performed various data collection and analytical activities on the Nisqually. Those activities include studies and data collection of the hydrology, hydraulics, and sedimentation properties near or within the study area (Nelson, 1987; Walder and Driedger, 1994; Walder and Driedger, 1995; Scott and Vallance, 1995; Scott, Vallance, and Pringle, 1995). The Nisqually, thus, has most of the necessary information for comparing fixed and mobile water surface profile models.

3.2.1 Study Location

The Nisqually River originates from the southwest slopes of Mt. Rainier National Park, Washington (Figure 3.1) (Nelson, 1987). The study area starts at the southwest boundary of Mt. Rainier and proceeds due west for about 5 miles. For most of its length, the Nisqually flows parallel to Washington State Route (SR) 706. The centerline of the Nisqually River is also the county line between Lewis and Pierce counties.

The river has broad floodplains with a meandering, braided stream pattern. There is very little development along the Nisqually. About 4 miles downstream from the Park boundary, a bridge crosses the Nisqually. This bridge provides access from Skate Creek Road to SR 706. The bridge slightly constricts the flood plain of the Nisqually. Topographic maps and aerial photographs show that manmade developments have very little influence on the hydrology and hydraulics of this portion of the river.

Upstream from the bridge site to the park boundary, the Federal Emergency Management Administration (FEMA) and Pierce County have designated a regulated floodway. The designated floodway encompasses the Pierce County portion of the 100-year flood plain. The FEMA-based regulations prevent development or encroachments in the regulated floodway. Preventing developments, thus, assures that manmade activities will not cause a rise in the 100-year flood elevations.

The FEMA regulations, however, only apply to the portion of the river lying in Pierce County. Lewis County chose not to have FEMA-based regulations that limit development in Nisqually River floodplains. Lewis County, thus, permits developments that may increase the 100-year flood elevations.

The above creates an unusual regulatory situation. Obviously, flood plain developments in Lewis County would affect the 100-year flood elevations of the Nisqually in both counties. Such developments could, thus, cause unwanted increases in the flood elevations on the Pierce County portion of the Nisqually.

The Pierce and Lewis County situation requires accurate and reliable water surface profiles. Future development will depend upon the computed flood profiles for this area. Thus, this location provides an opportunity to compare different flood modeling techniques. It should also show the influence that each model type can have on the selection of manmade features such as bridges.

3.2.2 Hydrology

This report uses flood hydrographs developed from US Geological Survey (USGS) data and methods (Cummans, Collings, and Nassar, 1975; Nelson, 1987). Near National, Washington, the USGS operates a gaging station (#12082500) a few miles downstream from the study area. At the gaging station, the Nisqually has a drainage area of 133 square miles. The study area has a drainage basin of about 75 square miles.

For the study area, FEMA had the USGS determine the flood boundaries in the late 1970's. Figure 3.2 presents a partial topographic map of the USGS study limits. Figure 3.2 also shows the general outline of the Nisqually River and its floodplains.

For their study, the USGS determined the peak values for the 10-year, 50-year, 100-year, and 500-year flood events. For rigid boundary models, the peak of the flood hydrograph is the only hydrologic concern for computing the related water surface profile. The USGS used the computer program, E431, to compute the FEMA flood elevations and boundaries. Assuming a rigid boundary, E431 uses a step backwater method to perform the flood analysis.

A mobile boundary model requires the complete flood hydrograph. This report uses the 25-year flood hydrograph from the USGS gage site as the base hydrograph. The hydrologic analysis consists of using simple flood peak ratios between the study area and the gage site. Using these ratios, the analysis adjusts the 25-year hydrograph at the gage station to match the flood peaks at the study area.

Figure 3.3 presents the hydrograph for the 25-year flood at the USGS gaging station.

It also shows the expected 10-(Q_{10}), 50-(Q_{50}), 100-(Q_{100}), and 500-year (Q_{500}) hydrographs for the selected study area. The hydrographs use a 12-minute interval for each flood wave. The study assumes that the site hydrograph has the same shape and duration as the hydrograph for the 25-year flood at the gaging station.

3.2.3 Sedimentation

At the study site, the Nisqually River has three primary sediment sources. They are the Tahoma Creek, Kautz Creek, and upper Nisqually River basins. All three sources originate in Mt. Rainier National Park (Figure 3.1) (Nelson, 1987). The selected study area begins just downstream from these sediment sources.

According to USGS studies, each of these basins experience large glacial outbursts that bring large loads of sediment to the main stem of the Nisqually (Scott, Vallance, and Pringle, 1995). The three basins have steep gradients compared to the main Nisqually basin (more than 10% versus 2% or less). Much of the deposition, thus, occurs at the confluences of these basins with the main stem of the Nisqually.

The glacial outbursts typically occur during late summer to early fall (Nelson, 1987; Scott, Vallance, and Pringle, 1995). These glacial outbursts have some effect on the flow rate of the main Nisqually stem. However, they do not occur at the same time as the main stem flood peaks. The main stem flood peaks normally occur from late spring to early summer.

The Nisqually mobile model assumes that the incoming sediment to the study reach is negligible during the flood wave. This assumption derives from the premise that the glacial outbursts have already deposited and shaped the upper reaches of the study site. The Nisqually River flood waves occur at a latter time (Nelson, 1987). These flood waves re-distribute through scour and deposition the previously deposited glacial sediments.

The mobile model uses sediment gradations obtained from pebble counts taken at the upstream and downstream end of the study site. The upstream sample site is near the confluence of Tahoma Creek with the Nisqually. The downstream site is just upstream from the Nisqually River bridge.

The study also assumes that the stream bed gradation initially changes in a uniform manner proceeding upstream to downstream (coarser to finer bed material). The model also assumes no variation in gradation across the stream cross-section. Based upon limited pebble counts and visual observations, this is a reasonable assumption. Figure 3.4 contains the gradation curves for the pebble counts. Overall, the Nisqually River has a gravelly cobble, stream bed.

3.2.4 Case Scenario Overview

For the Nisqually study, the case analysis included five case scenarios. The first scenario compared the water surface profiles of HEC-2 and BRI-STARS for a rigid boundary condition. The analysis included the 10-, 50-, 100-, and 500-year flood events. It did not include any bridges. Table 3.3 presents the results for the 100-year flood peak.

The second scenario compared the 10- and 100-year water surface profiles for the fixed and mobile boundary conditions. For this scenario, the study only used the BRI-STARS model. Table 3.4 presents the results for the 100-year water surface profiles. It also shows the relative changes in the stream bed at 0, 13, and 34 hours. These times represent the beginning, peak, and end of the flood hydrograph.

Using a third scenario, the study analyzed different bridge lengths at STA 3670. This analysis included both fixed and mobile boundary conditions. Using various bridge lengths, Table 3.5 presents the 100-year water surface elevations for the rigid and mobile boundary situations.

The fourth and fifth scenarios are similar to the third except the bridge is at STA 3120 and STA 5605. For these scenarios, Tables 3.6 and 3.7, respectively, present the results for the 100-year water surface elevations for the different bridge lengths.

3.2.5 Scenario 1.

This scenario routes the flood peaks for the 10-, 50-, 100-, and 500-year flood events through the selected study area. The channel boundaries do not change with time (rigid boundary condition). Both the HEC-2 and BRI-STARS models use the original FEMA flood study data. This data includes stream cross-sections (29 sections), Manning's roughness values (channels, floodplains), and planimetric distances between each cross-section. Both models also use contraction and expansion coefficients of 0.1 and 0.3, respectively. Furthermore, both models compute the water surface elevations for a steady state condition. The flow is subcritical and assumed to vary gradually between cross-sections.

As stated above, both models use the standard step approach to solve the water surface profile for each flood peak. Conceptually, both models use the same methods in their analysis. For the 100-year event, maximum flow depths vary from about 5' to 10'. Referring to Table 3.3, the "NET DIFF" column represents the "HEC-2" computed value subtracted from the "BRI-STARS" computed value. Table 3.3 shows that most of the computed elevation differences are within 5% of the computed flow depth (water surface elevation minus the minimum bed elevation).

Both the HEC-2 and BRI-STARS model use iterative procedures to solve equations 2-1 and 2-2. Both models use a maximum of 26 iterations to solve for the water surface elevation for each cross-section. BRI-STARS uses a convergence value of 0.001 feet compared to 0.01 feet for the HEC-2 model.

The fifth column of Table 3.3 shows the net water surface elevation difference between the two models (BRI-STARS value minus the HEC-2 value). A few of the cross-sections had elevation differences ranging from 5% to just under 15% of the computed flow depth. These cross-sections had significant changes in conveyance from the previous downstream cross-section. These changes were generally due to geometric changes (i.e., channel width, slope). Typically, the ratio of the current cross-section conveyance to the previous section conveyance exceeded 1.5. HEC-2 uses a conveyance based energy slope method (Eq. 2-4). BRI-STARS uses an average friction slope equation. This difference in energy slope equations probably causes most of the difference in the computed water surface elevations.

Using the same convergence value and energy slope equation should reduce the differences in the computed water surface elevations. The significant change in conveyance, however, does show that gradually varied flow may not exist between the current section and the next downstream cross-section. The modeler should, thus, add more cross-sections between the two sections. The two models usually compare well in their computed water surface elevations for the 100-year flood event.

3.2.6 Scenario 2.

This scenario compared the water surface profiles for the mobile and fixed boundary conditions. Given the small computational differences in HEC-2 and BRI-STARS, the comparisons included only the BRI-STARS models for the rigid and mobile boundary conditions.

Table 3.4 presents the results for the 100-year water surface profiles. This table shows that the flow depth for the mobile boundary model may differ by more than 30% from the fixed boundary value. For the two model types, this results in water surface elevation differences that exceed one foot at several cross-sections.

Before proceeding with an explanation for the computed differences, recall the assumptions and conditions for the mobile boundary model:

The model assumes that no sediment enters at the upstream location of the study area. It also assumes that the particle gradation changes uniformly from a gravelly, cobble bed to a cobbly, gravel bed. The uniform change occurs in the downstream direction. Pebble counts taken at upstream and downstream locations of the study area provide the basis for the BRI-STARS sediment gradations. Finally, the initial gradations do not vary across the stream cross-section.

At the downstream end, the model uses a rating curve to calculate the starting water surface elevation for each given discharge. The model does not adjust the rating curve for geometric changes in the downstream cross-section. Nor does the model have a downstream transmissive boundary. Such a feature would allow the sediment reaching the downstream boundary to pass without changing the cross-section geometry.

The study uses five stream tubes to distribute the flow across the stream cross-section. The model uniformly distributes the given discharge across the five stream tubes. The computed water surface elevation remains constant across the stream cross-section. The model, thus, uses equal conveyance to define the lateral location for each stream tube. The stream tube width will vary from cross-section to cross-section (Figure 2.3). The discharge per stream tube, however, does not vary from section to section.

The analysis uses Yang's (1984) gravel equation to compute the sediment loads from cross-section to cross-section. The model assumes that the active layer thickness is no more than eight inches. The model, thus, limits the sediment loads and the changes in the geometric boundary for each time step.

The mobile model uses a 12-minute time step between discharges. The cross-sections have an average spacing of about 900'. Average cross-section velocities range from about 4 feet per second (fps) to more than 9 fps. The selected time step should reflect both the speed of the flood wave and the speed that sediment moves along the stream.

The model uses six separate gradation sizes ranging from fine gravel (5 mm) to large cobbles (180 mm). Figure 3.4 presents the gradation curves for the selected sample sites. The assumed water temperature is 40 degrees Fahrenheit.

The mobile analysis does not widen the cross-section boundary. All boundary changes occur in the vertical direction.

Certain assumptions apply to both the rigid and mobile boundary models. These assumptions are similar to those for Scenario 1. For example, the expansion and contraction coefficients are 0.3 and 0.1, respectively. There are no loss adjustments for meanders.

From cross-section to cross-section, the left over-bank, right over-bank, and main channel flow distances are all equal. The analysis does not adjust roughness values for unequal flow lengths. The analysis uses the Manning's equation to solve for the water surface elevation for each time step. For the main channel, the roughness value ranges from 0.050 to 0.065. For the floodplains the values range from 0.080 to 0.18. These high values reflect the shallow flow over a very coarse stream bed and heavily vegetated flood plain.

For the standard step method, the assumed upstream water surface elevation should converge within 0.001' of the computed water surface elevation. The analysis limits the number of standard step iterations to 20.

For both models, the flow is gradually varied, subcritical, and one-dimensional. For the rigid model, the flow is steady state. For the mobile model, the flow is quasi-steady or steady state during each time step.

Except for the convergence value, the above assumptions are consistent with the HEC-2 and FEMA flood plain models.

Collectively, the above assumptions will influence the computed water surface elevations. For example, with no incoming sediment, the upstream cross-sections may exhibit excessive scour. This does not occur for the Nisqually case. Table 3.4 shows some minor degradation at STA 23285 (0.18 feet at the flood peak). At the upstream sections, the water surface elevations for the rigid and mobile models differ only a couple of tenths of a foot. This supports the original assumption that the incoming sediment to the Nisqually study area is negligible.

The coarse cobble bed at the upstream section limits the material that the Nisqually flood wave will transport from this region. The gradual change from a coarse cobble bed to a coarse gravel bed also reduces the chance for significant scour at anyone section. This approach allows for some incoming sediment to the downstream sections. As the bed material size decreases in the downstream direction, the incoming sediment reduces the potential for increased section scour.

At the downstream end, stations 0 through 1660 exhibit excessive scour and deposition. Compared to the rigid model, this causes differences in the stream bed and water surface elevations of several feet. As stated earlier, the model does not adjust the given water surface elevation at STA 0 for geometric changes to the stream section. It also does not pass the incoming sediment through STA 0. The model, thus, does not provide the proper adjustments to prevent the resultant oscillations between scour and deposition. Without proper hydraulics at STA 0, the excessive scour and deposition pattern extends upstream to STA 1660. The water surface elevations for this reach, therefore, do not represent reliable values (see Table 3.4).

The five stream tubes should adequately represent the subsection flow properties across the given cross-sections. The stream tube boundaries should lie at distinct breaks in the channel cross-section (main channel versus over-bank flow), or they should lie in homogenous subsections (three tubes falling within the main channel section). If a tube lies partially in the over-bank and partially in the main channel, the velocity and depth properties for the two distinct subsections will average out over the tube width. BRI-STARS may, thus, overstate the transport properties in the over-bank and understate these properties in the main channel. For the Nisqually case, this does not occur in enough instances to alter the results significantly.

The BRI-STARS model permits the option of using the Meyer-Peter and Müller (1948) or Yang (1984) equation for computing the gravel/cobble sediment transport quantities. The modeler also may enter a generic sediment rating curve. There was no available sediment rating curve for the Nisqually River.

Originally, the model was run using the Meyer-Peter and Müller (1948) method. Because of the coarse bed material and the relatively shallow flood flows, this appeared to be the most proper equation for the case study. The Meyer-Peter and Müller equation, however, predicts large quantities of sediment movement for each time step in this case. This appears inconsistent with field observations. Similarly to the downstream problems discussed above, the model computes excessive scour and deposition patterns for the given cross-sections.

Using the Yang (1984) equation, the BRI-STARS model computes smaller volumes of material transport. For each time step, this reduces the scour and deposition between the sections. The active layer thickness of eight inches, also, limits the scour and deposition for each time step. The combination of the Yang equation and the limited active layer creates a stable situation for the mobile boundary model.

As stated above, the mobile model used a 12-minute time step. The analysis was also carried out using other time steps (i.e., 6 minutes). The results did not change significantly. Each different time step requires re-computed discharges for the flood hydrograph. BRI-STARS also limits the number of time step iterations to 1000. The smallest possible time step is, thus, about 2 minutes for a 34 hour hydrograph. The analysis, therefore, did not emphasize the variation of time steps upon the computed water surface profiles for the mobile boundary situation.

The input data for the stream bed gradations and water temperatures should not have caused significant errors in the computed water surface elevations. These values come from field data.

The model includes the wide heavily, vegetated flood plains of the Nisqually River. Although the Nisqually will scour and deposit at different locations within each stream section, the overall width should not measurably change. The analysis should, thus, not need the BRI-STARS widening feature to improve the water surface profile computations.

Since the other above assumptions (i.e., expansion, contraction losses) apply to both the rigid and mobile models, these assumptions should not markedly influence the relative differences in the water surface profiles.

Disregarding the downstream sections from STA 0 to STA 1660, only seven of the 25 cross-sections have water surface elevation differences of more than 0.5' between the two model types. Referring to Table 3.4, the "NET WSEL" column represents the "RIGID WSEL" computed value subtracted from the "MOBILE WSEL" computed value. Using the maximum section flow depth, this represents at least a 5 to 10% difference. The following explains the differences in the two models.

From STA 13795 to STA 17245, the flow width varies from under 500' to over 1000'. This causes wide variation in the energy slopes (0.5 to 2%) and stream velocities (5 to 9 fps)from section to section. STA 16085, a narrow section, thus, experiences scour, while STA 13795, a wide section, experiences deposition. The rigid and mobile boundary models, therefore, have water surface elevation differences of -0.8' and 2.1' at STA 16085 and at STA 13795, respectively.

At STA 8535, this section has a more constricted flow width than the next upstream section at STA 9335 (325' versus 625'). This increases the local energy slope and velocity to nearly 2% and 11 fps, respectively. The mobile model responds with significant scour at STA 8535. The bed at STA 9335 remains stable. The slope, thus, increases between the two sections. This further causes an increase in the local velocity at STA 9335. The increase in velocity finally causes a decrease in the flow depth at STA 9335. In essence, potential energy (depth) converts to kinetic energy (velocity). The water surface elevation at STA

9335 drops about 1'.

At STA 7905, the section widens. This results in a decrease in the local energy slope and velocity. The scoured material from STA 8535 partially deposits at STA 7905. The increased bed elevation and flatter energy slope between STA 7905 (deposition) and STA 8535 (scour) causes a rise in the water surface elevation of 3.2' and 0.4', respectively. In this case, kinetic energy (velocity) converts to potential energy (depth).

At STA 7145, the scoured material from STA 8535 continues to deposit. The initial bed slope between STA 7145 and STA 7905 is less than 0.4%. With deposition, the bed slope between these two stations further decreases. Overall, the increased bed elevation and decreasing energy slope cause an increase in the water surface elevation of 1.8' at STA 7145.

The summary above demonstrates the inter-relationships between section geometry, hydraulic traits, and scour and deposition. These relationships clearly cause significant differences between water surface elevations for mobile and fixed boundary models. The summary represents only a simplified version of these processes. For example, STA 8535 eventually experiences deposition near the end of the flood hydrograph. The flatter energy slopes in this reach eventually causes deposition as the flood peak recedes. After scouring about 0.4' near the flood peak, the final thalweg elevation is about 0.7' higher than the flood peak value. This verifies the dynamic changes that mobile beds will experience as the section geometry, hydraulic traits, and sediment transport properties change over time.

3.2.7 Scenario 3.

Scenario 3 is Scenario 2 with a bridge at STA 3670 (see Figure 3.2). Except for the bridge, all assumptions for Scenario 2 apply to Scenario 3.

Figures 3.5, 3.6, 3.7, and 3.8 present the stream bed and water surface profiles for a bridge at STA 3670. These profiles represent the results of the 100-year flood event (10,400 cfs). The models used three different bridge lengths: 200', 250', and 315'.

Figure 3.9 presents a cross-section for the 200' bridge alternative. The selected cross-section lies at the bridge site (STA 3670). The section shows the change in the stream bed (SB) at the beginning (0 hours), peak (13 hours), and end of the flood hydrograph (34 hours). The figure also shows the water surface elevations at the flood peak for the rigid (WSR) and the mobile (WSM) models.

For the bridge analysis, the case study assumes that each bridge has spill-through abutments with two (horizontal) to one (vertical) side slopes. Each bridge also has a single 5' wide bridge pier with a rounded nose. Each bridge furthermore has well aligned and symmetrical abutments with the approaching flood waters. Figure 3-10 presents a typical bridge layout.

The bridge waterways analysis uses Figure 2.9 to compute a backwater loss coefficient. Because of the good alignment with the approaching flow, the analysis ignores losses related to skew and eccentricity. Although the analysis includes energy losses related to the bridge pier, the constricted opening represents most of the losses occurring at the bridge. At STA 3670, the model uses loss coefficients, K^*, of 0.3, 0.5, and 0.7 for the 315', 250', and 200' bridges, respectively.

BRI-STARS uses equation 2-17 and the above loss coefficients to compute the bridge backwater. The analysis applies equation 2-17 at STA 3670. The resultant backwater occurs at STA 4035.

Table 3.5 presents a comparison of the rigid and mobile boundary water surface elevations for each bridge alterative. The analysis included only BRI-STARS models for the rigid and mobile condition. The analysis did not include any HEC-2 bridge models.

The following summarizes the results of the analysis for the different bridge lengths. The mobile bed model produces measurably different water surface elevations compared to the fixed bed model. The differences become more apparent as the bridge length shortens. Using a 250' bridge (Figure 3.7), at STA 4035 the 100-year water surface elevation is about 1 foot less for the mobile situation compared to the fixed or rigid bed condition. For a 200' long bridge, the mobile model produces about 1.4' less backwater at STA 4035 than the fixed bed model. Figure 3.8 presents the bed and water surface profiles for the 200' bridge.

As the bridge shortens, the bridge section (STA 3670) experiences increased scour. The bridge section for the mobile model has a greater flow area than the non-scoured section for the fixed model (Figure 3.9). The mobile model, thus, has a lower velocity. The lower velocity generates smaller hydraulic losses through the bridge area. These local losses include the bridge losses, expansion/contraction losses, and slope friction losses. The reduction in these hydraulic or energy losses reduces the computed backwater depth at STA 4035.

The mobile bed model may allow an engineer to justify a shorter bridge. Using the fixed model, the 250' bridge causes about 2' of backwater (100-year) at STA 4035 compared to the no bridge situation (natural condition). This amount of backwater would violate many flood plain regulations (i.e., FEMA, FHWA) (AASHTO, 1999). The designing engineer would probably select a much longer bridge.

Using the mobile model, the 250' bridge produces a backwater increase of 1'. In many instances this would satisfy flood plain regulations. A 250' bridge at this site would cost about $ 750,000 to construct. The fixed bed model would require a much longer bridge to meet the typical backwater regulations (i.e., 300'). This could result in nearly a one-third increase in bridge construction costs (about $ 1,000,000 for a 300' bridge). Actual selection of the optimum bridge length would depend, however, on an assessment of the complete life-cycle costs.

The analysis shows measurable differences in the depositional pattern for STA 3120. For the 200' bridge, the stream bed cross-section at the end of the hydrograph is similar to that at the beginning of the hydrograph. For a 315' bridge, the stream cross-section experiences significant aggradation over the duration of the hydrograph (1' to 2'). The mobile model may, thus, show possible changes to local environments due to manmade structures (i.e., downstream destruction/construction of spawning beds).

The literature contains examples of channel behavior similar to those described above (i.e., expansion of the bridge section during large flood events) (Bradley, 1978; Linsley, Kohler, and Paulhus, 1982). Unfortunately, the typical engineer has had difficulty quantifying these processes into useable design information. BRI-STARS, however, produces quantified results that may have practical engineering and environmental value. These values include structure selection processes and their related impacts to the local environment.

3.2.8 Scenario 4.

This situation is the same as Scenario 3. except the bridge lies at STA 3120. The bridge layout at STA 3120 is also the same as the layout for STA 3670 (symmetry, abutment types, single pier). The bridge lengths do, however, differ from those at STA 3670. The rigid and mobile models used 480', 510', and 540' for the bridge lengths at STA 3120.

The bridge waterways analysis is also the same for STA 3120 as that for STA 3670. The loss coefficients, K^*, are 0.6, 0.75, and 0.9, for the bridge lengths of 540', 510', and 480', respectively. As with STA 3670, most of the bridge losses derive from constricting the natural stream channel and flood plains.

Table 3.6 presents a comparison of the rigid and mobile boundary water surface elevations for each bridge alternative. The analysis only includes BRI-STARS models for the rigid and mobile condition. The analysis does not include any HEC-2 bridge models.

The following summarizes the results of the analysis for the different bridge lengths. For the fixed bed model, the velocity head increases as the bridge length decreases at STA 3120. This results in backwater values of about 1' and 1.8' at STA 3670 for the 540' and 480' bridges, respectively.

The bridge at STA 3120 lies in a wide area. This section has a main channel width of about 700'. The upstream section at STA 3670 has a much narrower channel width (350'). For the mobile model, deposition occurs at STA 3120. This reduces the energy slope between STA 3120 and STA 3670. The reduced energy slope reduces energy losses due to friction. It also reduces the velocity head at STA 3120. This further reduces the energy losses due to the bridge constriction (see Eq. 2-17). For the 540' bridge, the backwater is only 0.2' at STA 3670.

The 480' bridge produces less deposition at STA 3120. This produces a slightly greater energy slope and velocity head at STA 3670. This results in an increasing backwater depth with decreasing bridge length. Although the backwater at STA 3670 is only 0.6', it is significantly greater than the backwater values generated for bridges of comparable length (i.e., 510' and 540').

In Scenario 3, the approaching channel section (STA 4035) has a natural width comparable to the natural width at the bridge location (STA 3670). In that case, the bridge length dominates the hydraulic and sedimentation processes at STA 3670. For example, the shorter bridge length increases the channel scour. This causes a smaller backwater elevation for the mobile model compared to the rigid model.

For Scenario 4, the above illustrates the influence of the natural stream morphology on bridge waterways. In this case, the model must use a much shorter bridge length before significant backwater occurs with the mobile condition. The morphology changes from a naturally narrower section (STA 3670) to a naturally wider section (STA 3120) that dominates the hydraulic and sedimentation processes at the bridge location. For longer lengths, the bridge section either aggrades or experiences no scour. This leads to a reduced energy slope and a lower velocity head through the bridge opening. The bridge losses and related backwater are, thus, much less for the mobile model.

Figure 3.11 shows the bed and water surface profiles for the 480' bridge. Figure 3.12 presents the water surface and channel cross-section for the 480' bridge section at STA 3120.

3.2.9 Scenario 5.

This situation is the same as Scenario 3 except the bridge is at STA 5605. The layout at STA 5605 is the same as the layout for STA 3670. The bridge lengths do differ. The rigid and mobile models used 288', 420', and 675' for the bridge lengths at STA 5605.

The bridge waterways analysis is also the same for STA 5605 as that for STA 3670. The loss coefficients, K^*, are 1.2, 0.6, and 0.2 for the 288', 420', and 675' bridge lengths, respectively. Most of the bridge losses derive from constricting the natural stream channel and flood plains.

Table 3.7 presents a comparison of the rigid and mobile boundary water surface elevations for each bridge alternative. The analysis only includes BRI-STARS models for the rigid and mobile condition. The analysis does not include any HEC-2 bridge models.

The following summarizes the results of the analysis for the different bridge lengths. Similar to Scenario 4, the bridge at STA 5605 lies in a wide area. This section has a main channel width of about 900'. The upstream section at STA 6165 has a much narrower channel width (550'). For the mobile model, deposition occurs at STA 5605 similarly to Scenario 4. Deposition also occurs, however, at STA 6165. With no bridge, this deposition provides a 100-year water surface elevation 0.30' higher than for the fixed boundary condition at STA 6165.

The 420' and 675' bridges also experience deposition at STA 5605 and STA 6165. With these bridge lengths, the mobile model produces a water surface elevation about 0.4' higher than the fixed model at STA 6165.

The 288' bridge finally constricts the natural section enough to cause some scour at the bridge site. This results in a lower water surface elevation for the mobile model compared to the fixed model at STA 6165. Figures 3.13 and 3.14 show profiles and the bridge section for the 288' alternative. Like Scenario 4, the natural stream morphology dominates the backwater conditions at the bridge site. Unlike Scenario 4, the complete river reach between the bridge site and the next upstream section lies in a deposition zone. This causes a higher water surface elevation at the upstream backwater location for the mobile model. In this case, the model must use a much shorter bridge length before the bridge begins to dominate the natural stream morphology (i.e., scour occurs at the bridge instead of deposition).

3.2.10 Summary of Nisqually Findings

The above scenarios show that mobile models may produce significantly different water surface profiles than fixed or rigid boundary models. These differences could affect river engineering designs in natural stream systems. Bridges in particular may require longer or possibly shorter lengths for such design constraints as economic costs or regulatory requirements (i.e., limits in backwater increases) (AASHTO, 1999). For mobile models, the direction of water surface changes are not easily predictable ahead of time but depend upon such factors as the natural morphology, manmade influences (bridges, etc.), hydrology, and systematic hydraulic/sediment transport characteristics.

Table 3.16 presents the summary backwater results for each Nisqually bridge site and length. h_{1M}* represents the backwater value for the mobile condition. h_{1R}* represents the backwater value for the rigid condition. h_{1R}* is the same as h_1* defined in Figure 2.8. h_{1M}*/h_{1R}* represents the ratio between the mobile and rigid boundary backwater values.

The above results also support the use of mobile models for many river engineering applications. They clearly provide more insight on the interaction of sediment and hydraulic processes than rigid river models. Unfortunately, mobile models require much more hydrologic and sediment data than rigid models. They may also require more assumptions and more analytical engineering skills.

3.3 Skagit River

This study focuses on the Skagit River Bridge near Newhalem, Washington. Using various bridge lengths, the Skagit study compares the bridge backwater for the fixed boundary condition to the mobile boundary condition. The method of analysis is quite similar to that presented in the Nisqually study.

3.3.1 Study Location, Hydrology, and Morphology

Starting about 3 miles upstream, a series of dams and reservoirs regulates most of the flow to the Skagit River bridge. Before the dams, this site experienced an estimated historic peak of about 115,000 cfs in 1815. Since 1924 (the inception of the dams), the maximum flood of record is 45,000 cfs (1932). From 1908 to 1924, the site experienced at least three floods exceeding 45,000 cfs. This data derives from USGS gaging station # 12178000. The gaging station lies almost one mile upstream of the bridge site (Figure 3.15).

The USACE has developed a hydrograph for the 100-year flood (Figure 3.16). They have included the influence of dams in the hydrograph. The bridge has an estimated 100-year flood peak of about 73460 cfs. For the mobile boundary portion, the study uses a flood duration of about 40 hours.

The Skagit bridge site has a cobble bed with boulder deposits (d_{50} of 75 to 80 mm - Figure 3.17). It has a fairly straight channel with high flood plains. The flood plains consist of large evergreens. Using Rosgen's (1996) classification system, the site is a B3 stream.

Currently, FHWA proposes a 350' bridge at this site. The proposed bridge would have 2 concrete piers, each having a width of about 3' to 5' (Figure 3.18). This particular bridge layout causes very little constriction of the main channel.

Overall, the Skagit sites meets most of the research constraints for performing a comparison between a mobile and a fixed boundary water surface profile (see Nisqually study for constraints).

3.3.2 Model Approach

The modeling approach is quite similar to that presented in the Nisqually study. The following presents some of the input factors.

Given the upstream dam, the mobile boundary model assumes no incoming sediment upstream. To insure a near equilibrium condition at the bridge site, the model uses extrapolated FHWA topographic data for about 1 mile upstream and ½ mile downstream of the bridge site (stations 0, 197, 517 (bridge), 869, and 1083, represent actual field surveyed cross sections).

The inclusion of the extra cross-sections insures that any excessive scour occurs sufficiently upstream of the bridge. The estimated 100-year flood of 73460 cfs is nearly double that of any recorded flood peak since the inception of the upstream dams. Thus, any excessive scour should occur immediately downstream from the dams. As for the additional downstream cross-sections, they act to prevent any artificial influences at the bridge site due to unadjusted downstream boundary conditions (i.e., lack of transmissive boundary).

The mobile model uses a time step of 0.00833 days (12 minutes), 200 time steps, an active layer thickness of about 180 mm, and Yang's (1984) method for estimating sediment loads. The stream cross-sections generally have a spacing of no more than 500'. Based upon a series of trial runs, the study found that these conditions produce the most stable results for a wide range of bridge lengths (i.e., model does not exhibit excessive oscillations between scour and deposition).

Assuming no bridges, the study tests the mobile condition for various situations. For example, the model does not work properly for the Parker (1982, 1990) or Meyer-Peter and

Müller (1948) sediment transport relations (excessive oscillation). Using various combinations of active layer thicknesses, time steps and gradations (well graded to uniformly graded), these sediment transport methods could not complete all the scour and deposition calculations for the full length of the hydrograph. Since most of the stream bed material is smaller than 100 mm, the Yang method seemed an acceptable sediment transport method for the study.

Using Yang's method and again no bridges, the study analyzed several combinations of time steps (2.4 to 12 minutes) and active layer thicknesses (180 mm to 9000 mm). Overall, the water surface profiles differed very little from one situation to the next (less than 1% difference in maximum flow depths). Borrowing from the Nisqually analysis, the Skagit study selected the combination of 12 minutes as the time step and an active layer thickness equal to the largest gradation group (180 mm). The 200 time steps resulted from operational limits. However, this allows for the study to use most of the Skagit flood hydrograph (40-hour duration).

Assuming no bridges, the Skagit study compared the fixed boundary profiles for HEC-2 and BRI-STARS. The two models had maximum flow depths differences of less than 2% for each of the FHWA surveyed cross sections.

Given the findings above, the Skagit study then compared 7 alternative bridge layouts for the fixed and mobile condition. For both conditions, the study used only the BRI-STARS model.

3.3.3 Model Results

Tables 3.8 and 3.9 show the profile results for each of the 7 bridge alternatives. The 7 bridge alternatives include a 235', 250', 265', 285', 300', 315', and a no bridge condition. The tables compare the resulting profiles for both the fixed and mobile boundary conditions. Table 3.8 and 3.9 separate the results into the water surface (WSEL) and bed elevation profiles, respectively. The water surface profile data represents the 100-year flood peak at 15 hours. The bed elevation data compares the results at 0 hours (fixed bed condition) to the mobile condition at 15 hours.

As Table 3.8 shows, the mobile condition consistently produces a lower water surface profile upstream of the bridge (STA 517) as compared to the fixed or rigid condition. As Table 3.16 illustrates, this is true for all bridge lengths. Figures 3.19, 3.21, and 3.23 present, as examples, the differences in the profiles for the no bridge, 300,' and the 265' bridge situations, respectively. Figures 3.22, and 3.24 illustrate the scour that occurs for the 300' and 265' bridges, respectively.

Figures 3.19 and 3.20 show some minor deposition for the no bridge condition. The natural cross-section at the bridge site is slightly wider than the upstream cross-sections. This results in relatively lower velocities. Thus, some deposition occurs at the site.

According to the mobile model output, the deposition for the no bridge alternative creates a more uniform flow condition through out the study reach. This results in a lower, but more uniform upstream water surface profile. For the no bridge situation, the lower profile for the mobile model, however, does fall within an expected computation difference of less than 1% when compared to the rigid model. When the models include the shorter bridge lengths and, thus, smaller openings, the local deposition converts to locally caused, bridge scour. For the mobile model, this local scour causes lower upstream water surface profiles compared to the rigid models for all selected bridge lengths. For the shorter bridge lengths, the water surface differences exceed those expected from simple computational differences (see Section 2.6).

3.3.4 Summary of Skagit Findings

For comparison, the study computed backwater at STA 869. This is about 350' upstream of the proposed bridge site. Referring to Table 3.16, the Skagit study shows that the mobile model would produce about 50 to 60% of the fixed model backwater for the same bridge layout. Using backwater design criteria, the mobile model would allow for a shorter bridge length compared to the fixed boundary model.

The Nisqually study also showed that mobile models could reduce the bridge length when compared to the backwater results produced with a fixed model. In this sense, both studies, thus, produce comparable results.

3.4 Stony Creek #1

This study focuses on a Stony Creek bridge near Hamilton City, Ca. Using various bridge lengths, the Stony Creek study compares the bridge backwater for the fixed boundary condition to the mobile boundary condition. The method of analysis is quite similar to that presented in the Nisqually and Skagit River studies.

3.4.1 Study Location, Hydrology, and Morphology

In 1992, the California Department of Transportation (CDOT) completed a hydrologic study of Stony Creek (Chang, Swanson, and Kondolf, 1992; Swanson and Kondolf, 1991). The study began at Black Butte Dam and proceeded downstream to the creek's confluence with the Sacramento River (Figure 3.25). The study covered about 25 miles of river length.

CDOT used the study to evaluate the influence of in-stream gravel mining operations on bridges crossing Stony Creek. In particular, they focused on the degradation and local scour of bridge foundations. To perform the study, they hired consultants (Michael Swanson & Associates, Howard Chang of San Diego University) to evaluate the area. In the process, they collected information on the hydrology, hydraulics, and sediment transport properties of Stony Creek.

Based upon the CDOT study (Chang, Swanson, and Kondolf, 1992; Swanson and Kondolf, 1991), the Black Butte dam significantly reduced the flood peaks into the Stony Creek system. Completed in 1963, the dam has reduced the 50-year flood peak from 80,000 cfs to about 20,000 cfs. Stony Creek has a stream bed consisting primarily of very fine to coarse size gravels with some sands. Since their inception, the Black Butte dam and ongoing gravel operations have influenced the channel patterns (braided to sinuous) and bed profiles (degrading to stable) of Stony Creek. Some reaches of the creek, however, have changed little since the start of human activities. Using the Rosgen stream classification system, the study area encompasses stream types C4, D4, and F4.

With some simplifications, the Stony Creek system does have a few potential locations that meet the research constraints for comparing fixed and mobile backwater values at bridge sites. In particular, the Highway 45 bridge near Hamilton City represents a fairly straight and stable reach within Stony Creek. There are also other potential sites for future case studies. This research project , thus, refers to the Highway 45 Bridge site study as "Stony Creek #1".

3.4.2 Model Approach

The modeling approach is quite similar to that presented in past studies. The model approach and results below present the author's own original model analysis for the selected study site. The following presents some of the input factors and assumptions.

The bridge lies at STA 17075. The study has a beginning upstream station of 27600 and an ending downstream station of 11600. Assuming no incoming sediment, the mobile model reaches a sediment equilibrium at the bridge site (incoming sediment equals outgoing sediment).

This equilibrium is due to the scoured material at the upstream end of the study area passing through the relatively uniform cross-sections at the middle and downstream reaches. The flow-generated sediment capacity of each middle to downstream cross-section (sediment demand) equals the incoming sediment load (supply). With no actual bridge at STA 17075, both the fixed and mobile model, thus, produce identical water surface profiles at the bridge site (zero bridge backwater) (see Figure 3.29). Again, this is due to the relative similarity in cross-section form through the bridge site. To accomplish this result, the Stony Creek #1 study uses the following additional assumptions.

The model uses a representative channel cross-section placed on a 0.1% slope. At STA 17075, Highway 45 crosses over a 620-foot long bridge. Based upon a HEC-RAS analysis, the energy slopes vary from 0.1% to 0.2%. The 620' bridge slightly constricts the natural channel and flood plain width of about 770'. To achieve a natural flow condition, the study model eliminates the 620' bridge section and repeats the 770' wide natural section throughout the study reach. The 0.1% slope derives from the morphological information contained in the CDOT report The Stony Creek #1 study, thus, starts with a uniform flow condition throughout the stream reach (see Figure 3.26).

The mobile model uses gravel gradations from the CDOT report. Figure 3.27 shows a d_{50} of 16 mm for Stony Creek #1. The overall gradation ranges from a very fine gravel to a very coarse gravel. Nearly 60% of the material, however, falls in the medium to coarse gravel size.

For Stony Creek #1, the study uses a modified hydrograph of the 1986 outflow hydrograph at Black Butte dam (see Figure 3.28). The BRI-STARS computer model limits the total number of time steps to 200 for an increment of 12 minutes. The study, thus, does not include the flatter portions of the outflow hydrograph.

The model uses the Yang method for estimating sediment loads. The CDOT report stated that the Yang method predicted morphological changes consistent with field collected stream channel survey. The mobile model also uses an active layer thickness of about 45 mm. This is consistent with past studies (active layer thickness equal to one times the geometric mean of the maximum size classification). For cross-section locations, the model uses a spacing of about 1000'. This is comparable to past studies.

Assuming no bridges, the Stony Creek #1 study compared the fixed boundary profiles for HEC-RAS and BRI-STARS. The HEC-RAS profiles used the HEC-2 conveyance approach. Using the representative natural cross-section on a repeated 0.1% slope, HEC-RAS and BRI-STARS had maximum flow depth differences of 1%.

Given the above findings, the Stony Creek #1 study compared 7 alternative bridge layouts for the fixed and mobile condition. For both conditions, the research used only the BRI-STARS model.

3.4.3 Model Results

Tables 3.10 and 3.11 show the profile results for each of the 7 bridge alternatives. The 7 bridge alternatives include a 175', 200', 225', 245', 290', 350', and a no bridge condition. The tables compare the resulting profiles for both the fixed and mobile boundary conditions. Tables 3.10 and 3.11 separate the results into the water surface (WSEL) and bed elevation profiles, respectively. The water surface profile data represents the 100-year flood peak at 23 hours. The bed elevation data compares the results at 0 hours (fixed bed condition) to the mobile condition at 23 hours.

As Table 3.10 shows, the mobile condition consistently produces a lower water surface profile upstream of the bridge (STA 17075) as compared to the fixed or rigid condition. As Table 3.16 illustrates, this is true for all bridge lengths. Figures 3.29, 3.31, and 3.33 present, as examples, the differences in the profiles for the no bridge, 290,' and the 175' bridge situations, respectively. Figures 3.30, 3.32, and 3.34, illustrate the scour that occurs for each respective bridge situation. The lower water surface profiles for the mobile models derive from this local bridge-related scour.

3.4.4 Summary of Stony Creek #1 Findings

For comparison, the study measured backwater at STA 17750. This is about 675' upstream of the proposed bridge site. Referring to Table 3.16, the Stony Creek #1 study shows that the mobile bed model would produce about 80 to 90% of the fixed model backwater for the same bridge layout . Table 3.16 also shows the mobile model would produce a smaller percentage of the fixed model backwater as the bridge length becomes shorter. This is due to an increase in local bridge scour relative to the smaller bridge opening.

Using typical backwater design criteria, the mobile model would probably allow for a slightly shorter bridge length compared to the fixed boundary model. The Nisqually and Skagit studies also showed that mobile models would allow for a shorter bridge length than a fixed model based upon backwater typical backwater design criteria(i.e., $h_1^* \leq$ one foot). In this sense, the completed studies produce comparable results.

3.5 Stony Creek #2

This study focuses on a Stony Creek bridge near Hamilton City, California. Using various bridge lengths, the Stony Creek study compares the bridge backwater for the fixed boundary condition to the mobile boundary condition. The method of analysis is quite similar to that presented in the Nisqually and Skagit River studies.

3.5.1 Study Location, Hydrology, and Morphology

Stony Creek #2 derives from the CDOT hydrologic study discussed in the Stony Creek #1study, Section 3.4 (Chang, Swanson, and Kondolf, 1992; Swanson and Kondolf, 1991). Stony Creek #2 also has the same stream hydrology and morphology as Stony Creek #1. The "P" bridge near Orland represents a fairly straight and stable reach within Stony Creek. Thus, it was selected as the location for Stony Creek #2 (Figure 3.35).

3.5.2 Model Approach

The modeling approach is quite similar to that presented in past studies. Similar to Stony Creek #1, the model approach and results represent the author's own original model analysis for the selected study site. The following presents some of the input factors and assumptions.

The bridge lies at STA 65400. The study has a beginning upstream station of 76100 and an ending downstream station of 59400. Assuming no incoming sediment, the mobile model reaches a sediment equilibrium at the bridge site (incoming sediment equals outgoing sediment).

This equilibrium is due to the scoured material at the upstream end of the study area passing through the relatively uniform cross-sections at the middle and downstream reaches. The flow-generated sediment capacity of each middle to downstream cross-section (sediment demand) equals the incoming sediment load (supply). With no actual bridge at STA 65400, both the fixed and mobile model, thus, produce identical water surface profiles throughout the relatively uniform bridge site (zero bridge backwater). To accomplish this result, the Stony Creek #2 study uses the following additional assumptions.

The models assume a representative channel cross-section placed on a 0.2% slope. STA 65400 has a natural channel and flood plain width of about 1200'. To achieve a natural flow condition, the study repeats the 1200' wide natural section throughout the study reach. The 0.2% slope derives from the morphological information contained in the CDOT report (Swanson and Kondolf, 1991). The Stony Creek #2 study, thus, starts with a uniform flow condition throughout the stream reach (Figures 3.36).

The mobile model uses gravel gradations from the CDOT report. Figure 3.37 shows a d_{50} of 8 mm for Stony Creek #2. The overall gradation ranges from a very fine gravel to a coarse gravel. Nearly 60% of the material, however, falls in the fine to medium gravel size.

For Stony Creek #2, the study uses a modified hydrograph of the 1986 outflow hydrograph at Black Butte Dam. It is the same modified hydrograph used for Stony Creek #1 (Figure 3.28). The computer model limits the total number of time steps to 200 for an increment of 0.00833 days (12 minutes). The study does not include the flat outflow hydrograph.

The model uses the Yang method for estimating sediment loads. The CDOT report stated that the Yang method predicted morphological changes consistent with field collected stream channel survey. The mobile model also uses an active layer thickness of about 22 mm. This is consistent with past studies (active layer thickness equal to one times the geometric mean of the maximum size classification). For cross-section locations, the model uses a spacing of about 1000'. This is comparable to past studies.

Assuming no bridges, the Stony Creek #2 study compared the fixed boundary profiles for HEC-RAS and BRI-STARS. The HEC-RAS profiles used the HEC-2 conveyance approach. Using the representative natural cross-section on a repeated 0.2% slope, HEC-RAS and BRI-STARS had maximum flow depth differences of 1%.

Given the above, the Stony #2 study compared 7 alternative bridge layouts for the fixed and mobile condition. For both conditions, the research used only the BRI-STARS model.

3.5.3 Model Results

Tables 3.12 and 3.13 show the profile results for each of the 7 bridge alternatives. The 7 bridge alternatives include a 185', 225', 245', 265', 345', 510', and a no bridge condition. The tables compare the resulting profiles for both the fixed and mobile boundary conditions. Tables 3.12 and 3.13 separate the results into the water surface (WSEL) and bed elevation profiles, respectively. The water surface profile data represents the 100-year flood peak at 23 hours. The bed elevation data compares the results at 0 hours (fixed bed condition) to the mobile condition at 23 hours.

As Table 3.12 shows, the mobile condition consistently produces a lower water surface profile upstream of the bridge (STA 65400) as compared to the fixed or rigid condition. As Table 3.16 illustrates, this is true for all bridge lengths. Figures 3.38, 3.40, and 3.42 present, as examples, in the profiles for the no bridge, 345', and the 245' bridge situations, respectively. Figures 3.39, 3.41, 3.43, illustrate the scour that occurs for each respective bridge situation. The lower water surface profiles for the mobile models occur because of this local bridge-related scour.

3.5.4 Summary of Stony Creek #2 Findings

For comparison, the study measured backwater at STA 66100. This is about 700' upstream of the proposed bridge site. Referring to Table 3.16, the Stony Creek #2 study shows that the mobile model would produce about 70 to 90% of the fixed model backwater for the same bridge layout. Similar to Stony Creek #1, Table 3.16 shows the mobile model would produce a smaller percentage of the fixed model backwater as the bridge length becomes shorter. This is due to an increase in local bridge scour relative to the smaller bridge opening.

Using typical backwater design criteria, the mobile model would probably allow for a shorter bridge length compared to the fixed boundary model. The Nisqually, Skagit, and Stony Creek #1 studies also showed that mobile models could reduce the bridge length when compared to the backwater results produced with a fixed model. In this sense, the completed studies, produce comparable results.

3.6 Gibbon River Bridge

This study focuses on a Gibbon River bridge near Madison Junction, Yellowstone National Park, WY. Using various bridge lengths, the Gibbon River study compares the bridge backwater for the fixed boundary condition to the mobile boundary condition. The method of analysis is quite similar to that presented in the Nisqually, Skagit River, and Stony Creek studies.

3.6.1 Study Location, Hydrology, and Morphology

At the proposed bridge site (Figure 3.44), the Gibbon River flows in a westerly direction through woody, mountainous terrain . The proposed bridge site lies in a relatively straight section of the river corridor (Figure 3.45).

Figure 3.45 shows a typical channel and flood plain section for the study site. The main channel of the Gibbon consists of a coarse gravel stream bed with some cobbles (Figure 3.46). Based upon a comparison of original bridge cross-sections taken in the 1930's to current stream cross-sections, the Gibbon has a fairly stable stream bed system (little aggradation or degradation). Similarly, the bushy, grassed flood plains appear fairly stable (well-vegetated with little or no braiding). The Gibbon has an approximate Rosgen stream classification of C4 to E4.

At the proposed bridge site, the Gibbon River has a drainage area of about 125 square miles. There are no manmade influences (i.e., dams, irrigation systems) up-stream of the proposed bridge site. Using a nearby USGS gaging station (# 06037000) and USGS regression equations for Montana (Omang, 1992) and Wyoming (Lowham, 1988), Figure 3.47 presents the 100-year flood hydrograph developed for the study. The attached hydrograph shows an estimated 100-year flood peak of about 2500 cubic feet per second.

Overall, the Gibbon River site meets the research constraints for comparing fixed and mobile backwater values at bridge sites.

3.6.2 Model Approach

The modeling approach is quite similar to that presented in past studies. The following presents some of the input factors and assumptions. The bridge lies at STA 9000. The study has a beginning upstream station of 20000 and an ending downstream station of 4000. Assuming no incoming sediment, the mobile model reaches a sediment equilibrium at the bridge site (incoming sediment equals outgoing sediment) for similar reasons discussed in Stony Creek #1 and Stony Creek #2 under Sections 3.4.2 and 3.5.2, respectively. Thus, with no actual bridge at STA 9000, both the fixed and mobile model produce identical water surface profiles at the bridge site (zero bridge backwater). To accomplish this result, the Gibbon River study uses the following additional assumptions:

The model assumes a representative channel cross-section placed on a 0.5% slope. STA 9000 has a natural channel and flood plain width of about 200'. To achieve a natural flow condition, the study repeats the 200' wide natural section throughout the study reach. The 0.5% slope is derived from typical stream cross-sections taken at the site and river slope computations from USGS quadrangle maps. Thus, the Gibbon River study starts with a uniform flow condition throughout the stream reach (Figure 3.45).

The mobile model uses only gravel and cobble gradations which come from on-site pebble counts. The stream bed does have small amounts of sand (probably less than 10% by volume) but this material is disregarded in the model. Figure 3.46 shows a d_{50} of 32 mm for the Gibbon River site. The overall gradation ranges from a fine gravel to a cobble size material. Nearly 75% of the material, however, falls in the coarse to very coarse gravel size.

Figure 3.47 shows a 40-hour duration for the 100-year flood hydrograph. Similarly to previous studies, the computer model limits the total number of time steps to 200 for an increment of 12 minutes. The study, thus, has a limited range of flows (1600 to 2500 cubic feet per second).

The model uses the Yang (1984) method for estimating sediment loads. The mobile model also uses an active layer thickness of about 90 mm. This is consistent with past studies (active layer thickness equal to one times the geometric mean of the maximum size classification). For cross-section locations, the model uses a spacing of about 1000'. This is comparable to past studies.

Assuming no bridges, the study compared the fixed boundary profiles for HEC-RAS and BRI-STARS. The HEC-RAS profiles used the HEC-2 conveyance approach. Using the representative natural cross-section on a repeated 0.5% slope, HEC-RAS and BRI-STARS had maximum flow depth differences of 1%.

Given the above findings, the Gibbon River study compared 7 alternative bridge layouts for the fixed and mobile condition. For both conditions, the study used only the BRI-STARS model.

3.6.3 Model Results

Tables 3.14 and 3.15 show the profile results for each of the 7 bridge alternatives. The 7 bridge alternatives include a 80', 85', 90', 95', 125', 165', and a no bridge condition. The tables compare the resulting profiles for both the fixed and mobile boundary conditions. Tables 3.14 and 3.15 separate the results into the water surface (WSEL) and bed elevation profiles, respectively. The water surface profile data represents the 100-year flood peak at 23 hours. The bed elevation data compares the results at 0 hours (fixed bed condition) to the mobile condition at 23 hours.

As Table 3.14 shows, the mobile condition consistently produces a lower water surface profile upstream of the bridge (STA 65400) as compared to the fixed or rigid condition. As Table 3.16 illustrates, this is true for all bridge lengths. Figures 3.48, 3.50, and 3.52 present, as examples, the differences in the profiles for the no bridge, 95', and the 85' bridge situations, respectively. Figures 3.49, 3.51, 3.53, illustrate the scour that occurs for each respective bridge situation. The lower water surface profiles for the mobile models derive from this local bridge-related scour.

3.6.4 Summary of Gibbon River Findings

For comparison, the study measured backwater at STA 9250. This is about 250' upstream of the proposed bridge site. Referring to Table 3.16, the Gibbon study shows that the mobile model would produce about 60 to 70% of the fixed model backwater for the same bridge layout. Unlike Stony Creek #1 and Stony Creek #2, Table 3.16 does not show the mobile model producing an ever smaller percentage ($h_{1M}*/h_{1R}*$) of the fixed model backwater as the bridge length becomes shorter. This is due to a smaller available supply of sediment in the stream bed for local scour as the bridge opening becomes smaller. For example, as the bridge opening reduces in size, the stream bed width at the bridge also becomes smaller. Thus, the smaller bridge opening has a smaller supply of bed material available for scour.

Using typical backwater design criteria, the mobile model would probably allow for a shorter bridge length compared to the fixed boundary model. The Nisqually, Skagit, and

Stony Creek studies also showed that mobile models could reduce the bridge length when compared to the backwater results produced with a fixed model. In this sense, the completed studies produce comparable results.

3.7 Conclusions

Table 3.16 presents the backwater comparisons for each of the selected studies. For a $h_{1M}^*/h_{1R}^* < 1$, the effect of using a mobile boundary model at a bridge is to reduce the upstream water surface elevations. This table illustrates that the above case studies generally produced lower water surface elevations for the mobile condition as compared to the fixed or rigid boundary condition when constructing an element such as a bridge. The Nisqually case at STA 5605 does produce a couple of notable exceptions.

The 420' and 675' bridges at STA 5605 produced a higher backwater elevation for the mobile versus rigid condition. As previously discussed, this occurs due to the natural elevation of the stream bed from local sediment deposition. Decreasing the bridge to a length of 288' increases the velocity through the opening and causes local scour of the opening. Once the bridge length begins to dominate the local morphological influences, the mobile model produces a lower backwater value than the rigid model.

If the selected bridge length represents the dominant influence on the local hydraulic and morphological characteristics, the above case studies demonstrates the hypothesis that the mobile model will produce a lower bridge backwater compared to the rigid model. For example, you cannot always expect the fixed boundary water surface profile to be greater than the mobile boundary profile unless you have established that the natural morphology is not a controlling or dominating influence at the bridge site.

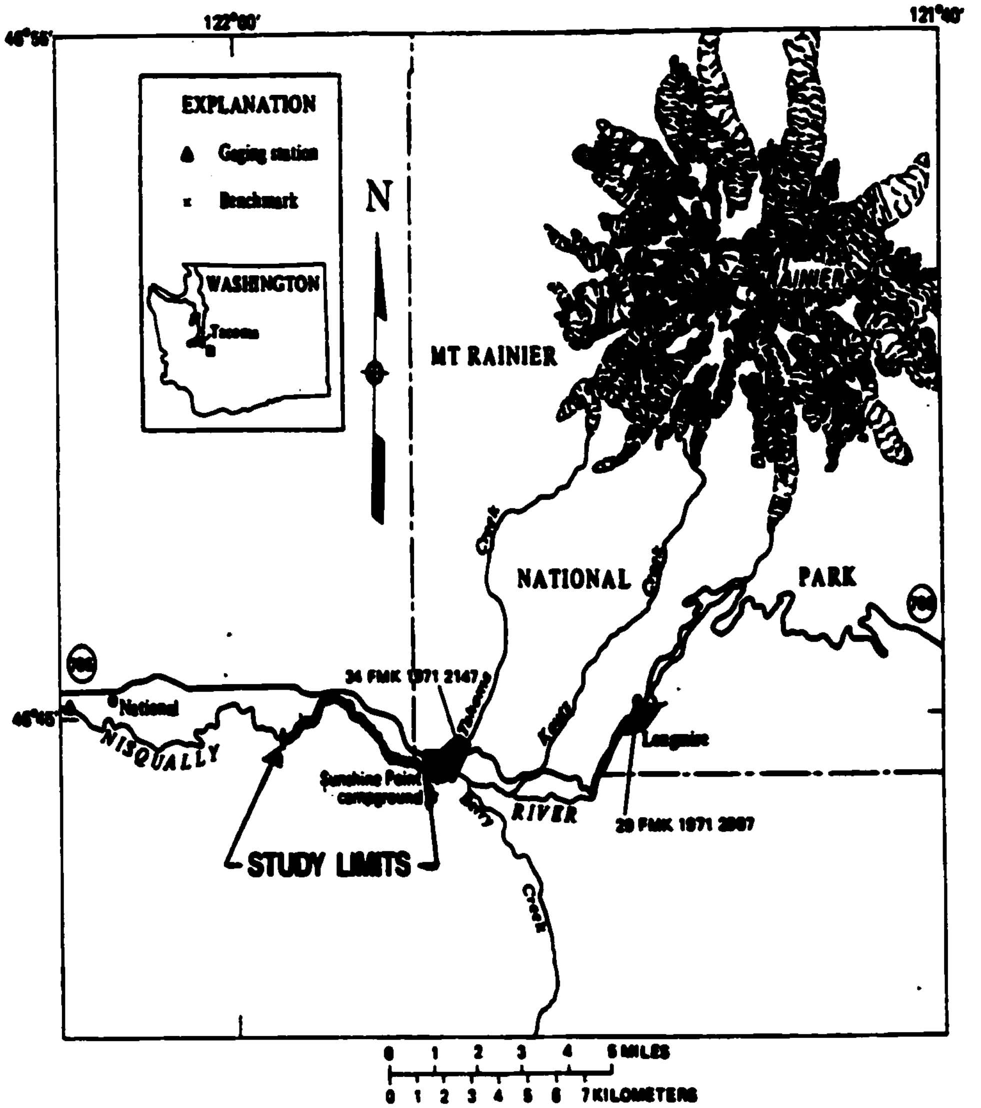

Figure 3.1 Nisqually River basin (Nelson, 1987)

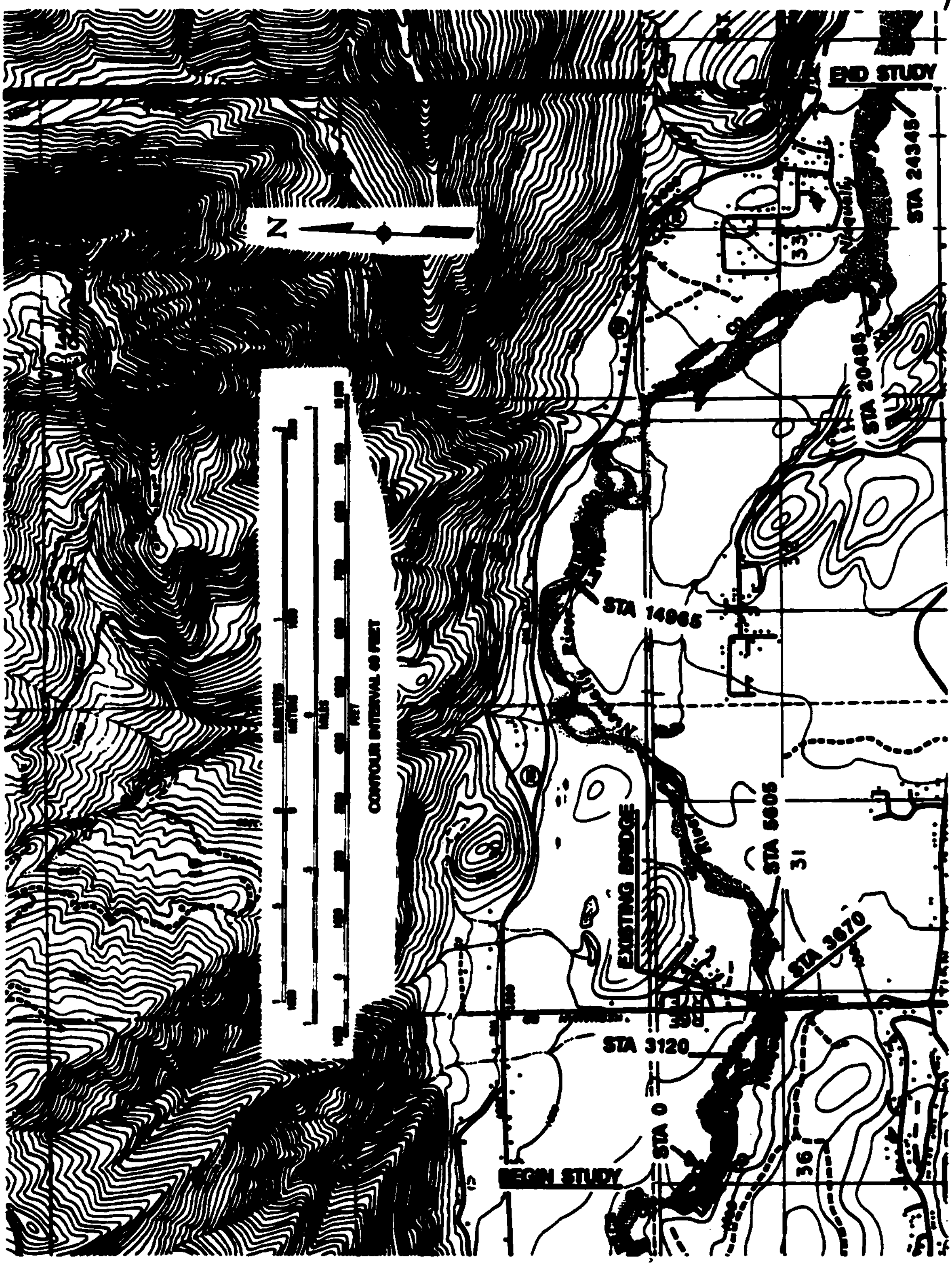

Figure 3.2 Nisqually study site

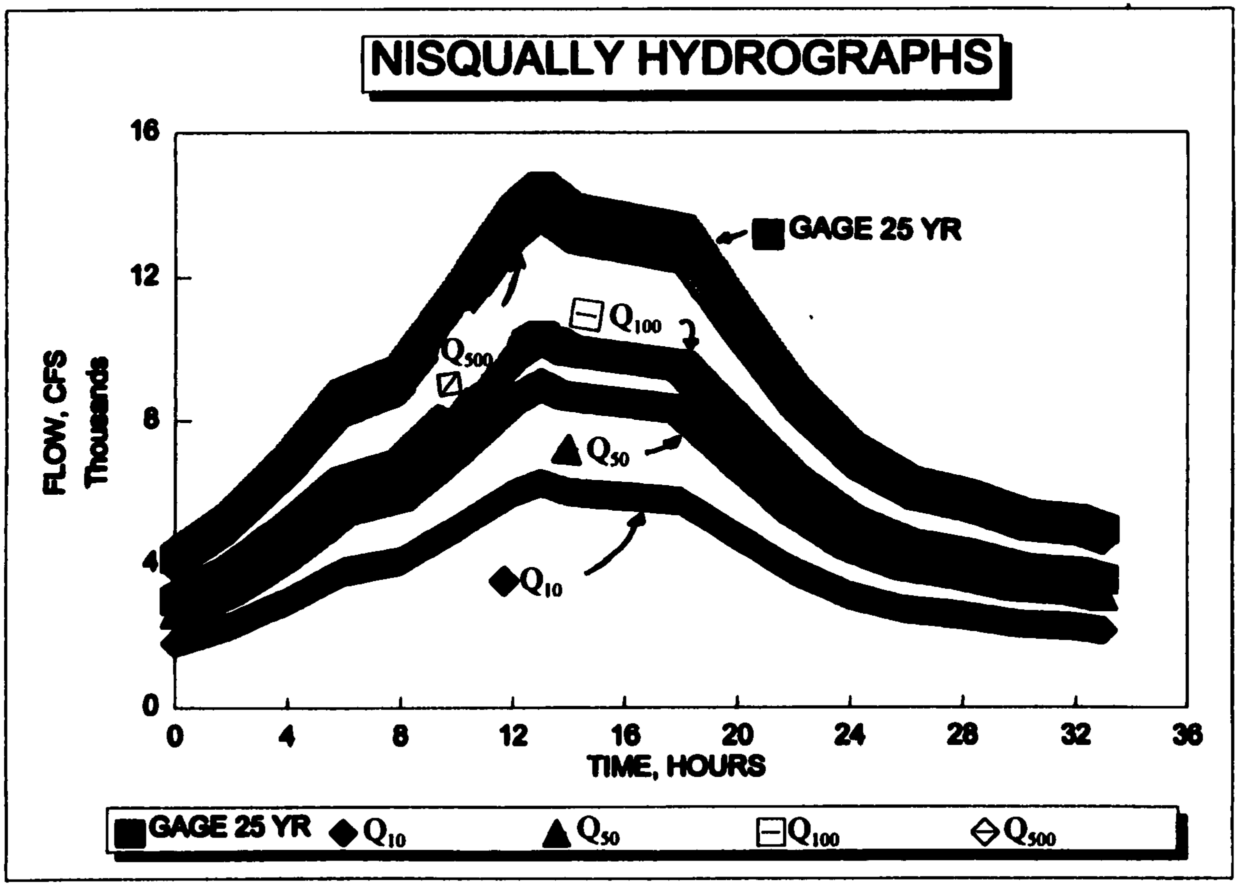

Figure 3.3 Nisqually hydrographs

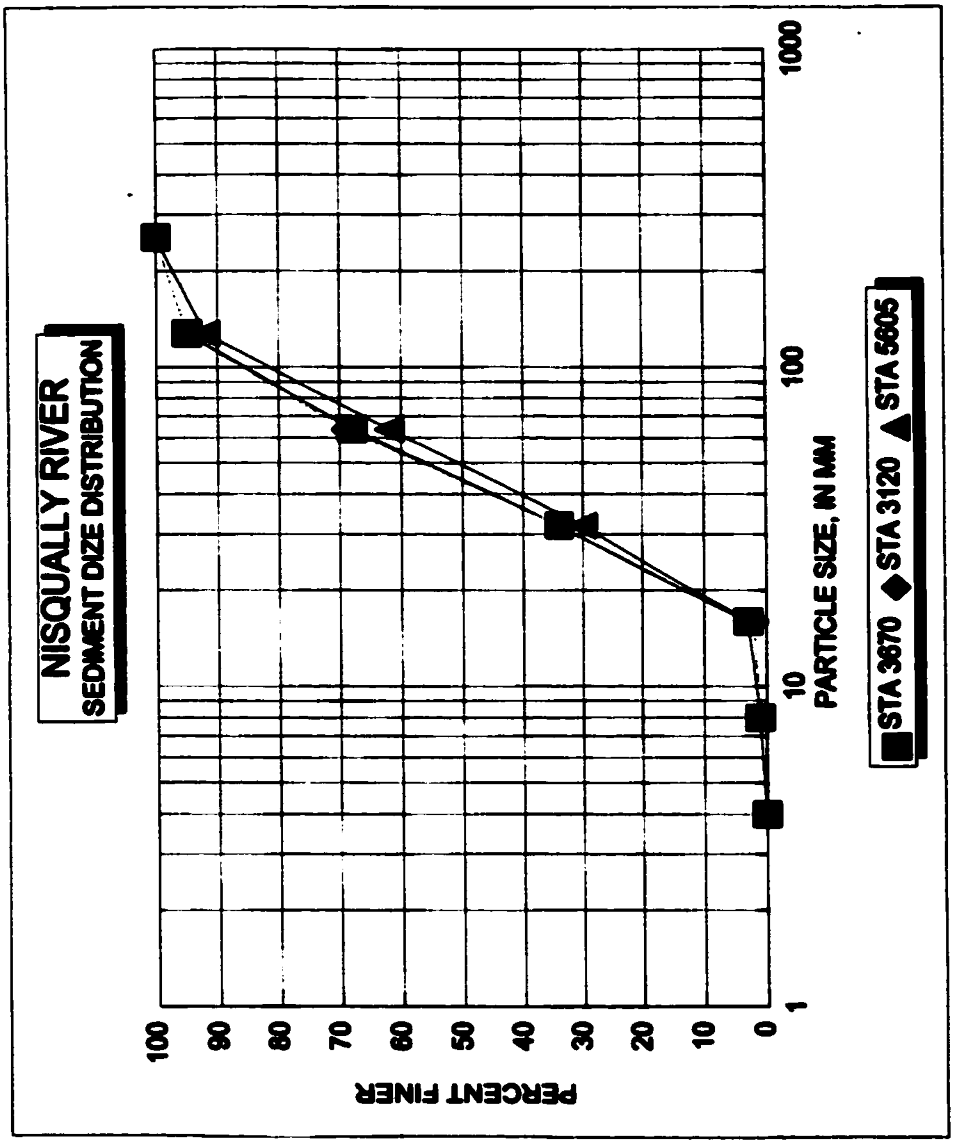

Figure 3.4 Nisqually gradations

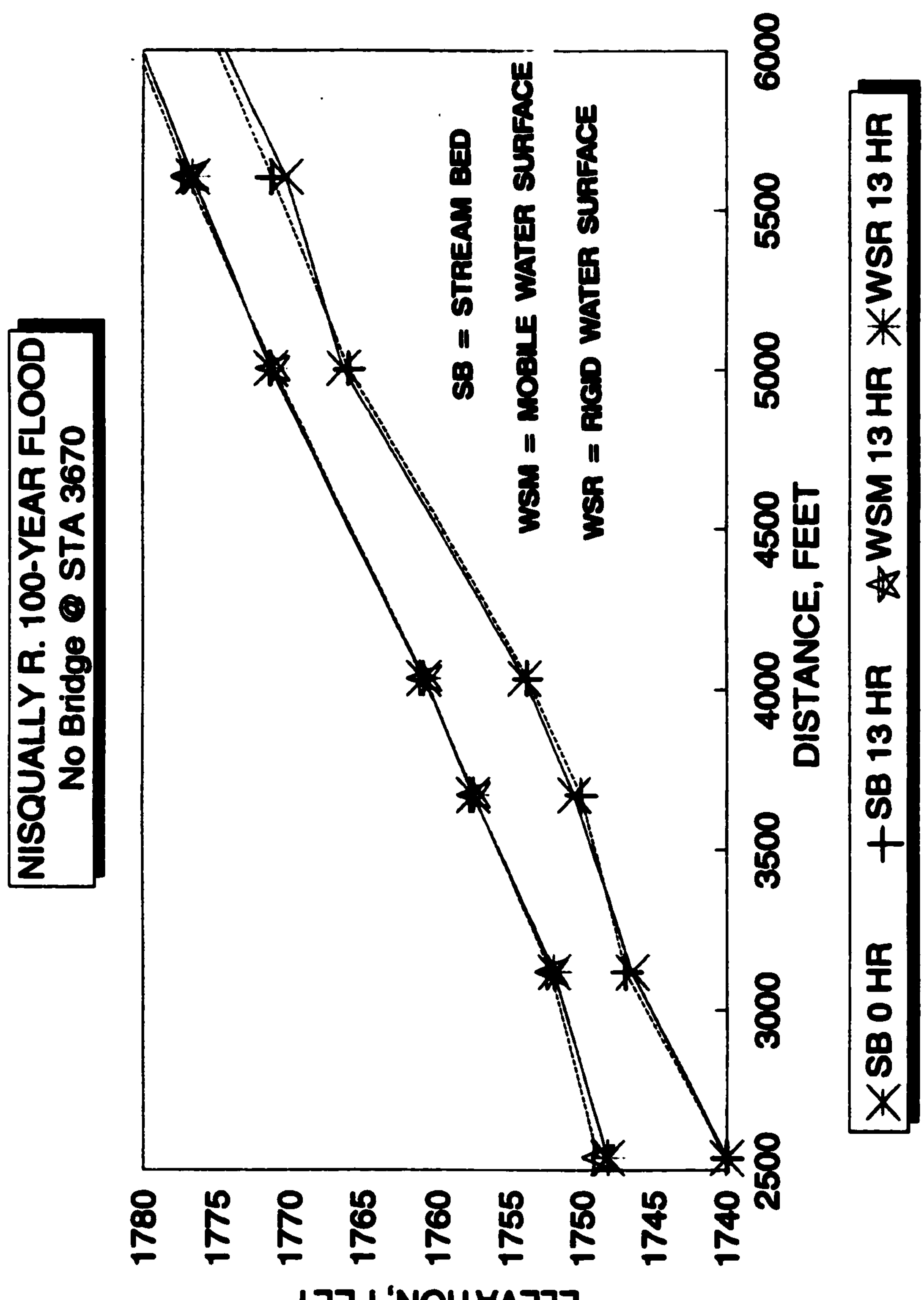

Figure 3.5 Nisqually profiles near STA 3670

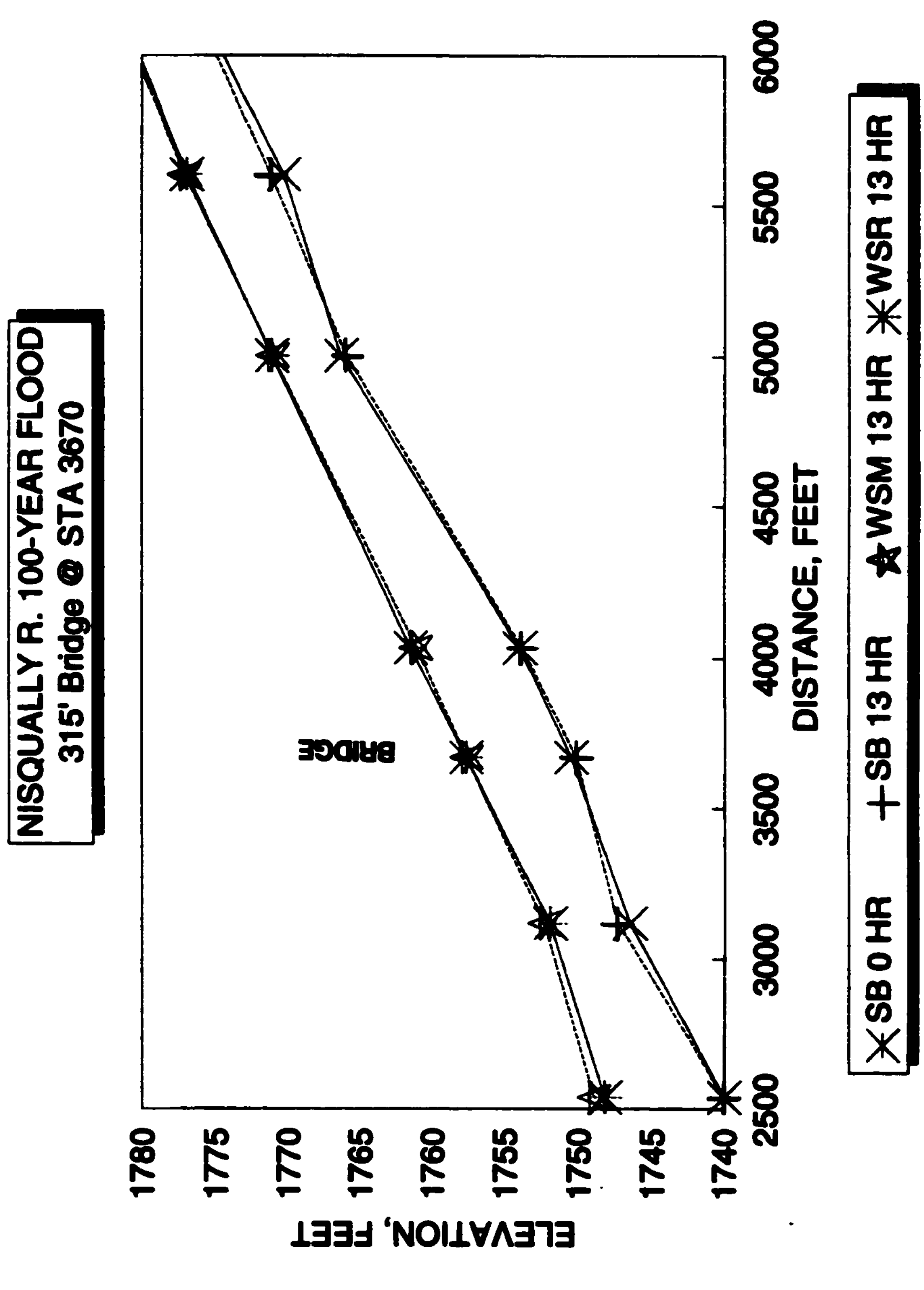

Figure 3.6 Nisqually profiles near STA 3670
315' bridge

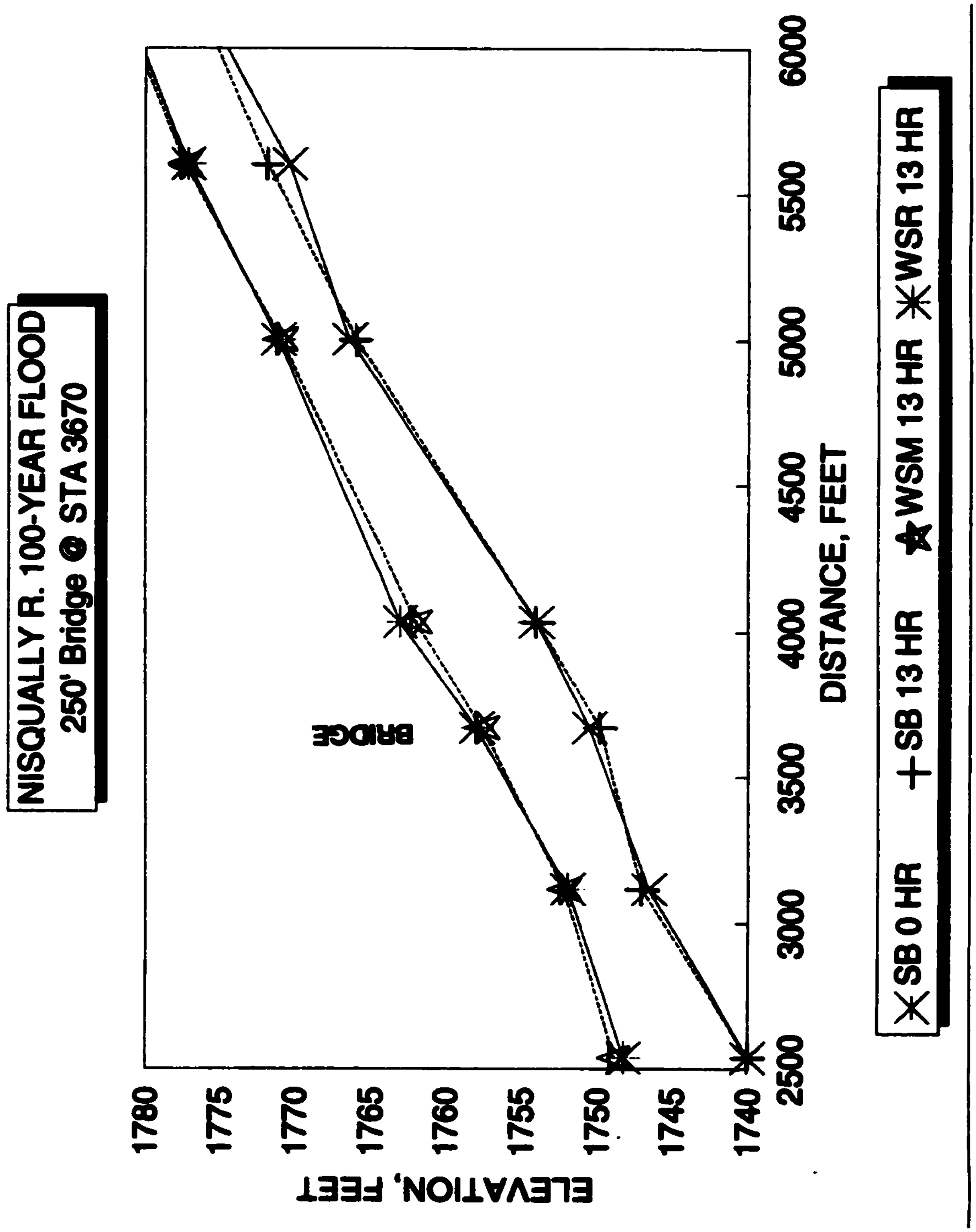

Figure 3.7 Nisqually profiles near STA 3670
250' bridge

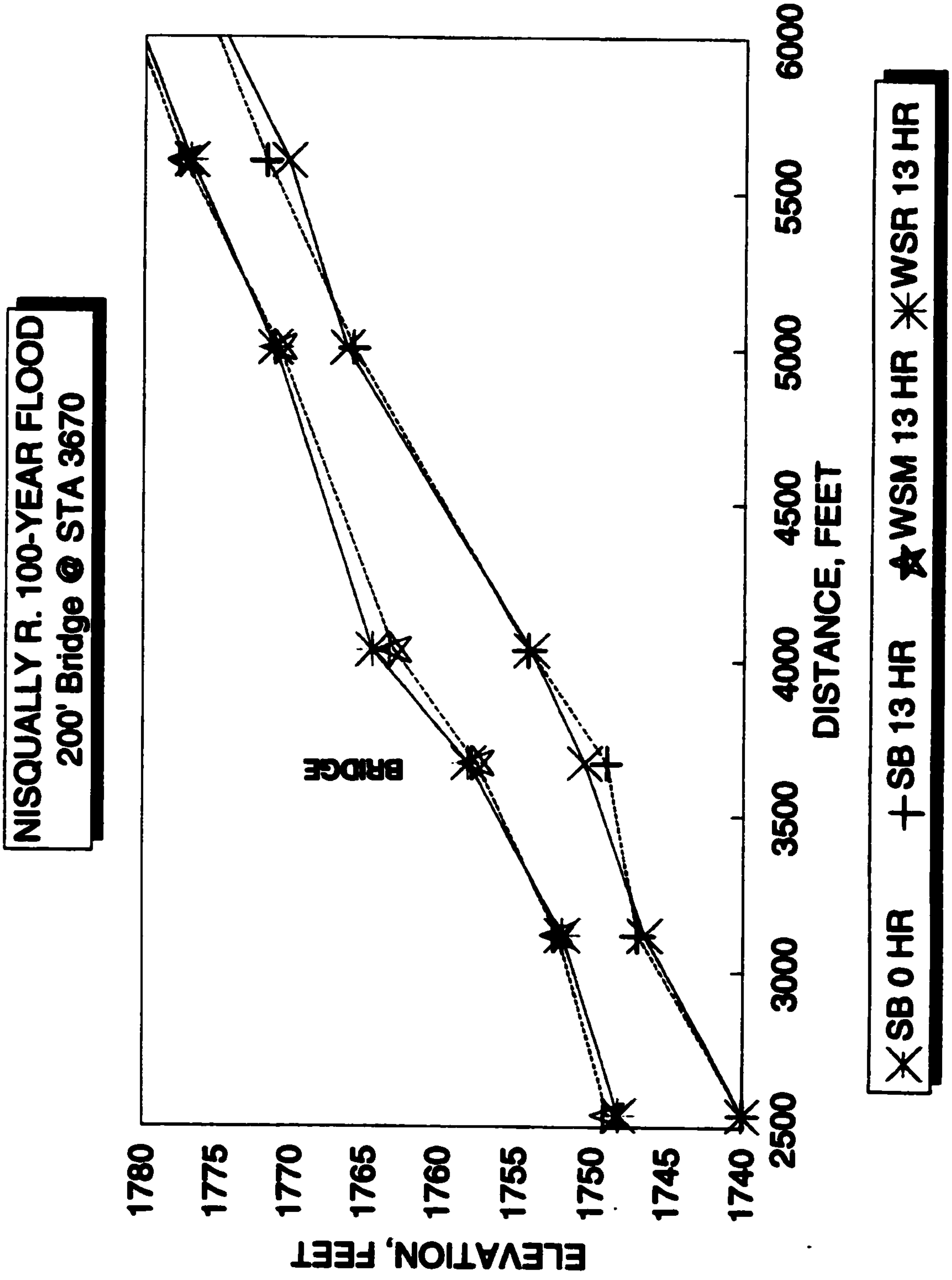

Figure 3.8 Nisqually profiles near STA 3670
200' bridge

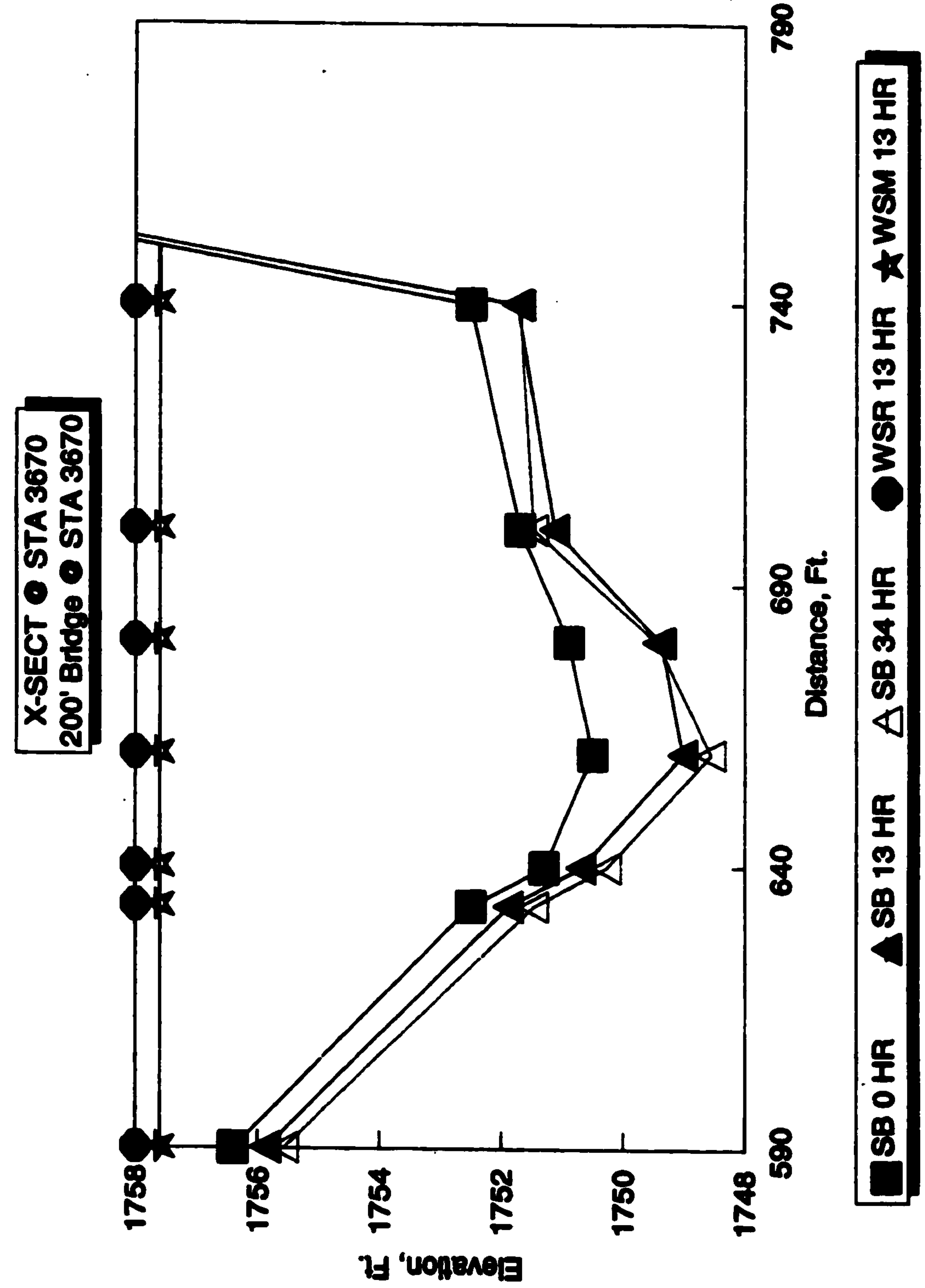

Figure 3.9 Nisqually cross-section at STA 3670
200' bridge

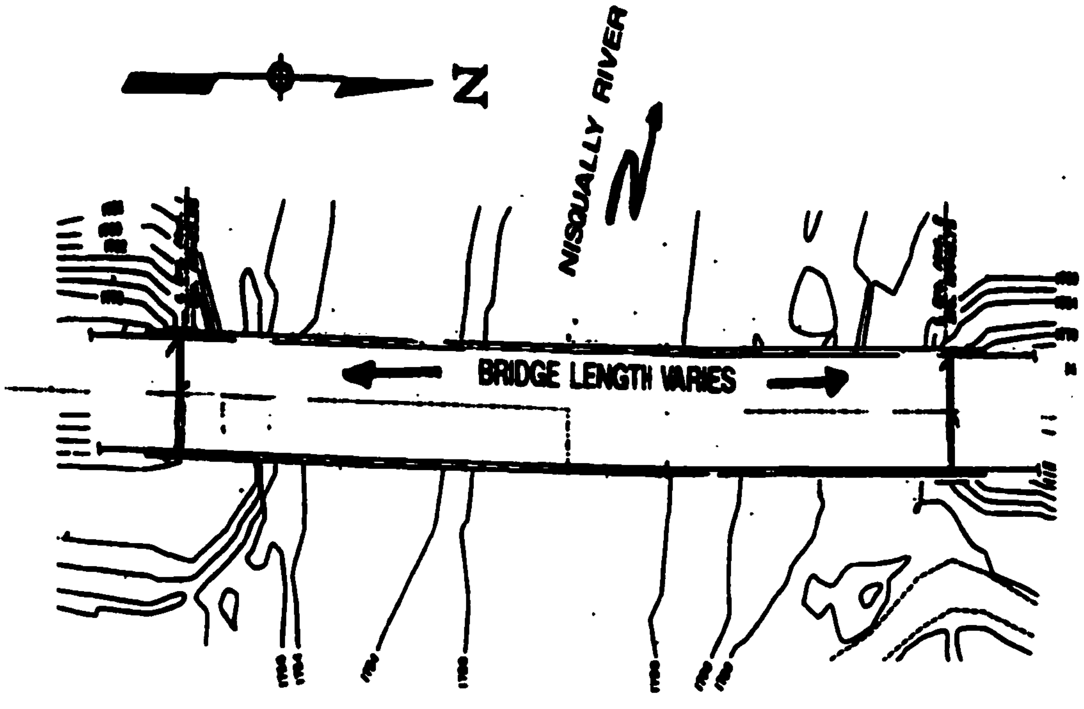

PLAN

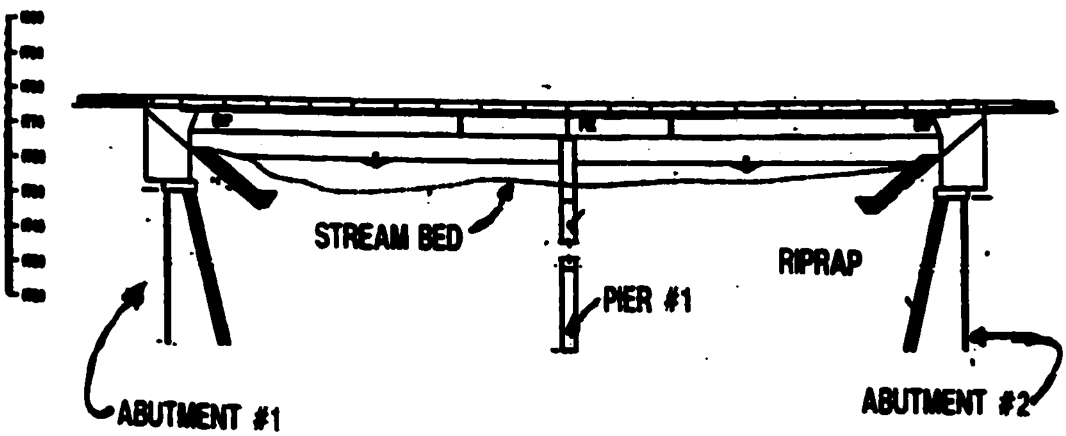

ELEVATION

Figure 3.10 Nisqually bridge layout

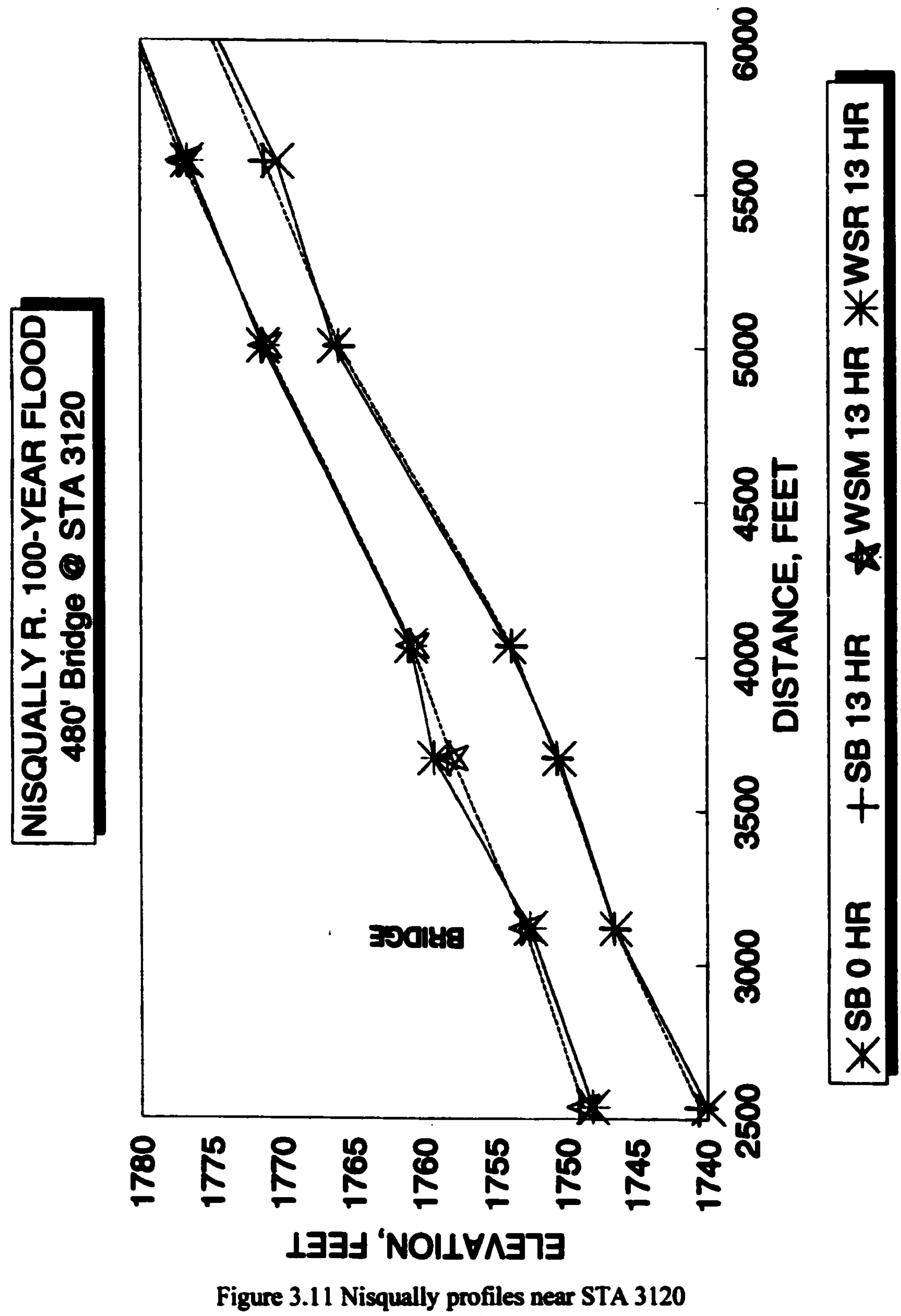

Figure 3.11 Nisqually profiles near STA 3120
480' bridge

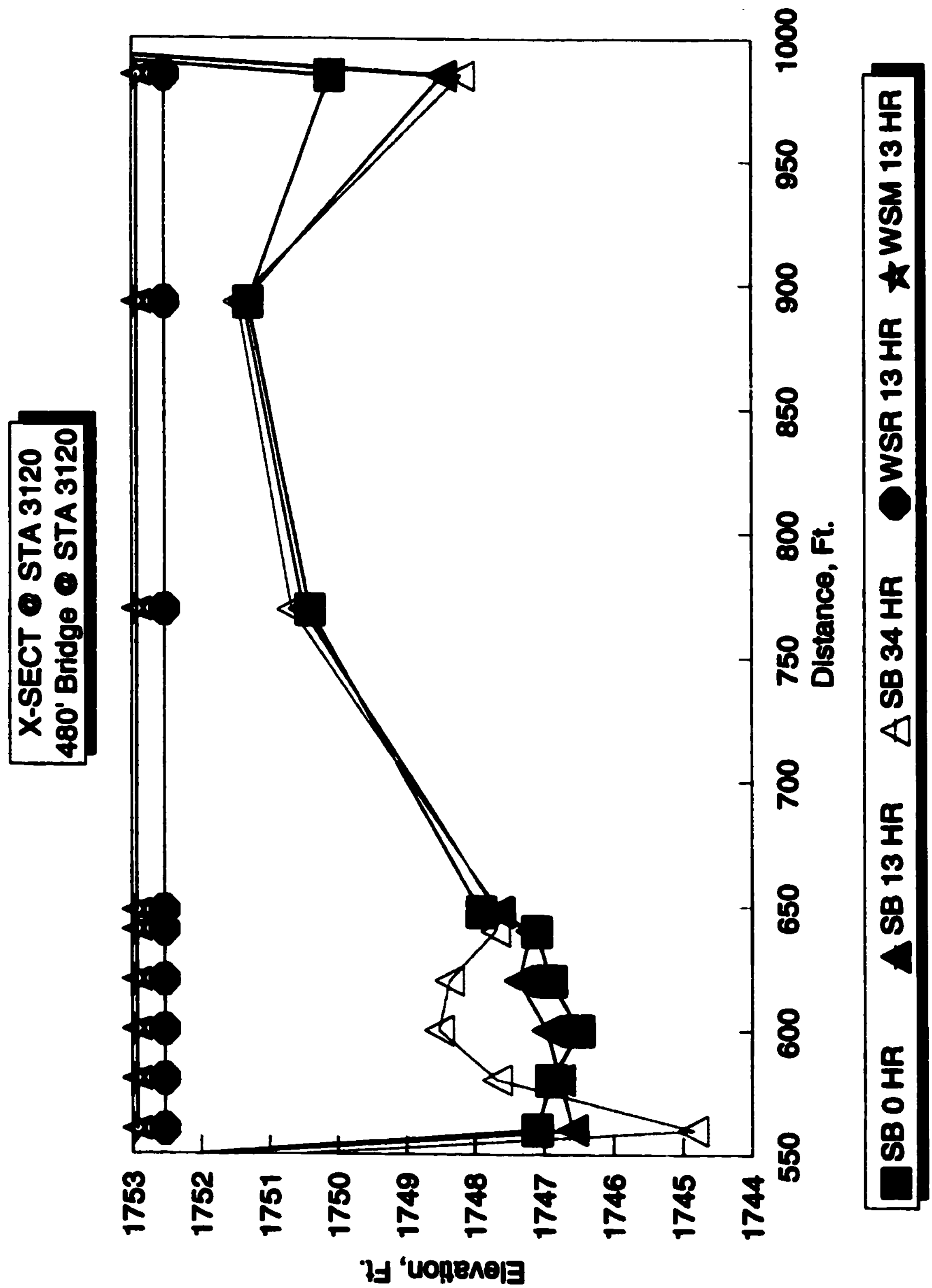

Figure 3.12 Nisqually cross-section at STA 3120
480' bridge

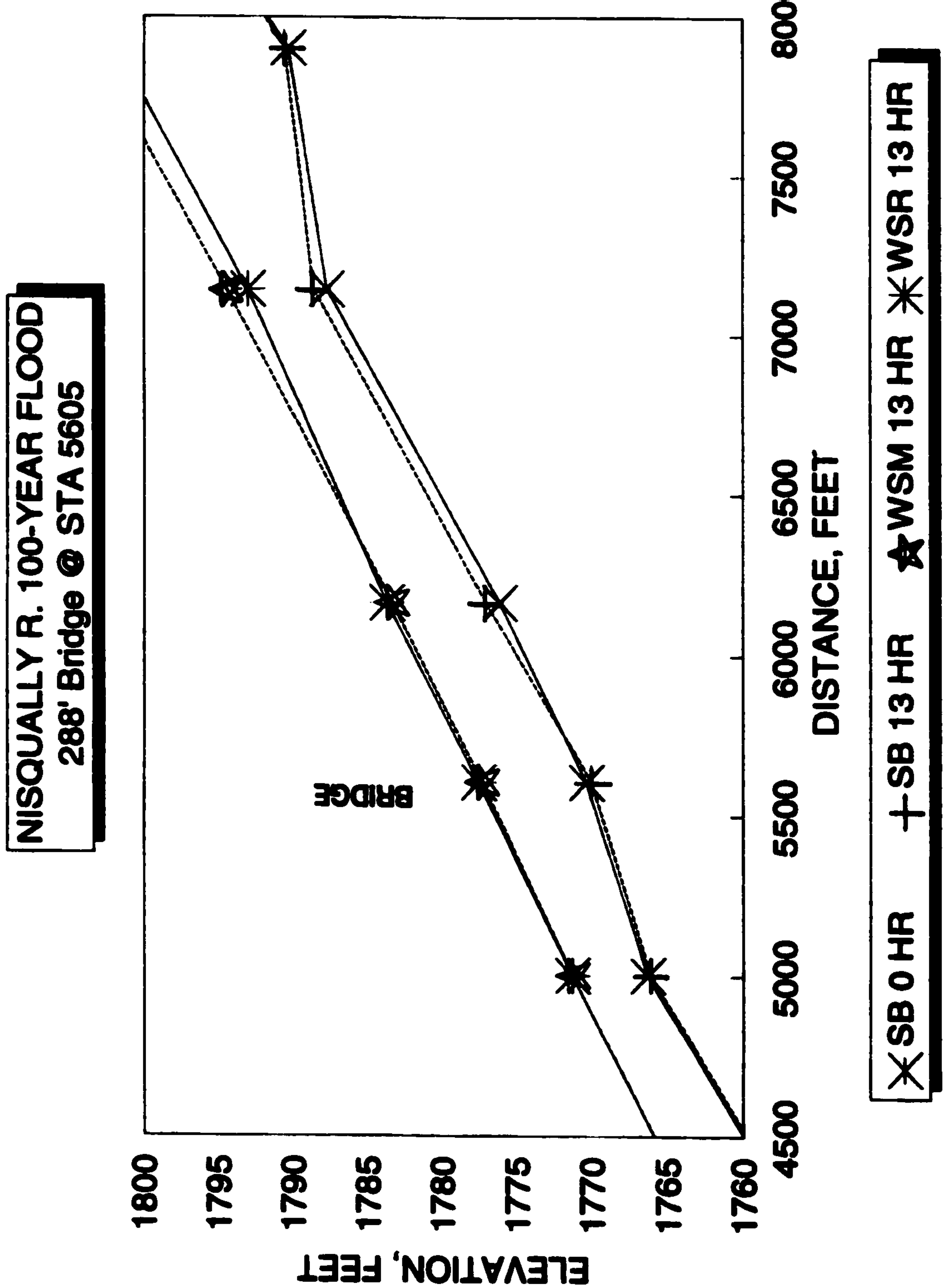

Figure 3.13 Nisqually profiles near STA 5605
288' bridge

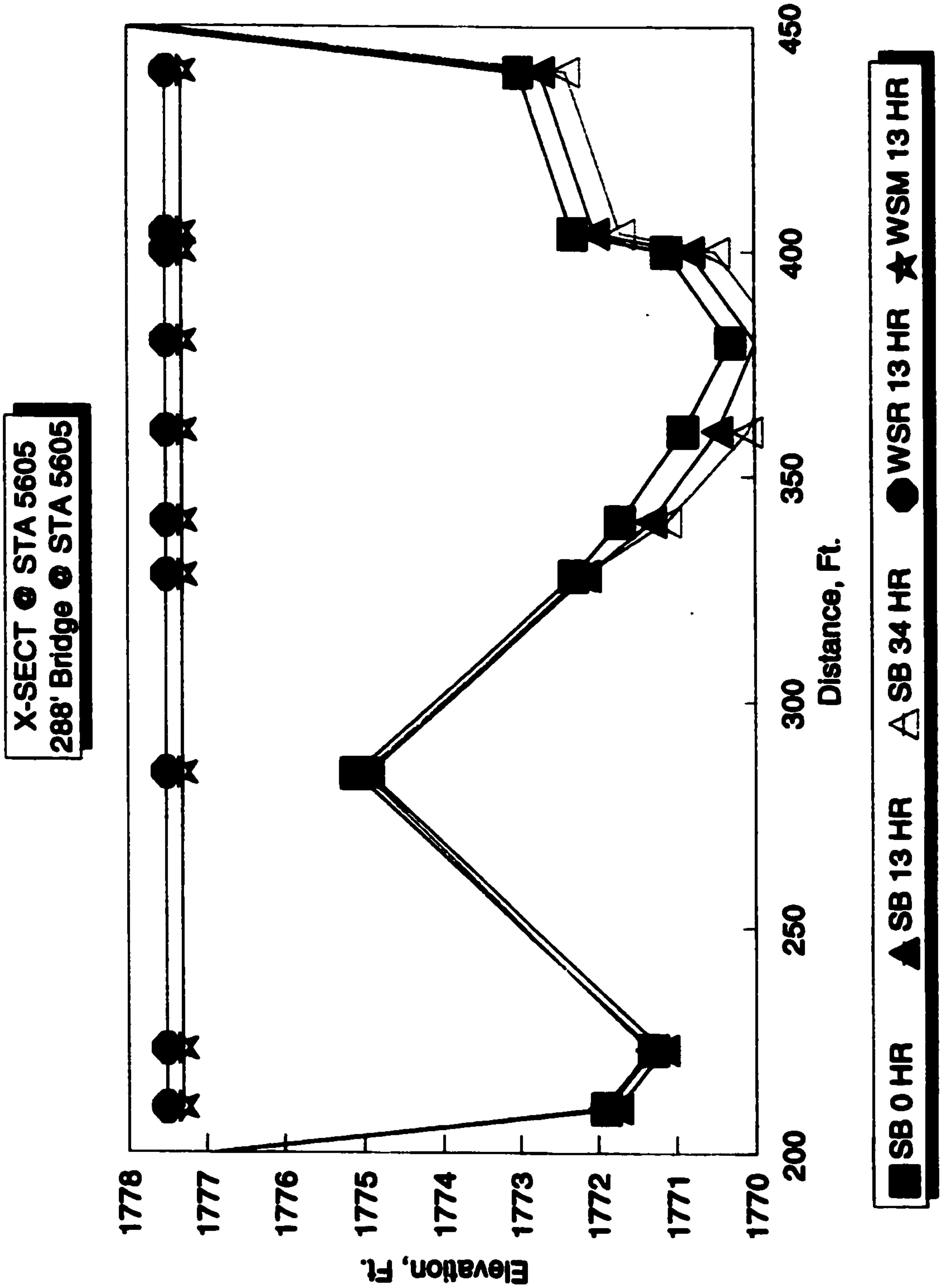

Figure 3.14 Nisqually cross-section at STA 5605
288' bridge

Figure 3.15 Skagit study site

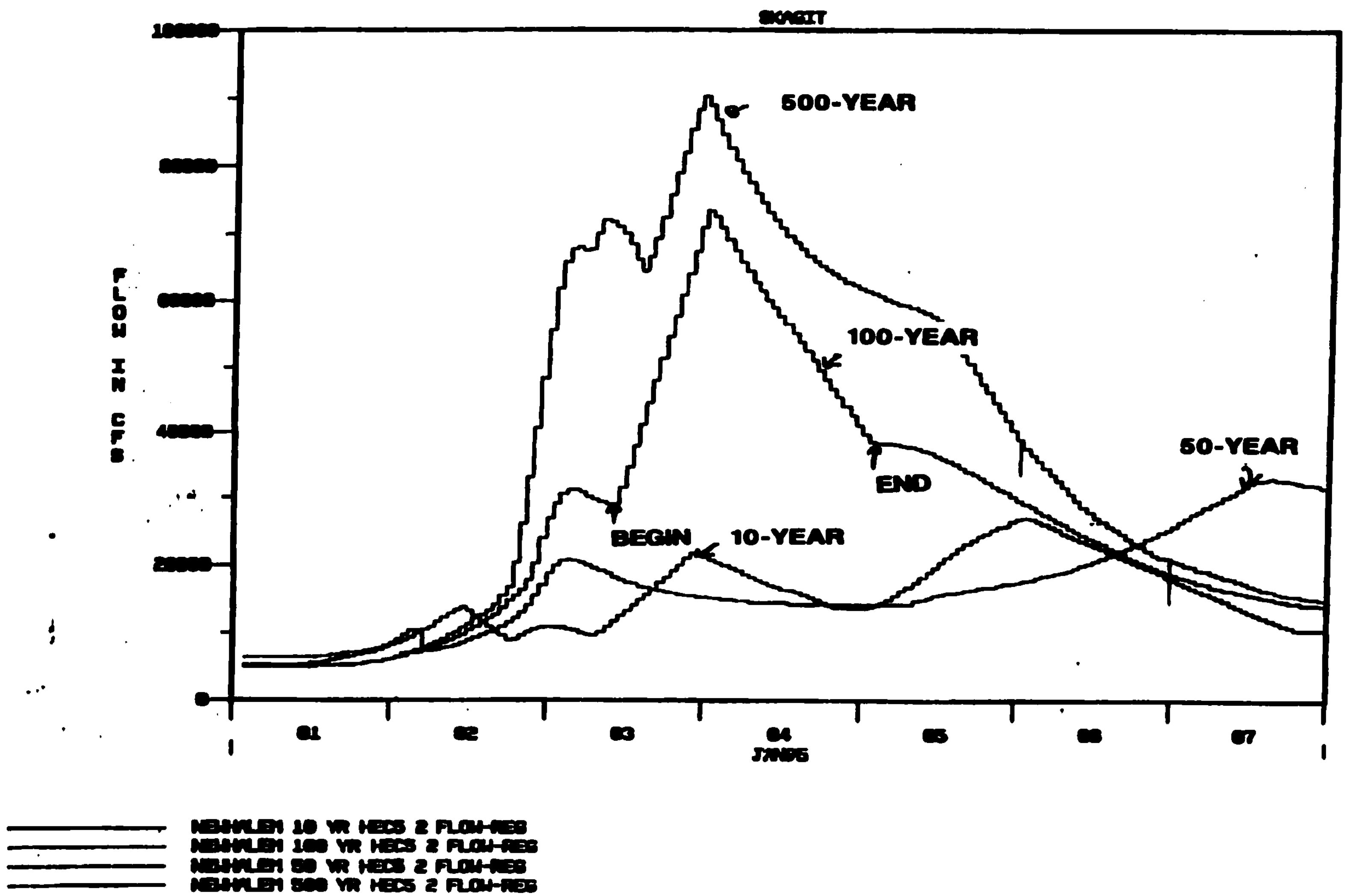

Figure 3.16 Skagit hydrographs

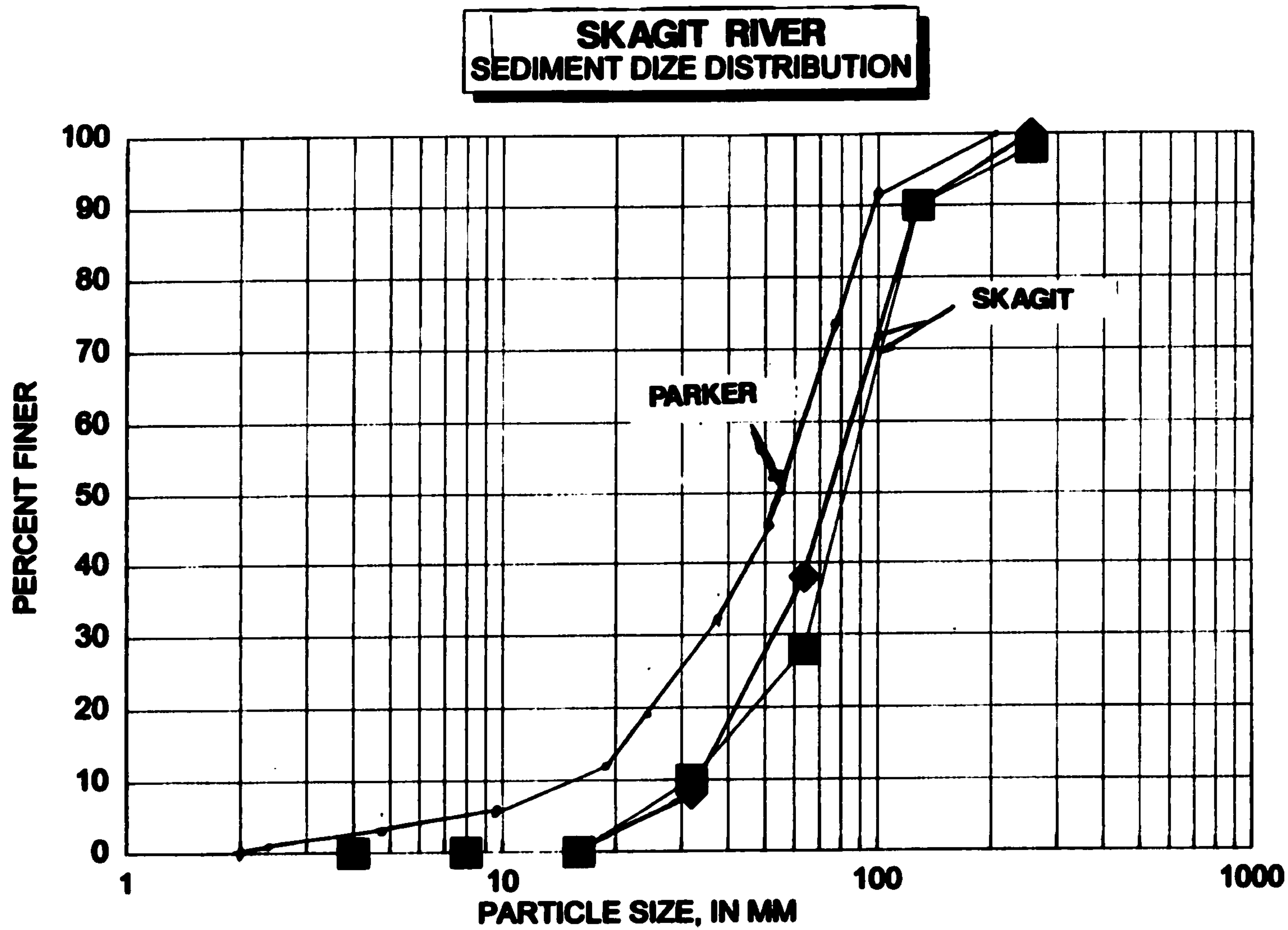

Figure 3.17 Skagit gradations

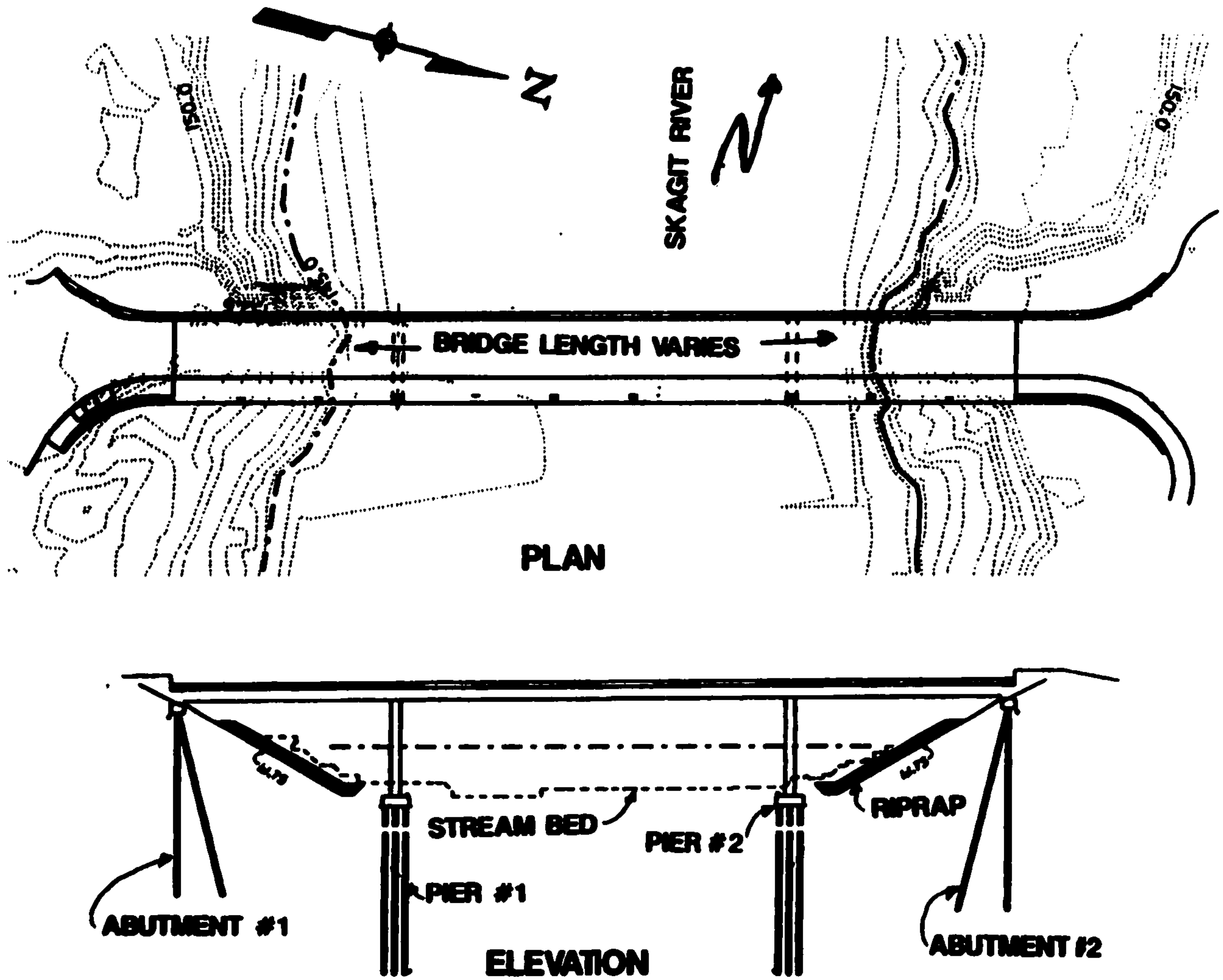

Figure 3.18 Skagit bridge layout

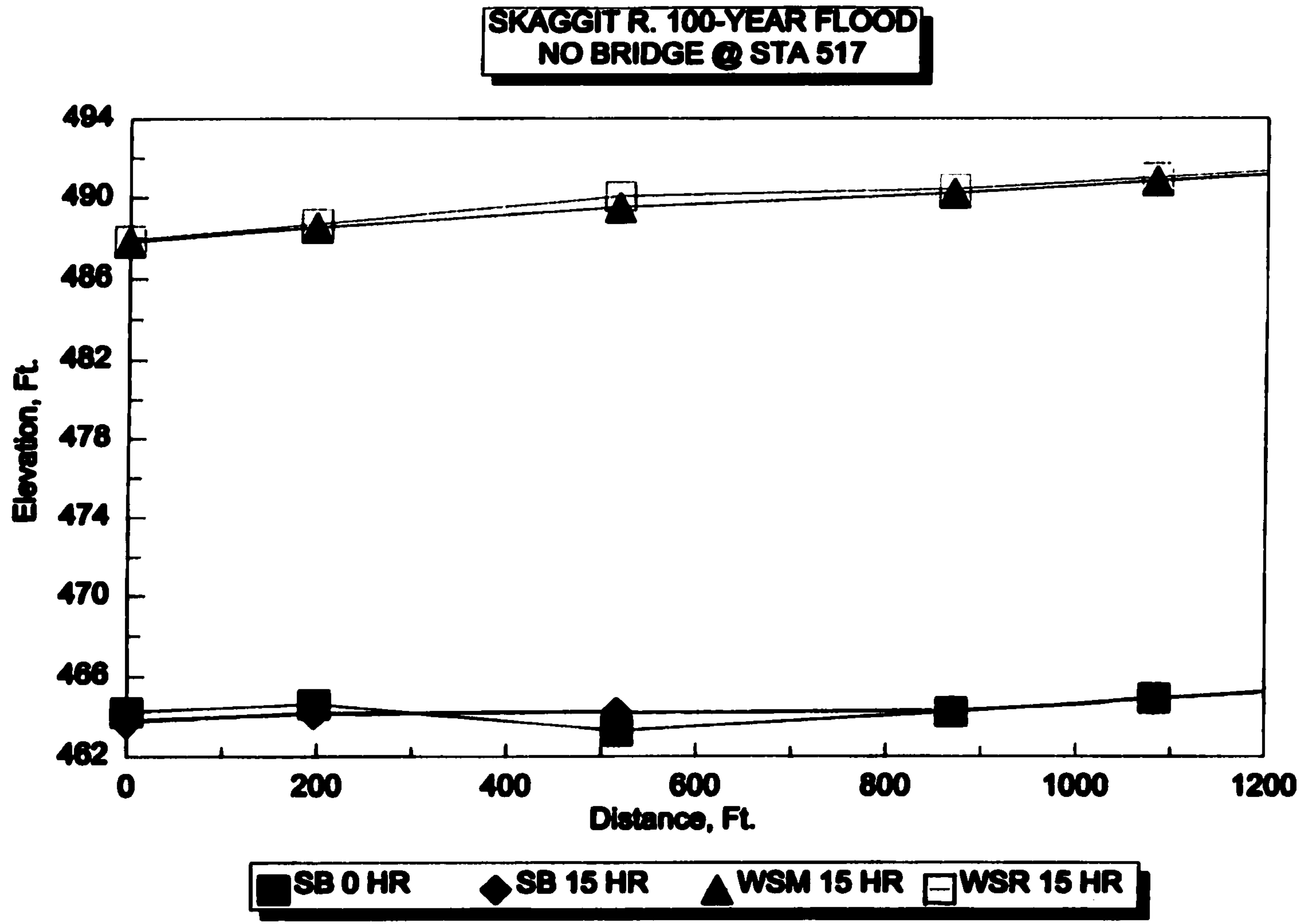

Figure 3.19 Skagit profiles, no bridge

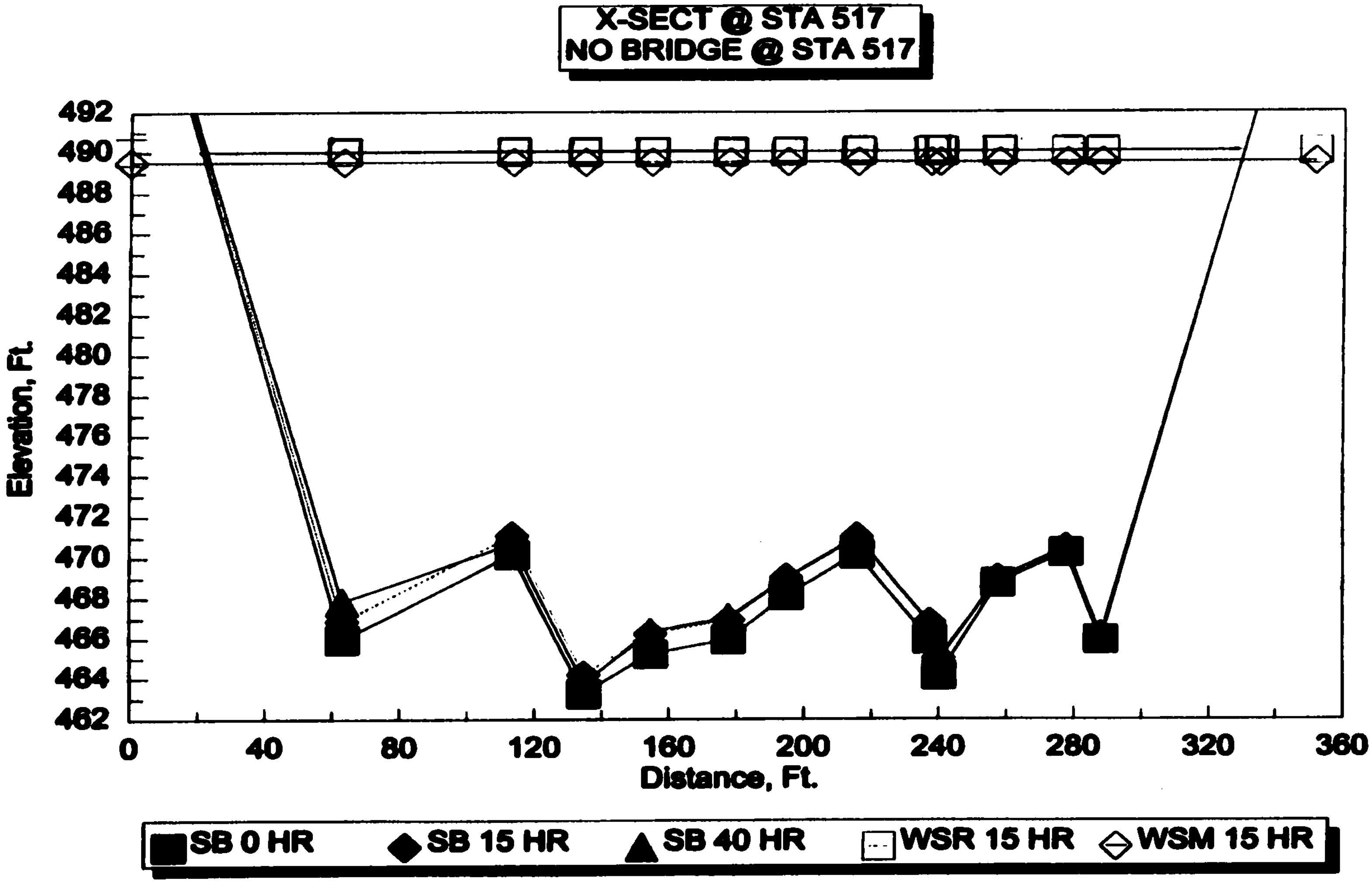

Figure 3.20 Skagit cross-section, no bridge

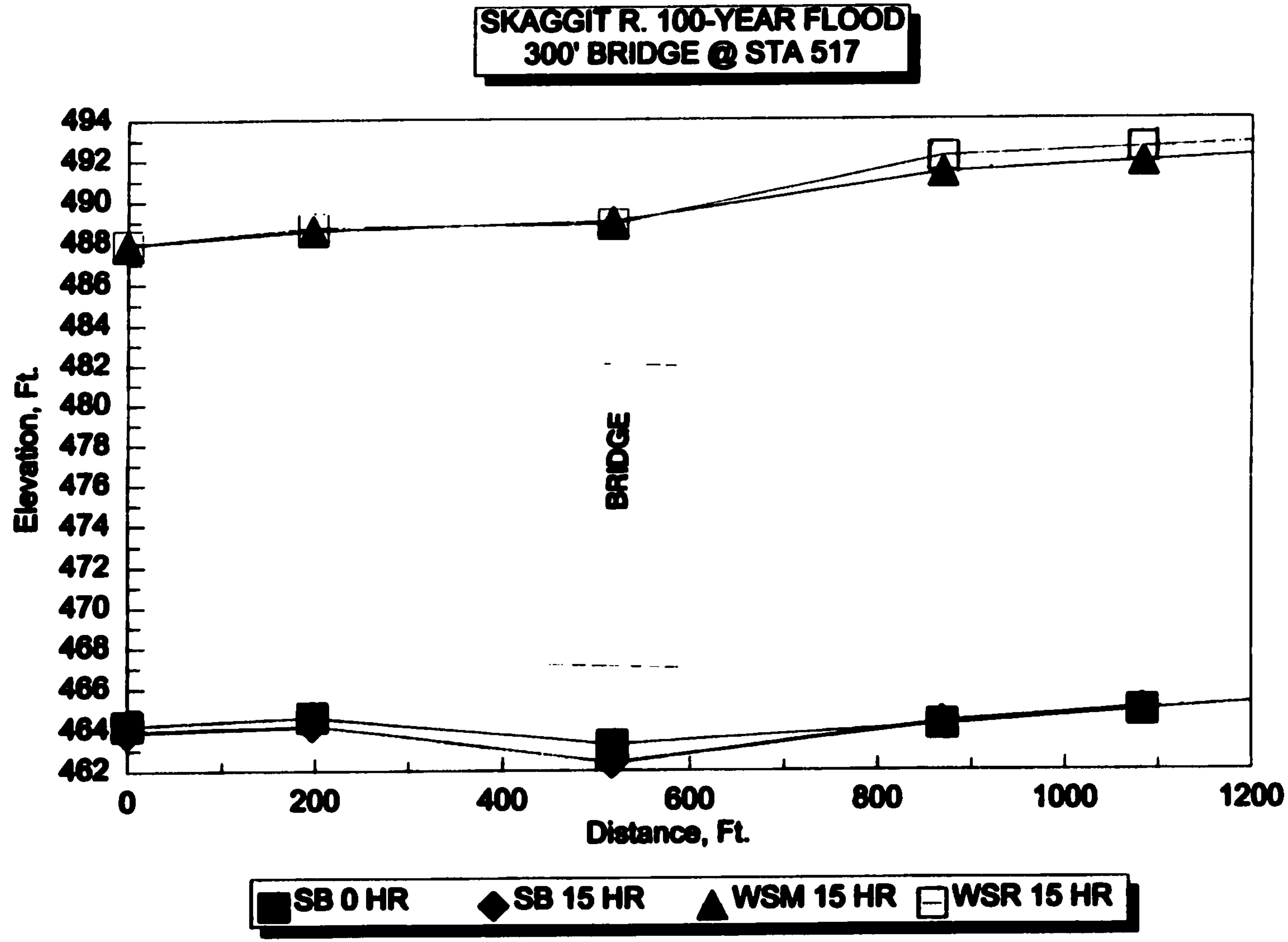

Figure 3.21 Skagit profiles, 300' bridge

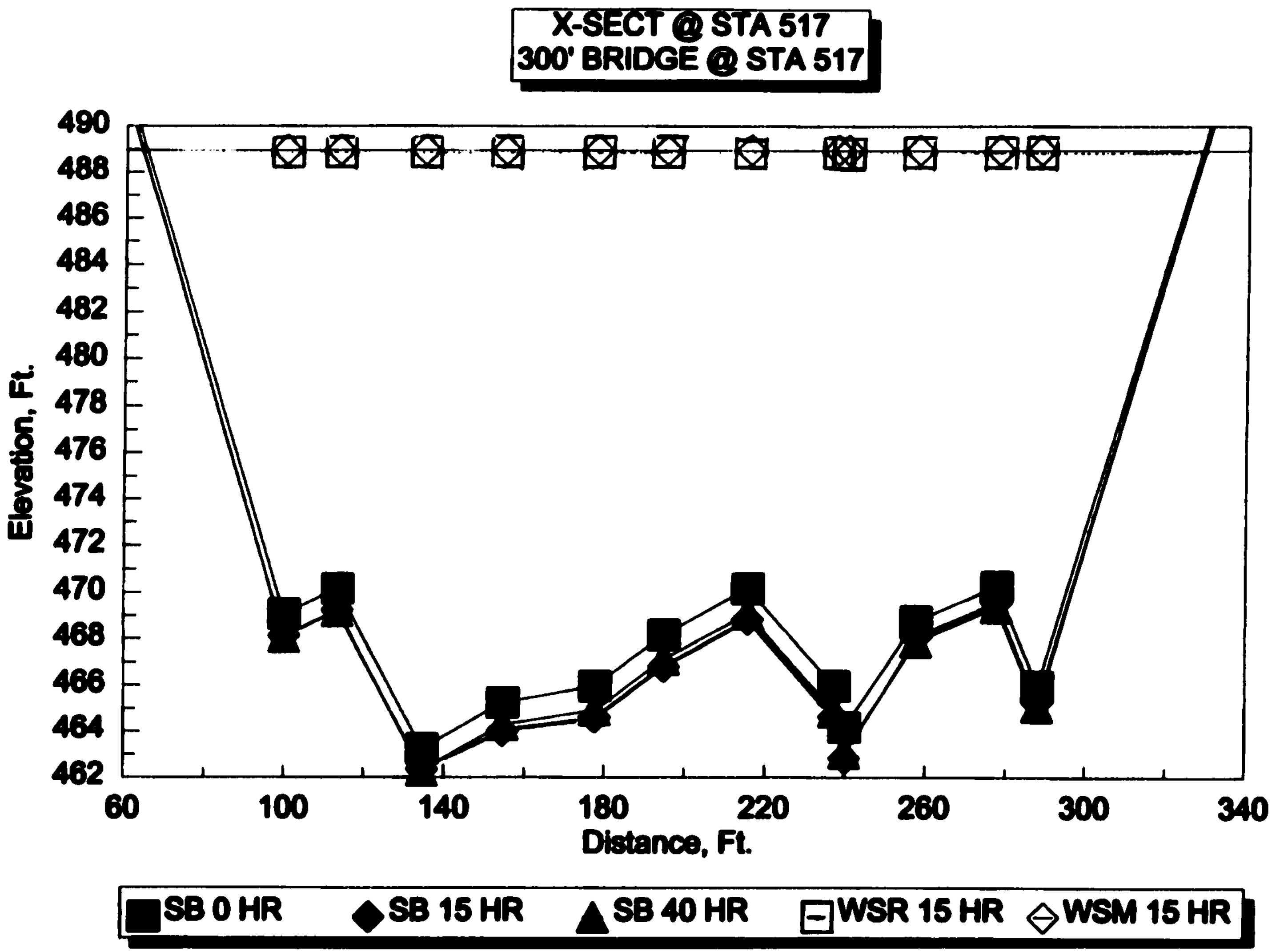

Figure 3.22 Skagit cross-section, 300' bridge

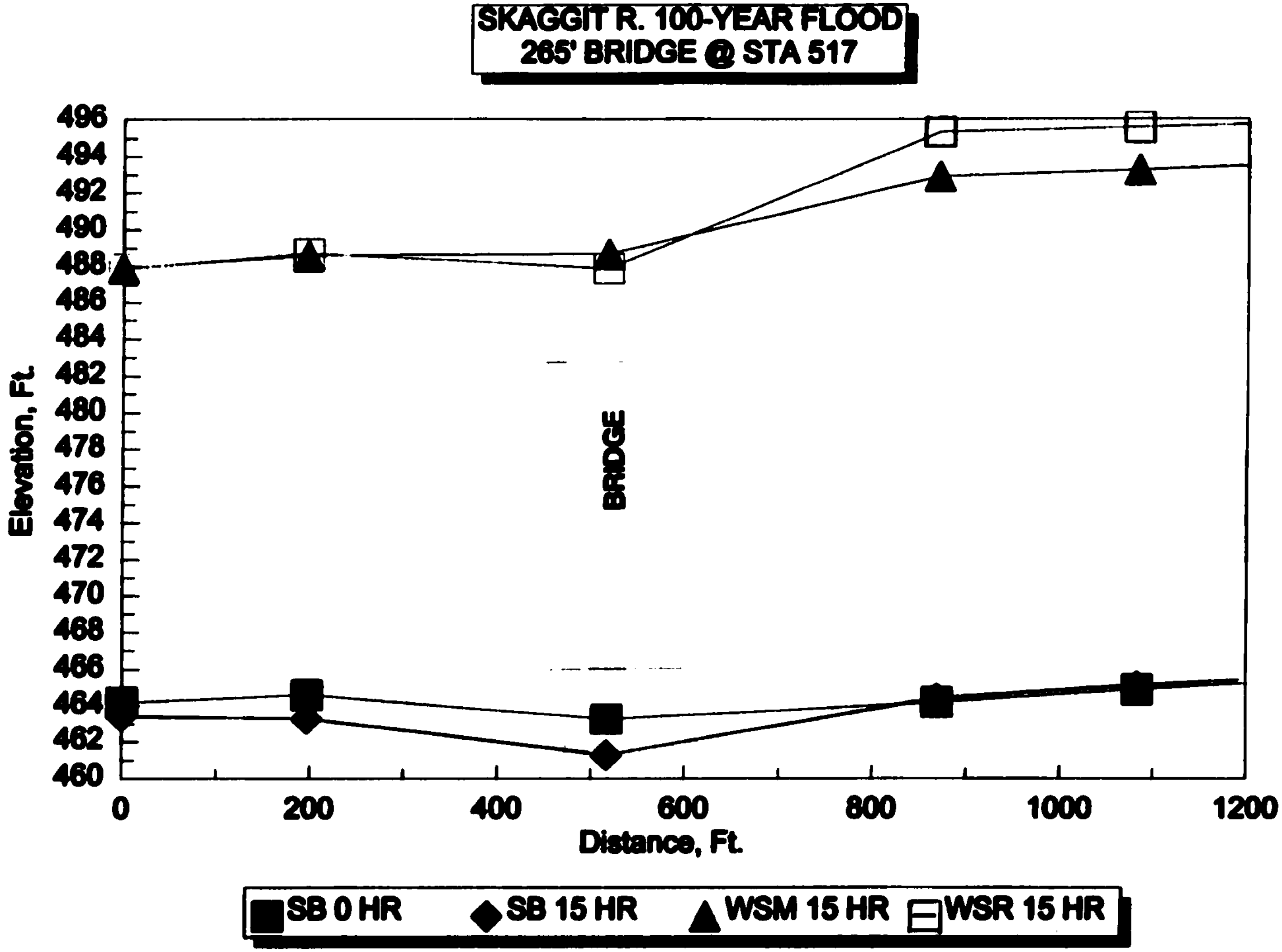

Figure 3.23 Skagit profiles, 265' bridge

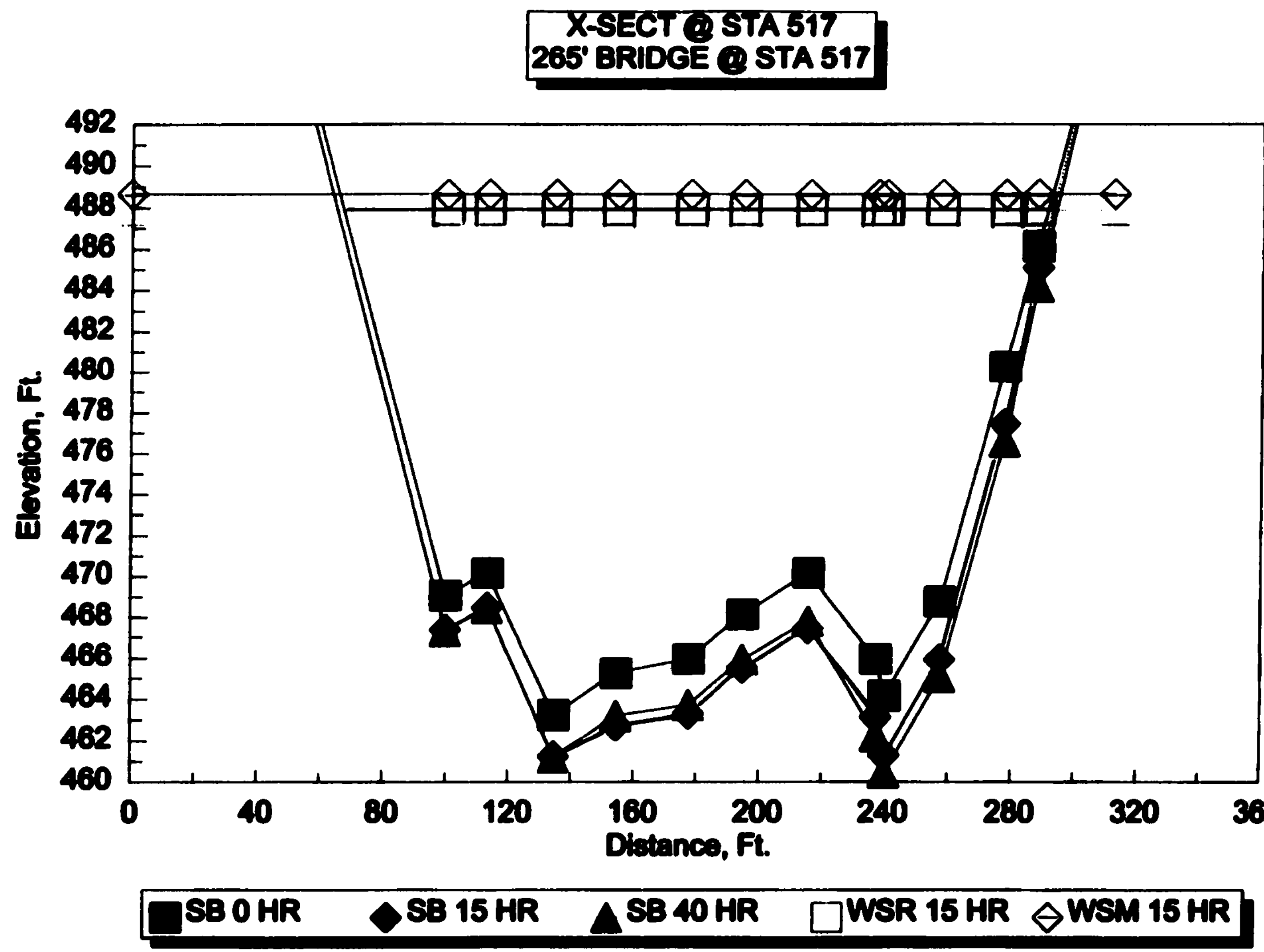

Figure 3.24 Skagit cross-section, 265' bridge

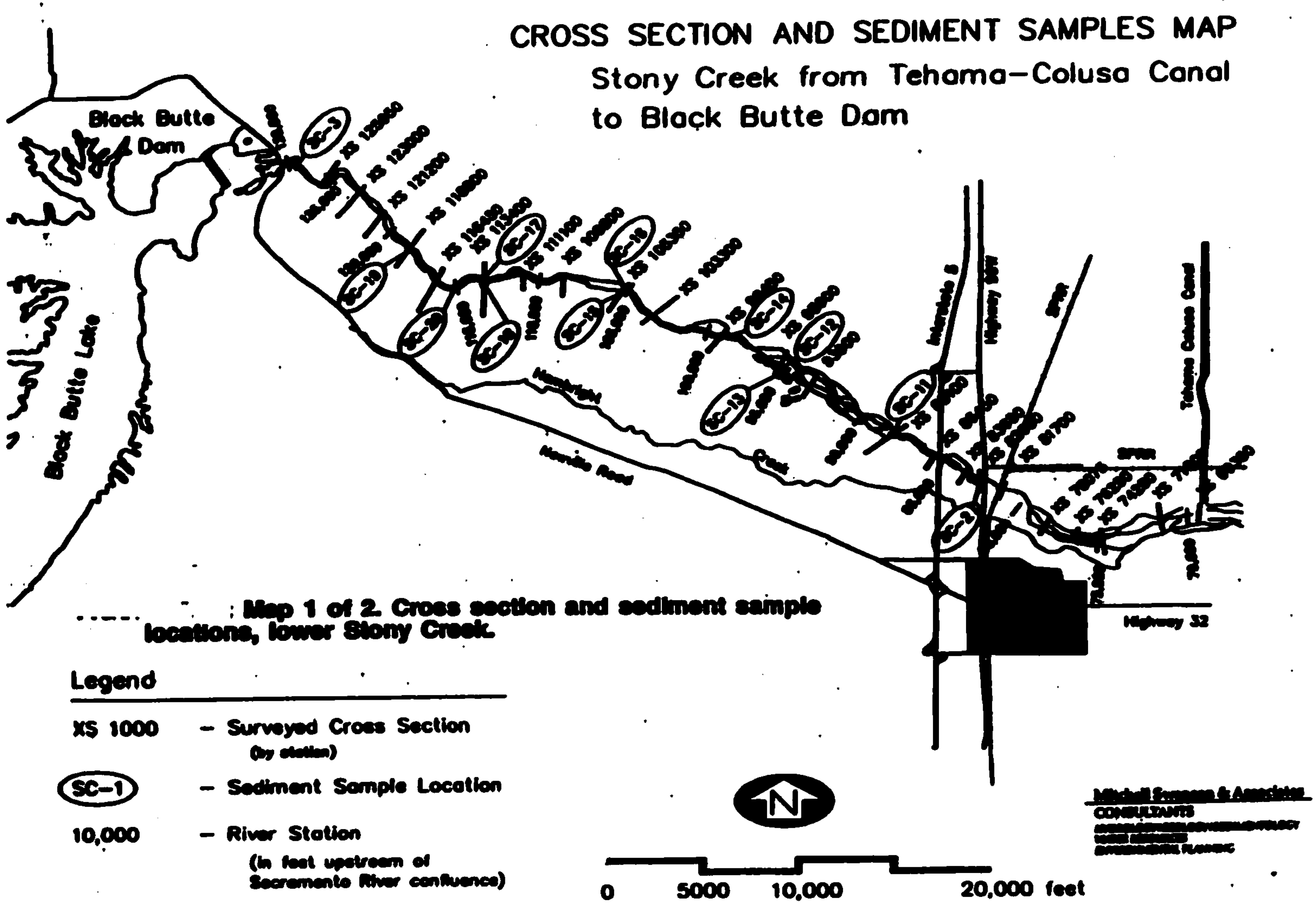

Figure 3.25 Stony Creek #1 study site (Swanson and Kondolf, 1991)

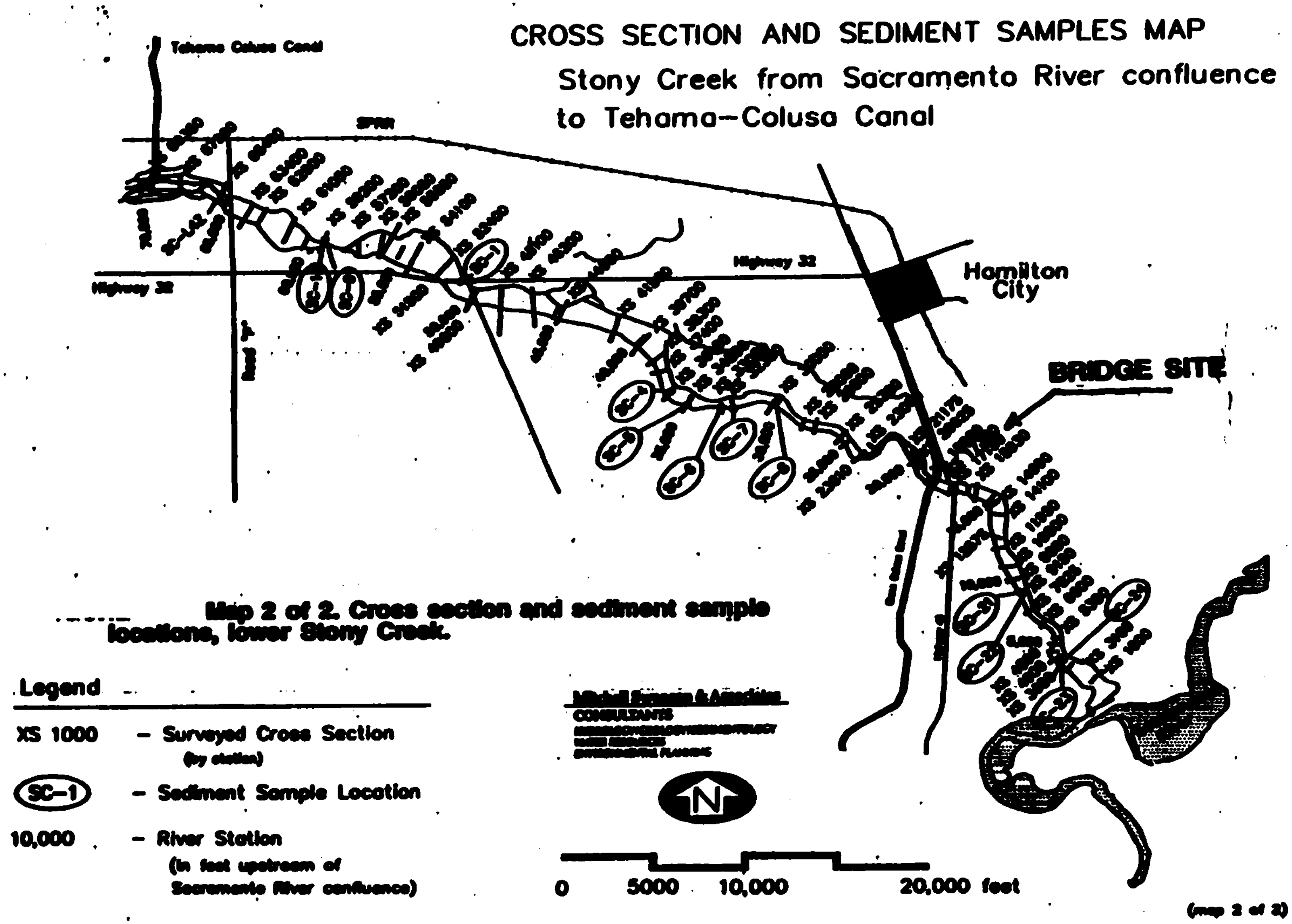

Figure 3.25 Stony Creek #1 study site(continued) (Swanson and Kondolf, 1991)

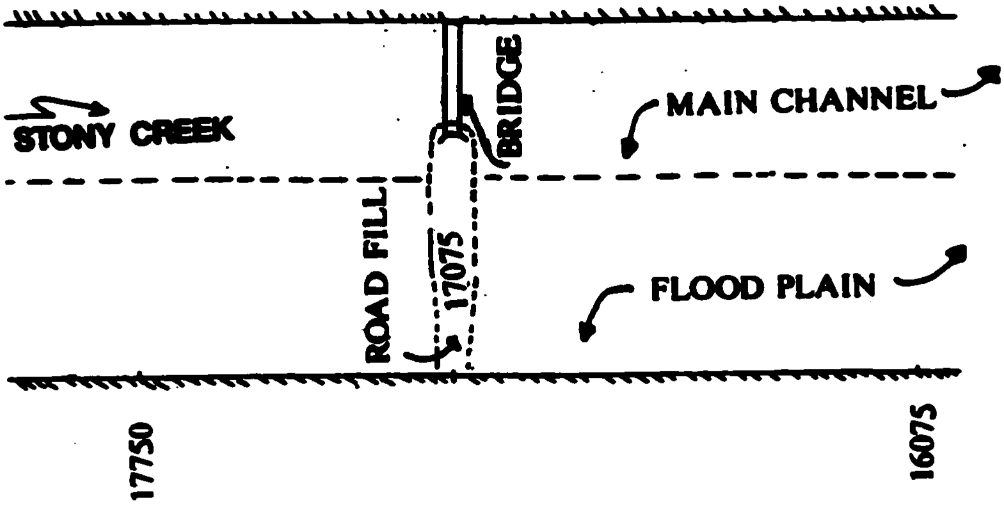

PLAN

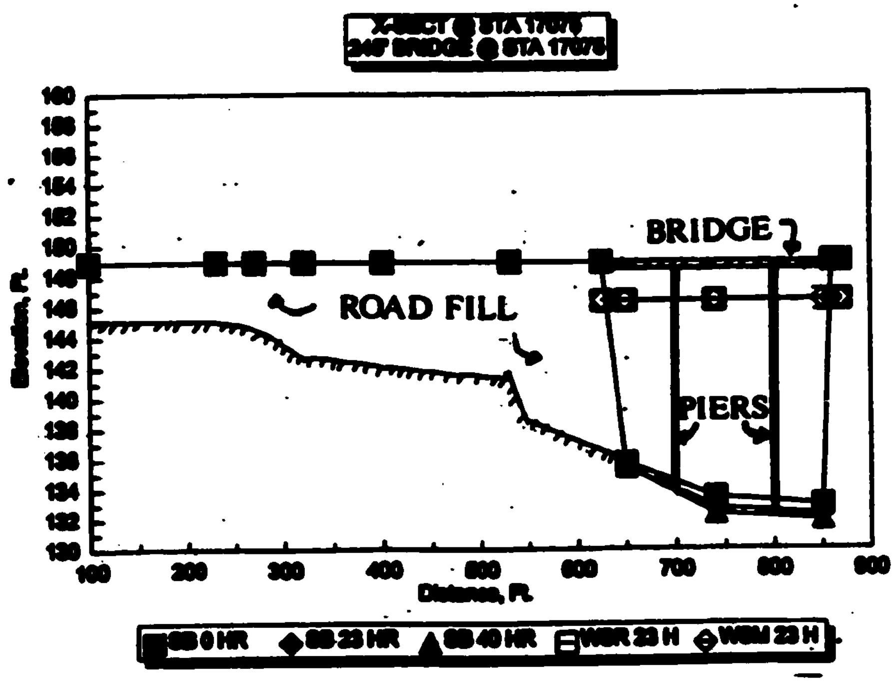

ELEVATION

Figure 3.26 Stony Creek #1 bridge layout

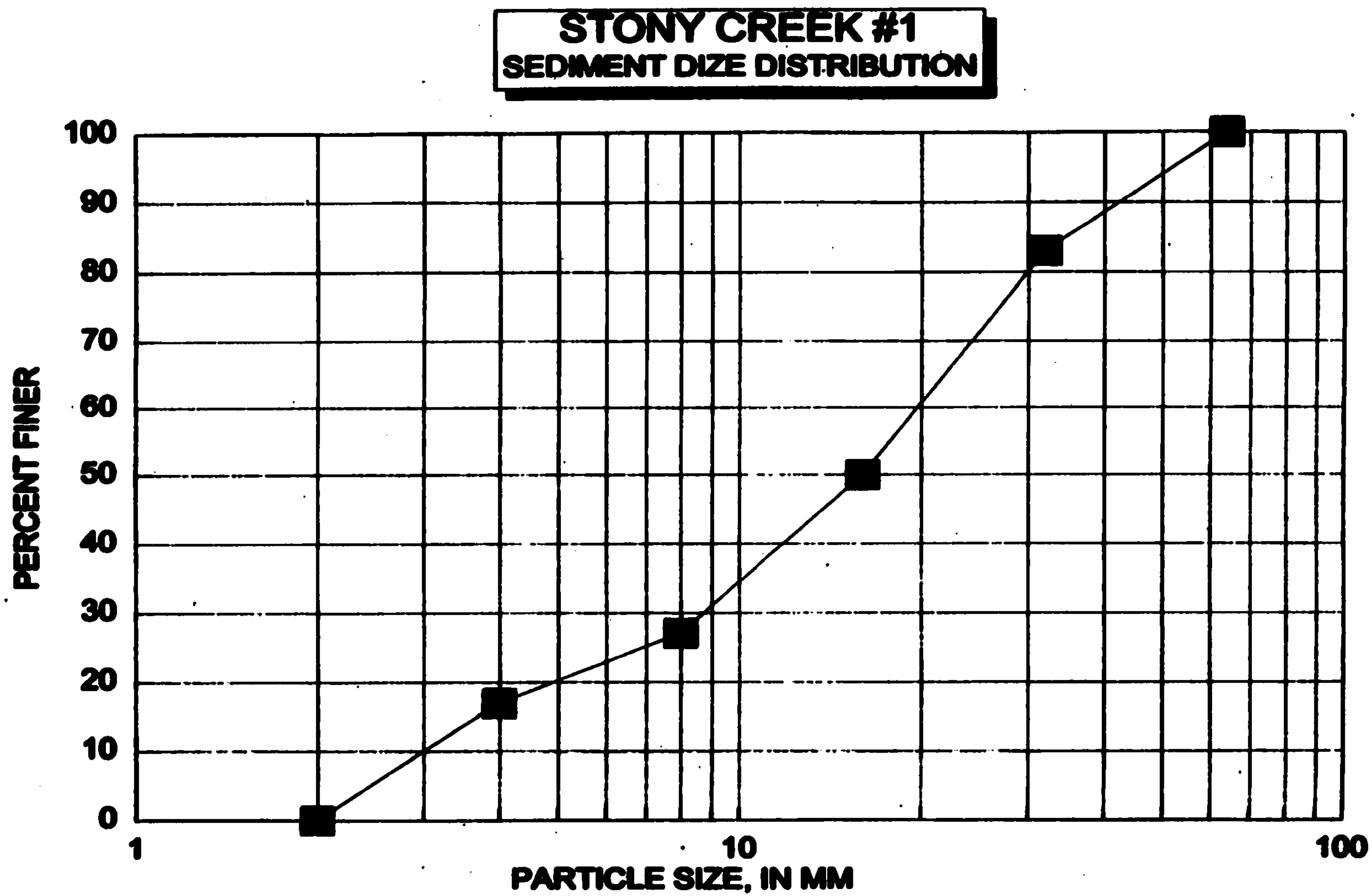

Figure 3.27 Stony Creek #1 gradations

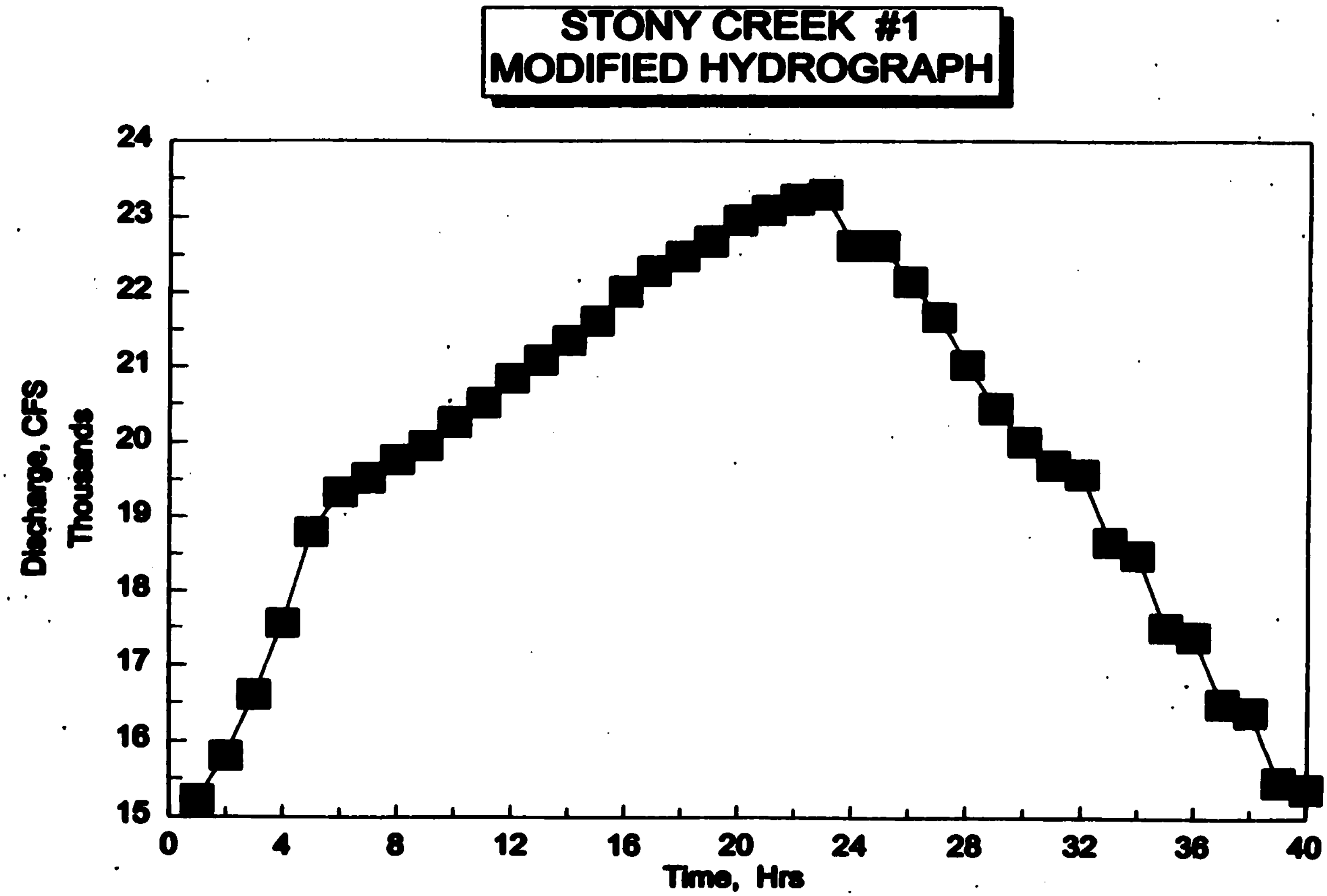

Figure 3.28 Stony Creek #1 hydrograph

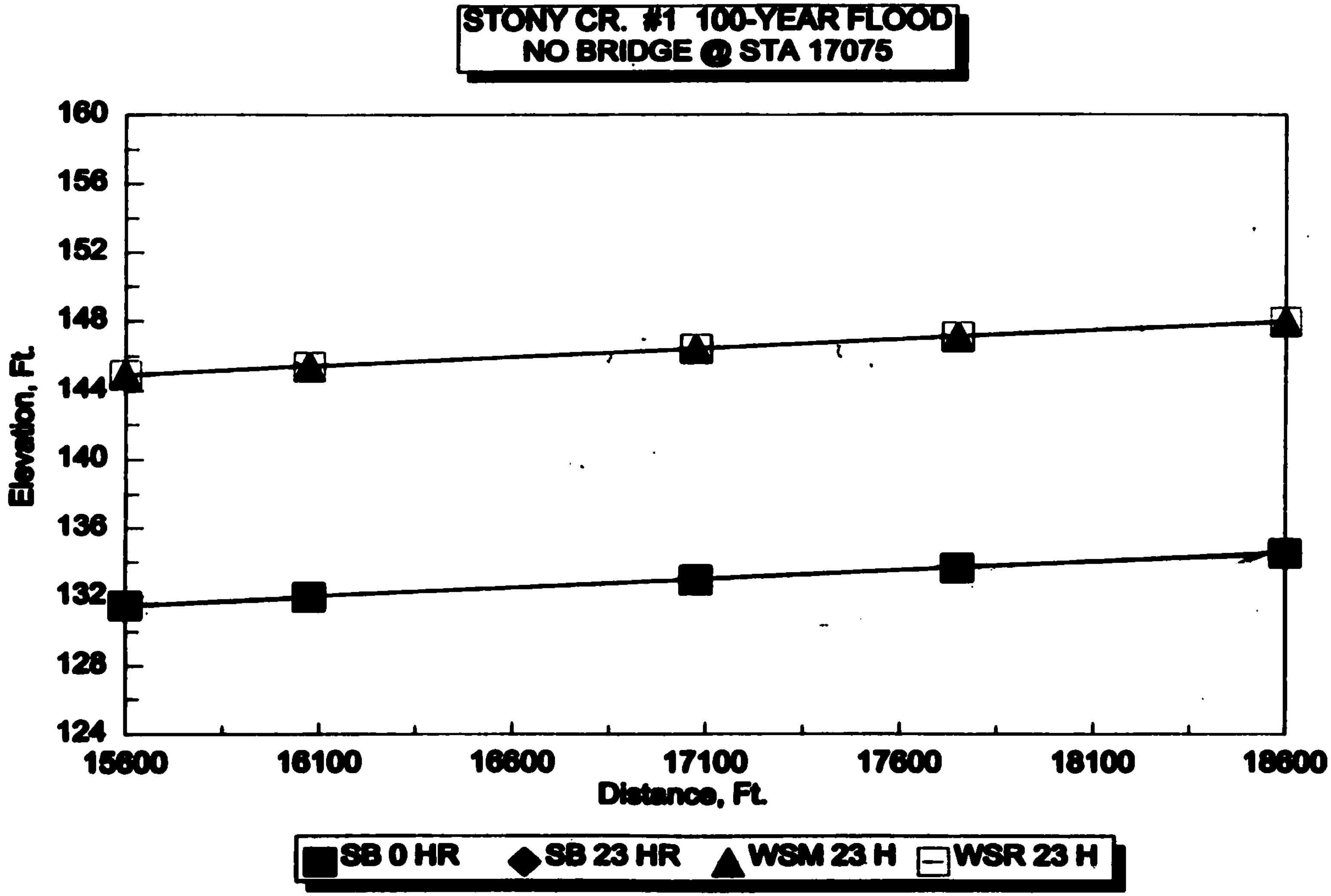

Figure 3.29 Stony Creek #1 profiles, no bridge

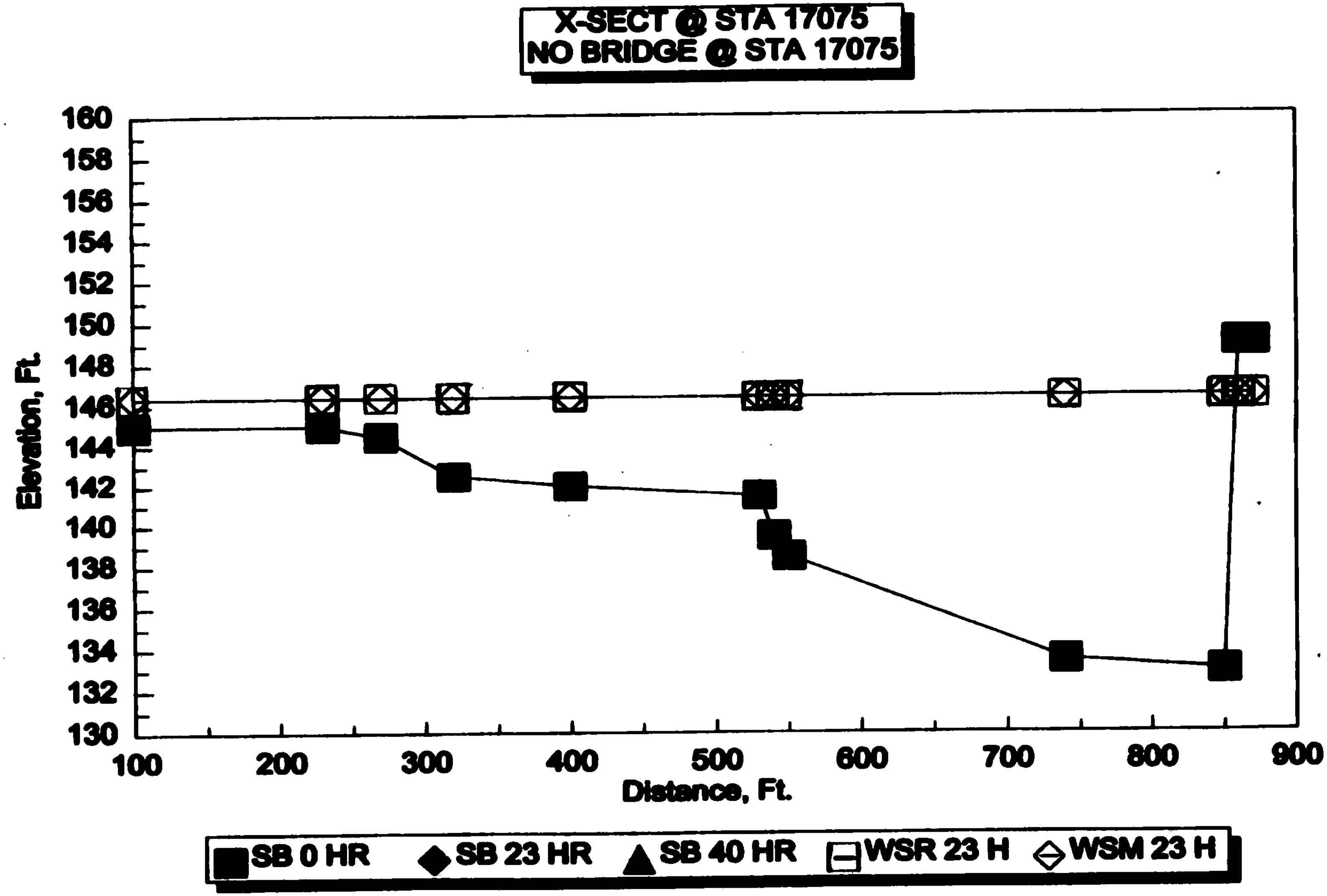

Figure 3.30 Stony Creek #1 cross-section, no bridge

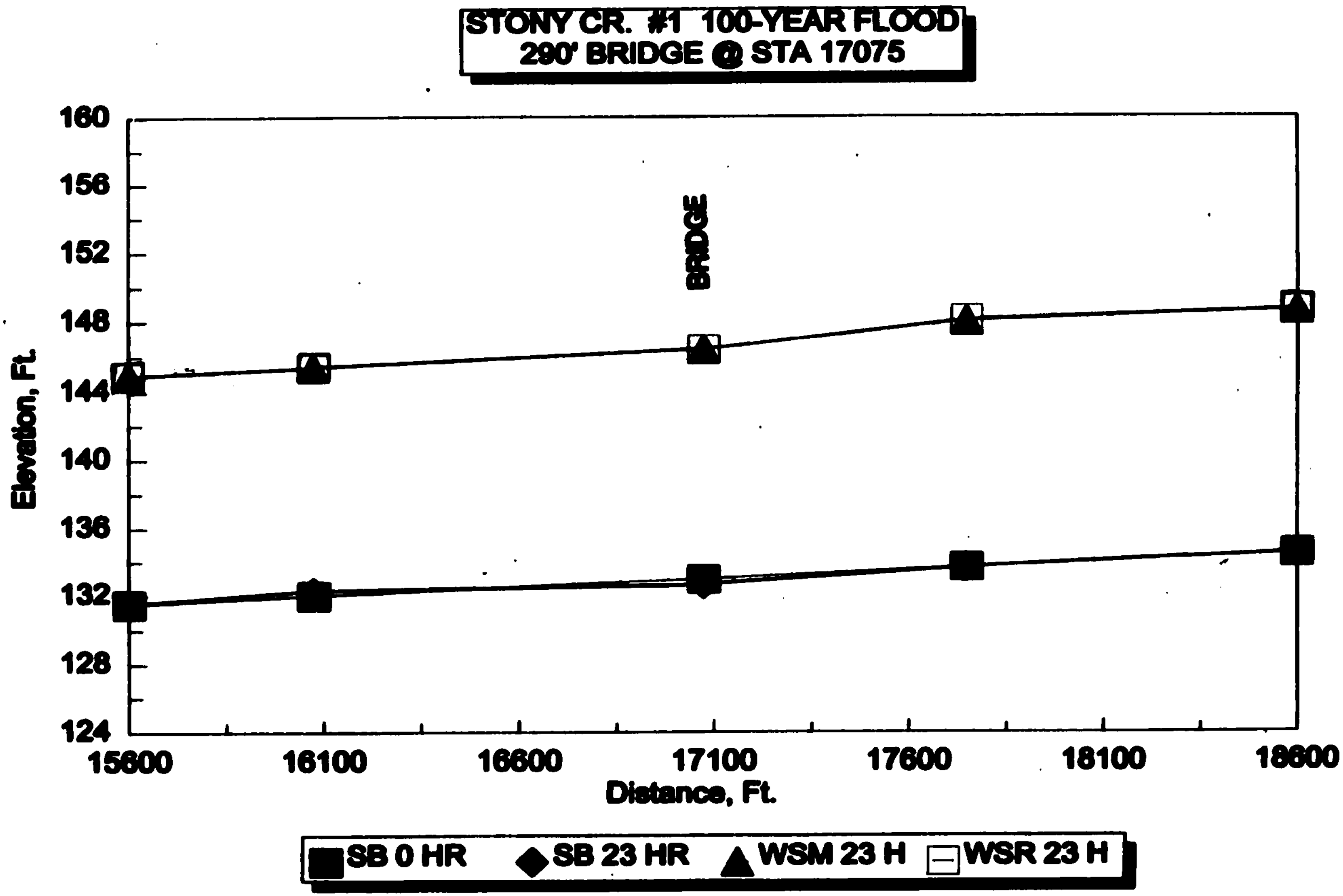

Figure 3.31 Stony Creek #1 profiles, 290' bridge

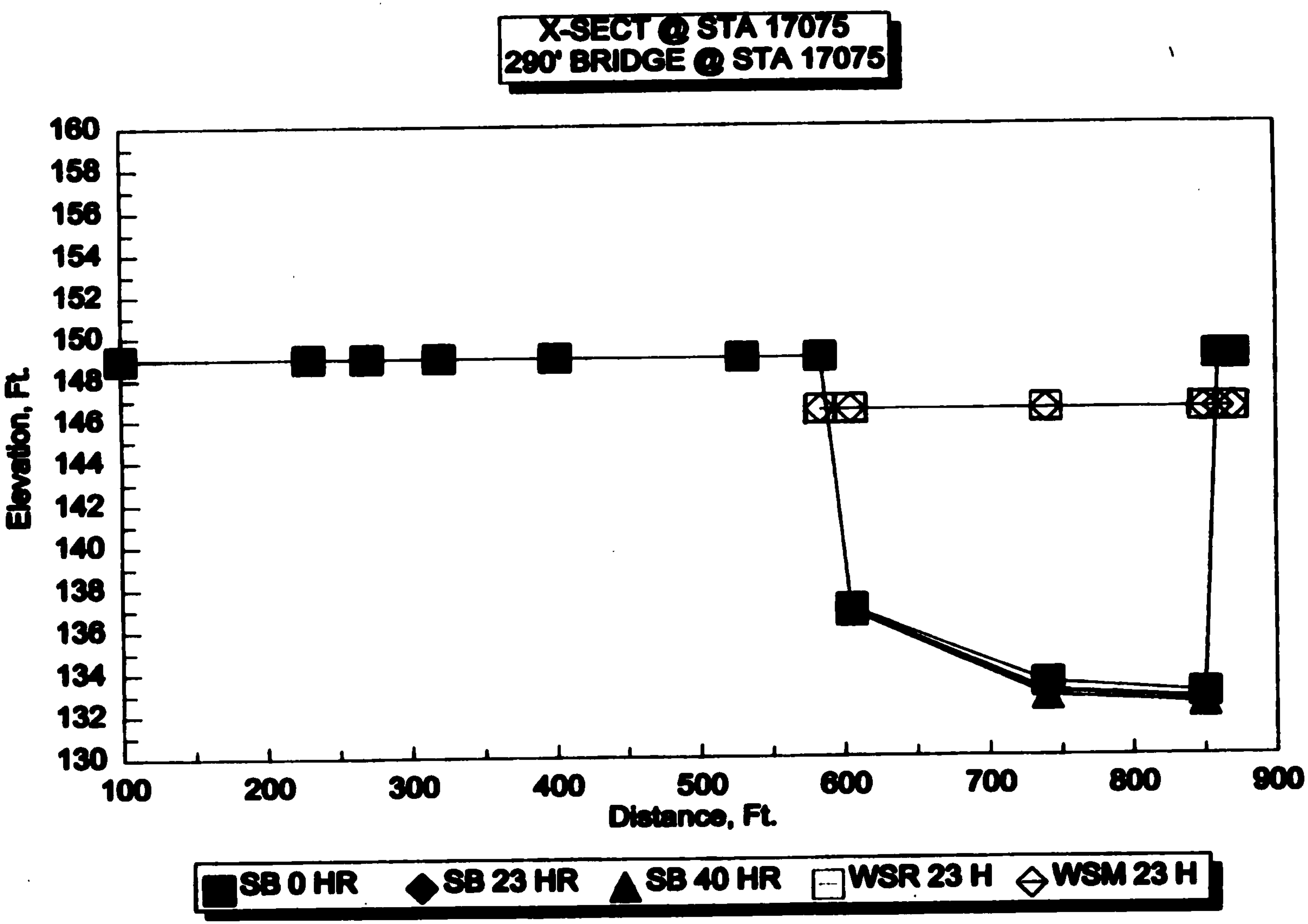

Figure 3.32 Stony Creek #1 cross-section, 290' bridge

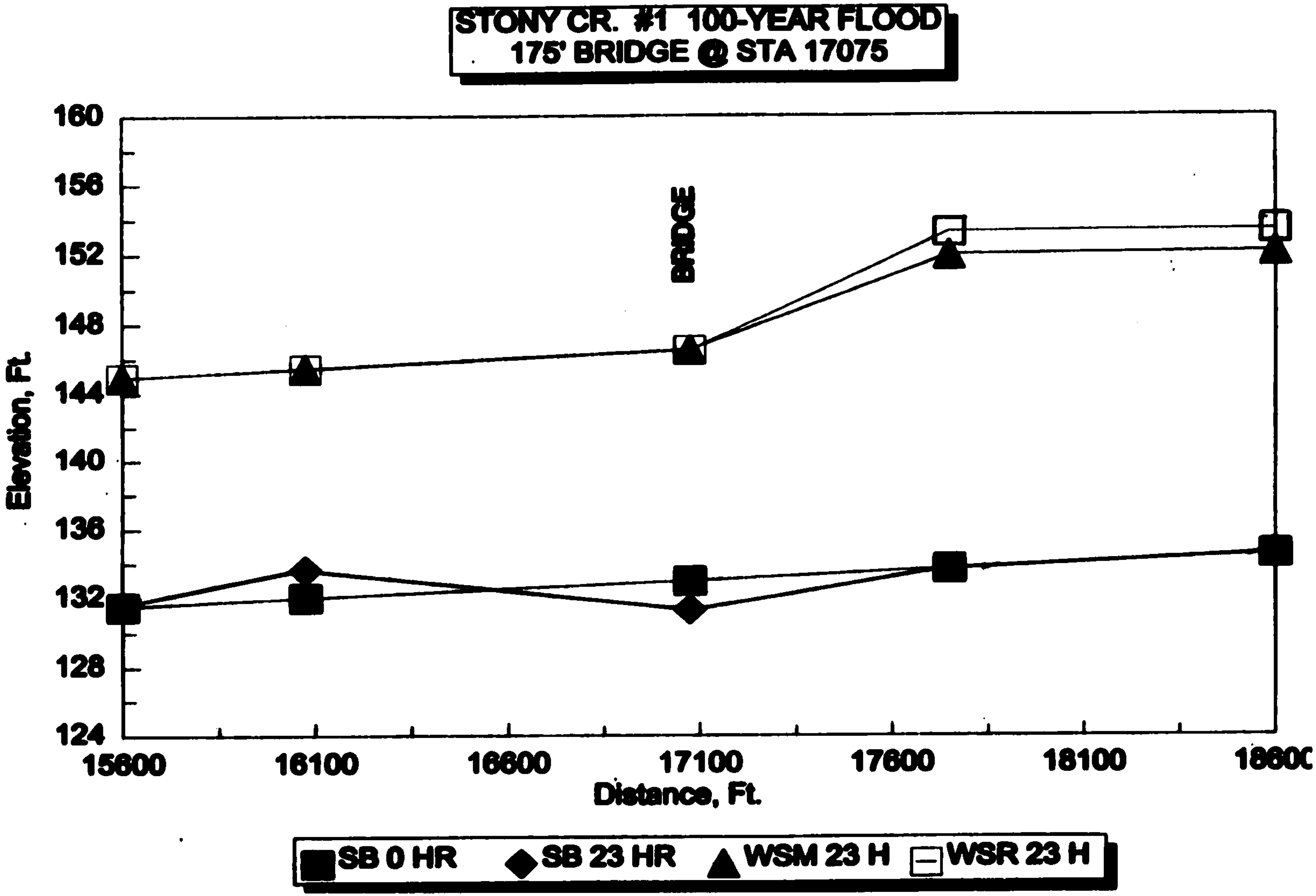

Figure 3.33 Stony Creek #1 profiles, 175' bridge

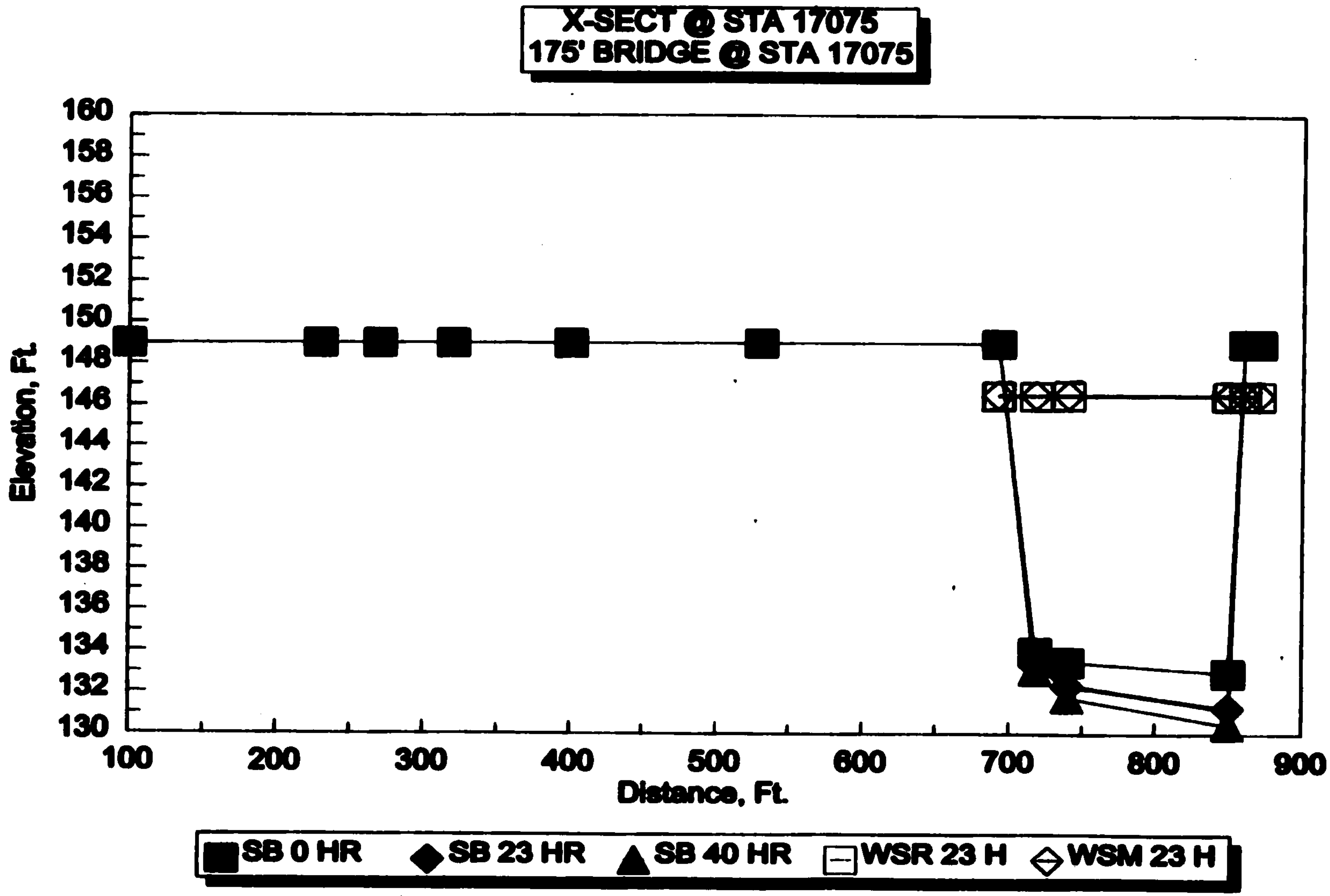

Figure 3.34 Stony Creek #1 cross-section, 175' bridge

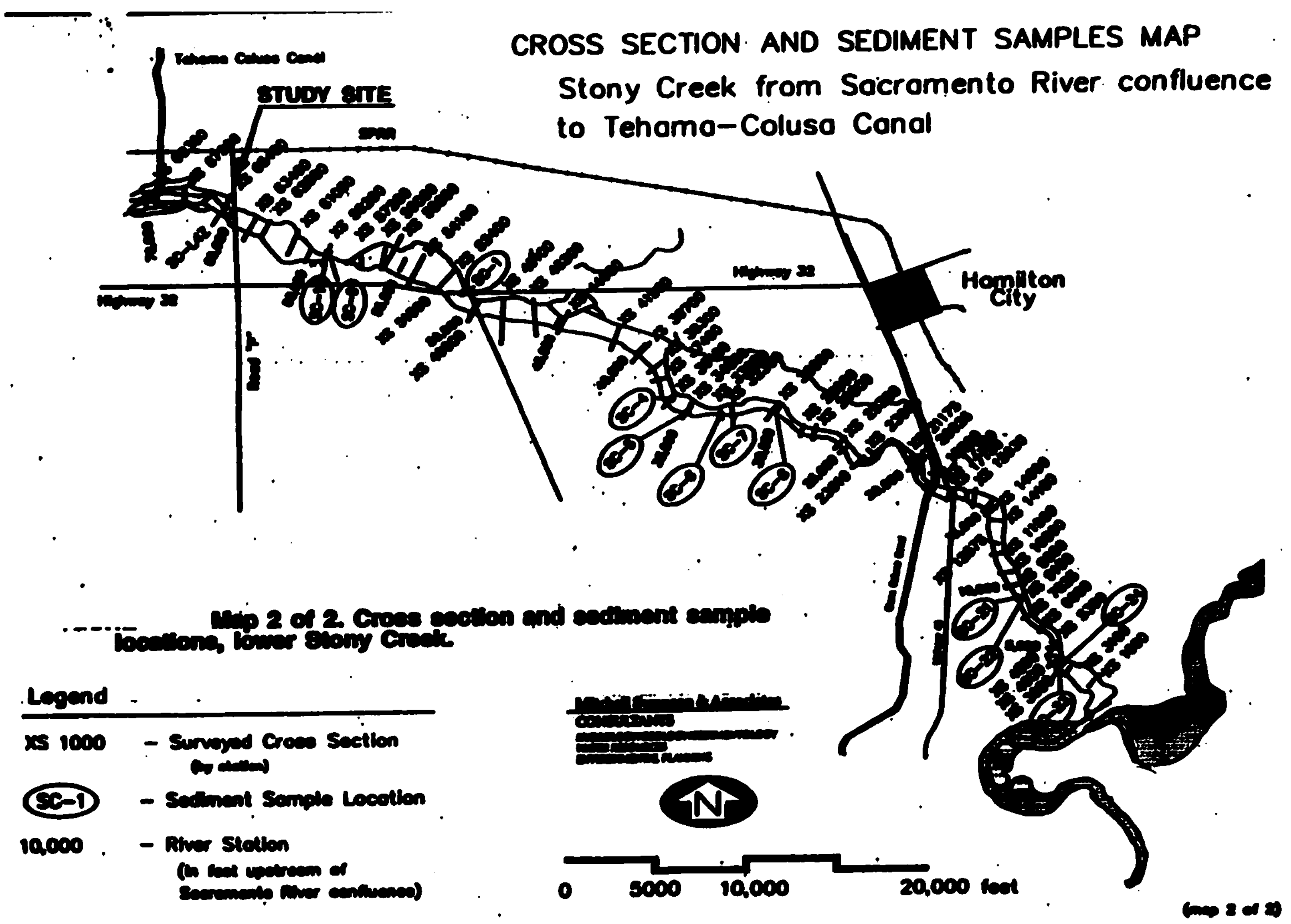

Figure 3.35 Stony Creek #2 study site (Swanson and Kondolf, 1991)

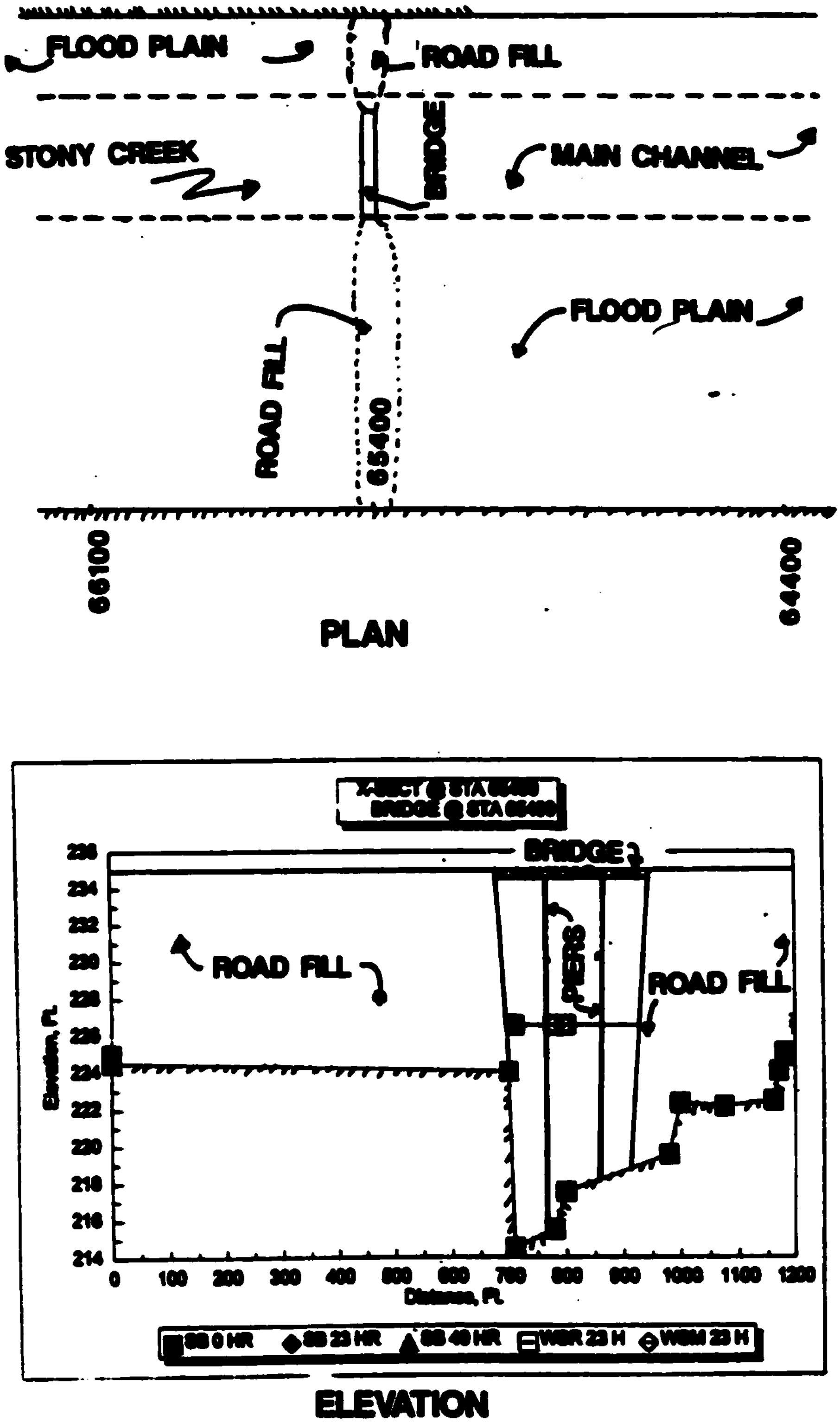

Figure 3.36 Stony Creek #2 bridge layout

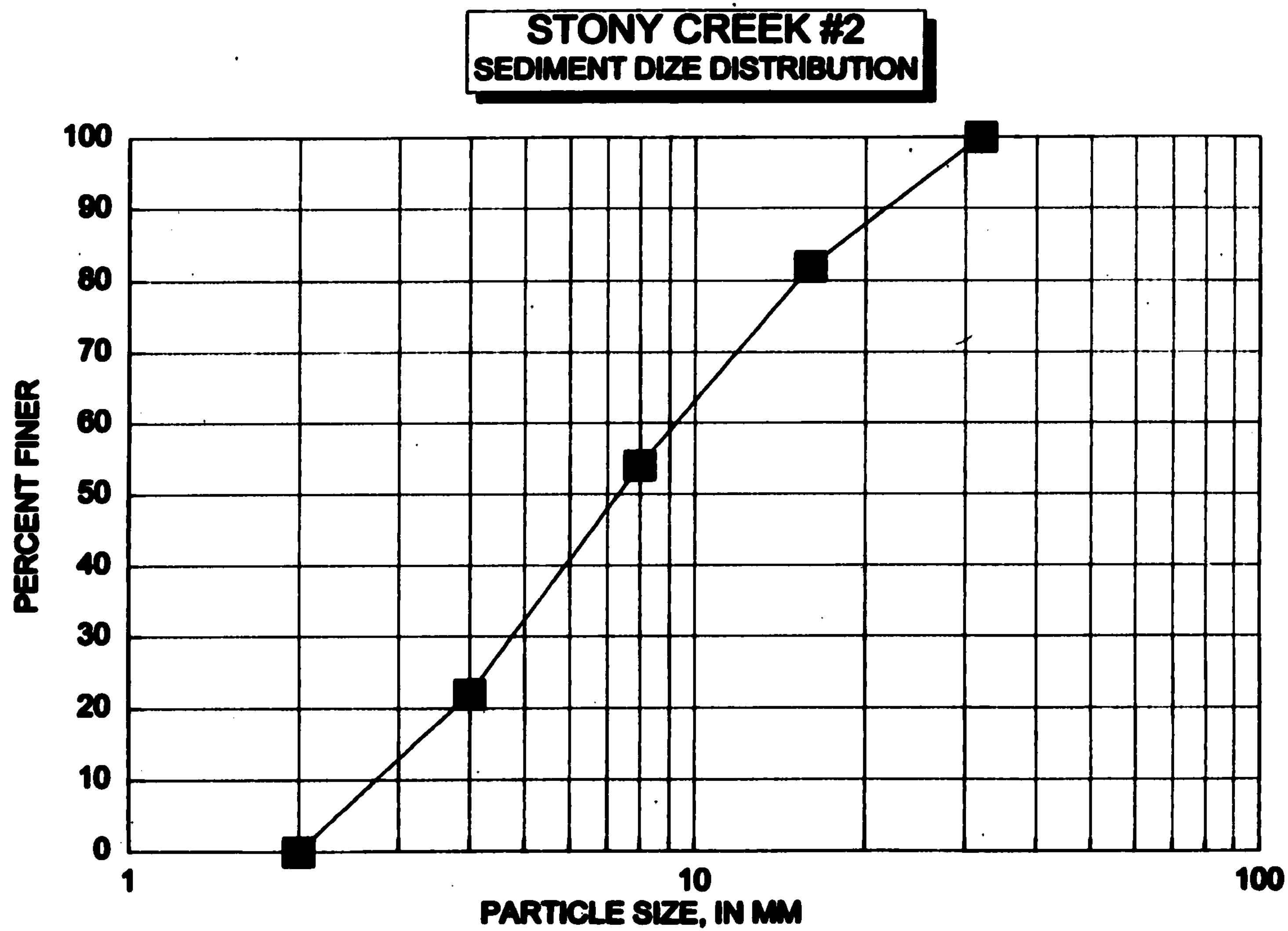

Figure 3.37 Stony Creek #2 gradations

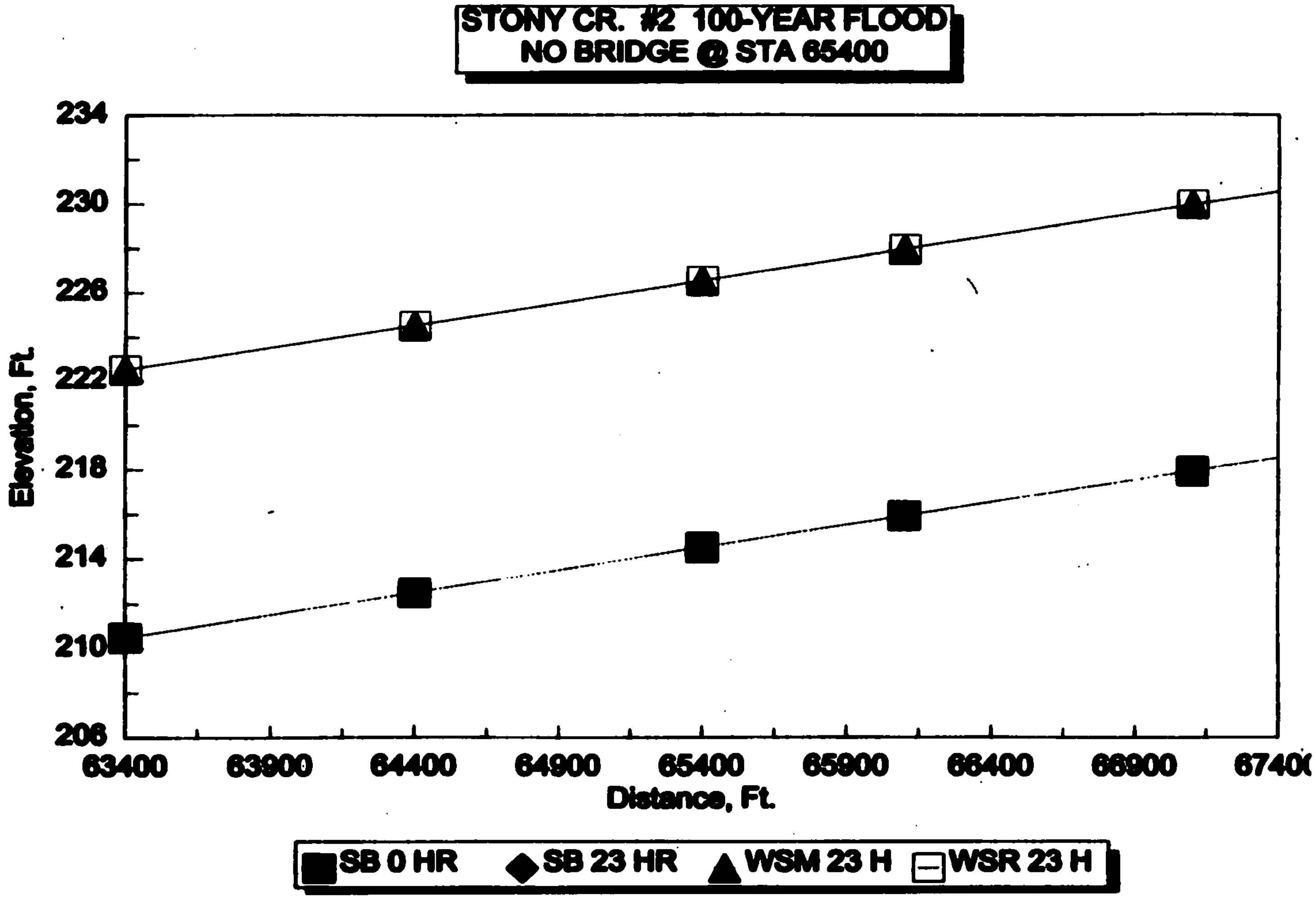

Figure 3.38 Stony Creek #2 profiles, no bridge

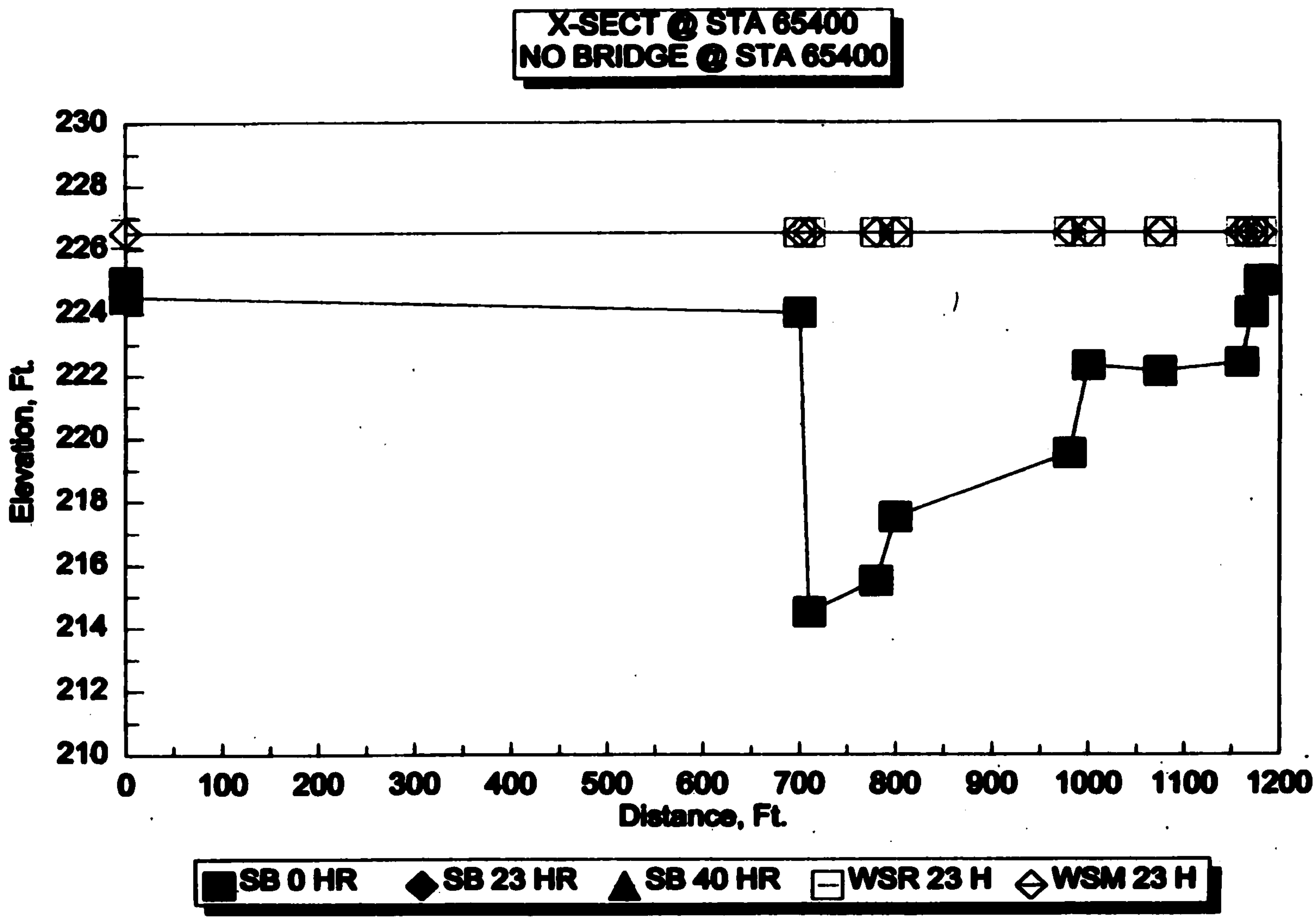

Figure 3.39 Stony Creek #2 cross-section, no bridge

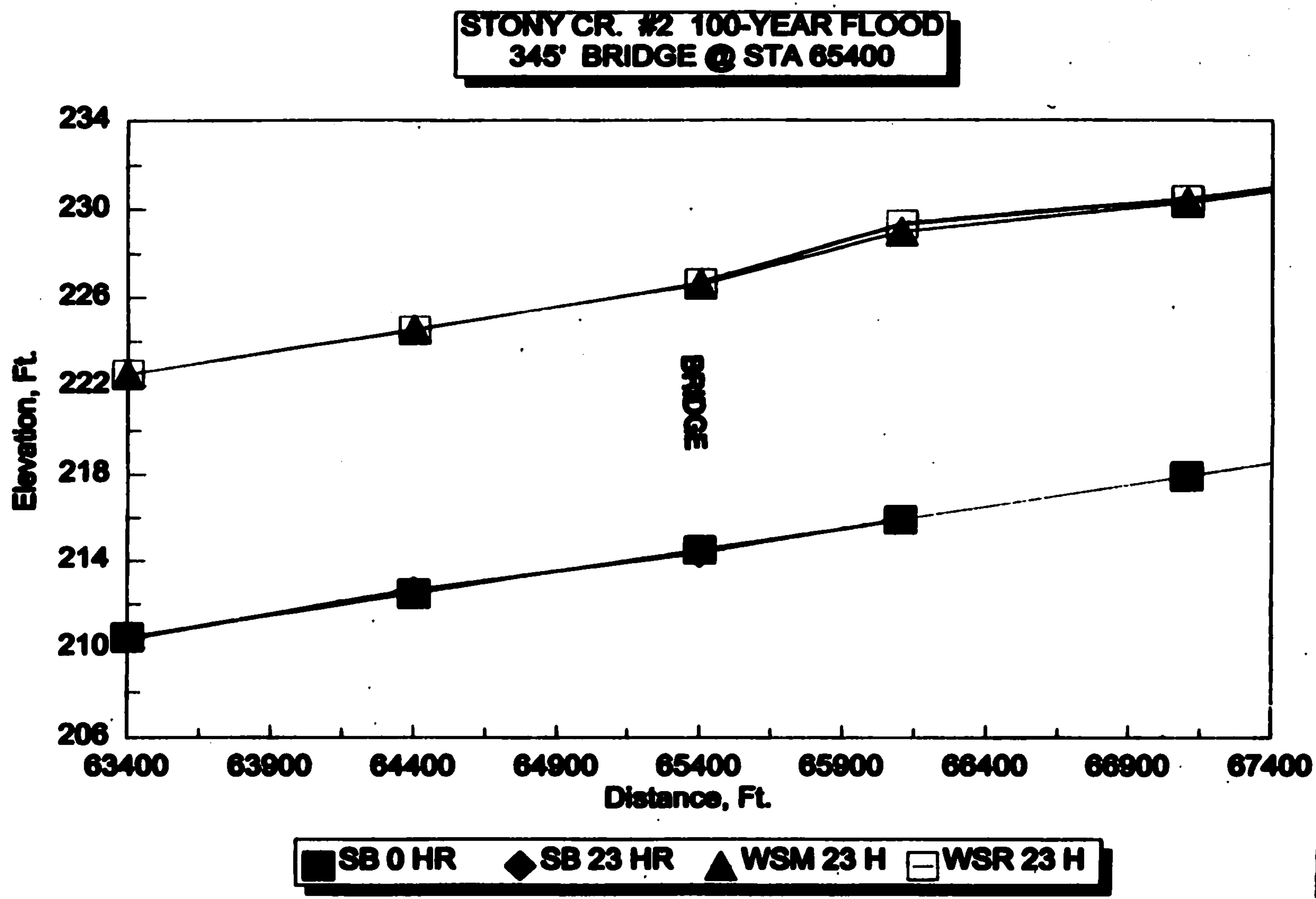

Figure 3.40 Stony Creek #2 profiles, 345' bridge

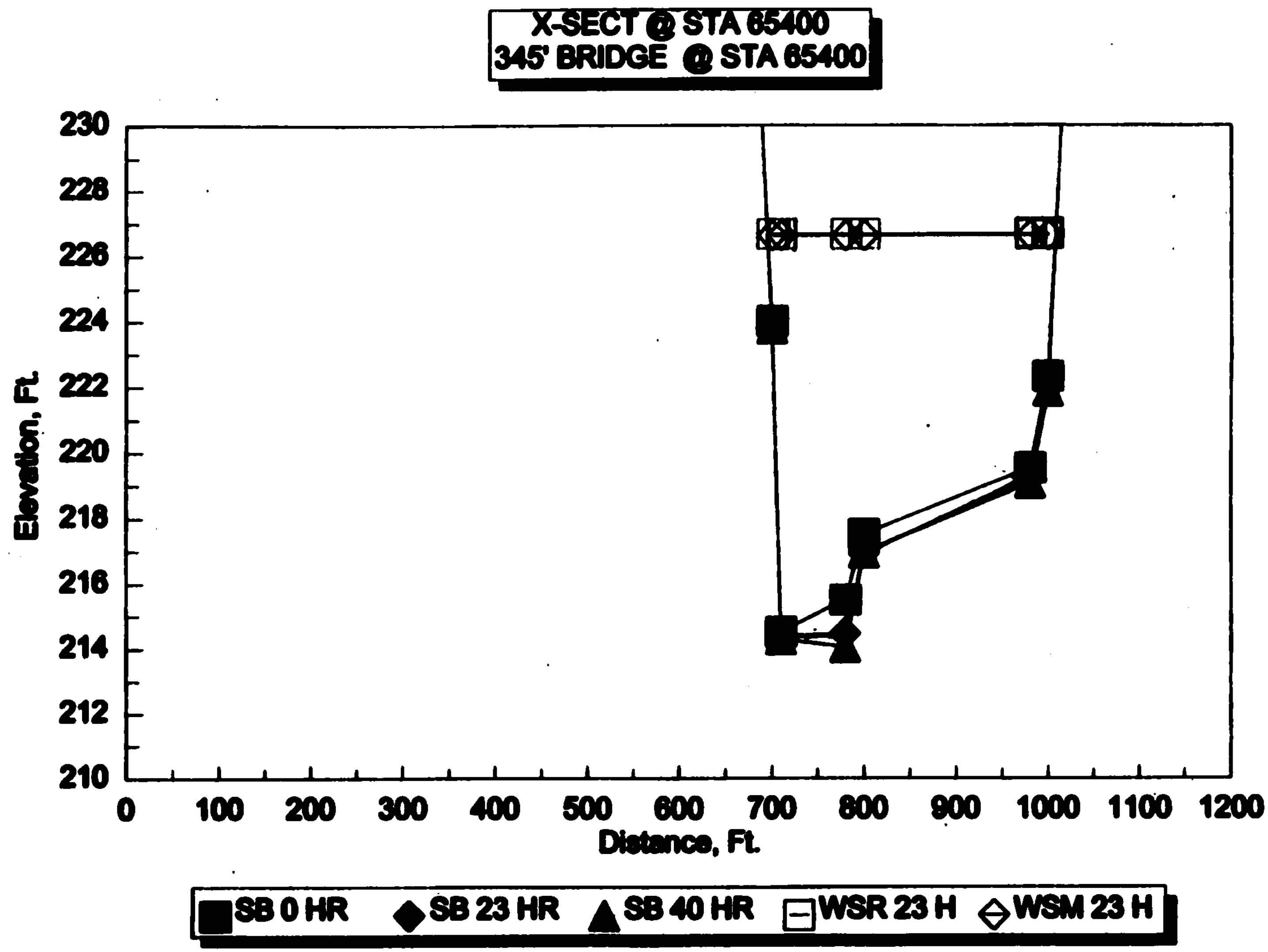

Figure 3.41 Stony Creek #2 cross-section, 345' bridge

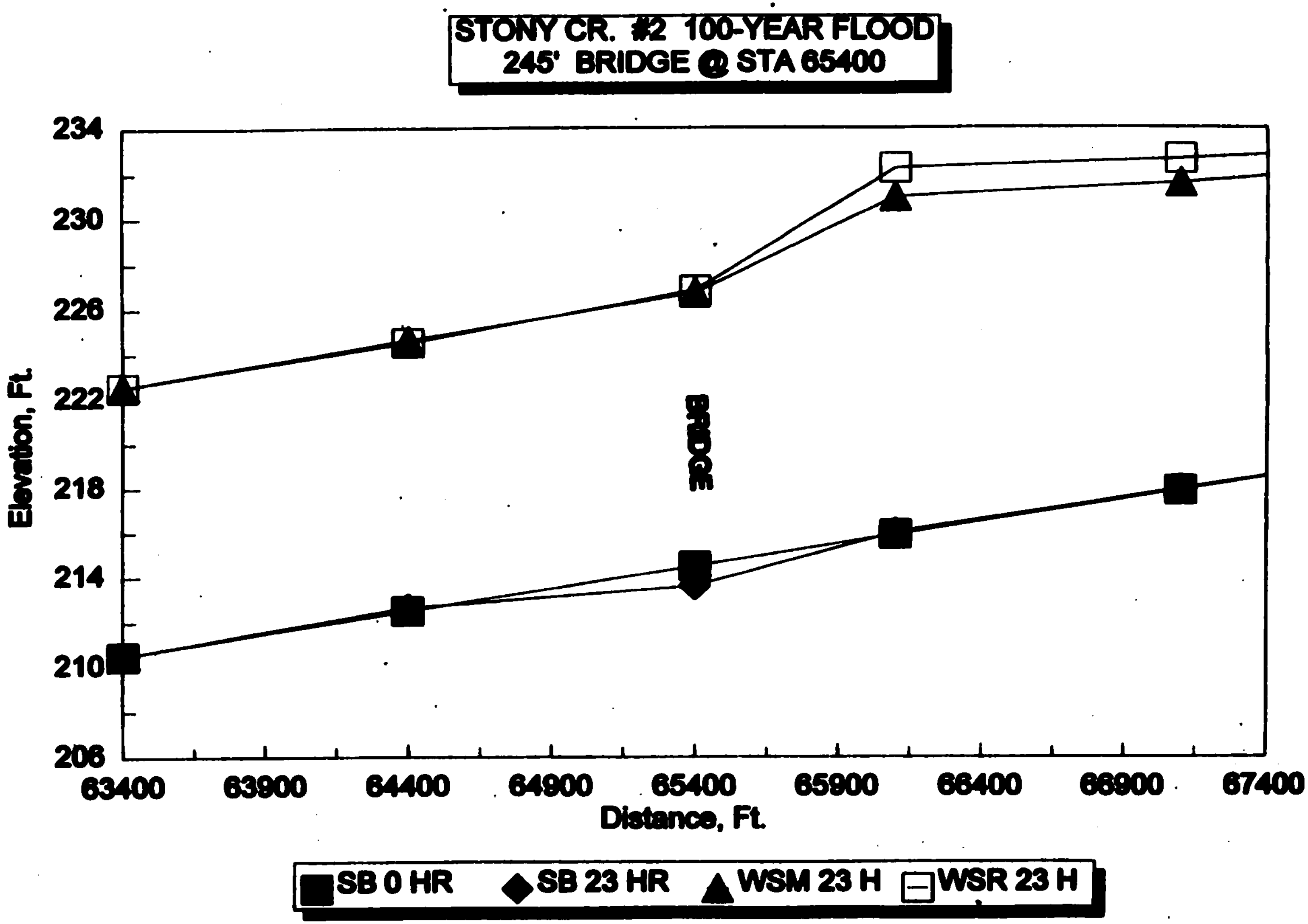

Figure 3.42 Stony Creek #2 profiles, 245' bridge

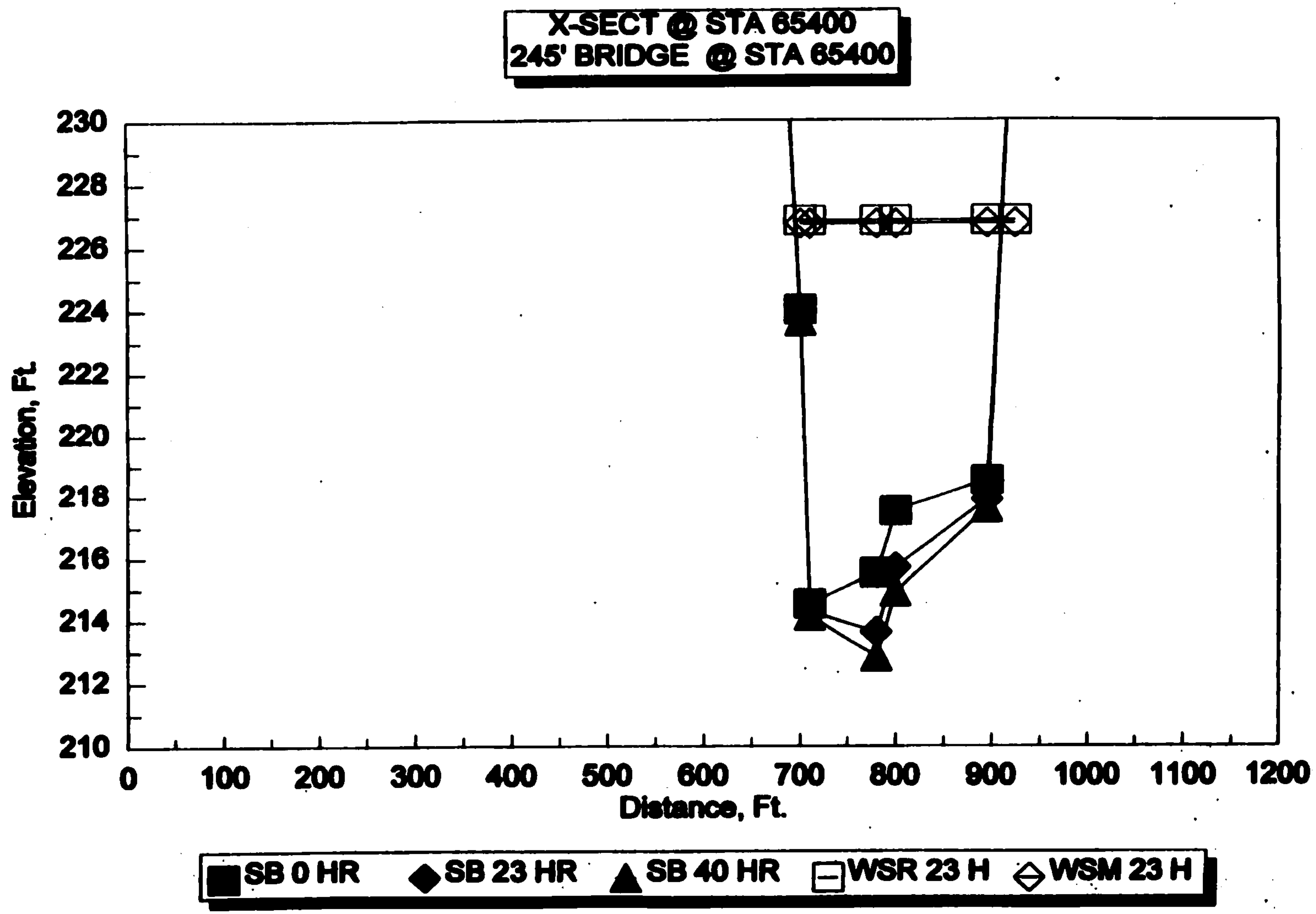

Figure 3.43 Stony Creek #2 cross-section, 245' bridge

Figure 3.44 Gibbon study site

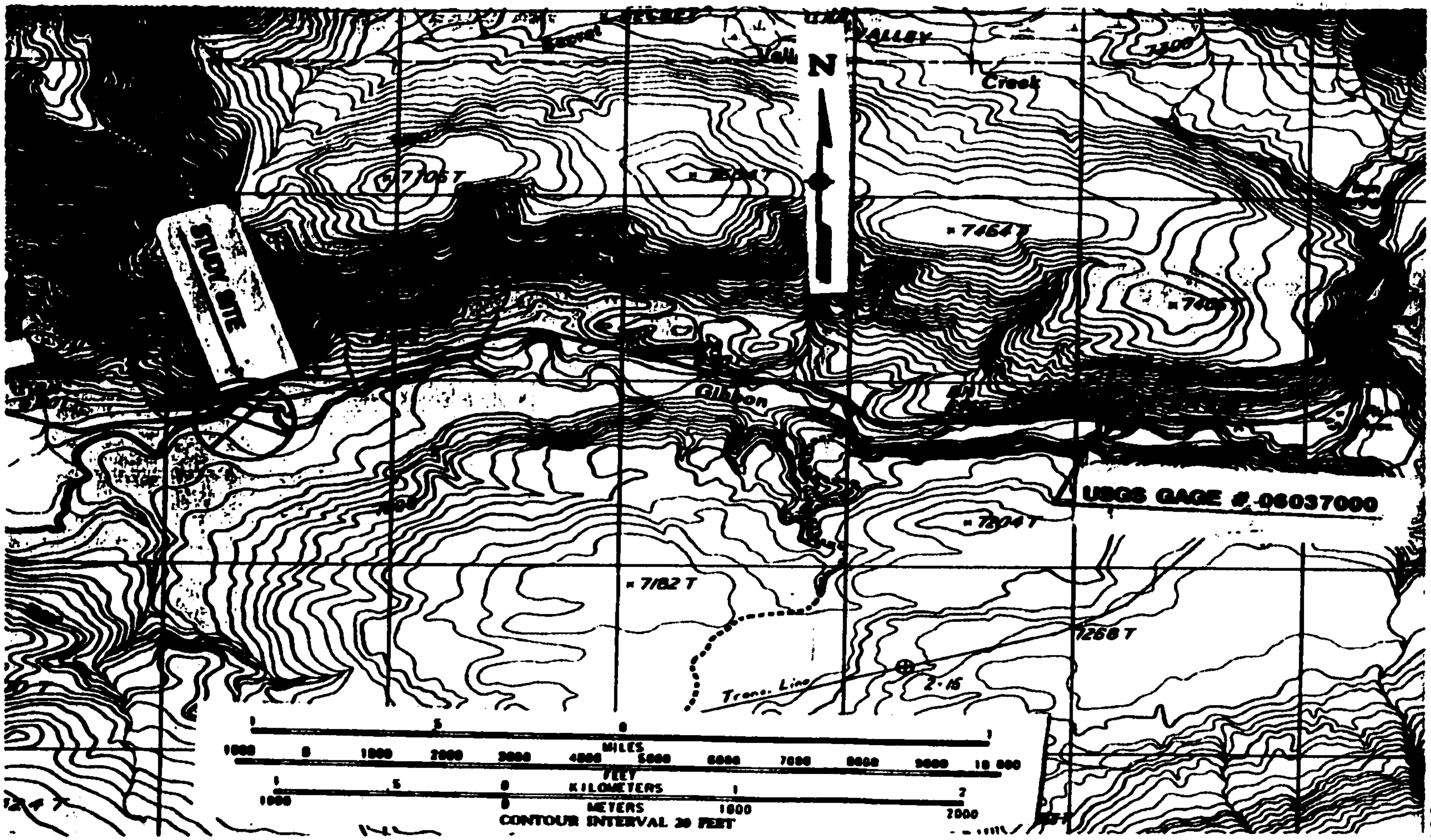

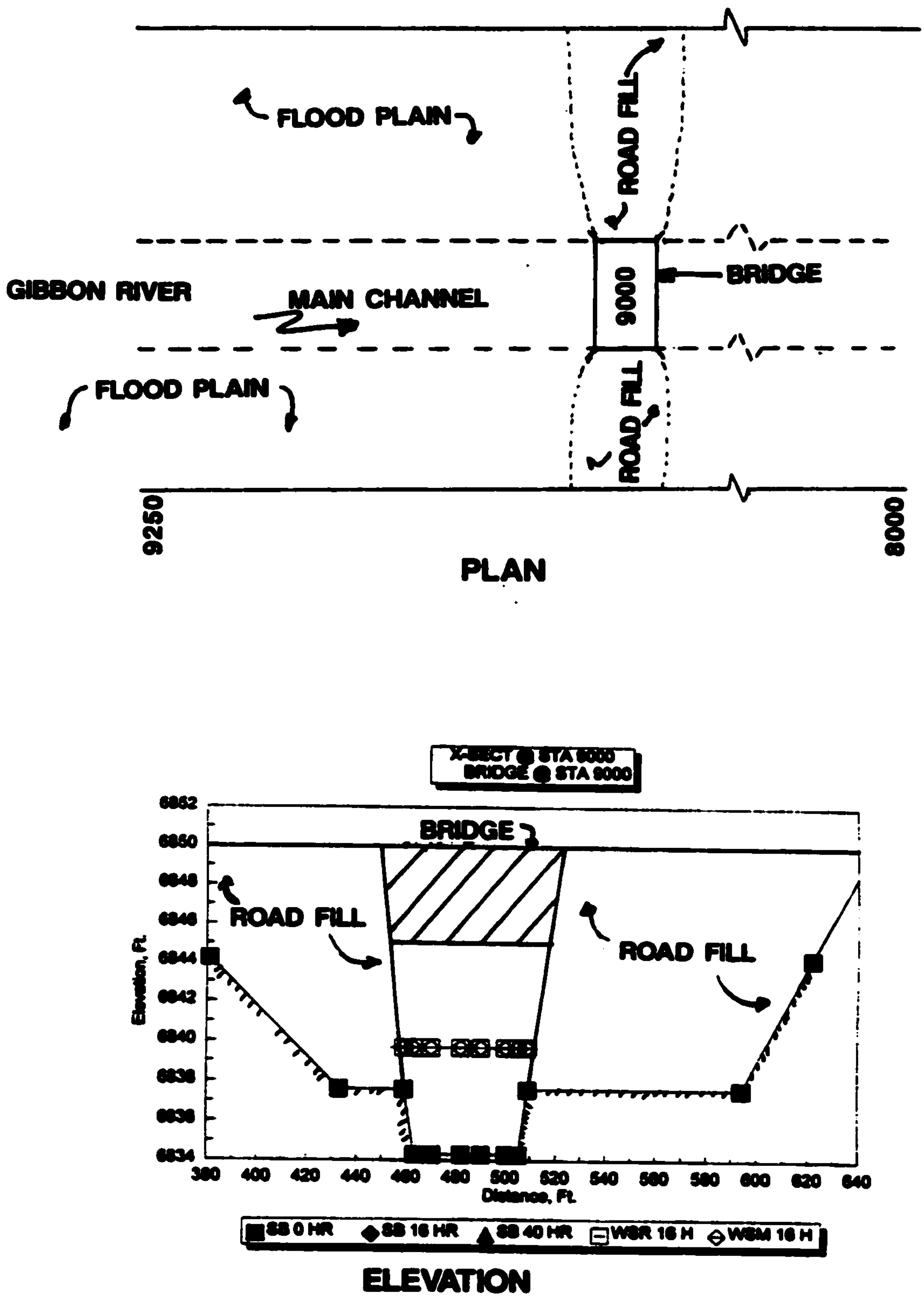

Figure 3.45 Gibbon bridge layout

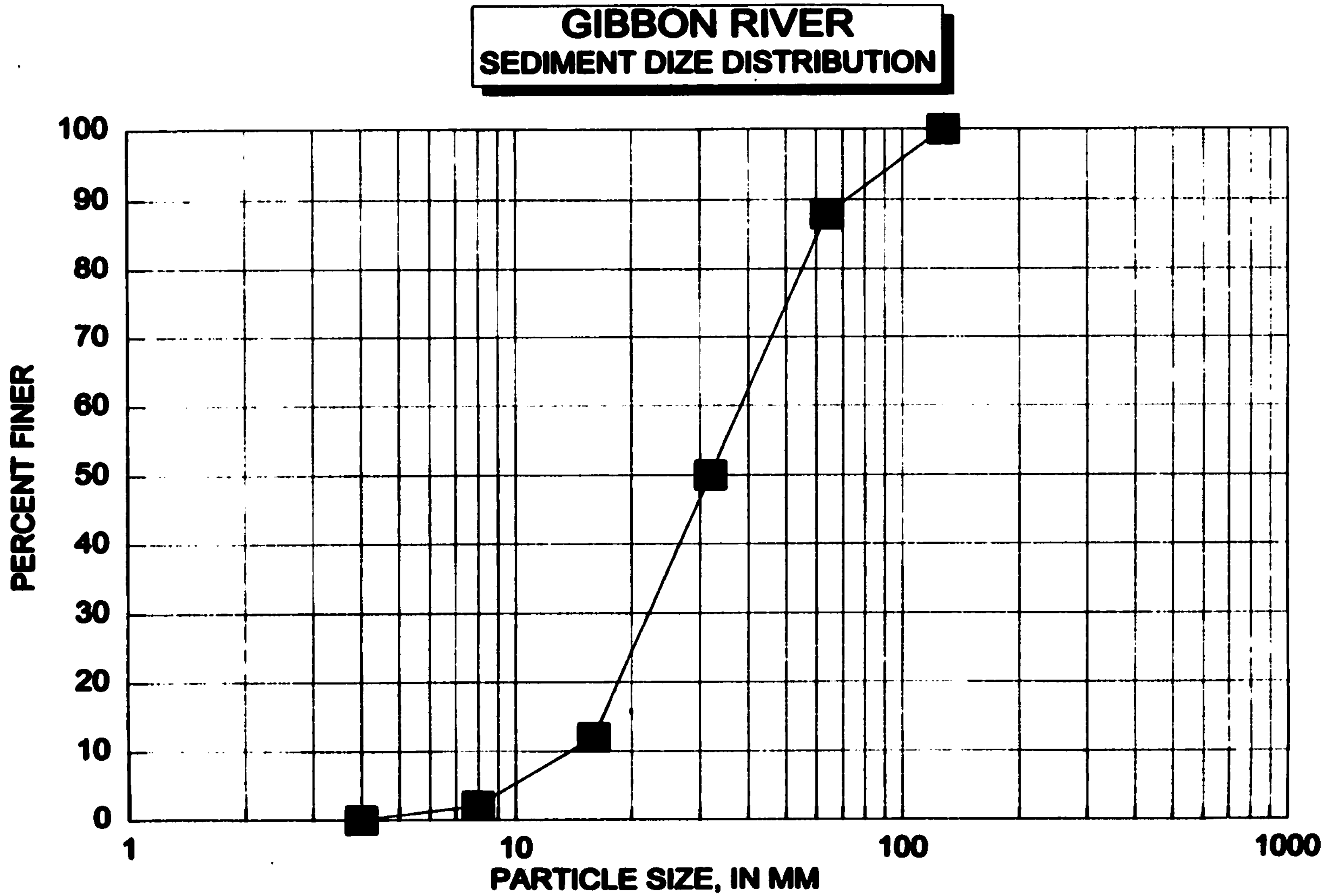

Figure 3.46 Gibbon gradation

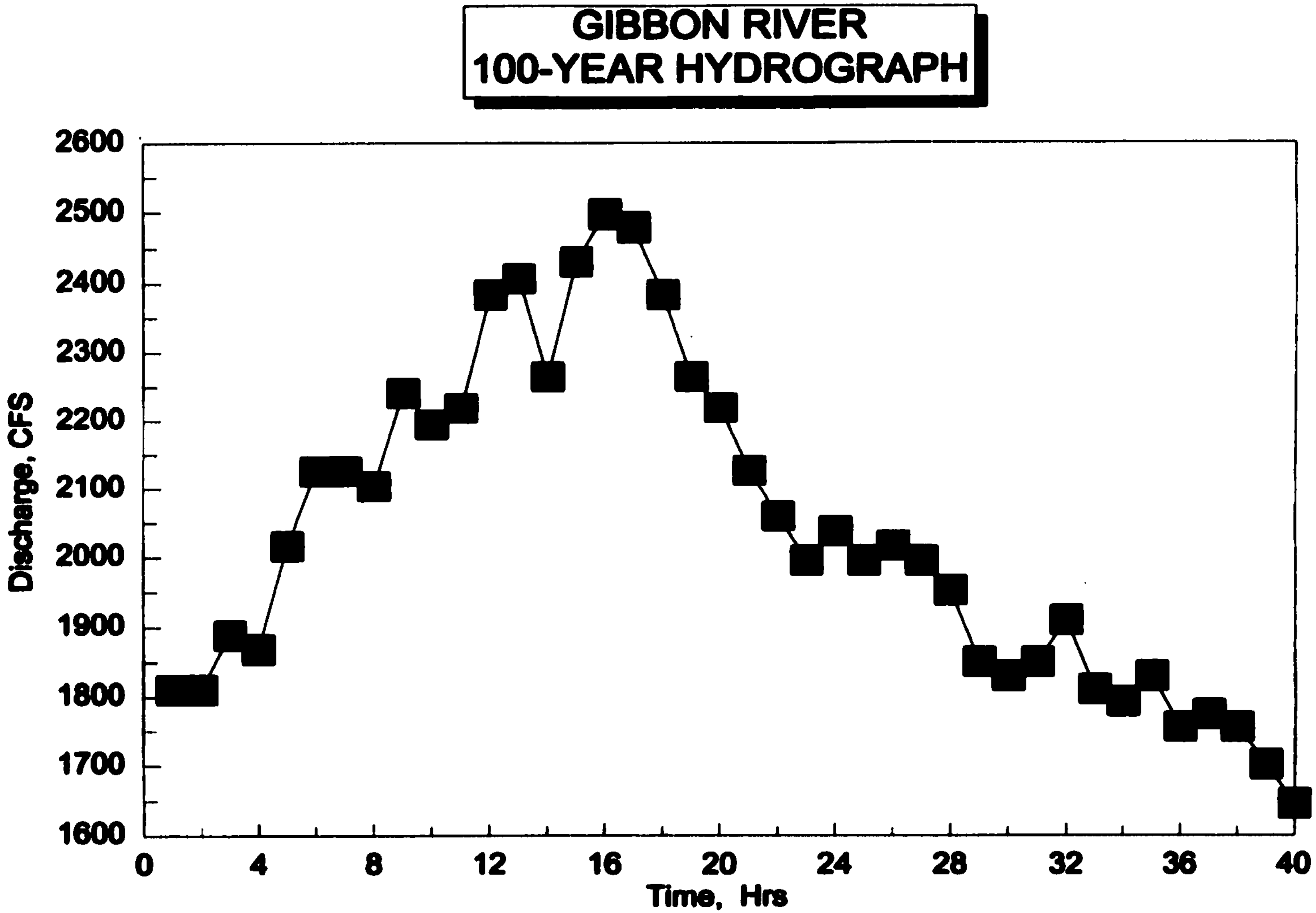

Figure 3.47 Gibbon hydrograph

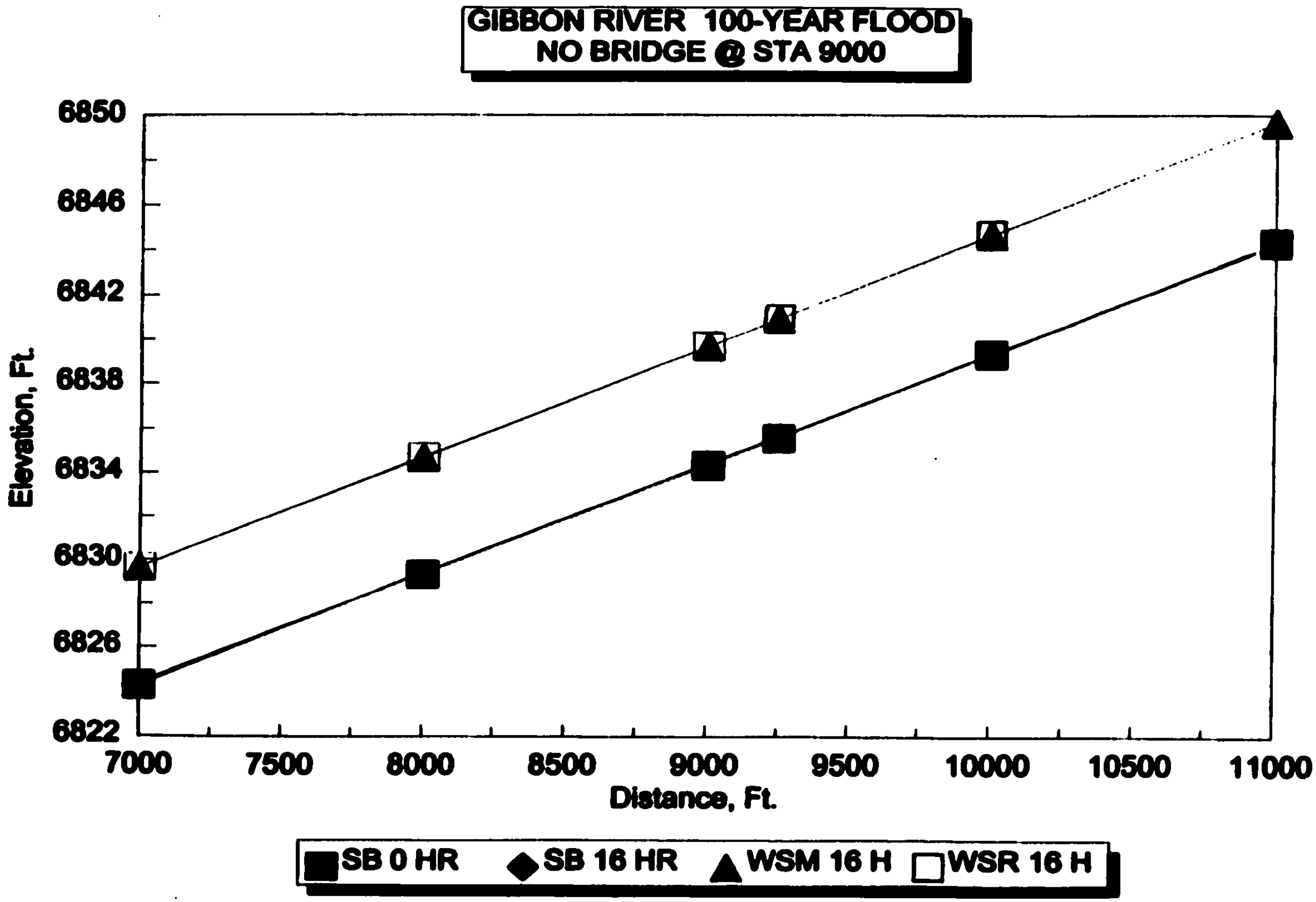

Figure 3.48 Gibbon profiles, no bridge

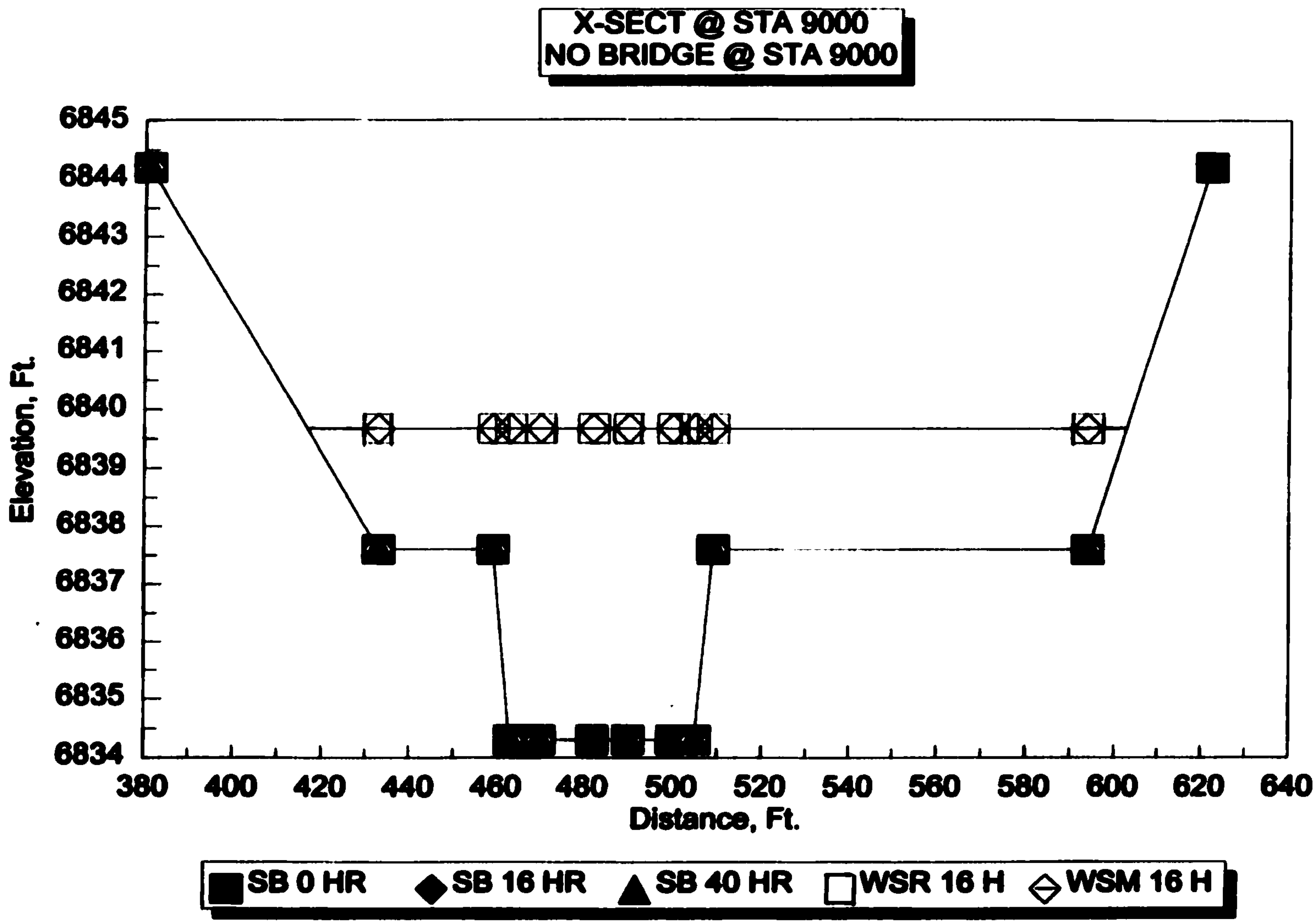

Figure 3.49 Gibbon cross-section, no bridge

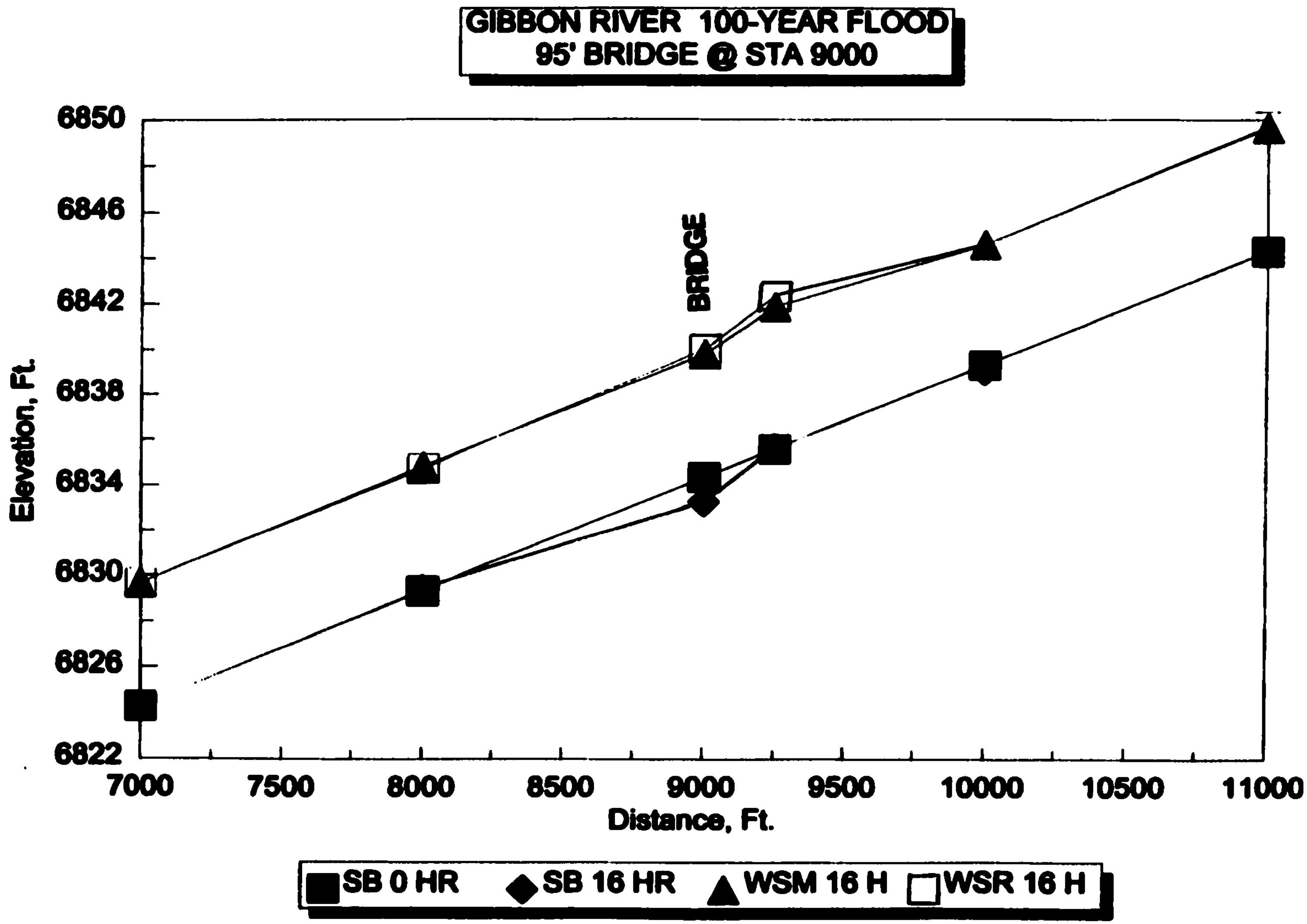

Figure 3.50 Gibbon profiles, 95' bridge

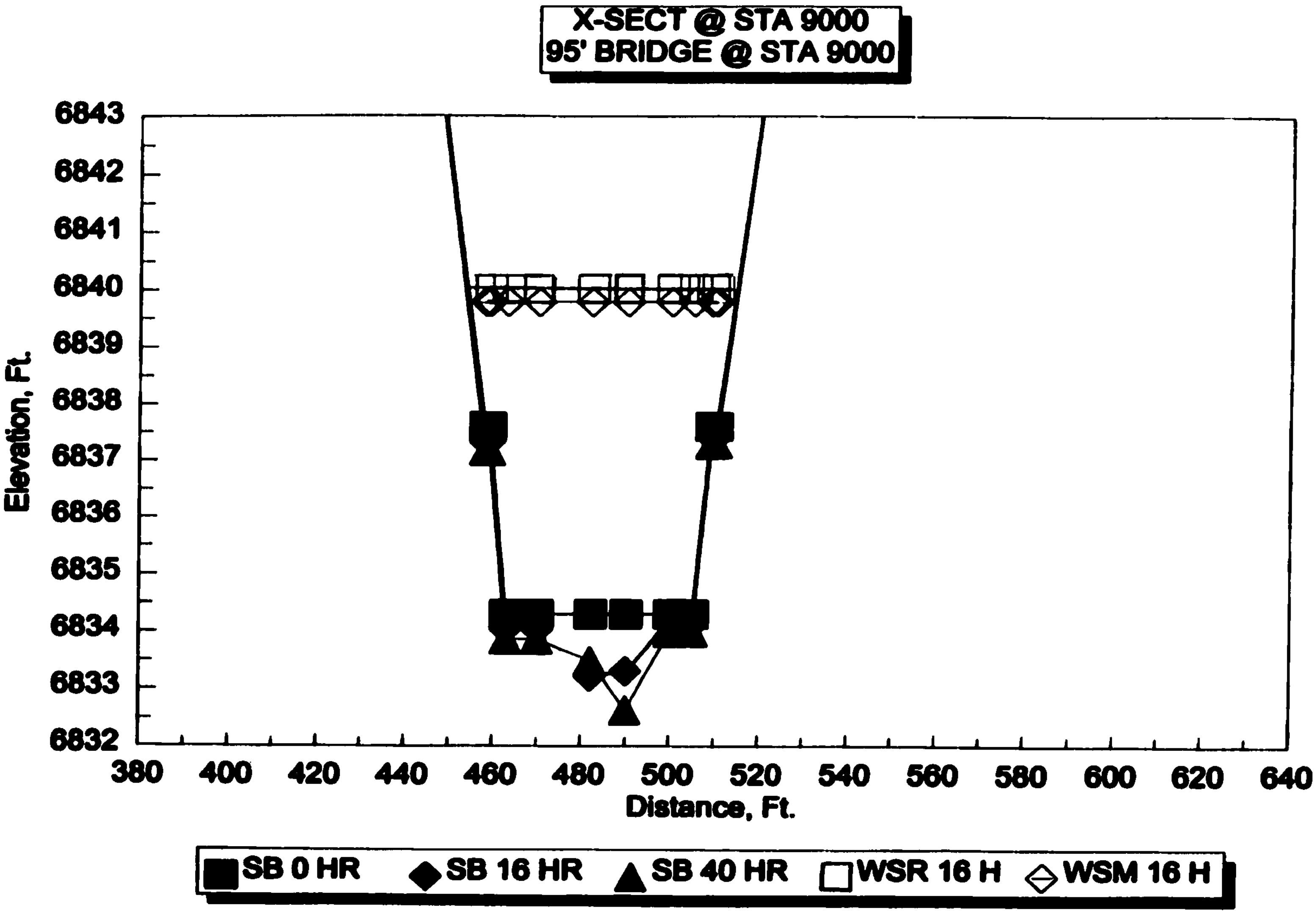

Figure 3.51 Gibbon cross-section, 95' bridge

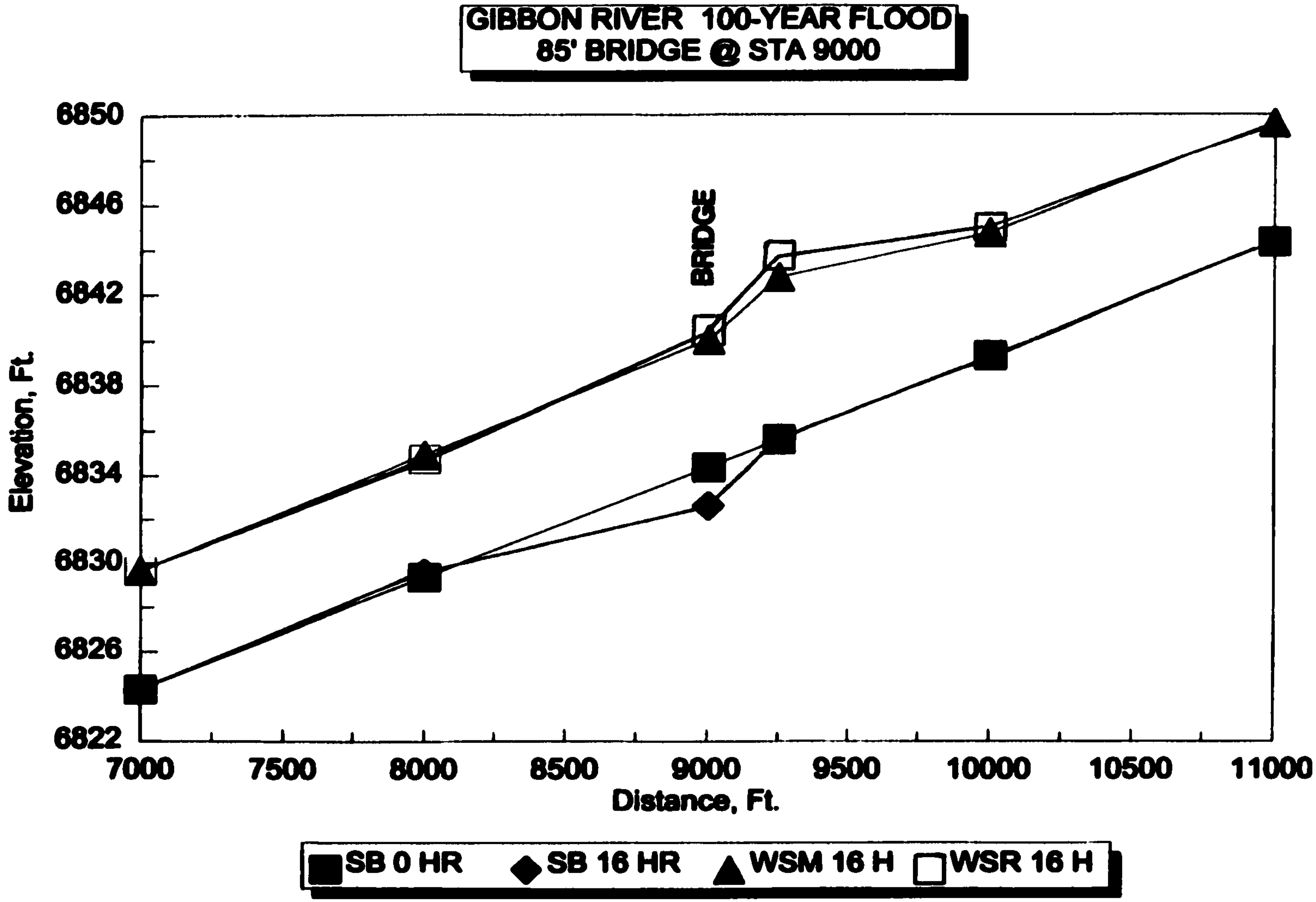

Figure 3.52 Gibbon profiles, 85' bridge

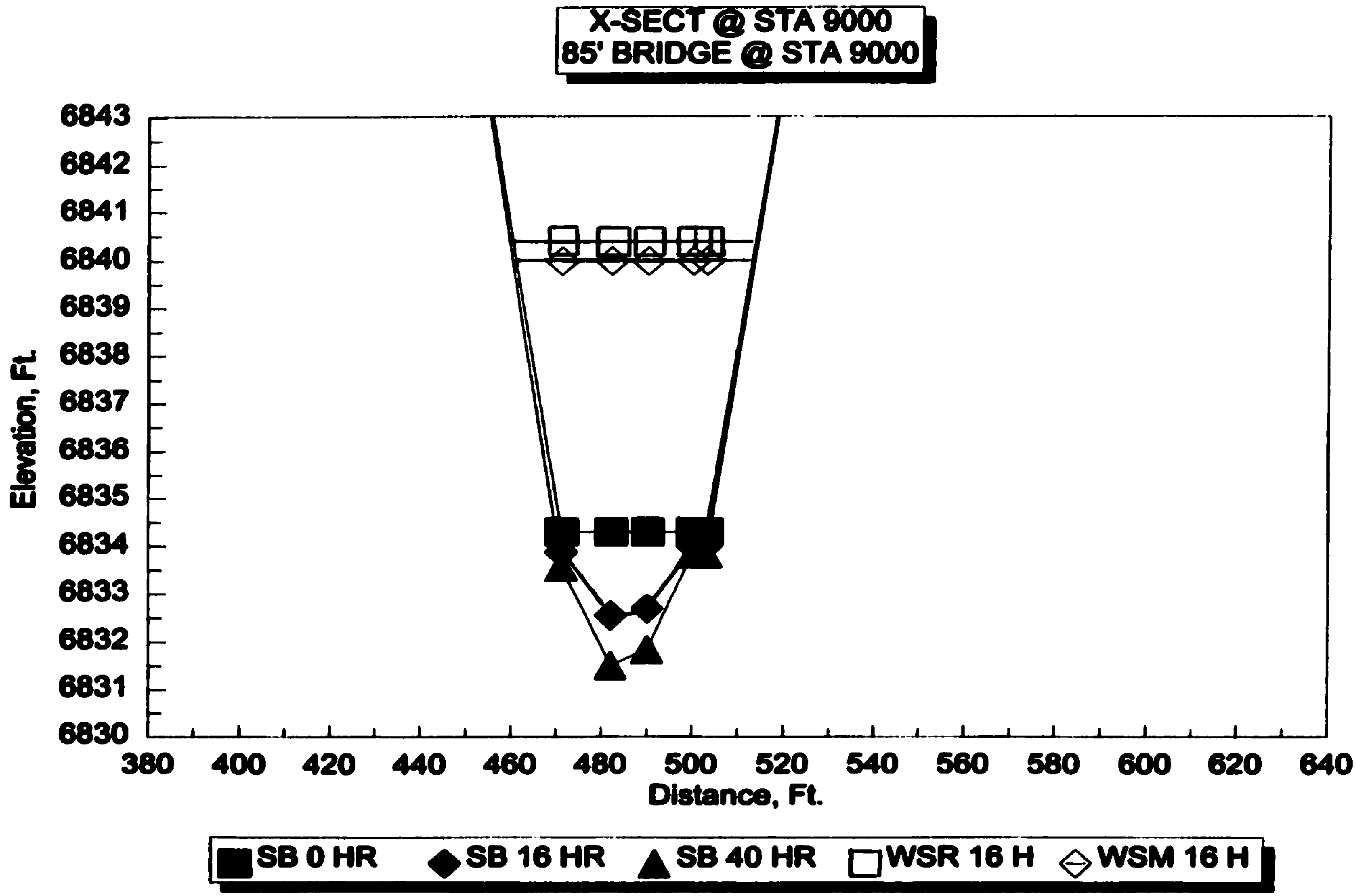

Figure 3.53 Gibbon cross-section, 85' bridge

Table 3.1 Morphological traits for selected case studies

Case	Sinuosity	Width/Depth	Entrenchment	Slope	Channel Material, d_{50}	Rosgen Class
Nisqually	Low to Moderate	High	Slight	0.001 to 0.02	Gravel, 45	D4
Skagit	Moderate	Moderate	Moderate to Entrenched	< 0.02	Cobble, 80	B3
Stony Creek #1	Moderate	Moderate to High	None to Entrenched	<0.02	Gravel, 16	D4 to F4
Stony Creek #2	Low to Moderate	Moderate to High	None to Moderate	0.001 to 0.02	Gravel, 8	C4 to D4
Gibbon	Moderate	Moderate	Slight	<0.02	Gravel, 32	C4 to E4

Sinuosity, width/depth, entrenchment, slope, and channel material as defined in Rosgen (1996).

Table 3.2 Typical hydraulic values for selected case studies

Case	Q100, cfs	Manning's n	Energy Slopes	Froude #	Flow Depths, ft	Velocities, fps	Flow Widths, ft
Nisqually*	10400	0.05 to 0.055	0.006 to 0.019	0.3 to 1.0	5 to 8	5 to 8	300 to 900
Skagit	73460	0.04	0.002 to 0.003	0.5 to 0.7	24 to 28	11 to 15	300 to 350
Stony Creek #1	23300	0.04	0.001 to 0.002	0.3 to 0.5	10 to 15	4 to 9	300 to 800
Stony Creek #2	23300	0.04	0.002	0.4 to 0.5	9 to 12	7 to 8	1100 to 1200
Gibbon	2500	0.04	0.005	0.5 to 0.6	5 to 6	7 to 8	150 to 200

* For Nisqually, the above values apply from Sta 1660 to Sta 7145

Table 3.3 Nisqually HEC-2/BRI-STARS comparisons

STATION	MINIMUM BED ELEVATION, ft.	HEC-2 WSEL, ft.	BRI-STARS WSEL, ft.	NET DIFF., ft
0	1714.00	1722.68	1722.68	0.00
500	1720.40	1727.46	1727.44	-0.02
1090	1729.00	1734.49	1734.33	-0.16
1660	1734.30	1740.37	1740.38	0.01
2540	1740.00	1747.39	1748.20	0.81
3120	1746.50	1751.77	1751.91	0.14
3670	1750.50	1757.97	1757.51	-0.46
4035	1754.00	1760.90	1760.90	0.00
5005	1766.30	1771.44	1771.28	-0.16
5605	1770.30	1776.68	1776.66	-0.02
6165	1776.10	1781.56	1781.51	-0.05
7145	1787.70	1793.84	1793.64	-0.20
7905	1790.30	1800.02	1800.00	-0.02
8535	1799.40	1805.20	1805.42	0.22
9335	1804.50	1813.14	1813.66	0.52
10495	1815.20	1820.66	1820.67	0.01
11735	1829.20	1834.98	1835.65	0.67
12695	1840.00	1847.71	1846.71	-1.00
13795	1847.10	1854.69	1854.73	0.04
14965	1861.70	1867.76	1868.06	0.30
16085	1877.00	1885.80	1885.33	-0.47
17245	1893.50	1900.21	1900.22	0.01
18245	1906.00	1912.23	1912.08	-0.15
19285	1918.50	1925.18	1925.26	0.08
20485	1940.10	1945.45	1945.23	-0.22
21345	1951.80	1958.35	1958.31	-0.04
22315	1963.90	1970.34	1970.20	-0.14
23285	1979.90	1984.63	1984.70	0.07
24345	1993.50	1999.49	1999.68	0.19

Table 3.4 Nisqually BRI-STARS mobile/rigid comparisons

NISQUALLY RIVER, 100-YEAR FLOOD

STA, ft	2977, cfs 0, hrs Bed Ele ft	10400, cfs 13, hrs Bed Ele ft	Net Bed Elev. Diff ft	10400, cf 13, hrs Bed Ele ft	3328, cfs 34, hrs Bed Ele ft	Net Bed Elev. Diff ft	2977, cfs 0, hrs Bed Ele ft	3328, cfs 34, hrs Bed Ele ft	Net Bed Elev. Diff ft	RIGID WSEL 10400, cf ft	MOBILE WSEL 10400, cf ft	Net WSEL Elev. Diff ft
24345	1993.50	1993.50	0.00	1993.50	1993.50	0.00	1993.50	1993.50	0.00	1999.68	1999.44	-0.24
23285	1979.90	1979.72	-0.18	1979.72	1979.49	-0.23	1979.90	1979.49	-0.41	1984.70	1984.73	0.03
22315	1963.90	1964.08	0.18	1964.08	1964.22	0.14	1963.90	1964.22	0.32	1970.20	1970.06	-0.14
21345	1951.80	1951.84	0.04	1951.84	1951.93	0.09	1951.80	1951.93	0.13	1958.31	1958.51	0.20
20485	1940.10	1940.12	0.02	1940.12	1940.19	0.07	1940.10	1940.19	0.09	1945.23	1945.09	-0.14
19285	1918.50	1918.41	-0.09	1918.41	1918.31	-0.10	1918.50	1918.31	-0.19	1925.26	1925.44	0.18
18245	1906.00	1906.19	0.19	1906.19	1906.43	0.24	1906.00	1906.43	0.43	1912.08	1911.86	-0.22
17245	1893.50	1893.47	-0.03	1893.47	1893.45	-0.02	1893.50	1893.45	-0.05	1900.22	1900.62	0.40
16085	1877.00	1876.96	-0.04	1876.96	1876.06	-0.90	1877.00	1876.06	-0.94	1885.33	1884.52	-0.81
14965	1861.70	1861.82	0.12	1861.82	1861.85	0.03	1861.70	1861.85	0.15	1866.06	1866.71	0.65
13795	1847.10	1848.35	1.25	1848.35	1853.28	4.93	1847.10	1853.28	6.18	1854.73	1856.80	2.07
12895	1840.00	1839.98	-0.02	1839.98	1839.68	-0.30	1840.00	1839.68	-0.32	1846.71	1846.99	0.28
11735	1829.20	1829.10	-0.10	1829.10	1828.99	-0.11	1829.20	1828.99	-0.21	1835.65	1835.51	-0.14
10495	1815.20	1815.33	0.13	1815.33	1815.52	0.19	1815.20	1815.52	0.32	1820.67	1820.99	0.32
9335	1804.50	1804.54	0.04	1804.54	1804.56	0.02	1804.50	1804.56	0.06	1813.66	1812.71	-0.95
8535	1799.40	1798.95	-0.45	1798.95	1799.68	0.73	1799.40	1799.68	0.28	1805.42	1805.83	0.41
7905	1790.30	1790.62	0.32	1790.62	1791.16	0.54	1790.30	1791.16	0.86	1800.00	1803.19	3.19
7145	1787.70	1788.95	1.25	1788.95	1789.07	0.12	1787.70	1789.07	1.37	1793.64	1795.43	1.79
6165	1776.10	1776.47	0.37	1776.47	1776.74	0.27	1776.10	1776.74	0.64	1781.51	1781.81	0.30
5605	1770.30	1771.23	0.93	1771.23	1772.84	1.61	1770.30	1772.84	2.54	1776.66	1777.01	0.35
5005	1766.30	1765.96	-0.34	1765.96	1765.48	-0.48	1766.30	1765.48	-0.82	1771.28	1771.14	-0.14
4035	1754.00	1753.79	-0.21	1753.79	1753.46	-0.33	1754.00	1753.46	-0.54	1760.90	1760.86	-0.04
3670	1750.50	1750.04	-0.46	1750.04	1749.36	-0.68	1750.50	1749.36	-1.14	1757.51	1757.47	-0.04
3120	1746.50	1746.94	0.44	1746.94	1747.40	0.46	1746.50	1747.40	0.90	1751.91	1752.15	0.24
2540	1740.00	1740.04	0.04	1740.04	1740.08	0.04	1740.00	1740.08	0.08	1748.20	1748.88	0.68
1660	1734.30	1737.65	3.35	1737.65	1739.11	1.46	1734.30	1739.11	4.81	1740.38	1743.54	3.16
1090	1729.00	1728.81	-0.19	1728.81	1728.77	-0.04	1729.00	1728.77	-0.23	1734.33	1740.95	6.62
500	1720.40	1727.29	6.89	1727.29	1726.79	-0.50	1720.40	1726.79	6.39	1727.44	1735.45	8.01
0	1714.00	1713.46	-0.54	1713.46	1712.96	-0.50	1714.00	1712.96	-1.04	1722.68	1722.44	-0.24

Table 3.5 Nisqually comparisons for STA 3670 bridge

NISQUALLY RIVER, 100-YEAR FLOOD
BRIDGE @ STA 3670

	No Bridge			315' Bridge			250' Bridge			200' Bridge		
	Rigid WSEL 10400 cfs	Mobile WSEL 10400 cfs	Net WSEL Elev. Diff	Rigid WSEL 10400 cfs	Mobile WSEL 10400 cfs	Net WSEL Elev. Diff	Rigid WSEL 10400 cfs	Mobile WSEL 10400 cfs	Net WSEL Elev. Diff	Rigid WSEL 10400 cfs	Mobile WSEL 10400 cfs	Net WSEL Elev. Diff
STA, ft	ft	ft	ft	ft	ft	ft	ft	ft	ft	ft	ft	ft
24345	1999.68	1999.44	-0.24	1999.68	1999.42	-0.26	1999.68	1999.42	-0.26	1999.68	1999.42	-0.26
23285	1984.70	1984.73	0.03	1984.70	1984.72	0.02	1984.70	1984.72	0.02	1984.70	1984.72	0.02
22315	1970.20	1970.06	-0.14	1970.20	1970.03	-0.17	1970.20	1970.03	-0.17	1970.20	1970.03	-0.17
21345	1958.31	1958.51	0.20	1958.31	1958.49	0.18	1958.31	1958.49	0.18	1958.31	1958.49	0.18
20465	1945.23	1945.09	-0.14	1945.23	1945.08	-0.15	1945.23	1945.08	-0.15	1945.23	1945.08	-0.15
19285	1925.26	1925.44	0.18	1925.26	1925.42	0.16	1925.26	1925.42	0.16	1925.26	1925.42	0.16
18245	1912.08	1911.86	-0.22	1912.08	1911.84	-0.24	1912.08	1911.84	-0.24	1912.08	1911.84	-0.24
17245	1900.22	1900.62	0.40	1900.22	1900.60	0.38	1900.22	1900.60	0.38	1900.22	1900.60	0.38
16065	1885.33	1884.52	-0.81	1885.33	1884.50	-0.83	1885.33	1884.50	-0.83	1885.33	1884.50	-0.83
14965	1868.06	1868.71	0.65	1868.06	1868.69	0.63	1868.06	1868.70	0.64	1868.06	1868.69	0.63
13795	1854.73	1856.80	2.07	1854.73	1856.78	2.05	1854.73	1856.78	2.05	1854.73	1856.77	2.04
12695	1846.71	1846.99	0.28	1846.71	1846.96	0.25	1846.71	1846.97	0.26	1846.71	1846.97	0.26
11735	1835.66	1835.51	-0.14	1835.65	1835.49	-0.16	1835.65	1835.49	-0.16	1835.65	1835.49	-0.16
10495	1820.67	1820.99	0.32	1820.67	1820.97	0.30	1820.67	1820.97	0.30	1820.67	1820.98	0.31
9335	1813.66	1812.71	-0.95	1813.65	1812.68	-0.97	1813.65	1812.66	-0.99	1813.65	1812.66	-0.99
8535	1805.42	1805.83	0.41	1805.42	1805.81	0.39	1805.42	1805.83	0.41	1805.42	1805.83	0.41
7905	1800.00	1803.19	3.19	1799.95	1803.18	3.23	1799.94	1803.23	3.29	1799.96	1803.24	3.28
7145	1793.64	1795.43	1.79	1793.67	1795.41	1.74	1793.68	1795.30	1.62	1793.67	1795.31	1.64
6165	1781.51	1781.81	0.30	1781.49	1781.79	0.30	1781.49	1781.86	0.37	1781.49	1781.86	0.37
5605	1776.66	1777.01	0.35	1776.93	1777.06	0.13	1777.07	1777.30	0.23	1776.85	1777.34	0.49
5005	1771.28	1771.14	-0.14	1771.12	1771.06	-0.06	1771.05	1770.94	-0.11	1771.16	1770.91	-0.25
4035	1760.90	1760.86	-0.04	1761.51	1761.11	-0.40	1762.98	1761.99	-0.99	1764.53	1763.12	-1.41
3670	1757.51	1757.47	-0.04	1757.64	1757.62	-0.02	1757.94	1757.59	-0.35	1758.07	1757.59	-0.48
3120	1751.91	1752.15	0.24	1751.91	1752.34	0.43	1751.91	1752.18	0.27	1751.91	1752.24	0.33
2540	1748.20	1748.88	0.68	1748.20	1748.93	0.73	1748.20	1748.85	0.65	1748.20	1748.92	0.72
1660	1740.38	1743.54	3.16	1740.38	1743.57	3.19	1740.38	1743.52	3.14	1740.38	1743.57	3.19
1090	1734.33	1740.95	6.62	1734.33	1740.97	6.64	1734.33	1740.94	6.61	1734.33	1740.98	6.65
500	1727.44	1735.45	8.01	1727.44	1735.47	8.03	1727.44	1735.51	8.07	1727.44	1735.47	8.03
0	1722.68	1722.44	-0.24	1722.68	1722.42	-0.26	1722.68	1722.47	-0.21	1722.68	1722.42	-0.26

Table 3.6 Nisqually comparisons for STA 3120 bridge

NISQUALLY RIVER, 100-YEAR FLOOD
BRIDGE @ STA 3120

	No Bridge			480' Bridge			510' Bridge			540' Bridge		
STA, ft	Rigid WSEL 10400 cfs ft	Mobile WSEL 10400 cfs ft	Net WSEL Elev. Diff ft	Rigid WSEL 10400 cfs ft	Mobile WSEL 10400 cfs ft	Net WSEL Elev. Diff ft	Rigid WSEL 10400 cfs ft	Mobile WSEL 10400 cfs ft	Net WSEL Elev. Diff ft	Rigid WSEL 10400 cfs ft	Mobile WSEL 10400 cfs ft	Net WSEL Elev. Diff ft
24345	1999.68	1999.44	-0.24	1999.68	1999.44	-0.24	1999.68	1999.44	-0.24	1999.68	1999.44	-0.24
23285	1984.70	1984.73	0.03	1984.70	1984.73	0.03	1984.70	1984.73	0.03	1984.70	1984.73	0.03
22315	1970.20	1970.06	-0.14	1970.20	1970.06	-0.14	1970.20	1970.05	-0.15	1970.20	1970.05	-0.15
21345	1958.31	1958.51	0.20	1958.31	1958.51	0.20	1958.31	1958.51	0.20	1958.31	1958.51	0.20
20485	1945.23	1945.09	-0.14	1945.23	1945.09	-0.14	1945.23	1945.09	-0.14	1945.23	1945.09	-0.14
19285	1925.26	1925.44	0.18	1925.26	1925.44	0.18	1925.26	1925.44	0.18	1925.26	1925.44	0.18
18245	1912.08	1911.86	-0.22	1912.08	1911.86	-0.22	1912.08	1911.86	-0.22	1912.08	1911.86	-0.22
17245	1900.22	1900.62	0.40	1900.22	1900.62	0.40	1900.22	1900.62	0.40	1900.22	1900.62	0.40
16085	1885.33	1884.52	-0.81	1885.33	1884.52	-0.81	1885.33	1884.53	-0.80	1885.33	1884.53	-0.80
14965	1868.06	1868.71	0.65	1868.06	1868.68	0.62	1868.06	1868.72	0.66	1868.06	1868.67	0.61
13795	1854.73	1856.80	2.07	1854.73	1856.81	2.08	1854.73	1856.79	2.06	1854.73	1856.80	2.07
12695	1846.71	1846.99	0.28	1846.71	1846.95	0.24	1846.71	1846.96	0.25	1846.71	1846.97	0.26
11735	1835.65	1835.51	-0.14	1835.65	1835.54	-0.11	1835.65	1835.51	-0.14	1835.65	1835.52	-0.13
10495	1820.67	1820.99	0.32	1820.67	1820.93	0.26	1820.67	1820.99	0.32	1820.67	1820.96	0.29
9335	1813.66	1812.71	-0.95	1813.66	1812.82	-0.84	1813.66	1812.72	-0.94	1813.66	1812.77	-0.89
8535	1805.42	1805.83	0.41	1805.42	1805.62	0.20	1805.41	1805.82	0.41	1805.41	1805.72	0.31
7905	1800.00	1803.19	3.19	1800.00	1802.64	2.64	1800.02	1803.17	3.15	1800.03	1802.90	2.87
7145	1793.64	1795.43	1.79	1793.64	1795.09	1.45	1793.63	1795.42	1.79	1793.62	1795.25	1.63
6165	1781.51	1781.81	0.30	1781.51	1781.79	0.28	1781.52	1781.82	0.30	1781.53	1781.81	0.28
5605	1776.66	1777.01	0.35	1776.65	1777.01	0.36	1776.60	1777.00	0.40	1776.57	1777.01	0.44
5005	1771.28	1771.14	-0.14	1771.29	1771.15	-0.14	1771.34	1771.15	-0.19	1771.36	1771.15	-0.21
4035	1760.90	1760.86	-0.04	1760.89	1760.81	-0.08	1760.79	1760.81	0.02	1760.74	1760.83	0.09
3670	1757.51	1757.47	-0.04	1759.27	1758.07	-1.20	1758.86	1757.65	-1.21	1758.47	1757.70	-0.77
3120	1751.91	1752.15	0.24	1752.53	1752.93	0.40	1752.45	1753.31	0.86	1752.33	1753.00	0.67
2540	1748.20	1748.88	0.68	1748.20	1748.86	0.66	1748.20	1749.26	1.06	1748.20	1749.15	0.95
1660	1740.38	1743.54	3.16	1740.38	1742.39	2.01	1740.38	1742.63	2.25	1740.38	1742.65	2.27
1090	1734.33	1740.95	6.62	1734.33	1740.32	5.99	1734.33	1740.79	6.46	1734.33	1740.55	6.22
500	1727.44	1735.45	8.01	1727.44	1735.16	7.72	1727.44	1735.85	8.41	1727.44	1735.55	8.11
0	1722.68	1722.44	-0.24	1722.68	1721.70	-0.98	1722.68	1721.70	-0.98	1722.68	1721.70	-0.98

Table 3.7 Nisqually comparisons for STA 5605 bridge

NISQUALLY RIVER, 100-YEAR FLOOD
BRIDGE @ STA 5605

	No Bridge			288' Bridge			420' Bridge			675' Bridge		
STA, ft	Rigid WSEL 10400 cfs ft	Mobile WSEL 10400 cfs ft	Net WSEL Elev. Diff ft	Rigid WSEL 10400 cfs ft	Mobile WSEL 10400 cfs ft	Net WSEL Elev. Diff ft	Rigid WSEL 10400 cfs ft	Mobile WSEL 10400 cfs ft	Net WSEL Elev. Diff ft	Rigid WSEL 10400 cfs ft	Mobile WSEL 10400 cfs ft	Net WSEL Elev. Diff ft
24345	1999.68	1999.44	-0.24	1999.67	1999.44	-0.23	1999.68	1999.44	-0.24	1999.68	1999.44	-0.24
23285	1984.70	1984.73	0.03	1984.70	1984.73	0.03	1984.70	1984.73	0.03	1984.70	1984.73	0.03
22315	1970.20	1970.06	-0.14	1970.19	1970.05	-0.14	1970.20	1970.06	-0.14	1970.20	1970.06	-0.14
21345	1958.31	1958.51	0.20	1958.31	1958.51	0.20	1958.31	1958.51	0.20	1958.31	1958.51	0.20
20485	1945.23	1945.09	-0.14	1945.23	1945.10	-0.13	1945.23	1945.09	-0.14	1945.23	1945.09	-0.14
19285	1925.26	1925.44	0.18	1925.26	1925.45	0.19	1925.26	1925.44	0.18	1925.26	1925.44	0.18
18245	1912.08	1911.86	-0.22	1912.08	1911.85	-0.23	1912.08	1911.86	-0.22	1912.08	1911.86	-0.22
17245	1900.22	1900.62	0.40	1900.23	1900.63	0.40	1900.22	1900.62	0.40	1900.22	1900.62	0.40
16085	1885.33	1884.52	-0.81	1885.32	1884.54	-0.78	1885.33	1884.52	-0.81	1885.33	1884.52	-0.81
14985	1868.06	1868.71	0.65	1868.06	1868.74	0.68	1868.06	1868.73	0.67	1868.06	1868.72	0.66
13795	1854.73	1856.80	2.07	1854.70	1856.82	2.12	1854.73	1856.78	2.05	1854.73	1856.79	2.06
12895	1846.71	1846.99	0.28	1846.75	1846.99	0.24	1846.71	1847.03	0.32	1846.71	1847.01	0.30
11735	1835.65	1835.51	-0.14	1835.63	1835.50	-0.13	1835.65	1835.49	-0.16	1835.65	1835.50	-0.15
10495	1820.67	1820.99	0.32	1820.71	1821.01	0.30	1820.67	1821.06	0.39	1820.67	1821.01	0.34
9335	1813.66	1812.71	-0.95	1813.29	1812.64	-0.65	1813.58	1812.57	-1.01	1813.67	1812.65	-1.02
8535	1805.42	1805.83	0.41	1805.58	1805.96	0.38	1805.45	1806.05	0.60	1805.41	1805.92	0.51
7905	1800.00	1803.19	3.19	1801.81	1803.46	1.65	1800.90	1803.74	2.84	1800.13	1803.41	3.28
7145	1793.64	1795.43	1.79	1792.98	1794.44	1.46	1793.22	1795.10	1.88	1793.55	1795.37	1.82
6165	1781.51	1781.81	0.30	1783.68	1783.33	-0.35	1781.99	1782.38	0.39	1781.58	1781.96	0.38
5605	1776.66	1777.01	0.35	1777.51	1777.30	-0.21	1776.99	1777.17	0.18	1776.72	1777.08	0.36
5005	1771.28	1771.14	-0.14	1771.28	1771.28	0.00	1771.28	1771.18	-0.10	1771.28	1771.14	-0.14
4035	1760.90	1760.86	-0.04	1760.90	1760.87	-0.03	1760.90	1760.86	-0.04	1760.90	1760.86	-0.04
3670	1757.51	1757.47	-0.04	1757.51	1757.34	-0.17	1757.51	1757.47	-0.04	1757.51	1757.47	-0.04
3120	1751.91	1752.15	0.24	1751.91	1752.29	0.38	1751.91	1752.15	0.24	1751.91	1752.15	0.24
2540	1748.20	1748.88	0.68	1748.20	1749.44	1.24	1748.20	1748.88	0.68	1748.20	1748.88	0.68
1860	1740.38	1743.54	3.16	1740.38	1742.89	2.51	1740.38	1743.54	3.16	1740.38	1743.54	3.16
1090	1734.33	1740.95	6.62	1734.33	1739.56	5.23	1734.33	1740.95	6.62	1734.33	1740.95	6.62
500	1727.44	1735.45	8.01	1727.44	1734.34	6.90	1727.44	1735.45	8.01	1727.44	1735.45	8.01
0	1722.68	1722.44	-0.24	1722.68	1722.22	-0.46	1722.68	1722.44	-0.24	1722.68	1722.44	-0.24

Table 3.8 Skagit water surface profiles

SKAGIT RIVER, 100-YEAR FLOOD
BRIDGE @ STA 517

STA, ft	No Bridge Rigid WSEL 73480 cfs ft	No Bridge Mobile WSEL 73480 cfs ft	Net WSEL Elev. Diff ft	315' Bridge Rigid WSEL 73480 cfs ft	315' Bridge Mobile WSEL 73480 cfs ft	Net WSEL Elev. Diff ft	300' Bridge Rigid WSEL 73480 cfs ft	300' Bridge Mobile WSEL 73480 cfs ft	Net WSEL Elev. Diff ft	285' Bridge Rigid WSEL 73480 cfs ft	285' Bridge Mobile WSEL 73480 cfs ft	Net WSEL Elev. Diff ft
5583		502.38			502.45			502.51			502.59	
5083		501.88			501.74			501.81			501.90	
4583		500.33			500.42			500.51			500.62	
4083		499.00			499.12			499.23			499.37	
3583		497.86			497.82			497.96			498.15	
3083	496.38	496.31	-0.07	496.63	496.53	-0.10	496.93	496.71	-0.22	497.41	496.94	-0.47
2583	495.05	494.96	-0.09	495.39	495.25	-0.14	495.78	495.47	-0.31	496.37	495.76	-0.61
2083	493.72	493.60	-0.12	494.16	493.97	-0.19	494.66	494.26	-0.40	495.38	494.61	-0.77
1583	492.36	492.22	-0.14	492.96	492.70	-0.26	493.58	493.05	-0.53	494.47	493.49	-0.98
1083	490.99	490.81	-0.18	491.79	491.44	-0.35	492.56	491.87	-0.69	493.62	492.40	-1.22
583	490.42	490.20	-0.22	491.32	490.91	-0.41	492.16	491.38	-0.78	493.29	491.96	-1.33
517	490.05	489.51	-0.54	490.24	490.19	-0.05	489.84	489.97	0.13	489.56	489.89	0.33
197	488.69	488.50	-0.19	488.69	488.53	-0.16	488.69	488.55	-0.14	488.69	488.53	-0.16
0	487.88	487.82	-0.06	487.88	487.85	-0.03	487.88	487.87	-0.01	487.88	487.87	-0.01
-500	486.36	486.35	-0.01	486.36	486.36	0.00	486.36	486.37	0.01	486.36	486.37	0.01
-1000	484.84	484.84	0.00	484.84	484.84	0.00	484.84	484.85	0.01	484.84	484.86	0.01
-1500	483.30	483.30	0.00	483.30	483.30	0.00	483.30	483.30	0.00	483.30	483.30	0.00
-2000	481.73	481.73	0.00	481.73	481.73	0.00	481.73	481.73	0.00	481.73	481.73	0.00

STA, ft	265' Bridge Rigid WSEL 73480 cfs ft	265' Bridge Mobile WSEL 73480 cfs ft	Net WSEL Elev. Diff ft	250' Bridge Rigid WSEL 73480 cfs ft	250' Bridge Mobile WSEL 73480 cfs ft	Net WSEL Elev. Diff ft	235' Bridge Rigid WSEL 73480 cfs ft	235' Bridge Mobile WSEL 73480 cfs ft	Net WSEL Elev. Diff ft
5583		502.74			503.25			504.00	
5083		502.06			502.61			503.42	
4583		500.83			501.50			502.47	
4083		499.83			500.47			501.81	
3583		498.47			499.48			500.82	
3083	498.47	497.34	-1.13	501.60	498.56	-3.04	503.78	500.10	-3.68
2583	497.64	496.25	-1.39	501.12	497.70	-3.42	503.44	499.46	-3.98
2083	496.88	495.21	-1.67	500.71	496.92	-3.79	503.15	498.90	-4.25
1583	496.19	494.21	-1.98	500.34	496.20	-4.14	502.89	498.40	-4.49
1083	495.58	493.26	-2.32	500.03	495.55	-4.48	502.68	497.98	-4.70
583	495.35	492.89	-2.46	499.91	495.32	-4.59	502.58	497.81	-4.77
517	487.87	488.65	0.78	487.92	487.05	-0.87	499.12	496.02	-3.10
197	488.69	488.57	-0.12	488.69	488.59	-0.10	488.69	488.58	-0.11
0	487.88	487.90	0.02	487.88	487.95	0.07	487.88	487.97	0.09
-500	486.36	486.39	0.03	486.36	486.42	0.06	486.36	486.43	0.07
-1000	484.84	484.85	0.01	484.84	484.86	0.02	484.84	484.87	0.03
-1500	483.3	483.30	0.00	483.30	483.31	0.01	483.30	483.31	0.01
-2000	481.73	481.73	0.00	481.73	481.73	0.00	481.73	481.73	0.00

Table 3.9 Skagit stream bed profiles

SKAGIT RIVER, 100-YEAR FLOOD
BRIDGE @ STA 517

STA, ft	No Bridge 29146, cfs 0, hrs Bed Ele ft	No Bridge 73480, cfs 15, hrs Bed Ele ft	Net Bed Elev. Diff ft	315' Bridge 29146, cfs 0, hrs Bed Ele ft	315' Bridge 73480, cfs 15, hrs Bed Ele ft	Net Bed Elev. Diff ft	300' Bridge 29146, cfs 0, hrs Bed Ele ft	300' Bridge 73480, cfs 15, hrs Bed Ele ft	Net Bed Elev. Diff ft	285' Bridge 29146, cfs 0, hrs Bed Ele ft	285' Bridge 73480, cfs 15, hrs Bed Ele ft	Net Bed Elev. Diff ft
5583	476.80	476.80	0.00	476.80	476.80	0.00	476.80	476.80	0.00	476.80	476.80	0.00
5083	475.30	472.85	-2.45	475.30	472.87	-2.43	475.30	472.89	-2.41	475.30	472.91	-2.39
4583	474.00	472.97	-1.03	474.00	472.99	-1.01	474.00	473.02	-0.98	474.00	473.05	-0.95
4083	472.70	472.52	-0.18	472.70	472.56	-0.14	472.70	472.59	-0.11	472.70	472.61	-0.09
3583	471.40	471.35	-0.05	471.40	471.36	-0.04	471.40	471.38	-0.02	471.40	471.40	0.00
3083	470.10	470.07	-0.03	470.10	470.10	0.00	470.10	470.11	0.01	470.10	470.13	0.03
2583	469.80	469.78	-0.02	469.80	469.81	0.01	469.80	469.83	0.03	469.80	469.85	0.05
2083	467.50	467.48	-0.02	467.50	467.52	0.02	467.50	467.54	0.04	467.50	467.57	0.07
1583	466.20	466.17	-0.03	466.20	466.22	0.02	466.20	466.26	0.06	466.20	466.29	0.09
1083	464.90	464.86	-0.04	464.90	464.94	0.04	464.90	464.99	0.09	464.90	465.03	0.13
888	464.20	464.24	0.04	464.20	464.31	0.11	464.20	464.35	0.15	464.20	464.38	0.18
517	463.25	464.18	0.93	463.25	462.74	-0.51	463.25	462.34	-0.91	463.25	462.10	-1.15
197	464.60	464.11	-0.49	464.60	464.22	-0.38	464.60	464.17	-0.43	464.60	463.73	-0.87
0	464.20	463.70	-0.50	464.20	463.90	-0.30	464.20	463.86	-0.34	464.20	463.68	-0.52
-500	462.70	462.23	-0.47	462.70	462.43	-0.27	462.70	462.47	-0.23	462.70	462.45	-0.25
-1000	461.20	460.89	-0.31	461.20	461.02	-0.18	461.20	461.07	-0.13	461.20	461.09	-0.11
-1500	459.70	459.55	-0.15	459.70	459.61	-0.09	459.70	459.64	-0.06	459.70	459.66	-0.04
-2000	458.20	458.15	-0.05	458.20	458.18	-0.02	458.20	458.19	-0.01	458.20	458.20	0.00

STA, ft	265' Bridge 29146, cfs 0, hrs Bed Ele ft	265' Bridge 73480, cfs 15, hrs Bed Ele ft	Net Bed Elev. Diff ft	250' Bridge 29146, cfs 0, hrs Bed Ele ft	250' Bridge 73480, cfs 15, hrs Bed Ele ft	Net Bed Elev. Diff ft	236' Bridge 29146, cfs 0, hrs Bed Ele ft	236' Bridge 73480, cfs 15, hrs Bed Ele ft	Net Bed Elev. Diff ft
5583	476.80	476.80	0.00	476.80	476.80	0.00	476.80	476.80	0.00
5083	475.30	472.95	-2.35	475.30	473.08	-2.22	475.30	473.27	-2.03
4583	474.00	473.12	-0.88	474.00	473.30	-0.70	474.00	473.54	-0.46
4083	472.70	472.64	-0.06	472.70	472.70	0.00	472.70	472.78	0.08
3583	471.40	471.42	0.02	471.40	471.48	0.08	471.40	471.51	0.11
3083	470.10	470.18	0.08	470.10	470.21	0.11	470.10	470.23	0.13
2583	469.80	469.89	0.09	469.80	469.93	0.13	469.80	469.93	0.13
2083	467.50	467.61	0.11	467.50	467.64	0.14	467.50	467.61	0.11
1583	466.20	466.32	0.12	466.20	466.33	0.13	466.20	466.29	0.09
1083	464.90	465.07	0.17	464.90	465.05	0.15	464.90	464.99	0.09
888	464.20	464.38	0.18	464.20	464.33	0.13	464.20	464.28	0.08
517	463.25	461.29	-1.96	463.25	459.15	-4.10	463.25	459.19	-4.06
197	464.60	463.29	-1.31	464.60	462.31	-2.29	464.60	461.58	-3.02
0	464.20	463.45	-0.75	464.20	463.09	-1.11	464.20	462.87	-1.33
-500	462.70	462.43	-0.27	462.70	462.39	-0.31	462.70	462.40	-0.30
-1000	461.20	461.12	-0.08	461.20	461.16	-0.04	461.20	461.22	0.02
-1500	459.70	459.69	-0.01	459.70	459.73	0.03	459.70	459.77	0.07
-2000	458.20	458.21	0.01	458.20	458.23	0.03	458.20	458.26	0.06

Table 3.10 Stony Creek #1 water surface profiles

STONY CREEK #1, 100-YEAR FLOOD
BRIDGE @ STA 17075

STA, ft	No Bridge Rigid WSEL 23300 cfs ft	No Bridge Mobile WSEL 23300 cfs ft	Net WSEL Elev. Diff ft	360' Bridge Rigid WSEL 23300 cfs ft	360' Bridge Mobile WSEL 23300 cfs ft	Net WSEL Elev. Diff ft	290' Bridge Rigid WSEL 23300 cfs ft	290' Bridge Mobile WSEL 23300 cfs ft	Net WSEL Elev. Diff ft	245' Bridge Rigid WSEL 23300 cfs ft	245' Bridge Mobile WSEL 23300 cfs ft	Net WSEL Elev. Diff ft
27600	156.89	156.86	-0.03	156.90	156.87	-0.03	156.92	156.89	-0.03	156.96	156.92	-0.04
26600	155.89	155.88	-0.01	155.90	155.89	-0.01	155.93	155.92	-0.01	155.99	155.96	-0.03
25600	154.89	154.89	0.00	154.91	154.91	0.00	154.95	154.94	-0.01	155.04	155.01	-0.03
24600	153.89	153.89	0.00	153.92	153.92	0.00	153.98	153.97	-0.01	154.11	154.07	-0.04
23600	152.89	152.89	0.00	152.93	152.93	0.00	153.02	153.01	-0.01	153.21	153.15	-0.06
22600	151.89	151.89	0.00	151.96	151.95	-0.01	152.09	152.07	-0.02	152.35	152.27	-0.08
21600	150.89	150.89	0.00	150.99	150.98	-0.01	151.18	151.15	-0.03	151.54	151.43	-0.11
20600	149.89	149.89	0.00	150.04	150.03	-0.01	150.30	150.26	-0.04	150.79	150.65	-0.14
19600	148.89	148.89	0.00	149.11	149.10	-0.01	149.48	149.42	-0.06	150.12	149.94	-0.18
18600	147.90	147.90	0.00	148.20	148.19	-0.01	148.71	148.64	-0.07	149.53	149.30	-0.23
17750	147.06	147.06	0.00	147.47	147.45	-0.02	148.12	148.02	-0.10	149.09	148.82	-0.27
17075	146.38	146.38	0.00	146.41	146.41	0.00	146.41	146.42	0.01	146.41	146.43	0.02
16075	145.39	145.39	0.00	145.39	145.39	0.00	145.39	145.39	0.00	145.39	145.39	0.00
15600	144.92	144.92	0.00	144.92	144.92	0.00	144.92	144.92	0.00	144.92	144.92	0.00
14600	143.93	143.93	0.00	143.93	143.93	0.00	143.93	143.93	0.00	143.93	143.93	0.00
13600	142.95	142.95	0.00	142.95	142.95	0.00	142.95	142.95	0.00	142.95	142.95	0.00
12600	141.98	141.98	0.00	141.98	141.98	0.00	141.98	141.98	0.00	141.98	141.98	0.00
11600	141.03	141.03	0.00	141.03	141.03	0.00	141.03	141.03	0.00	141.03	141.03	0.00

STA, ft	225' Bridge Rigid WSEL 23300 cfs ft	225' Bridge Mobile WSEL 23300 cfs ft	Net WSEL Elev. Diff ft	200' Bridge Rigid WSEL 23300 cfs ft	200' Bridge Mobile WSEL 23300 cfs ft	Net WSEL Elev. Diff ft	175' Bridge Rigid WSEL 23300 cfs ft	175' Bridge Mobile WSEL 23300 cfs ft	Net WSEL Elev. Diff ft
27600	157.00	156.95	-0.05	157.10	157.02	-0.08	157.51	157.23	-0.28
26600	156.06	156.01	-0.04	156.20	156.10	-0.10	156.76	156.39	-0.37
25600	155.13	155.08	-0.05	155.34	155.20	-0.14	156.08	155.60	-0.48
24600	154.24	154.16	-0.08	154.53	154.34	-0.19	155.48	154.88	-0.60
23600	153.39	153.28	-0.11	153.78	153.53	-0.25	154.96	154.23	-0.73
22600	152.60	152.45	-0.15	153.11	152.78	-0.33	154.52	153.65	-0.87
21600	151.88	151.67	-0.21	152.52	152.10	-0.42	154.15	153.17	-0.98
20600	151.23	150.97	-0.26	152.00	151.50	-0.50	153.85	152.75	-1.10
19600	150.66	150.34	-0.32	151.57	150.98	-0.59	153.60	152.41	-1.19
18600	150.17	149.79	-0.38	151.21	150.55	-0.66	153.39	152.13	-1.26
17750	149.82	149.39	-0.43	150.95	150.23	-0.72	153.25	151.93	-1.32
17075	146.41	146.44	0.03	146.42	146.45	0.03	146.44	146.50	0.06
16075	145.39	145.40	0.01	145.39	145.40	0.01	145.39	145.40	0.01
15600	144.92	144.92	0.00	144.92	144.92	0.00	144.92	144.92	0.00
14600	143.93	143.93	0.00	143.93	143.93	0.00	143.93	143.93	0.00
13600	142.95	142.95	0.00	142.95	142.95	0.00	142.95	142.95	0.00
12600	141.98	141.98	0.00	141.98	141.98	0.00	141.98	141.98	0.00
11600	141.03	141.03	0.00	141.03	141.03	0.00	141.03	141.03	0.00

Table 3.11 Stony Creek #1 stream bed profiles

STONY CEREEK #1, 100-YEAR FLOOD
BRIDGE @ STA 17075

STA, ft	No Bridge 15220, cfs 0, hrs Bed Ele ft	No Bridge 23300, cfs 23, hrs Bed Ele ft	Net Bed Elev. Diff ft	350' Bridge 15220, cfs 0, hrs Bed Ele ft	350' Bridge 23300, cfs 23, hrs Bed Ele ft	Net Bed Elev. Diff ft	290' Bridge 15220, cfs 0, hrs Bed Ele ft	290' Bridge 23300, cfs 23, hrs Bed Ele ft	Net Bed Elev. Diff ft	245' Bridge 15220, cfs 0, hrs Bed Ele ft	245' Bridge 23300, cfs 23, hrs Bed Ele ft	Net Bed Elev. Diff ft
27600	143.50	143.50	0.00	143.50	143.50	0.00	143.50	143.50	0.00	143.50	143.50	0.00
26600	142.50	142.36	-0.14	142.50	142.36	-0.14	142.50	142.36	-0.14	142.50	142.36	-0.14
25600	141.50	141.48	-0.02	141.50	141.49	-0.01	141.50	141.49	-0.01	141.50	141.49	-0.01
24600	140.50	140.50	0.00	140.50	140.50	0.00	140.50	140.50	0.00	140.50	140.50	0.00
23600	139.50	139.50	0.00	139.50	139.50	0.00	139.50	139.50	0.00	139.50	139.51	0.01
22600	138.50	138.50	0.00	138.50	138.50	0.00	138.50	138.50	0.00	138.50	138.51	0.01
21600	137.50	137.50	0.00	137.50	137.50	0.00	137.50	137.51	0.01	137.50	137.51	0.01
20600	136.50	136.50	0.00	136.50	136.50	0.00	136.50	136.51	0.01	136.50	136.52	0.02
19600	135.50	135.50	0.00	135.50	135.51	0.01	135.50	135.51	0.01	135.50	135.52	0.02
18600	134.50	134.50	0.00	134.50	134.51	0.01	134.50	134.52	0.02	134.50	134.52	0.02
17750	133.65	133.65	0.00	133.65	133.66	0.01	133.65	133.67	0.02	133.65	133.67	0.02
17075	132.97	132.97	0.00	132.97	132.86	-0.11	132.97	132.63	-0.34	132.97	132.31	-0.66
16075	131.97	131.97	0.00	131.97	132.05	0.08	131.97	132.23	0.26	131.97	132.51	0.54
15600	131.50	131.50	0.00	131.50	131.50	0.00	131.50	131.51	0.01	131.50	131.52	0.02
14600	130.50	130.50	0.00	130.50	130.50	0.00	130.50	130.50	0.00	130.50	130.50	0.00
13600	129.50	129.50	0.00	129.50	129.50	0.00	129.50	129.50	0.00	129.50	129.50	0.00
12600	128.50	128.50	0.00	128.50	128.50	0.00	128.50	128.50	0.00	128.50	128.50	0.00
11600	127.50	127.50	0.00	127.50	127.50	0.00	127.50	127.50	0.00	127.50	127.50	0.00

STA, ft	225' Bridge 15220, cfs 0, hrs Bed Ele ft	225' Bridge 23300, cfs 23, hrs Bed Ele ft	Net Bed Elev. Diff ft	200' Bridge 15220, cfs 0, hrs Bed Ele ft	200' Bridge 23300, cfs 23, hrs Bed Ele ft	Net Bed Elev. Diff ft	175' Bridge 15220, cfs 0, hrs Bed Ele ft	175' Bridge 23300, cfs 23, hrs Bed Ele ft	Net Bed Elev. Diff ft
27600	143.50	143.50	0.00	143.50	143.50	0.00	143.50	143.50	0.00
26600	142.50	142.37	-0.13	142.50	142.37	-0.13	142.50	142.40	-0.10
25600	141.50	141.49	-0.01	141.50	141.49	-0.01	141.50	141.50	0.00
24600	140.50	140.50	0.00	140.50	140.51	0.01	140.50	140.51	0.01
23600	139.50	139.51	0.01	139.50	139.51	0.01	139.50	139.52	0.02
22600	138.50	138.51	0.01	138.50	138.52	0.02	138.50	138.52	0.02
21600	137.50	137.52	0.02	137.50	137.52	0.02	137.50	137.51	0.01
20600	136.50	136.52	0.02	136.50	136.52	0.02	136.50	136.51	0.01
19600	135.50	135.52	0.02	135.50	135.51	0.01	135.50	135.51	0.01
18600	134.50	134.52	0.02	134.50	134.51	0.01	134.50	134.50	0.00
17750	133.65	133.67	0.02	133.65	133.66	0.01	133.65	133.65	0.00
17075	132.97	132.06	-0.91	132.97	131.75	-1.22	132.97	131.28	-1.69
16075	131.97	132.74	0.77	131.97	133.07	1.10	131.97	133.62	1.65
15600	131.50	131.53	0.03	131.50	131.54	0.04	131.50	131.57	0.07
14600	130.50	130.50	0.00	130.50	130.50	0.00	130.50	130.50	0.00
13600	129.50	129.50	0.00	129.50	129.50	0.00	129.50	129.50	0.00
12600	128.50	128.50	0.00	128.50	128.50	0.00	128.50	128.50	0.00
11600	127.50	127.50	0.00	127.50	127.50	0.00	127.50	127.50	0.00

Table 3.12 Stony Creek #2 water surface profiles

STONY CREEK #2, 100-YEAR FLOOD
BRIDGE @ STA 65400

STA, ft	No Bridge Rigid WSEL 23300 cfs ft	No Bridge Mobile WSEL 23300 cfs ft	Net WSEL Elev. Diff ft	510' Bridge Rigid WSEL 23300 cfs ft	510' Bridge Mobile WSEL 23300 cfs ft	Net WSEL Elev. Diff ft	345' Bridge Rigid WSEL 23300 cfs ft	345' Bridge Mobile WSEL 23300 cfs ft	Net WSEL Elev. Diff ft	265' Bridge Rigid WSEL 23300 cfs ft	265' Bridge Mobile WSEL 23300 cfs ft	Net WSEL Elev. Diff ft
76100	247.91	247.76	-0.15	247.91	247.76	-0.15	247.91	247.76	-0.15	247.91	247.76	-0.15
75100	245.91	245.82	-0.09	245.91	245.82	-0.09	245.91	245.82	-0.09	245.91	245.82	-0.09
74100	243.91	243.90	-0.01	243.91	243.90	-0.01	243.91	243.90	-0.01	243.91	243.90	-0.01
73100	241.91	241.91	0.00	241.91	241.91	0.00	241.91	241.91	0.00	241.91	241.91	0.00
72100	239.91	239.91	0.00	239.91	239.91	0.00	239.91	239.91	0.00	239.91	239.91	0.00
71100	237.91	237.91	0.00	237.91	237.91	0.00	237.91	237.91	0.00	237.92	237.92	0.00
70100	235.91	235.91	0.00	235.91	235.91	0.00	235.91	235.92	0.01	235.96	235.94	-0.02
69100	233.91	233.91	0.00	233.92	233.92	0.00	233.93	233.94	0.01	234.14	234.04	-0.10
68100	231.91	231.91	0.00	231.94	231.95	0.01	232.04	232.03	-0.01	232.69	232.34	-0.35
67100	229.91	229.91	0.00	230.08	230.09	0.01	230.44	230.31	-0.13	231.74	231.05	-0.69
66100	227.91	227.91	0.00	228.55	228.47	-0.08	229.31	228.98	-0.33	231.19	230.23	-0.96
65400	226.51	226.51	0.00	226.58	226.56	-0.02	226.65	226.61	-0.04	226.78	226.70	-0.08
64400	224.51	224.51	0.00	224.51	224.52	0.01	224.51	224.54	0.03	224.51	224.59	0.08
63400	222.51	222.51	0.00	222.51	222.51	0.00	222.51	222.51	0.00	222.51	222.52	0.01
62400	220.51	220.51	0.00	220.51	220.51	0.00	220.51	220.51	0.00	220.51	220.51	0.00
61400	218.51	218.51	0.00	218.51	218.51	0.00	218.51	218.51	0.00	218.51	218.51	0.00
60400	216.52	216.53	0.01	216.52	216.53	0.01	216.52	216.53	0.01	216.52	216.53	0.01
59400	214.58	214.58	0.00	214.58	214.58	0.00	214.58	214.58	0.00	214.58	214.58	0.00

STA, ft	245' Bridge Rigid WSEL 23300 cfs ft	245' Bridge Mobile WSEL 23300 cfs ft	Net WSEL Elev. Diff ft	225' Bridge Rigid WSEL 23300 cfs ft	225' Bridge Mobile WSEL 23300 cfs ft	Net WSEL Elev. Diff ft	185' Bridge Rigid WSEL 23300 cfs ft	185' Bridge Mobile WSEL 23300 cfs ft	Net WSEL Elev. Diff ft
76100	247.91	247.76	-0.15	247.91	247.76	-0.15	247.91	247.76	-0.15
75100	245.91	245.82	-0.09	245.91	245.82	-0.09	245.91	245.82	-0.09
74100	243.91	243.90	-0.01	243.91	243.90	-0.01	243.93	243.91	-0.02
73100	241.91	241.91	0.00	241.91	241.91	0.00	242.04	241.93	-0.11
72100	239.91	239.91	0.00	239.93	239.92	-0.01	240.43	240.02	-0.41
71100	237.93	237.92	-0.01	238.00	237.95	-0.05	239.30	238.29	-1.01
70100	236.04	235.97	-0.07	236.30	236.06	-0.24	238.83	236.94	-1.89
69100	234.43	234.15	-0.28	235.04	234.40	-0.64	238.25	236.08	-2.17
68100	233.30	232.63	-0.67	234.27	233.17	-1.10	238.04	235.59	-2.45
67100	232.63	231.58	-1.05	233.83	232.41	-1.42	237.92	235.33	-2.59
66100	232.25	230.97	-1.28	233.59	231.99	-1.60	237.84	235.18	-2.66
65400	226.83	226.73	-0.10	226.89	226.78	-0.11	227.03	226.93	-0.10
64400	224.51	224.61	0.10	224.51	224.63	0.12	224.51	224.71	0.20
63400	222.51	222.52	0.01	222.51	222.52	0.01	222.51	222.53	0.02
62400	220.51	220.51	0.00	220.51	220.51	0.00	220.51	220.51	0.00
61400	218.51	218.51	0.00	218.51	218.51	0.00	218.51	218.52	0.01
60400	216.52	216.53	0.01	216.52	216.53	0.01	216.52	216.53	0.01
59400	214.58	214.58	0.00	214.58	214.58	0.00	214.58	214.58	0.00

Table 3.13 Stony Creek #2 stream bed profiles

STONY CEREEK #2, 100-YEAR FLOOD
BRIDGE @ STA 65400

STA, ft	No Bridge 15220, cfs 0, hrs Bed Ele ft	23300, cfs 23, hrs Bed Ele ft	Net Bed Elev. Diff ft	510' Bridge 15220, cfs 0, hrs Bed Ele ft	23300, cfs 23, hrs Bed Ele ft	Net Bed Elev. Diff ft	345' Bridge 15220, cfs 0, hrs Bed Ele ft	23300, cfs 23, hrs Bed Ele ft	Net Bed Elev. Diff ft	285' Bridge 15220, cfs 0, hrs Bed Ele ft	23300, cfs 23, hrs Bed Ele ft	Net Bed Elev. Diff ft
76100	235.90	235.90	0.00	235.90	235.90	0.00	235.90	235.90	0.00	235.90	235.90	0.00
75100	233.90	233.89	-0.01	233.90	233.89	-0.01	233.90	233.89	-0.01	233.90	233.89	-0.01
74100	231.90	231.90	0.00	231.90	231.90	0.00	231.90	231.90	0.00	231.90	231.90	0.00
73100	229.90	229.90	0.00	229.90	229.90	0.00	229.90	229.90	0.00	229.90	229.90	0.00
72100	227.90	227.90	0.00	227.90	227.90	0.00	227.90	227.90	0.00	227.90	227.90	0.00
71100	225.90	225.90	0.00	225.90	225.90	0.00	225.90	225.90	0.00	225.90	225.90	0.00
70100	223.90	223.90	0.00	223.90	223.90	0.00	223.90	223.90	0.00	223.90	223.90	0.00
69100	221.90	221.90	0.00	221.90	221.90	0.00	221.90	221.90	0.00	221.90	221.90	0.00
68100	219.90	219.90	0.00	219.90	219.90	0.00	219.90	219.90	0.00	219.90	219.90	0.00
67100	217.90	217.90	0.00	217.90	217.90	0.00	217.90	217.90	0.00	217.90	217.90	0.00
66100	215.90	215.90	0.00	215.90	215.90	0.00	215.90	215.90	0.00	215.90	216.05	0.15
65400	214.50	214.50	0.00	214.50	214.38	-0.12	214.50	214.35	-0.15	214.50	213.93	-0.57
64400	212.50	212.50	0.00	212.50	212.57	0.07	212.50	212.58	0.08	212.50	212.61	0.11
63400	210.50	210.50	0.00	210.50	210.50	0.00	210.50	210.50	0.00	210.50	210.50	0.00
62400	208.50	208.50	0.00	208.50	208.50	0.00	208.50	208.50	0.00	208.50	208.50	0.00
61400	206.50	206.50	0.00	206.50	206.50	0.00	206.50	206.50	0.00	206.50	206.50	0.00
60400	204.50	204.50	0.00	204.50	204.50	0.00	204.50	204.50	0.00	204.50	204.50	0.00
59400	202.50	202.50	0.00	202.50	202.50	0.00	202.50	202.50	0.00	202.50	202.50	0.00

STA, ft	245' Bridge 15220, cfs 0, hrs Bed Ele ft	23300, cfs 23, hrs Bed Ele ft	Net Bed Elev. Diff ft	225' Bridge 15220, cfs 0, hrs Bed Ele ft	23300, cfs 23, hrs Bed Ele ft	Net Bed Elev. Diff ft	185' Bridge 15220, cfs 0, hrs Bed Ele ft	23300, cfs 23, hrs Bed Ele ft	Net Bed Elev. Diff ft
76100	235.90	235.90	0.00	235.90	235.90	0.00	235.90	235.90	0.00
75100	233.90	233.89	-0.01	233.90	233.89	-0.01	233.90	233.89	-0.01
74100	231.90	231.90	0.00	231.90	231.90	0.00	231.90	231.90	0.00
73100	229.90	229.90	0.00	229.90	229.90	0.00	229.90	229.90	0.00
72100	227.90	227.90	0.00	227.90	227.90	0.00	227.90	227.90	0.00
71100	225.90	225.90	0.00	225.90	225.90	0.00	225.90	225.90	0.00
70100	223.90	223.90	0.00	223.90	223.90	0.00	223.90	223.90	0.00
69100	221.90	221.90	0.00	221.90	221.90	0.00	221.90	221.97	0.07
68100	219.90	219.90	0.00	219.90	219.90	0.00	219.90	219.93	0.03
67100	217.90	217.95	0.05	217.90	217.97	0.07	217.90	217.90	0.00
66100	215.90	215.90	0.00	215.90	215.94	0.04	215.90	215.90	0.00
65400	214.50	213.62	-0.88	214.50	213.31	-1.19	214.50	213.36	-1.14
64400	212.50	212.63	0.13	212.50	212.65	0.15	212.50	212.70	0.20
63400	210.50	210.50	0.00	210.50	210.50	0.00	210.50	210.50	0.00
62400	208.50	208.50	0.00	208.50	208.50	0.00	208.50	208.50	0.00
61400	206.50	206.50	0.00	206.50	206.50	0.00	206.50	206.50	0.00
60400	204.50	204.50	0.00	204.50	204.50	0.00	204.50	204.50	0.00
59400	202.50	202.50	0.00	202.50	202.50	0.00	202.50	202.50	0.00

Table 3.14 Gibbon water surface profiles

GIBBON RIVER, 100-YEAR FLOOD
BRIDGE @ STA 9000

	No Bridge			165' Bridge			125' Bridge			95' Bridge		
STA, ft	Rigid WSEL 2500 cfs ft	Mobile WSEL 2500 cfs ft	Net WSEL Elev. Diff ft	Rigid WSEL 2500 cfs ft	Mobile WSEL 2500 cfs ft	Net WSEL Elev. Diff ft	Rigid WSEL 2500 cfs ft	Mobile WSEL 2500 cfs ft	Net WSEL Elev. Diff ft	Rigid WSEL 2500 cfs ft	Mobile WSEL 2500 cfs ft	Net WSEL Elev. Diff ft
20000	6894.67	6894.57	-0.10	6894.67	6894.57	-0.10	6894.67	6894.57	-0.10	6894.67	6894.57	-0.10
19000	6889.67	6889.50	-0.17	6889.67	6889.50	-0.17	6889.67	6889.50	-0.17	6889.67	6889.50	-0.17
18000	6884.67	6884.66	-0.01	6884.67	6884.66	-0.01	6884.67	6884.66	-0.01	6884.67	6884.66	-0.01
17000	6879.67	6879.66	-0.01	6879.68	6879.66	-0.02	6879.68	6879.66	-0.02	6879.67	6879.66	-0.01
16000	6874.67	6874.67	0.00	6874.66	6874.67	0.01	6874.66	6874.67	0.01	6874.67	6874.67	0.00
15000	6869.67	6869.67	0.00	6869.69	6869.66	-0.03	6869.69	6869.66	-0.03	6869.68	6869.66	-0.02
14000	6864.67	6864.67	0.00	6864.65	6864.67	0.02	6864.64	6864.68	0.04	6864.66	6864.68	0.02
13000	6859.67	6859.67	0.00	6859.71	6859.66	-0.05	6859.72	6859.66	-0.06	6859.69	6859.65	-0.04
12000	6854.67	6854.67	0.00	6854.62	6854.67	0.05	6854.61	6854.67	0.06	6854.64	6854.68	0.04
11000	6849.67	6849.67	0.00	6849.77	6849.67	-0.10	6849.79	6849.68	-0.11	6849.73	6849.68	-0.05
10000	6844.67	6844.67	0.00	6844.54	6844.63	0.09	6844.52	6844.58	0.06	6844.59	6844.59	0.00
9250	6840.92	6840.92	0.00	6841.35	6841.18	-0.17	6841.84	6841.49	-0.35	6842.39	6841.89	-0.50
9000	6839.67	6839.67	0.00	6839.78	6839.65	-0.13	6839.90	6839.69	-0.21	6840.02	6839.80	-0.22
8000	6834.68	6834.67	-0.01	6834.68	6834.72	0.04	6834.68	6834.74	0.06	6834.68	6834.77	0.09
7000	6829.66	6829.67	0.01	6829.66	6829.67	0.01	6829.66	6829.67	0.01	6829.66	6829.67	0.01
6000	6824.69	6824.67	-0.02	6824.69	6824.67	-0.02	6824.69	6824.67	-0.02	6824.69	6824.67	-0.02
5000	6819.65	6819.65	0.00	6819.65	6819.65	0.00	6819.65	6819.65	0.00	6819.65	6819.65	0.00
4000	6814.71	6814.71	0.00	6814.71	6814.71	0.00	6814.71	6814.71	0.00	6814.71	6814.71	0.00

	90' Bridge			85' Bridge			80' Bridge		
STA, ft	Rigid WSEL 2500 cfs ft	Mobile WSEL 2500 cfs ft	Net WSEL Elev. Diff ft	Rigid WSEL 2500 cfs ft	Mobile WSEL 2500 cfs ft	Net WSEL Elev. Diff ft	Rigid WSEL 2500 cfs ft	Mobile WSEL 2500 cfs ft	Net WSEL Elev. Diff ft
20000	6894.67	6894.57	-0.10	6894.67	6894.57	-0.10	6894.67	6894.57	-0.10
19000	6889.67	6889.50	-0.17	6889.67	6889.50	-0.17	6889.66	6889.50	-0.16
18000	6884.67	6884.66	-0.01	6884.68	6884.66	-0.02	6884.68	6884.66	-0.02
17000	6879.67	6879.66	-0.01	6879.66	6879.66	0.00	6879.65	6879.67	0.02
16000	6874.67	6874.67	0.00	6874.69	6874.67	-0.02	6874.70	6874.66	-0.04
15000	6869.67	6869.66	-0.01	6869.64	6869.66	0.02	6869.63	6869.67	0.04
14000	6864.67	6864.68	0.01	6864.71	6864.67	-0.04	6864.74	6864.67	-0.07
13000	6859.67	6859.65	-0.02	6859.61	6859.66	0.05	6859.57	6859.65	0.08
12000	6854.67	6854.69	0.02	6854.79	6854.69	-0.10	6854.87	6854.73	-0.14
11000	6849.68	6849.67	-0.01	6849.52	6849.63	0.11	6849.44	6849.51	0.07
10000	6844.66	6844.61	-0.05	6845.02	6844.75	-0.27	6845.61	6845.05	-0.56
9250	6842.68	6842.10	-0.58	6843.71	6842.74	-0.97	6844.82	6843.56	-1.26
9000	6840.08	6839.83	-0.25	6840.40	6840.00	-0.40	6840.62	6840.14	-0.48
8000	6834.68	6834.78	0.10	6834.68	6834.88	0.20	6834.68	6834.93	0.25
7000	6829.66	6829.67	0.01	6829.66	6829.68	0.02	6829.66	6829.68	0.02
6000	6824.69	6824.67	-0.02	6824.69	6824.67	-0.02	6824.69	6824.67	-0.02
5000	6819.65	6819.65	0.00	6819.65	6819.65	0.00	6819.65	6819.65	0.00
4000	6814.71	6814.71	0.00	6814.71	6814.71	0.00	6814.71	6814.71	0.00

Table 3.15 Gibbon stream bed profiles

GIBBON RIVER, 100-YEAR FLOOD
BRIDGE @ STA 9000

No Bridge 1811, cfs 0, hrs Bed Ele ft	No Bridge 2500, cfs 16, hrs Bed Ele ft	Net Bed Elev. Diff ft	165' Bridge 1811, cfs 0, hrs Bed Ele ft	165' Bridge 2500, cfs 16, hrs Bed Ele ft	Net Bed Elev. Diff ft	125' Bridge 1811, cfs 0, hrs Bed Ele ft	125' Bridge 2500, cfs 16, hrs Bed Ele ft	Net Bed Elev. Diff ft	95' Bridge 1811, cfs 0, hrs Bed Ele ft	95' Bridge 2500, cfs 16, hrs Bed Ele ft	Net Bed Elev. Diff ft
6889.30	6889.30	0.00	6889.30	6889.30	0.00	6889.30	6889.30	0.00	6889.30	6889.30	0.00
6884.30	6883.51	-0.79	6884.30	6883.51	-0.79	6884.30	6883.51	-0.79	6884.30	6883.51	-0.79
6879.30	6879.26	-0.04	6879.30	6879.26	-0.04	6879.30	6879.26	-0.04	6879.30	6879.26	-0.04
6874.30	6874.29	-0.01	6874.30	6874.29	-0.01	6874.30	6874.29	-0.01	6874.30	6874.28	-0.02
6869.30	6869.29	-0.01	6869.30	6869.29	-0.01	6869.30	6869.29	-0.01	6869.30	6869.29	-0.01
6864.30	6864.30	0.00	6864.30	6864.29	-0.01	6864.30	6864.30	0.00	6864.30	6864.29	-0.01
6859.30	6859.30	0.00	6859.30	6859.29	-0.01	6859.30	6859.29	-0.01	6859.30	6859.29	-0.01
6854.30	6854.30	0.00	6854.30	6854.30	0.00	6854.30	6854.30	0.00	6854.30	6854.30	0.00
6849.30	6849.30	0.00	6849.30	6849.28	-0.02	6849.30	6849.25	-0.05	6849.30	6849.25	-0.05
6844.30	6844.30	0.00	6844.30	6844.30	0.00	6844.30	6844.30	0.00	6844.30	6844.30	0.00
6839.30	6839.30	0.00	6839.30	6839.19	-0.11	6839.30	6839.06	-0.24	6839.30	6839.04	-0.26
6835.55	6835.55	0.00	6835.55	6835.55	0.00	6835.55	6835.58	0.03	6835.55	6835.59	0.04
6834.30	6834.30	0.00	6834.30	6833.65	-0.65	6834.30	6833.48	-0.82	6834.30	6833.23	-1.07
6829.30	6829.30	0.00	6829.30	6829.30	0.00	6829.30	6829.30	0.00	6829.30	6829.37	0.07
6824.30	6824.29	-0.01	6824.30	6824.28	-0.02	6824.30	6824.29	-0.01	6824.30	6824.30	0.00
6819.30	6819.30	0.00	6819.30	6819.30	0.00	6819.30	6819.30	0.00	6819.30	6819.30	0.00
6814.30	6814.26	-0.04	6814.30	6814.26	-0.04	6814.30	6814.26	-0.04	6814.30	6814.26	-0.04
6809.30	6809.30	0.00	6809.30	6809.30	0.00	6809.30	6809.30	0.00	6809.30	6809.30	0.00

STA, ft	90' Bridge 1811, cfs 0, hrs Bed Ele ft	90' Bridge 2500, cfs 16, hrs Bed Ele ft	Net Bed Elev. Diff ft	85' Bridge 1811, cfs 0, hrs Bed Ele ft	85' Bridge 2500, cfs 16, hrs Bed Ele ft	Net Bed Elev. Diff ft	80' Bridge 1811, cfs 0, hrs Bed Ele ft	80' Bridge 2500, cfs 16, hrs Bed Ele ft	Net Bed Elev. Diff ft
20000	6889.30	6889.30	0.00	6889.30	6889.30	0.00	6889.30	6889.30	0.00
19000	6884.30	6883.51	-0.79	6884.30	6883.51	-0.79	6884.30	6883.51	-0.79
18000	6879.30	6879.26	-0.04	6879.30	6879.26	-0.04	6879.30	6879.26	-0.04
17000	6874.30	6874.28	-0.02	6874.30	6874.29	-0.01	6874.30	6874.29	-0.01
16000	6869.30	6869.29	-0.01	6869.30	6869.29	-0.01	6869.30	6869.30	0.00
15000	6864.30	6864.29	-0.01	6864.30	6864.29	-0.01	6864.30	6864.28	-0.02
14000	6859.30	6859.29	-0.01	6859.30	6859.30	0.00	6859.30	6859.30	0.00
13000	6854.30	6854.30	0.00	6854.30	6854.29	-0.01	6854.30	6854.23	-0.07
12000	6849.30	6849.25	-0.05	6849.30	6849.30	0.00	6849.30	6849.30	0.00
11000	6844.30	6844.30	0.00	6844.30	6844.26	-0.04	6844.30	6844.02	-0.28
10000	6839.30	6839.08	-0.22	6839.30	6839.30	0.00	6839.30	6839.32	0.02
9250	6835.55	6835.59	0.04	6835.55	6835.57	0.02	6835.55	6835.55	0.00
9000	6834.30	6833.10	-1.20	6834.30	6832.56	-1.74	6834.30	6832.20	-2.10
8000	6829.30	6829.38	0.08	6829.30	6829.52	0.22	6829.30	6829.58	0.28
7000	6824.30	6824.30	0.00	6824.30	6824.30	0.00	6824.30	6824.30	0.00
6000	6819.30	6819.30	0.00	6819.30	6819.30	0.00	6819.30	6819.30	0.00
5000	6814.30	6814.26	-0.04	6814.30	6814.26	-0.04	6814.30	6814.26	-0.04
4000	6809.30	6809.30	0.00	6809.30	6809.30	0.00	6809.30	6809.30	0.00

Table 3.16 Summary of case backwater values

Case	Bridge Length ft	h_{1M}^* ft	h_{1R}^* ft	h_{1M}^*/h_{1R}^*
Nisqually(3670)	None	-0.04	0.00	N/A
	315	0.21	0.61	0.34
	250	1.09	2.08	0.52
	200	2.22	3.63	0.61
Nisqually(5605)	None	0.30	0.00	N/A
	675	0.45	0.07	6.43
	420	0.87	0.48	1.81
	288	1.82	2.20	0.83
Nisqually(3120)	None	-0.04	0.00	N/A
	540	0.19	0.96	0.20
	510	0.14	1.35	0.10
	480	0.56	1.76	0.32
Skagit(517)	None	-0.22	0.00	N/A
	315	0.49	0.90	0.54
	300	0.96	1.74	0.55
	285	1.54	2.87	0.54
	265	2.47	4.93	0.50
	250	4.90	9.49	0.52
	235	7.39	12.43	0.59

h_{1R}^* is defined in Figure 2.8 as h_1^*. h_{1M}^* is similarly defined. However, it represents the difference in the upstream(no bridge) rigid boundary elevation and the upstream(with bridge) mobile boundary elevation.

Table 3.16 Summary of case backwater values(continued)

Case	Bridge Length ft	h^*_{IM} ft	h^*_{IR} ft	h^*_{IM}/h^*_{IR}
Stony #1(17075)	None	0.00	0.00	N/A
	350	0.40	0.42	0.95
	290	0.97	1.07	0.91
	245	1.77	2.04	0.87
	225	2.34	2.77	0.84
	200	3.18	3.90	0.82
	175	4.88	6.20	0.79
Stony #2(65400)	None	0.00	0.00	N/A
	510	0.56	0.64	0.88
	345	1.07	1.40	0.76
	265	2.32	3.28	0.71
	245	3.06	4.34	0.71
	225	4.08	5.68	0.72
	185	7.27	9.93	0.73
Gibbon(9000)	None	0.00	0.00	N/A
	165	0.26	0.43	0.60
	125	0.57	0.92	0.62
	95	0.97	1.47	0.66
	90	1.18	1.76	0.67
	85	1.82	2.79	0.65
	80	2.64	3.90	0.68

For each of the above cases, the bridge station location is shown in parentheses.

CHAPTER 4: STATISTICAL RELATIONSHIPS AND SENSITIVITY ANALYSIS

4.1 Overview

This chapter evaluates the assumption that there are certain fixed boundary, hydraulic parameters for estimating mobile boundary, bridge backwater elevations from fixed boundary water surface elevations. It also provides recommended values for certain physical and operational parameters in applying mobile models. To accomplish these goals, the chapter presents the relationships and sensitivity between bridge backwater and key hydraulic/sediment parameters.

Section 4.2 evaluates the relationship between fixed boundary hydraulic variables and the relative differences in the backwater values for a rigid boundary model versus a mobile boundary model. If there is a positive correlation between the fixed hydraulic variables and the relative differences in the rigid/mobile backwater values, then these fixed hydraulic variables may be used to estimate the mobile bridge, backwater values. Section 4.3 assesses a backwater correction factor for bridge scour. This scoured-based correction factor may provide an estimate of the potential reduction in backwater for a mobile model versus a fixed boundary model.

Section 4.4 focuses on the sensitivity of the mobile boundary backwater values to various physical and operational model parameters. From the sensitivity analysis, the thesis develops recommended values for certain mobile boundary model parameters. Section 4.5 summarizes the results of the statistical analysis from Section 4.2, the use of the backwater correction factor of Section 4.3, and the sensitivity results of Section 4.4. Overall, this chapter lays a foundation for applying mobile boundary models at bridge crossings.

4.2 Bridge Backwater Relationships

This section evaluates the relationship between fixed boundary hydraulic variables and the relative differences in the backwater values for the rigid boundary model versus the mobile boundary model. If there is a positive correlation between the fixed hydraulic variables and the ratio of the rigid/mobile backwater values, then these fixed hydraulic variables may possibly predict the mobile bridge, backwater values. Section 2.5 presented an analytical overview of the variables that determine the computed backwater values for the rigid and mobile models.

In particular, equation 2-17 presented a simplified functional relationship between backwater, h_1^*, and the bridge- related losses, K^*, and the bridge cross-section velocity, V. For reference, equation 2-17 is re-stated below.

$$h_1^* = K^* \alpha_2 \frac{V_{n2}^2}{2g} \tag{2-17}$$

For the selected case studies, K^* and V primarily represent functions of the total volume of flow per unit time, Q, the upstream flow within the projected bridge length, Q_b, and the total flow area at the bridge crossing, A. The computed backwater becomes a function of the ratio of Q_b to Q and Q to A.

For the rigid and mobile models, Q and Q_b are the same. Due to scour and deposition, A will differ for the rigid and mobile boundary models. The search for a relationship between the fixed or rigid boundary model and mobile model, thus, focuses on flow area, A, and the parameters that influence A at the bridge section.

Using the results from the case studies developed in Chapter 3, Table 4.1 summarizes those variables associated with the bridge cross-section area, A,

where: Q_b = flow in portion of channel within projected length of bridge at upstream backwater section, cubic feet per second (cfs)

Q_{100} = total discharge for 100-year flood, cfs

h_{1M}^* = backwater for the mobile model, feet (ft)

h_{1R}^* = backwater for the rigid model, ft

A_{SM} = area of scour at bridge section for mobile boundary condition, square feet, (sq ft)

A = area of flow at bridge section, sq ft

F_u = Froude number for upstream backwater section

F_b = Froude number for bridge section

SP_d = unit stream power (Eq. 2-18, velocity times energy slope) for downstream reach, feet per second (fps)

SP_u = unit stream power for upstream reach, fps

τ_b = shear stress for bridge section, pounds per square foot (lbs/ft^2)

τ_{cr} = critical shear stress for bridge section, lbs/ft^2

Unless otherwise stated, all the above values represent fixed boundary conditions. From Table 4.1, the following observations stand out:

As the opening ratio, Q_b/Q_{100}, decreases, the computed backwater for both model types increases. This is an expected result since the bridge loss coefficient, K^*, and thus the backwater, increases with a decrease in the bridge opening ratio (decrease in bridge length).

Similarly, each bridge site produces a decrease in flow area, A, and generally an increase in scour, A_{SM}, with a decrease in bridge length. As stated above, the computed backwater is inversely related to the flow area. Also, as the flow area decreases, the bridge cross-section velocity increases (Q remains constant as A decreases), and thus, the local scour area increases (see section 2.5.4 for sediment transport analysis).

With an increase in upstream backwater and a decrease in bridge flow area, the Froude value upstream, F_u, decreases and at the bridge, F_b increases. This occurs with a decrease in bridge length for each case. The Froude value is a ratio of velocity to the square root of flow depth. With a decrease in bridge length, the upstream depth increases and the velocity decreases. At the bridge cross-section, the opposite occurs.

For unit stream power, SP_u represents the average of the velocities at the bridge and the upstream backwater section times the energy slope between the bridge and backwater sections. Likewise, SP_d represents the average of the velocities at the bridge and the downstream section near full flow expansion times the energy slope between the bridge and downstream section. In this study, SP_d and SP_u generally increase with a decrease in bridge length.

For shear stress, τ_b represents the energy slope times a depth length scale (the hydraulic radius) times the unit weight of water (assumed at 62.4 lbs/ft^3) at the bridge. For the critical shear stress, τ_{cr} represents the critical shields value (approximately 0.06 for gravel) times the submerged specific weight of the bed particle (103 lbs/ft^3) times the mean grain size, d_{50}, of the stream bed (see Table 3.1 for values). In this study, τ_b/τ_{cr} generally increases with a decrease in bridge length.

Using the dimesionless ratio of h_{1M}^* to h_{1R}^* as the dependent variable and Q_b / Q_{100}, A_{SM} / A, F_u / F_b, SP_d / SP_u and τ_b/τ_{cr} as independent variables, a regression analysis (linear, multiple) shows little or no correlation among the variables (i.e., r^2 of about 0 for all combination of variables; 0 = no correlation, 1 = a perfect correlation). The presented hydraulic parameters for fixed boundaries cannot, thus, be used to predict bridge backwater elevations deriving from mobile boundary models.

For the regression analysis, the data includes only those backwater values in which the bridge represents a dominating influence. If the selected bridge length had a Froude ratio (F_u / F_b) of less than one, then the research accepted the bridge as the dominating hydraulic influence at the study site. With this criterion, the regression analysis included 31 of the 33 bridge lengths from the five case studies.

4.3 Backwater Correction Factor For Bridge Scour

With limited research and a lack of correlation between backwater values and the influencing variables shown in Table 4.1, the research focuses on the correction factor for backwater with scour presented in HDS No. 1 (Bradley, 1978). Figure 4.1 reproduces the correction factor curve. The curve was derived mainly from flume data using a sand bed and scaled bridge abutments to produce contraction scour.

Using the rigid boundary hydraulic values in the contraction scour equations from HEC-18, "Evaluating Scour at Bridges", (FHWA, 1995), Table 4.2 presents the predicted area of bridge scour, A_{SR}. The table also presents the predicted ratio of mobile boundary backwater to rigid boundary backwater (predicted h_{1M}^* / h_{1R}^*) from Figure 4.1 for each A_{SR}

/ A. In Table 4.2, the model h_{1M}^*/h_{1R}^* values represent the values from the BRI-STARS models (mobile and rigid) of Chapter 3. These are the same values presented in Table 4.1 for each case study. Figure 4.2 shows the plot of the modeled h_{1M}^* / h_{1R}^* (Table 4.1 values) versus the predicted h_{1M}^* / h_{1R}^* (Figure 4.1 values).

Figure 4.2 shows at least three outlier data points. These three points represent the three bridge lengths at Sta 3120 in the Nisqually case. As stated in Chapter 3, the Sta 3120 bridge site lies in a natural deposition zone. Thus, the natural morphology dominates the backwater characteristics for the selected bridge lengths. The bridge dominance criterion of $F_u / F_b \leq 1$ did not hold for this situation. Nonetheless, this criterion did predict the hydraulic dominance of 28 bridge lengths out of 31 (over 90%) for the selected case studies.

Disregarding the three outliers, the ratio of predicted to modeled h_{1M}^* / h_{1R}^* ratios ($R_{p/m}$) has a mean of about 1.03 and a standard deviation of about 0.34. The r^2 correlation value between the predicted and modeled h_{1M}^* / h_{1R}^* is less than 0.2. Assuming a normally distributed population, however, the sample/model data has a 90% chance that there is a relationship with the prediction curve of Figure 4.1 (a t-statistic value of 1.71 for 26 degrees of freedom with a 0.10 level of significance) (Miller and Freund, 1977).

Figure 4.3 presents the data in Figure 4.2 with the best fitting line and related confidence limits. As an example, assuming a predicted h_{1M}^* / h_{1R}^* value of 0.7 from Figure 4.1 for an A_{SR}/A value of 0.25, the corresponding modeled h_{1M}^* / h_{1R}^* would have a value of about 0.69 from Figure 4.3. For a rigid model backwater value of 1', the mobile boundary value would equate to about 0.69'.

For a rigid backwater value, h_{1R}^* of 1', the user would expect the actual mobile model backwater value, h_{1M}^*, to range on average from 0.65' to 0.74' in 90% of the population cases. For an individual or single case, the user would expect the mobile model to produce a backwater value, h_{1M}^*, ranging from 0.45' to 0.93'. Equation 4-1 presents the linear relationship(best fit) between the predicted h_{1M}^* / h_{1R}^* and the modeled h_{1M}^* / h_{1R}^* values of Figure 4.3.

$$Y_M = 0.46145 + 0.323218X_P \qquad (4\text{-}1)$$

Where: Y_M = Modeled h_{1M}^* / h_{1R}^*

X_P = Predicted h_{1M}^* / h_{1R}^*

4.4 Sensitivity Analysis

The sensitivity analysis focuses on active layer thickness, time steps, sediment gradations, and sediment transport equations. These parameters are the primary physical and operational variables of the mobile boundary model. From the sensitivity analysis, the thesis recommends values for these mobile boundary model parameters. The case studies (Nisqually, Skagit, Stony #1, Stony #2, and Gibbon) use the following parameter values:

Active layer thickness = One times the geometric mean of the maximum gradation size (D(NF)). See Table 4.3 for the active layer thicknesses for each case.

Time step(dt) = 12 minutes.

Sediment gradations = See Table 4.3 for gradations for each case study.

Sediment transport equation = Yang's (1984) method for gravel beds.

For sensitivity purposes, the analysis alters only one of the above parameters while leaving all the other parameters the same. The following summarizes the sensitivity results.

4.4.1 Active Layer Thickness

Based upon the results presented in Chapter 3, the mobile models with the largest mean grain sizes generally produce the largest backwater differences compared to the rigid boundary models. The sensitivity analysis, thus, starts with increasing the active layer thickness for Stony Creek #1, Stony Creek #2, and Gibbon River cases to equal the thickness of the Nisqually and Skagit case studies. Table 4.4 and the following discussion present the results of altering the active layer thickness:

Gibbon River - The original case study uses an active layer thickness of 91 mm. Doubling the active layer thickness to 181 mm matches the thicknesses of the Nisqually and Skagit studies. Table 4.4 shows that doubling the thickness does not alter the backwater results for any of the bridge lengths for this case. This result indicates that an active layer thickness of one does not limit the supply of sediment available for transport (demand-limited model).

For confirmation, the analysis includes various active layer thicknesses less than one times the geometric mean of the largest gradation size (less than 91 mm). For the 80' and 95' bridges, no changes in backwater occur for the mobile model until the active layer thickness becomes less than 0.1 of D (NF). In essence, the mobile model does not become supply-limited until the active layer thickness nearly equals 0.1 of the D (NF). As the active layer thickness continues to decline, the mobile backwater values increase until they match the rigid boundary model values.

Stony Creek #1 - The original case study uses an active layer thickness of about 45 mm. Similar to Gibbon, the analysis starts with increasing the active layer thickness to match the Nisqually and Skagit studies. This requires an active layer thickness of four times the D(NF). Like Gibbon, increasing the active layer thickness does not alter the mobile backwater values (demand-limited). Conversely, decreasing the active layer thickness to 0.05 of D (NF) does not alter the results for the 245' bridge. The model, thus, does not become supply-limited until the active layer thickness becomes less than 0.05 of D (NF). Similar to Gibbon, the mobile backwater values approach the fixed model values as the active layer thickness continues to decline.

Stony Creek #2 - The original case study uses an active layer thickness of 23 mm. The analysis started with increasing the active layer thickness to match the Nisqually and Skagit studies (8 D(NF)). Similar to Gibbon and Stony #1, increasing the active layer thickness does not alter the mobile backwater values for any of the bridge lengths (demand-limited).

For further confirmation, the analysis reduces the active layer thickness to 0.1 of D (NF) before the mobile backwater value for the 265' bridge begins to increase toward the fixed boundary value. The model, therefore, becomes supply-limited as the active layer thickness reduces to less than 0.6 of D (NF). Similar to Gibbon and Stony Creek #1, the mobile backwater values approach the fixed model values as the active layer thickness continues to decline.

Skagit River - For this case, the analysis looks at a wide range of active layer thicknesses (0.1 to 20 D(NF)) for the 285' bridge. Increasing the active layer thickness in this case does reduce the mobile backwater (supply-limited). For example, an active layer thickness of 5.0 D (NF) causes the mobile backwater to decline from 1.54' (1.0 D (NF)) to 1.29'. Conversely, reducing the active layer thickness to 0.1 D (NF) increases the backwater value to 2.43'. The fixed boundary value is 2.87' for the 285' bridge.

The above results justify using a minimum active layer thickness equal to one times the geometric mean of the largest gradation size (D (NF)). This insures an adequate supply of bed material for transport during a given time step. In demand-limited cases, increasing the active layer thickness to greater than D (NF) will not alter the results. In supply-limited cases (Skagit), increasing the active layer thickness 100% resulted in decreasing the computed backwater by 10%. In the same situation, increasing the active layer thickness by 400% causes a decrease in backwater of only 16%. Overall, an active layer thickness equal to D(NF) provides a reasonable starting value for a mobile boundary model (Hsu, 1991).

4.4.2 Time Step

Table 4.5 presents the results for analyzing different time steps at selected locations and bridge lengths. For each of the case studies, changing the time step does not alter the results to any measurable degree (less than a 2% change in the backwater depth). The following justifies the selected time steps:

2.4 minutes - This value represents the approximate time for the flood wave to travel from section to section. It is basically the distance between cross- sections (500' to 1000' feet) divided by the average channel velocity (5 to 10 feet per second). This yields a value of about one to two minutes. For convenience of computation, the analysis used 2.4 minutes or 1000 time steps (maximum limit) for a 40 hour hydrograph.

12 minutes and 60 minutes - The model also must simulate the movement of sediment near the bed (Lynn and Goodwin, 1997). Assuming a logarithmic velocity profile, the flood wave will exhibit a much slower velocity near the bed as compared to the overall average velocity. Using 0.1 of the average flood velocity (approximately the shear velocity), the time step increases to 20 to 30 minutes. Furthermore, flood values, sediment movements (saltation, suspension), and sediment sizes in motion will vary for each time step. To cover

variation in the values, the sensitivity analysis uses 12 and 60 minutes for the water/sediment time steps.

Molinas (1994) presents model data that shows very little differences in stream bed elevations for time steps ranging from nearly zero to three days (base = one day). Table 4.5 results support his findings.

For the selected times, the mobile boundary model prorates the distribution of sediment for each step. For example, the 60-minute time step will have about 5 times the total sediment load as the 12-minute time step. The 60-minute version of the model, however, has only one-fifth the total time steps as the 12-minute version of the model (40 steps versus 200 steps). The two model versions, therefore, produce comparable water surface profiles. Similarly, the 2.4-minute time step produces a profile comparable to the 12-minute time step. Using a 2.4-minute time step has less material in transport per step but has more time steps than if 12-minutes were used (1000 steps versus 200 steps). The two versions of the model produce nearly identical bridge backwater values.

The selected time step should vary with active layer thickness. As discussed above, however, three of the five cases represent demand-limited situations. Thus, increasing such supply limiting factors as active layer thickness and the time step does not alter the computed backwater results. Decreasing the active layer thickness to less than 1 D (NF) and the time step to less than a couple of minutes seems unreasonable (starts to approximate a fixed boundary model). As stated above, the model should allow for an adequate supply of material for transport during each time step. Similarly for the selected time step, the sediment particles should not travel faster than the water particles due to their larger mass. Overall, a time step of 12 minutes with an active layer thickness equal to one D (NF) should provide reasonable supply parameters for a mobile model (Molinas, 1997) with flood velocities on the order of 5 to 15 feet per second.

4.4.3 Gradation Variations

Table 4.5 presents the results for analyzing different gradation variations for Gibbon and Skagit River bridges. For Gibbon River, the 80' bridge produces only slight differences in bridge backwater results (less than a 5% variation). Shifting the original stream bed gradation downward by one size group produces no change at all. For example, the analysis tested Gibbon gradation ranges from 2 mm to 64 mm, instead of the actual 4 mm to 128 mm range. The 2 to 64 mm groups also have the same proportional distribution as the original 4 to 128 mm size groups.

Although using a smaller gradation shows an increase in transported material, the stream bed changes at the bridge site occur so as not to alter the computed backwater. Some bridge sections experience greater deposition and others greater scour. The flow depths, thus, differ from the original case but so do the bed elevations and some other hydraulic properties (i.e., changes in hydraulic bridge losses due to an expanded cross-section). The differences in flow depths and bed elevations, however, are less than 0.1' compared to the original model.

For a uniform size of 32 mm (original d_{50}), the model results show slightly more material in transport than with the full gradation. It, thus, produces a little less backwater. For the larger uniform size of 64 mm (original d_{90}), the model shows slightly less material in transport. It, therefore, produces a little more backwater compared to the original model run using a full gradation.

In the Skagit model, the 285' bridge has larger reductions in backwater than the Gibbon model due to variation in grain size. The elevations measure in tenths of a foot compared to the few hundredths of a foot for Gibbon. Shifting the stream bed gradation downward without altering the proportion of each size group produces a reduction in mobile backwater of 20%. The smaller gradation produces only 42% of the rigid model backwater values versus 54% of the rigid model backwater values for the original gradation. Similarly, a uniform gradation of 75 mm (original d_{50}), produces a comparable backwater reduction to the smaller gradation distribution.

In both of the above Skagit gradation cases (reduced gradation and uniform size), the model has more material available for transport than in the original case study. In both the reduced and uniform gradations, all six groups are available for transport. For the original case, the model will not transport about 10% of the particles using the Yang (1984) equation

(128 to 256 mm range). The model comparisons for the Skagit, thus, may over state the actual differences in computed backwater.

The modeler should use great care in sampling for stream bed gradations at a given bridge site (Molinas and Wu, 1998). Generally, the sensitivity results show a decrease in backwater for smaller graded materials (i.e., increased scour at the bridge site). The Gibbon, and for the most part the Skagit, produce only slightly different backwater results (a few hundredths of a foot) for the above differences in gradation sizes and distributions.

4.4.4 Sediment Transport Equations

This portion of the analysis compared the Meyer-Peter and Müller (1948) and Parker (1982, 1990) sediment transport equations to the Yang (1984) equation. Both comparisons start with a time step equal to 12 minutes and an active layer thickness equal to one times the representative grain size. The representative grain size for Meyer-Peter and Müller (1948) normally range from the d_{50} to d_{65} of the original gradation. For Parker (1982, 1990), the analysis uses the d_{50}. Table 4.5 presents a partial summary of the following results.

For the Meyer-Peter and Müller (MPM) (1948) method, the Nisqually, Skagit, and Gibbon cases generally produce 5 to 10 times the transported tonnage per 12-minute time step compared to the Yang (1984) equation. Given the large volume of sediment transported, these cases generally produce unstable oscillations. The model, thus, fails to complete the sediment/backwater calculations for the full hydrograph or the model produces unreliable backwater results (i.e., negative value for Gibbon). The cross-sections near and at the bridge also experience several feet more of scour or deposition compared to the Yang (1984) results.

The oscillations derive from large deposits or scour at each time step. This causes large changes in bed and water surface slopes. As the slopes, in particular the energy slope, increase, ever greater increases occur in the sediment transported (scour or deposition at each time step), continuing to increase the absolute value of the slopes to greater values. The model begins to oscillate back and forth like a wave between large values of deposition and scour, and large differences in positive and negative slopes, from time step to time step. The differences or oscillations begin to produce model results that do not match physical observations. In extreme cases, the oscillations become so great that they exceed numerical limitations of the model and the model ceases computations (Molinas, 1997).

To stabilize the model using the MPM (1948) method, the analysis reduces the active layer thickness for the Gibbon River case (80' bridge) to 0.05 of the representative sediment size (d_m = 37 mm, one size only) for the 12-minute time step. This produces a backwater value of 3.42'. This compares to 2.65' for the Yang method and 3.90' for the rigid model. The MPM model, however, still produces several times the tonnage per time step as the Yang model.

As a final MPM (1948) comparison, the analysis uses the 245' bridge of Stony Creek #1. Stony Creek #1 has a representative grain size, d_m, of 19 mm (again one size only). For an active layer thickness of one times the d_m, the MPM (1948) model produces a backwater value of about 0.97'. This compares to a Yang (1984) value of 1.77' and a rigid model value of 2.04'. For an active layer thickness of 0.05 d_m (d_m = D(NF) in this case), the MPM (1948) produces a comparable backwater value of 1.80'. The bed elevations near and at the bridge also compare well with the Yang (1984) results. The MPM (1948), however, still produces much larger volumes of transported materials.

Of the above cases used for the above MPM (1948) comparisons, Stony Creek #1 has the smallest active layer thicknesses. The smaller thicknesses help stabilize the model and produce results more comparable to the Yang (1984) results. Given the consistently larger volumes of sediment loads computed with MPM (1948) compared to the Yang (1984) method, the MPM (1948) models may require a smaller active layer thickness than for Yang (1984) to produce stable and reliable results.

Using the Parker (1982, 1990) method, the analysis evaluates the Skagit, Gibbon, and Stony Creek #1 cases. For an active layer thickness of 1.0 D (NF) and a time step of 12 minutes, the Parker (1982, 1990) method produces similar results to the MPM (1948) results for the selected bridge sites. For example, the Parker (1982, 1990) method generally produces 5 to 10 times the bed load of the Yang method for each time step. Also, the bridge sections generally experience several more vertical feet of scour.

For the 80' bridge on the Gibbon, active layer thicknesses of 1.0 and 0.05 D (NF) produce backwater values of 0.33' and 3.49', respectively. These compare to 2.65' for the Yang (1984) method and 3.90' for the rigid model. For Gibbon, the D (NF) equals a d_{50} of 32 mm. The 1.0 D (NF) produces very large loads and unstable channel and flood plain sections. The 0.05 D (NF) produces more stable results (smaller sediment loads).

For the 245' bridge on Stony Creek #1, active layer thicknesses of 1.0 and 0.1 D (NF) produce backwater values of 0.68' and 1.74', respectively. These compare to 1.77' with Yang (1984) and 2.04' with the rigid model. Similar to Gibbon, the smaller active layer thickness produces smaller load and more stable channel changes.

The Parker (1982, 1990) method like the MPM (1948) method requires much smaller active layer thicknesses than Yang's (1984) method to produce stable results. The unstable results (oscillations, abrupt deposition or scour) occur from large computed volumes of sediment loads for each time step. While an active layer thickness of 1.0 D (NF) works well with Yang (1984), the MPM (1948) and Parker (1982, 1990) methods need more analysis to determine a desirable D (NF) factor.

The above results, however, indicate that an active layer thickness less than one times the representative or d_{50} grain size probably provides the most stable and reliable results for the MPM (1948) and Parker (1982, 1990) methods. Physically, however, one would expect the active layer thickness to be at least as large as the particle sizes in transport (i.e., d_{50}, d_m). Therefore, a method that requires an active layer thickness less than the representative or d_{50} grain size to produce mathematically stable results may not truly produce physically representative backwater values.

For operational purposes, the analysis primarily uses a 12-minute time step for the MPM (1948) and Parker (1982, 1990) methods. For the Yang (1984) method, the time step sensitivity analysis does not produce differing results for a 2.4-minute versus a 12-minute time step. On the Skagit, a 2.4-minute time step does not alter the results for the MPM (1948) or Parker (1982, 1990) methods. Reducing the time step further also creates potential operational problems (limited number of time steps) and increases the computation time.

4.4.5 Summary of Sensitivity Results

The following summarizes the above results:

Active layer thickness - Using Yang (1984), an active layer thickness of 1.0 D (NF) provides a reasonable operational value for the mobile model. Values greater than 1.0 D (NF) generally lead to an additional supply of sediment that the model does not mathematically transport (sediment supply exceeds demand). The computed mobile backwater value, therefore, does not appreciably change from the 1.0 D(NF) value. Conversely, decreasing the active layer thickness until sediment demand exceeds supply leads to backwater values approaching the rigid model values.

Time step - For reasons previously discussed, the analysis uses time steps ranging from 2.4 minutes to 60 minutes. Altering the time step does not measurably alter the computed backwater values (less than 2% variation in values). The original 12-minute time step, thus, provides a reasonable operational value for the mobile model.

Stream bed gradations - Varying the stream bed gradation (uniform versus well-graded, downsizing gradation distribution) generally does not change the backwater results. Using smaller particles, however, does cause some reduction in backwater values. Smaller particles lead to an increase in transported sediment loads and, thus, greater bridge scour. Increased bridge scour normally reduces the bridge backwater. Assuming the engineer or researcher uses care in collecting sediment data, minor variations in sediment distribution should not affect the backwater results.

Sediment transport equations - The MPM (1948) and Parker (1982, 1990) methods require much smaller active layer thicknesses than the Yang (1984) method to produce a stable mobile model. Both methods computed much larger sediment loads than the Yang (1984) method. As stated above, the MPM (1948) and Parker (1982, 1990) methods require more analysis to determine a desirable D (NF) factor. Until then, the Yang (1984) method produces a more orderly and stable model for the given parameters (i.e., active layer thickness, time step, cross-section spacing).

4.5 Summary

The following summarizes the discussion and results from this chapter:

- Bridge backwater relationships - Fixed boundary, hydraulic parameters such as shear stress, Froude values, area of scour, unit stream power, and opening ratio cannot be used to predict bridge backwater elevations deriving from mobile boundary models. This conclusion comes from a statistical analysis of the data presented in Table 4.1. A regression analysis showed little or no correlation between the hydraulic parameters of fixed boundary models and the computed bridge backwater of mobile models. The data derives from the case studies presented in Chapter 3.
- Backwater correction factor - Figure 4.3 and Equation 4-1 present a relationship between a modeled backwater ratio (mobile/rigid) and a predicted backwater ratio. The modeled h_{1M}^* / h_{1R}^* values derive from the modeled results of Chapter 3. The predicted h_{1M}^* / h_{1R}^* values derive from Figure 4.1 (Bradley, 1978). Although the relationship between these two variables is statistically weak, it does provide a strong enough relationship for assessing the potential reduction in backwater if a mobile model is used in the bridge waterways analysis instead of a rigid boundary model.
- Bridge dominance - A Froude ratio (upstream value to bridge value) of less than one proved a reliable indicator of whether the bridge is the dominating morphologic feature at a given site. If a bridge is the dominating feature, then it is the primary influence on the local sedimentation processes. In this case, the bridge site has the potential to scour. The potential scour produces a potential reduction in bridge backwater that a mobile model will possibly predict but a rigid boundary model can not predict.
- Sensitivity analysis - Using BRI-STARS, the sensitivity analysis generated recommended values for active layer thickness, time step, stream bed gradations, and sediment transport equations. The analysis supports an active layer thickness of 1.0 D(NF) (geometric mean of the maximum stream bed gradation size). For time step, the analysis recommends 12 minutes as a reasonable value. For stream bed gradations, the research recommends only

careful collection of representative stream bed sediment gradations. As for sediment transport equations, the presented research recommends the Yang (1984) method for coarse-bedded streams.

Collectively, the above results suggest guidelines for applying mobile boundary models at bridge crossings.

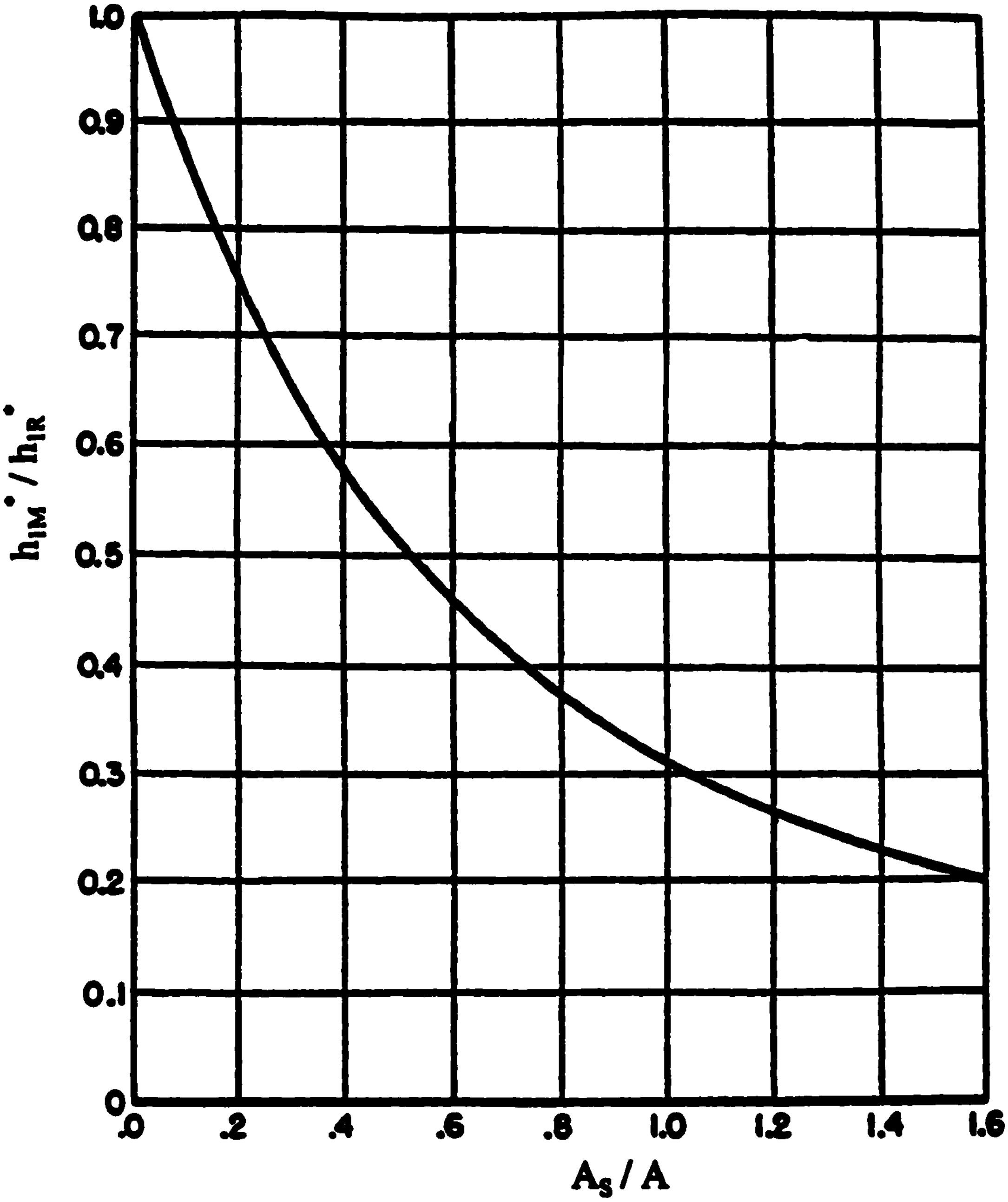

Figure 4.1 Correction factor for backwater with scour (Bradley, 1978)

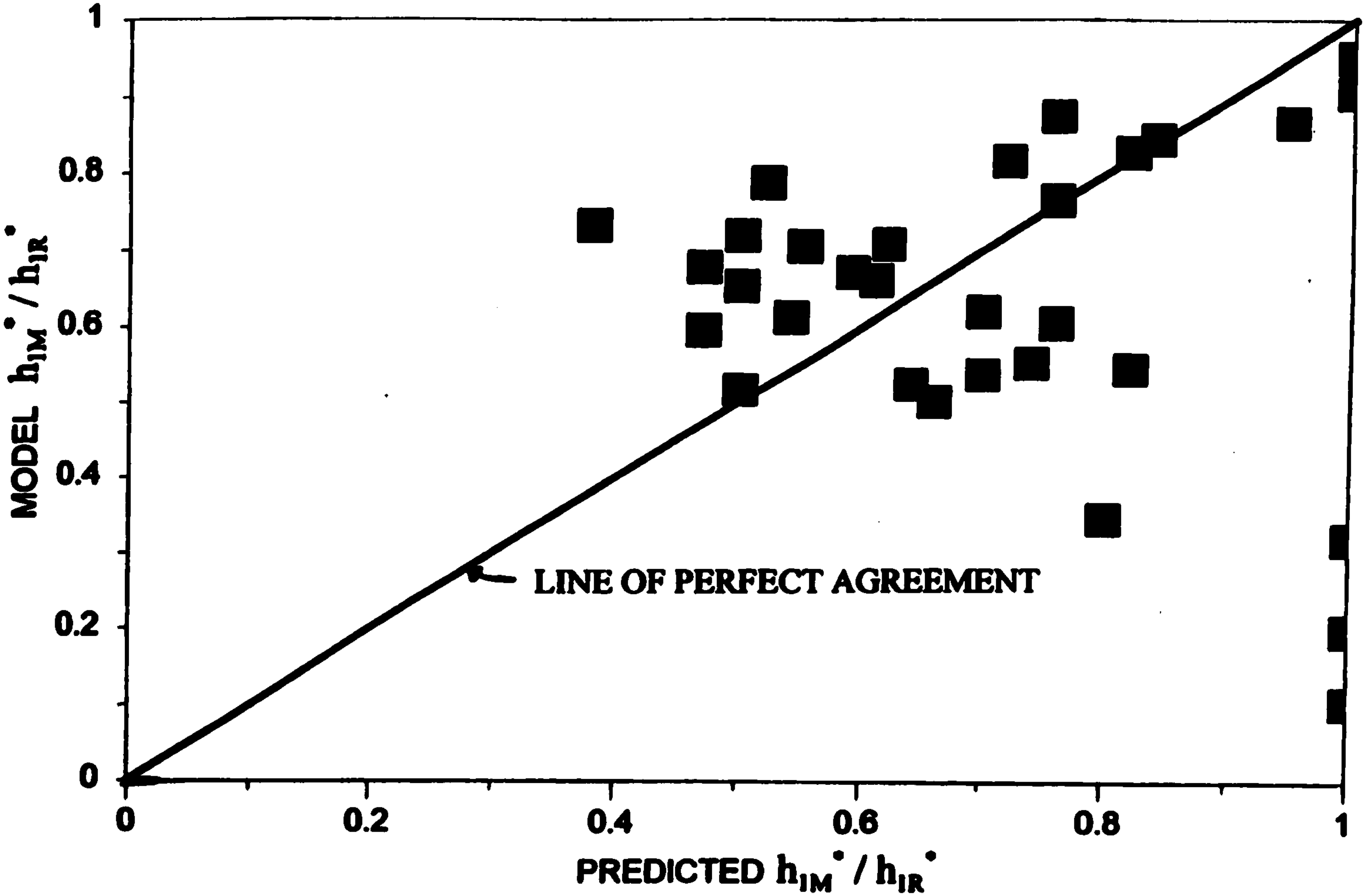

Figure 4.2 Modeled h_{IM}^{*} / h_{IR}^{*} versus the predicted h_{IM}^{*} / h_{IR}^{*}

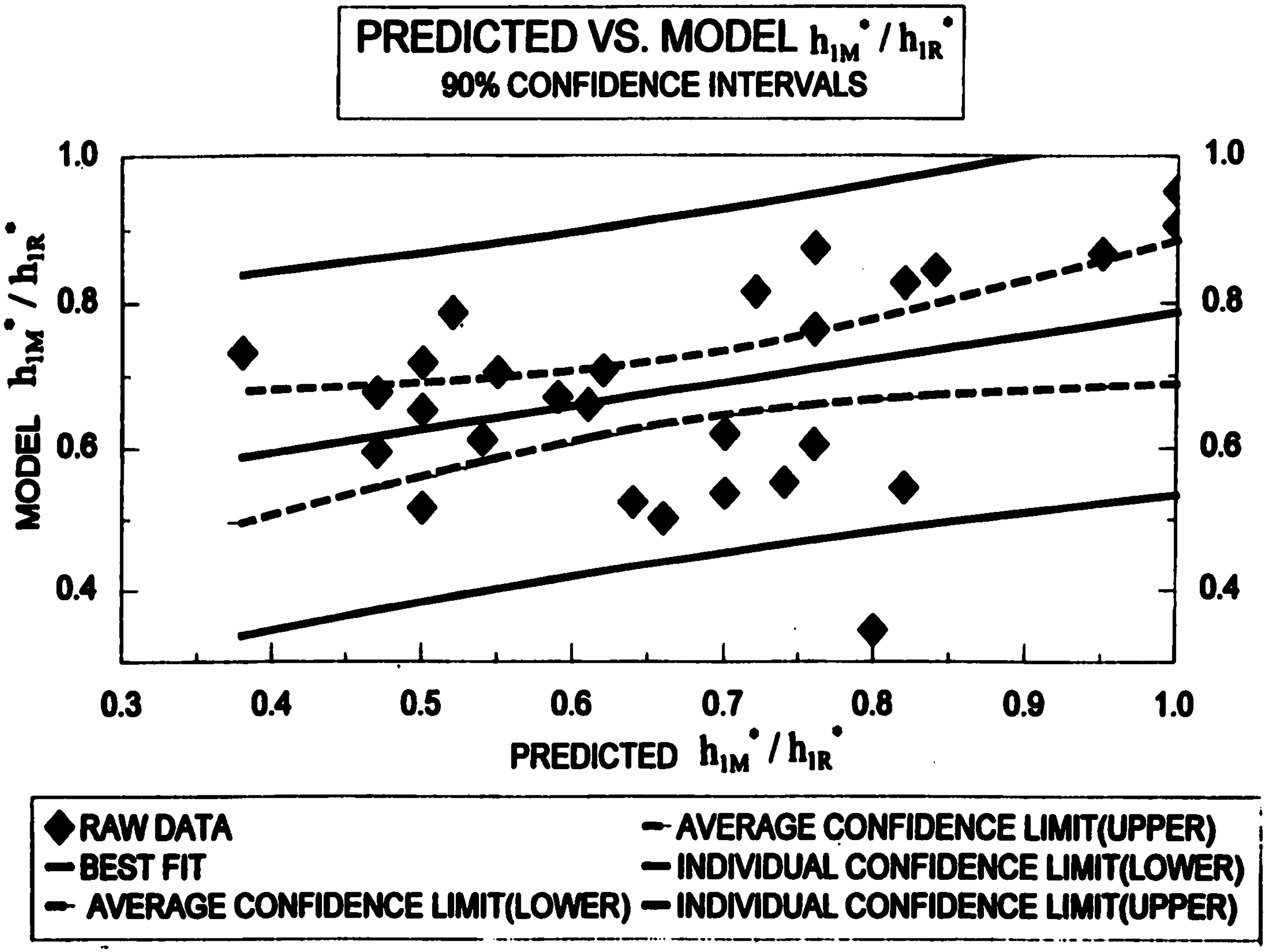

Figure 4.3 Modeled h_{1M}^{*} / h_{1R}^{*} versus the predicted h_{1M}^{*} / h_{1R}^{*} with best fitting line and confidence limits

Table 4.1 Summary of key hydraulic parameters

Nisqually River, 100-Year Flood

@ STA 3670 Bridge Length	Q_b cfs	Q_{100} cfs	$\frac{Q_b}{Q_{100}}$	h_{1M}^* ft	h_{1R}^* ft	$\frac{h_{1M}^*}{h_{1R}^*}$	A_{SM} sq ft	A sq ft	$\frac{A_{SM}}{A}$	F_u	F_b	$\frac{F_u}{F_b}$
No Bridge	10400	10400	1.00	-0.04	0.00	N/A	14	1409	0.01	0.73	0.84	0.87
315' Bridge	9400	10400	0.90	0.21	0.61	0.34	81	1203	0.07	0.61	0.78	0.78
250' Bridge	8250	10400	0.79	1.09	2.08	0.52	151	1025	0.15	0.43	0.87	0.49
200' Bridge	6600	10400	0.63	2.22	3.63	0.61	138	897	0.15	0.39	0.91	0.43

@ STA 5605 Bridge Length	Q_b cfs	Q_{100} cfs	$\frac{Q_b}{Q_{100}}$	h_{1M}^* ft	h_{1R}^* ft	$\frac{h_{1M}^*}{h_{1R}^*}$	A_{SM} sq ft	A sq ft	$\frac{A_{SM}}{A}$	F_u	F_b	$\frac{F_u}{F_b}$
No Bridge	10400	10400	1.00	0.30	0.00	N/A	-482	2313	-0.21	0.78	0.54	1.44
675' Bridge	9400	10400	0.90	0.45	0.07	6.43	-422	2068	-0.20	0.75	0.52	1.44
420' Bridge	7280	10400	0.70	0.87	0.48	1.81	-139	1558	-0.09	0.61	0.61	1.00
288' Bridge	5200	10400	0.50	1.82	2.20	0.83	71	1180	0.06	0.33	0.75	0.44

@ STA 3120 Bridge Length	Q_b cfs	Q_{100} cfs	$\frac{Q_b}{Q_{100}}$	h_{1M}^* ft	h_{1R}^* ft	$\frac{h_{1M}^*}{h_{1R}^*}$	A_{SM} sq ft	A sq ft	$\frac{A_{SM}}{A}$	F_u	F_b	$\frac{F_u}{F_b}$
No Bridge	10400	10400	1.00	-0.04	0.00	N/A	-125	1717	-0.07	0.84	0.78	1.08
540' Bridge	7280	10400	0.70	0.19	0.96	0.20	-76	1423	-0.05	0.70	0.86	0.81
510' Bridge	6760	10400	0.65	0.14	1.35	0.10	-12	1370	-0.01	0.58	0.89	0.65
480' Bridge	6240	10400	0.60	0.56	1.76	0.32	71	1317	0.05	0.49	0.91	0.54

Table 4.1 Summary of key hydraulic parameters(continued)

Skagit River, 100-Year Flood
Bridge @ STA 517

@ STA 517 Bridge Length	Q_b cfs	Q_{100} cfs	$\frac{Q_b}{Q_{100}}$	h_{1M}^* ft	h_{1R}^* ft	$\frac{h_{1M}^*}{h_{1R}^*}$	A_{SM} sq ft	A sq ft	$\frac{A_{SM}}{A}$	F_u	F_b	$\frac{F_u}{F_b}$
No Bridge	73460	73460	1.00	-0.22	0.00	N/A	-250	6127	-0.04	0.65	0.53	1.23
315' Bridge	69787	73460	0.95	0.49	0.90	0.54	130	5241	0.02	0.61	0.64	0.95
300' Bridge	66114	73460	0.90	0.96	1.74	0.55	270	4854	0.06	0.58	0.70	0.83
285' Bridge	62441	73460	0.85	1.54	2.87	0.54	380	4415	0.09	0.54	0.75	0.72
265' Bridge	58770	73460	0.80	2.47	4.93	0.50	490	3924	0.12	0.48	0.85	0.56
250' Bridge	55095	73460	0.75	4.90	9.49	0.52	700	3597	0.19	0.36	1.00	0.36
235' Bridge	51422	73460	0.70	7.39	12.43	0.59	740	3550	0.21	0.30	1.00	0.30

Stony Creek #1, 100-Year Flood
Bridge @ Sta 17075

@ STA 17075 Bridge Length	Q_b cfs	Q_{100} cfs	$\frac{Q_b}{Q_{100}}$	h_{1M}^* ft	h_{1R}^* ft	$\frac{h_{1M}^*}{h_{1R}^*}$	A_{SM} sq ft	A sq ft	$\frac{A_{SM}}{A}$	F_u	F_b	$\frac{F_u}{F_b}$
No Bridge	23300	23300	1.00	0.00	0.00	N/A	0	4948	0.00	0.40	0.39	1.03
350' Bridge	20970	23300	0.90	0.40	0.42	0.95	25	3607	0.01	0.36	0.35	1.03
290' Bridge	18640	23300	0.80	0.97	1.07	0.91	65	3095	0.02	0.32	0.40	0.80
245' Bridge	16310	23300	0.70	1.77	2.04	0.87	130	2675	0.05	0.27	0.46	0.59
225' Bridge	15145	23300	0.65	2.34	2.77	0.84	160	2469	0.06	0.24	0.50	0.48
200' Bridge	13980	23300	0.60	3.18	3.90	0.82	170	2222	0.08	0.20	0.55	0.36
175' Bridge	11650	23300	0.50	4.88	6.20	0.79	160	1926	0.08	0.15	0.64	0.23

Table 4.1 Summary of key hydraulic parameters(continued)

Stony Creek #2, 100-Year Flood
Bridge @ STA 65400

@ STA 65400 Bridge Length	Q_b cfs	Q_{100} cfs	$\frac{Q_b}{Q_{100}}$	h_{1M}* ft	h_{1R}* ft	$\frac{h_{1M}*}{h_{1R}*}$	A_{SM} sq ft	A sq ft	$\frac{A_{SM}}{A}$	F_u	F_b	$\frac{F_u}{F_b}$
No Bridge	23300	23300	1.00	0.00	0.00	N/A	0	4953	0.00	0.58	0.58	1.00
510' Bridge	20970	23300	0.90	0.56	0.64	0.88	68	3398	0.02	0.47	0.52	0.90
345' Bridge	18640	23300	0.80	1.07	1.40	0.76	136	2698	0.05	0.37	0.54	0.69
265' Bridge	16310	23300	0.70	2.32	3.28	0.71	220	2177	0.10	0.23	0.64	0.36
245'Bridge	15145	23300	0.65	3.06	4.34	0.71	230	2017	0.11	0.19	0.68	0.28
225' Bridge	13980	23300	0.60	4.08	5.68	0.72	220	1862	0.12	0.15	0.74	0.20
185' Bridge	11650	23300	0.50	7.27	9.93	0.73	200	1539	0.13	0.08	0.88	0.09

Gibbon River, 100-Year Flood
Bridge @ STA 9000

@ STA 65400 Bridge Length	Q_b cfs	Q_{100} cfs	$\frac{Q_b}{Q_{100}}$	h_{1M}* ft	h_{1R}* ft	$\frac{h_{1M}*}{h_{1R}*}$	A_{SM} sq ft	A sq ft	$\frac{A_{SM}}{A}$	F_u	F_b	$\frac{F_u}{F_b}$
No Bridge	2498	2498	1.00	0.00	0.00	N/A	0	510	0.00	0.75	0.75	1.00
165' Bridge	2250	2498	0.90	0.26	0.43	0.60	16	426	0.04	0.61	0.75	0.81
125' Bridge	2125	2498	0.85	0.57	0.92	0.62	25	350	0.07	0.50	0.76	0.66
95' Bridge	2000	2498	0.80	0.97	1.47	0.66	26	288	0.09	0.40	0.74	0.54
90' Bridge	1875	2498	0.75	1.18	1.76	0.67	30	284	0.11	0.36	0.75	0.48
85' Bridge	1750	2498	0.70	1.82	2.79	0.65	40	261	0.15	0.26	0.81	0.32
80' Bridge	1500	2498	0.60	2.64	3.90	0.68	55	247	0.22	0.20	0.86	0.23

Table 4.1 Summary of key hydraulic parameters(continued)

Nisqually River, 100-Year Flood

@ STA 3670 Bridge Length	Q_b cfs	Q_{100} cfs	$\frac{Q_b}{Q_{100}}$	h_{1M}^* ft	h_{1R}^* ft	$\frac{h_{1M}^*}{h_{1R}^*}$	SP_u fps	SP_d	$\frac{SP_u}{SP_d}$	τ_{cr}	τ_b	τ_b/τ_{cr}
No Bridge	10400	10400	1.00	-0.04	0.00	N/A	0.07311	0.07117	1.03	0.93	1.64	1.77
315' Bridge	9400	10400	0.90	0.21	0.61	0.34	0.08465	0.07250	1.17	0.93	2.07	2.23
250' Bridge	8250	10400	0.79	1.09	2.08	0.52	0.10464	0.07847	1.33	0.93	2.63	2.84
200' Bridge	6600	10400	0.63	2.22	3.63	0.61	0.12346	0.09506	1.30	0.93	3.40	3.67

@ STA 5605 Bridge Length	Q_b cfs	Q_{100} cfs	$\frac{Q_b}{Q_{100}}$	h_{1M}^* ft	h_{1R}^* ft	$\frac{h_{1M}^*}{h_{1R}^*}$	SP_u fps	SP_d	$\frac{SP_u}{SP_d}$	τ_{cr}	τ_b	τ_b/τ_{cr}
No Bridge	10400	10400	1.00	0.30	0.00	N/A	0.04694	0.05492	0.85	0.99	0.66	0.67
675' Bridge	9400	10400	0.90	0.45	0.07	6.43	0.05028	0.05575	0.90	0.99	0.75	0.76
420' Bridge	7280	10400	0.70	0.87	0.48	1.81	0.06379	0.05522	1.16	0.99	1.24	1.26
288' Bridge	5200	10400	0.50	1.82	2.20	0.83	0.08807	0.05835	1.51	0.99	2.09	2.12

@ STA 3120 Bridge Length	Q_b cfs	Q_{100} cfs	$\frac{Q_b}{Q_{100}}$	h_{1M}^* ft	h_{1R}^* ft	$\frac{h_{1M}^*}{h_{1R}^*}$	SP_u fps	SP_d	$\frac{SP_u}{SP_d}$	τ_{cr}	τ_b	τ_b/τ_{cr}
No Bridge	10400	10400	1.00	-0.04	0.00	N/A	0.03521	0.07311	0.48	0.93	1.25	1.35
540' Bridge	7280	10400	0.70	0.19	0.96	0.20	0.04669	0.06398	0.73	0.93	1.60	1.72
510' Bridge	6760	10400	0.65	0.14	1.35	0.10	0.04987	0.06250	0.80	0.93	1.70	1.83
480' Bridge	6240	10400	0.60	0.56	1.76	0.32	0.05301	0.06268	0.85	0.93	1.78	1.92

Table 4.1 Summary of key hydraulic parameters(continued)

Skagit River, 100-Year Flood
Bridge @ STA 517

@ STA 517 Bridge Length	Q_b cfs	Q_{100} cfs	$\frac{Q_b}{Q_{100}}$	h_{1M}* ft	h_{1R}* ft	$\frac{h_{1M}*}{h_{1R}*}$	SP_u fps	SP_d	$\frac{SP_u}{SP_d}$	τ_{cr}	τ_b	τ_b/τ_{cr}
No Bridge	73460	73460	1.00	-0.22	0.00	N/A	0.03204	0.03262	0.98	1.61	2.30	1.43
315' Bridge	69787	73460	0.95	0.49	0.90	0.54	0.04490	0.04727	0.95	1.61	3.13	1.95
300' Bridge	66114	73460	0.90	0.96	1.74	0.55	0.05760	0.06128	0.94	1.61	3.74	2.33
285' Bridge	62441	73460	0.85	1.54	2.87	0.54	0.07463	0.08364	0.89	1.61	4.38	2.73
265' Bridge	58770	73460	0.80	2.47	4.93	0.50	0.10677	0.12920	0.83	1.61	5.56	3.46
250' Bridge	55095	73460	0.75	4.90	9.49	0.52	0.23387	0.18983	1.23	1.61	6.58	4.10
235' Bridge	51422	73460	0.70	7.39	12.43	0.59	0.31901	0.21831	1.46	1.61	6.69	4.16

Stony Creek #1, 100-Year Flood
Bridge @ Sta 17075

@ STA 17075 Bridge Length	Q_b cfs	Q_{100} cfs	$\frac{Q_b}{Q_{100}}$	h_{1M}* ft	h_{1R}* ft	$\frac{h_{1M}*}{h_{1R}*}$	SP_u fps	SP_d	$\frac{SP_u}{SP_d}$	τ_{cr}	τ_b	τ_b/τ_{cr}
No Bridge	23300	23300	1.00	0.00	0.00	N/A	0.00467	0.00469	1.00	0.33	0.43	1.32
350' Bridge	20970	23300	0.90	0.40	0.42	0.95	0.00663	0.00679	0.98	0.33	0.84	2.55
290' Bridge	18640	23300	0.80	0.97	1.07	0.91	0.00872	0.01017	0.86	0.33	1.08	3.31
245' Bridge	16310	23300	0.70	1.77	2.04	0.87	0.01169	0.01602	0.73	0.33	1.44	4.40
225' Bridge	15145	23300	0.65	2.34	2.77	0.84	0.01390	0.02096	0.66	0.33	1.68	5.14
200' Bridge	13980	23300	0.60	3.18	3.90	0.82	0.01764	0.02923	0.60	0.33	2.08	6.35
175' Bridge	11650	23300	0.50	4.88	6.20	0.79	0.02487	0.04866	0.51	0.33	2.75	8.40

Table 4.1 Summary of key hydraulic parameters(continued)

Stony Creek #2, 100-Year Flood
Bridge @ STA 65400

@ STA 65400 Bridge Length	Q_b cfs	Q_{100} cfs	$\frac{Q_b}{Q_{100}}$	h_{1M}* ft	h_{1R}* ft	$\frac{h_{1M}*}{h_{1R}*}$	SP_u fps	SP_d	$\frac{SP_u}{SP_d}$	τ_{cr}	τ_b	τ_b/τ_{cr}
No Bridge	23300	23300	1.00	0.00	0.00	N/A	0.00940	0.00940	1.00	0.16	0.47	2.90
510' Bridge	20970	23300	0.90	0.56	0.64	0.88	0.01355	0.01190	1.14	0.16	1.00	6.22
345' Bridge	18640	23300	0.80	1.07	1.40	0.76	0.01788	0.01569	1.14	0.16	1.57	9.76
265' Bridge	16310	23300	0.70	2.32	3.28	0.71	0.02663	0.02601	1.02	0.16	2.35	14.62
245'Bridge	15145	23300	0.65	3.06	4.34	0.71	0.03105	0.03341	0.93	0.16	2.72	16.92
225' Bridge	13980	23300	0.60	4.08	5.68	0.72	0.03674	0.04385	0.84	0.16	3.15	19.62
185' Bridge	11650	23300	0.50	7.27	9.93	0.73	0.05595	0.08322	0.67	0.16	4.52	28.16

Gibbon River, 100-Year Flood
Bridge @ STA 9000

@ STA 9000 Bridge Length	Q_b cfs	Q_{100} cfs	$\frac{Q_b}{Q_{100}}$	h_{1M}* ft	h_{1R}* ft	$\frac{h_{1M}*}{h_{1R}*}$	SP_u fps	SP_d	$\frac{SP_u}{SP_d}$	τ_{cr}	τ_b	τ_b/τ_{cr}
No Bridge	2498	2498	1.00	0.00	0.00	N/A	0.024426	0.024514	1.00	0.62	0.61	0.99
165' Bridge	2250	2498	0.90	0.26	0.43	0.60	0.028235	0.024765	1.14	0.62	0.87	1.41
125' Bridge	2125	2498	0.85	0.57	0.92	0.62	0.033455	0.027169	1.23	0.62	1.28	2.07
95' Bridge	2000	2498	0.80	0.97	1.47	0.66	0.039833	0.032785	1.21	0.62	1.88	3.05
90' Bridge	1875	2498	0.75	1.18	1.76	0.67	0.040737	0.036137	1.13	0.62	1.93	3.12
85' Bridge	1750	2498	0.70	1.82	2.79	0.65	0.047451	0.044867	1.06	0.62	2.24	3.62
80' Bridge	1500	2498	0.60	2.64	3.90	0.68	0.052347	0.060362	0.87	0.62	2.47	4.00

Table 4.2 Model versus Predicted $\frac{h_{IM}^*}{h_{IR}^*}$

Project	Sta	Bridge Length, ft	h_{IM}^* ft	h_{IR}^* ft	Model $\frac{h_{IM}^*}{h_{IR}^*}$	A_{SR} sq ft	A sq ft	$\frac{A_{SR}}{A}$	Predicted $\frac{h_{IM}^*}{h_{IR}^*}$	$R_{p/m}$
NISQUALL	3670	315	0.21	0.61	0.34	200	1203	0.17	0.80	2.32
NISQUALL	3670	250	1.09	2.08	0.52	334	1025	0.33	0.64	1.22
NISQUALL	3670	200	2.22	3.63	0.61	398	897	0.44	0.54	0.88
NISQUALL	5605	288	1.82	2.20	0.83	171	1180	0.14	0.82	0.99
NISQUALL	3120	540	0.19	0.96	0.20	0	1423	0.00	1.00	5.05
NISQUALL	3120	510	0.14	1.35	0.10	0	1370	0.00	1.00	9.64
NISQUALL	3120	480	0.56	1.76	0.32	0	1317	0.00	1.00	3.14
SKAGIT	517	315	0.49	0.90	0.54	721	5241	0.14	0.82	1.51
SKAGIT	517	300	0.96	1.74	0.55	1049	4854	0.22	0.74	1.34
SKAGIT	517	285	1.54	2.87	0.54	1098	4415	0.25	0.70	1.30
SKAGIT	517	265	2.47	4.93	0.50	1227	3924	0.31	0.66	1.32
SKAGIT	517	250	4.90	9.49	0.52	1970	3597	0.55	0.50	0.97
SKAGIT	517	235	7.39	12.43	0.59	2089	3550	0.59	0.47	0.79
STONY #1	17075	350	0.40	0.42	0.95	0	3607	0.00	1.00	1.05
STONY #1	17075	290	0.97	1.07	0.91	0	3095	0.00	1.00	1.10
STONY #1	17075	245	1.77	2.04	0.87	85	2675	0.03	0.95	1.09
STONY #1	17075	225	2.34	2.77	0.84	265	2469	0.11	0.84	0.99
STONY #1	17075	200	3.18	3.90	0.82	486	2222	0.22	0.72	0.88
STONY #1	17075	175	4.88	6.20	0.79	976	1926	0.51	0.52	0.66
STONY #2	65400	510	0.56	0.64	0.88	663	3398	0.20	0.76	0.87
STONY #2	65400	345	1.07	1.40	0.76	545	2698	0.20	0.76	0.99
STONY #2	65400	265	2.32	3.28	0.71	811	2177	0.37	0.62	0.88

Table 4.2 Model versus Predicted $\frac{h_{IM}^*}{h_{IR}^*}$ (continued)

Project	Sta	Bridge Length ft	h_{IM}^* ft	h_{IR}^* ft	Model $\frac{h_{IM}^*}{h_{IR}^*}$	A_{SR} sq ft	A sq ft	$\frac{A_{SR}}{A}$	Predicted $\frac{h_{IM}^*}{h_{IR}^*}$	$R_{p/m}$
STONY #2	65400	245	3.06	4.34	0.71	923	2017	0.46	0.55	0.78
STONY #2	65400	225	4.08	5.68	0.72	1023	1862	0.55	0.50	0.70
STONY #2	65400	185	7.27	9.93	0.73	1239	1539	0.81	0.38	0.52
GIBBON	9000	165	0.26	0.43	0.60	81	426	0.19	0.76	1.26
GIBBON	9000	125	0.57	0.92	0.62	88	350	0.25	0.70	1.13
GIBBON	9000	95	0.97	1.47	0.66	105	288	0.36	0.61	0.92
GIBBON	9000	90	1.18	1.76	0.67	111	284	0.39	0.59	0.88
GIBBON	9000	85	1.82	2.79	0.65	136	261	0.52	0.50	0.77
GIBBON	9000	80	2.64	3.90	0.68	149	247	0.60	0.47	0.69

Table 4.3 Sediment size distribution and active layer thickness

Sediment Size Distribution
All Cases

					Nisqually Bridges		
Gradation mm	Skagit % Passing	Stony #1 % Passing	Stony #2 % Passing	Gibbon % Passing	Sta 3120 % Passing	Sta 3670 % Passing	Sta 5605 % Passing
--------	--------	--------	--------	--------	--------	--------	--------
2	0	0	0	0	0	0	0
4	0	17	22	0	0	0	0
8	0	27	54	2	1	1	2
16	0	50	82	12	2	3	3
32	8	83	100	50	34	34	31
64	38	100		88	69	68	63
128	90			100	95	95	93
256	100				100	100	100

Active Layer Thickness
All Cases

					Nisqually Bridges		
	Skagit mm	Stony #1 mm	Stony #2 mm	Gibbon mm	Sta 3120 mm	Sta 3670 mm	Sta 5605 mm
	--------	--------	--------	--------	--------	--------	--------
D(NF)	181	45	23	91	181	181	181

Table 4.4 Sensitivity results for active layer thickness

<u>Active Layer Thickness = A_L * Geometric Mean of Maximum Gradation (D(NF))</u>

Time Step, dt = 12 minutes

Sediment Transport Equation = Yang's (1984)

Gibbon River, 100-Year Flood
Bridge @ Sta 9000

@ Sta 9000 Bridge Length	Q_b cfs	Q_{100} cfs	$\frac{Q_b}{Q_{100}}$	$A_L = 1$ h_{IM}^* ft	$A_L = 2$ h_{IM}^* ft	h_{IR}^* ft
No Bridge	2498	2498	1.00	0.00	0.00	0.00
165' Bridge	2250	2498	0.90	0.26	0.26	0.43
125' Bridge	2125	2498	0.85	0.57	0.56	0.92
95' Bridge	2000	2498	0.80	0.97	0.96	1.47
90' Bridge	1875	2498	0.75	1.18	1.18	1.76
85' Bridge	1750	2498	0.70	1.82	1.81	2.79
80' Bridge	1500	2498	0.60	2.64	2.64	3.90

Stony Creek #1, 100-Year Flood
Bridge @ STA 17075

@ Sta 17075 Bridge Length	Q_b cfs	Q_{100} cfs	$\frac{Q_b}{Q_{100}}$	$A_L = 1$ h_{IM}^* ft	$A_L = 4$ h_{IM}^* ft	h_{IR}^* ft
No Bridge	23300	23300	1.00	0.00	0.00	0.00
350' Bridge	20970	23300	0.90	0.40	0.40	0.42
290' Gridge	18640	23300	0.80	0.97	0.97	1.07
245' Bridge	16310	23300	0.70	1.77	1.77	2.04
225' Bridge	15145	23300	0.65	2.34	2.33	2.77
200' Bridge	13980	23300	0.60	3.18	3.18	3.90
175' Bridge	11650	23300	0.50	4.88	4.87	6.20

Stony Creek #2, 100-Year Flood
Bridge @ Sta 65400

@ Sta 65400 Bridge Length	Q_b cfs	Q_{100} cfs	$\frac{Q_b}{Q_{100}}$	$A_L = 1$ h_{IM}^* ft	$A_L = 8$ h_{IM}^* ft	h_{IR}^* ft
No Bridge	23300	23300	1.00	0.00	0.00	0.00
510' Bridge	20970	23300	0.90	0.56	0.56	0.64
345' Bridge	18640	23300	0.80	1.07	1.07	1.40
265' Bridge	16310	23300	0.70	2.32	2.32	3.28
245' Bridge	15145	23300	0.65	3.06	3.05	4.34
225' Bridge	13980	23300	0.60	4.08	4.07	5.68
185' Bridge	11650	23300	0.50	7.27	7.24	9.93

Table 4.4 Sensitivity results for active layer thickness(continued)

Selected Locations and Bridge Lengths

Location and Bridge Length	Q_b cfs	Q_{100} cfs	$\frac{Q_b}{Q_{100}}$	$A_L = 20$ h_{IM}^* ft	$A_L = 10$ h_{IM}^* ft	$A_L = 5$ h_{IM}^* ft	$A_L = 2$ h_{IM}^* ft	$A_L = 1$ h_{IM}^* ft	$A_L = 0.5$ h_{IM}^* ft	$A_L = 0.1$ h_{IM}^* ft	$A_L = .05$ h_{IM}^* ft	$A_L = .01$ h_{IM}^* ft	h_{IR}^* ft
Gibbon River 95' Bridge	2000	2498	0.80					0.97	0.97	0.99			1.47
Gibbon River 80' Bridge	1500	2498	0.60					2.64	2.65	2.65	2.82		3.90
Stony Creek #1 245' Bridge	16310	23300	0.70					1.77	1.77	1.77	1.77	1.92	2.04
Stony Creek #2 265' Bridge	16310	23300	0.70					2.32	2.32	2.46	2.73	3.14	3.28
Skagit River 285' Bridge	62441	73460	0.85	1.23	1.25	1.29	1.39	1.54	1.77	2.43			2.87

Table 4.5 Sensitivity Results for Time Step, Gradation Variation and Sediment Transport Equations

Time Step, dt, in Minutes

Active Layer Thickness = 1 * D(NF); Sediment Transport Equation = Yang's (1984)

Location and Bridge Length	Q_b cfs	Q_{100} cfs	$\frac{Q_b}{Q_{100}}$	dt = 2.4 m h_{IM}^* ft	dt = 12 m h_{IM}^* ft	dt = 60 m h_{IM}^* ft	h_{IR}^* ft
Gibbon River, 80' Bridge	1500	2498	0.60	2.63	2.64	2.69	3.90
Stony Creek #1, 245' Bridge	16310	23300	0.70	1.77	1.77	1.78	2.04
Stony Creek #2, 265' Bridge	16310	23300	0.70	2.32	2.32	2.34	3.28
Skagit River, 285' Bridge	62441	73460	0.85	1.54	1.54	1.57	2.87

Variations in Sediment Gradation

Active Layer Thickness = 1 * D(NF); Sediment Transport Equation = Yang's (1984)

Time Step, dt = 12 minutes

Location and Bridge Length	Q_b cfs	Q_{100} cfs	$\frac{Q_b}{Q_{100}}$	Actual Size h_{IM}^* ft	One Size Gradation Reduction h_{IM}^* ft	Uniform Distribution d_{50} h_{IM}^* ft	Uniform Distribution d_{90} h_{IM}^* ft	h_{IR}^* ft
Gibbon River 80' Bridge	1500	2498	0.60	2.64	2.64	2.57	2.72	3.90
Skagit River 285' Bridge	62441	73460	0.85	1.54	1.20	1.14		2.87

d_{50} = 32 and 75 mm for Gibbon and Skagit, respectively.
d_{90} = 64 mm for Gibbon.

Table 4.5 Sensitivity Results for Time Step, Gradation Variation and Sediment Transport Equations(continued)

Sediment Transport Equations

Time Step, dt = 12 minutes

Location and Bridge Length	Q_b cfs	Q_{100} cfs	$\frac{Q_b}{Q_{100}}$	Yang $A_L = 1$ h_{IM}^* ft	MPM $A_L = 1$ h_{IM}^* ft	MPM $A_L = .05$ h_{IM}^* ft	Parker $A_L = 1$ h_{IM}^* ft	Parker $A_L = 0.1$ h_{IM}^* ft	Parker $A_L = .05$ h_{IM}^* ft	h_{IR}^* ft
Gibbon River 80' Bridge	1500	2498	0.60	2.64	-0.14	3.42	0.33		3.49	3.90
Stony Creek #1 245' Bridge	16310	23300	0.70	1.77	0.97	1.80	0.68	1.74		2.04

For Yang, the active layer thickness equals 1 * D(NF). For Gibbon and Stony #1, D(NF) is 91 and 45 mm, respectively.
For MPM, the active layer thickness equals A_L * d_m. For Gibbon and Stony #1, d_m is 37 and 19 mm, respectively.
For Parker, the active layer thickness equals A_L * d_{50}. For Gibbon and Stony #1, d_{50} is 32 and 16 mm, respectively.

CHAPTER 5: APPLYING MOBILE MODELS AT BRIDGE CROSSINGS

5.1 Overview

This chapter introduces a method for applying mobile boundary models to coarse-bedded bridge crossings. Before presenting this process, Section 5.1.1 briefly discusses the hydraulic design of bridges. This subsection is presented to place Sections 5.2 through 5.8 in their proper context.

Section 5.1.2 presents a summary of the general processes for applying mobile boundary models at bridge crossings. Table 5.1 presents the overall process for applying these models. This subsection also briefly discusses the content contained in Sections 5.2 through 5.8.

5.1.1 Hydraulic Design of Bridges

There is no single approach for the hydraulic design of bridges crossing stream systems. Instead, engineers commonly use an accumulation of hydraulic design criteria and design methods for bridge crossings. These criteria and methods are summarized in such publications as AASHTO's Model Drainage Manual (1999), AASHTO's Highway Drainage Guidelines (1999), and FHWA's Federal Lands Highway Project Development and Design Manual (1996-2000).

In the most basic terms, the hydraulic design of a bridge includes determining its length, depth, and height. Sometimes these parameters are intertwined and the computed water surface profile plays a major role in the design of each parameter. In some instances, the profile may directly affect only one bridge design parameter such as length, for example.

The following steps summarize the general design criteria and approach employed in the hydraulic design of bridges:

1. Determine the quantitative and qualitative design criteria - To hydraulically design the selected bridge site, the engineer must determine the required design criteria. The design criteria may include such items as regulated limits on bridge backwater increases (e.g., one foot for 100-year flood); potential damage to adjacent property; hazard to life; government

regulations on fish, wildlife, wetlands, water quality, and flood plains; and life cycle costing (i.e., initial bridge costs, maintenance). Collectively, these items will often set many limits on the possible bridge alternatives.

2. Select the design flood(s) - To meet the design criteria under Step 1, the engineer will evaluate a bridge crossing for a wide range of floods and for the conditions associated with each flood. For example, FEMA, FHWA, and various other agencies use the 100-year flood as the base or design flood for determining bridge backwater elevations. For determining foundation depth and types, FHWA (1995) recommends a "super" flood such as a 500-year flood. For environmental reasons (i.e., fish passage, water quality), regulatory agencies (i.e., USACE, USFWS) may require hydraulic evaluations for flood peaks of a more common occurrence, such as a 2-year frequency. In general, the hydraulic engineer will evaluate the a bridge crossing for a wide range of floods and conditions associated with each flood.

3. Perform physical site evaluation - To evaluate each design flood, the engineer performs a physical site evaluation. This requires such information as data collection (e.g., field survey, high water marks), morphologic evaluations (e.g., Rosgen stream type, sediment yields), hydrology (e.g., 100-year flood determination), and sedimentation assessment (e.g., bed gradations, aggrading or degrading bed).

4. Determine existing water surface profile - Before analyzing the potential bridge alternatives, the engineer evaluates the existing hydraulic conditions at the site. This typically requires a hydraulic computer model such as HEC-RAS or BRI-STARS or FESWMS-2D. The engineer selects the model that contains the computational methods that best describes the design flood conditions (one dimensional or two dimensional, fixed or mobile, etc.).

5. Select the design bridge length(s) - Using the information from Steps 1 through 4, the engineer will select the potential bridge length(s) for computing the associated water surface profiles. This assumes that the bridge location, alignment, and basic design are set (piers, etc.). The upstream profile or bridge backwater is normally a function of the selected bridge length (the longer the bridge length, the less the relative bridge backwater). The

selected bridge length typically determines the bridge opening and the bridge backwater is primarily a function of the bridge opening.

6. Compute the proposed water surface profile(s) - This is done for the selected bridge length(s) using the same methods and considerations as those used for the existing water surface profile.

7. Evaluate the proposed bridge length(s) relative to the computed profile(s)- Generally, the engineer evaluates each alternative bridge length in terms of the given design criteria (Step 1). Using an assessment or analysis of the capital costs and associated risks, the engineer will typically recommend the bridge length that has the lowest life-cycle costs. This assumes the recommended bridge length meets the other SEE constraints (social, economic, and environmental) (OFR, 1999). The computed water surface profile represents the hydraulic evaluation of how well the selected bridge length(s) meet the SEE constraints.

8. Select the minimum bridge clearance - Once the engineer or modeler has determined the design bridge length, he or she will determine the minimum bridge clearance. This is usually the vertical clearance between the low chord elevation of the bridge and the computed water surface profile for the given design flood. Generally, the engineer will determine a minimum vertical clearance or freeboard based upon an evaluation of data collection errors, model errors, and on the passage of debris and ice.

9. Determine the bridge foundation depths - This step typically depends upon a hydraulic scour evaluation (e.g., for 500-year flood), geotechnical evaluation (e.g., bedrock, alluvial deposits), and structural design criteria (e.g., load capability and load distributions for various bridge layouts). Collectively, the selected foundation depths, types, and layout are a function of costs, construction, and regulatory constraints.

The above steps represent one typical process for the hydraulic design of bridges. Clearly, many variations are possible. For example, highway design constraints may limit the height of the bridge. Thus, the engineer would possibly have to select a longer and more expensive bridge rather than a shorter, higher bridge or possibly reduce the desirable vertical clearance.

Regardless of the particular design approach, the above outline illustrates the role of the mobile model analysis in the hydraulic design of bridges. In particular, the mobile model analysis will play a significant role in Steps 4, 5, and 6. Assuming a more accurate water surface profile and scour depths from the mobile analysis, the following approach may also lead to a more accurate determination of the minimum bridge clearance and foundation depths.

5.1.2 Summary of Applying Mobile Models at Bridge Crossings

Table 5.1 presents the overall process for applying mobile models at bridge crossings. In this process, the modeler or user first determines the applicability of the models to the given bridge site. The initial process includes a fixed boundary analysis of the site and an assessment of the site's morphological characteristics (e.g., aggrading, degrading, sediment transport traits, bridge influence on sedimentation processes). If the natural morphology dominates the resulting backwater curves or water surface profiles at the site, then the mobile model becomes the model of choice for the site. If the bridge layout represents the dominant morphological feature at the site, then the modeler can use a cost-based approach to determine whether or not to use a mobile model. If the user selects the mobile model, then the backwater results are compared to those of the fixed boundary model. Ultimately, the user applies this process to select the optimum bridge layout for the given design criteria (i.e., bridge backwater limits versus bridge length).

Section 5.2 lists the preferred physical attributes for identifying bridge sites applicable to the process presented in Table 5.1. Section 5.3 summarizes the requirements for performing a fixed boundary analysis at a given bridge site. Section 5.4 presents an approach for determining the relationship or dominance of the bridge layout relative to the natural morphology. Section 5.5 provides an approach for comparing the cost of using a mobile vs. fixed boundary model and the potential economic benefits (e.g., reduced bridge costs). Section 5.6 presents an approach for using the mobile model (i.e., physical and operational parameters). Section 5.7 discusses the mobility of the bridge approaches or banks and their influence on the bridge backwater values and in selecting an optimum bridge length. Section 5.8 summarizes the information presented in Sections 5.1 through 5.7.

5.2 Identifying Potential Cases/Sites

Preferably, the potential bridge site should have the general attributes presented in Section 2.3 for the previously discussed case studies of Chapter 3. These attributes consist of the stream hydraulics, stream hydrology and morphology, sediment traits, and bridge hydraulics. The following summarizes those preferred attributes from Section 2.3 and presented in Table 5.2.

Ideally, the flow at the bridge site is one-dimensional with subcritical and gradually varied flow. These conditions should prevail throughout the study reach. Since the case studies have a peak flood range of 2500 to 75000 cfs, the research also recommends a similar range of flows for the process shown in Table 5.1. The main portion of the flood hydrograph should have a duration of one to two days.

For the morphology, the site should have a main channel and floodplains with long-term stability and definition (vegetated flood plains, gravel channel beds, etc.). The reach geometry should have fairly uniform widths and slopes. The stream slopes should range from 0.1% to 3%. Overall, the stream system should have moderate sinuosity, moderate entrenchment, and moderate bank width to depth ratios (10 to 40) as defined in Rosgen (1996).

For the sediment traits, the main channel bed should consist of gravel to cobble beds. The bed should have a dominating bed size (i.e., armored or uniform gradation). Sediment inflow should approximately equal sediment outflow. The stream shear stresses should exceed the critical shear stresses of the main channel bed or boundary (sediment in transport during the given flood event).

The bridge opening should represent the dominant hydraulic feature of the bridge layout. The selected site should have minimal skew or eccentricity. Also the piers should have little influence on the water surface profile. Energy-based methods should be able to compute a reasonably, accurate bridge water surface profile of the site (i.e., preferably no hydraulic jumps).

Again, the above represents preferred attributes. However, Tables 3.1 and 3.2 show a wide range of morphological and hydraulic traits for the actual case studies in Chapter 3.

Thus, the user may still apply the Table 5.1 process to bridge sites that in some instances lack some of the preferred physical attributes.

5.3 Fixed Boundary Analysis

After identifying the potential bridge site, the modeler should perform a fixed boundary analysis. Typical bridge design guidelines and government regulations will generally require such an analysis for a given flood event(s) (AASHTO, 1999). As stated earlier, this type of analysis consists of determining the water surface profile at the bridge site for a given flood event (i.e., bridge backwater analysis for 100-year flood). From a bridge design and regulatory perspective, the fixed boundary water surface profile analysis represents the minimum hydraulic analysis for a given bridge site (AASHTO, 1999).

For this analysis, the modeler must collect various data, develop the overall stream water surface profile, and address the bridge hydraulics. Sections 2.4, 2.5.1, and 2.5.3, respectively, discuss each of these topics in detail. The following summarizes the discussions from those sections.

The required data includes stream cross-sections, design peak floods, stream bed gradations, and boundary roughness values. Assuming flow conditions as discussed Section 5.2 (subcritical, gradually varied, one-dimensional), the fixed boundary analysis uses the standard step method to compute the general stream water surface profile (i.e., no bridge). For the model, the user could use HEC-2 (USACE, 1990) or BRI-STARS (Molinas, 1994 and Molinas, 1998) or HECRAS (USACE, 1998).

If the user anticipates the possibility of performing a mobile boundary analysis, then BRI-STARS is a reasonable model for using the process outlined in Table 5.1. To represent the bridge, the user simply adjusts the cross-section at the bridge site to match the proposed bridge layout. For the bridge section, the user must also apply the bridge backwater coefficient, K^*, defined in equation 2-17. The BRI-STARS model uses this additional data to compute the water surface profile for the given bridge layout. Otherwise, many other available mobile boundary models have the option to be operated in a fixed boundary mode (e.g., HEC-6).

For a given location along the upstream water surface profile, the user computes the difference in the water surface elevations for the no bridge and selected bridge alternative(s). This difference represents the fixed boundary backwater value(s), h_{1R}^*. Table 5.3 presents the process for the fixed boundary analysis that leads to the computed backwater values.

5.4 Bridge Domination Analysis

After completing the fixed boundary analysis, the user should assess whether or not the bridge is the dominating morphological feature at the proposed site. This assessment consists of two steps. First, the user evaluates the natural morphology (e.g., sedimentation processes, Rosgen (1996) classification). Second, the user evaluates the upstream versus the bridge section Froude value criterion (i.e., $F_u / F_b \leq 1$). Collectively, these two assessments should provide the user with the necessary physical information for choosing between a mobile and fixed boundary model.

The user should assess the natural morphology with the main objective of determining whether or not the given bridge site is in sedimentation equilibrium. This assessment is performed with the assumption of no bridge at the proposed site. For example, with no bridge, does the sediment inflow at the bridge site approximately equal the sediment outflow? If yes, then the proposed bridge layout becomes the potential dominating morphological feature.

Unfortunately, an assessment of the natural morphology in terms of its dominance versus a proposed bridge structure is very subjective. For example, as Table 3.1 shows, the case studies include a large range of morphological types. Using the Rosgen (1996) channel classification scheme, the case studies included types B, C, D, E, and F. The research only ignored highly entrenched (and generally hydraulically steep) channel types such A and G. For Rosgen (1996) classified stream types B through F, each type had bridge layouts that dominated or influenced the water surface profile more than the natural morphology (no bridge, mobile boundary scenario).

As stated under Section 5.2, the user should generally select bridge sites with fairly uniform channel widths and slopes. For the Nisqually case studies at STA 3120 and STA

5605, these sites produced data outliers because each site had a natural stream width much greater than the approaching upstream channel section. In one case (STA 3120), this greater width produced a mobile boundary backwater curve much lower than the rigid boundary curve. For different reasons, the second case (STA 5605) produced a mobile boundary curve higher than the fixed boundary curve. Sections 3.2.8 and 3.2.9 give detail explanations for these outlying results.

While the user should consider the morphological features of the study area (entrenchment, sinuosity, width/depth ratio, slope, channel material, etc.), simply assessing or classifying the general stream morphology (i.e., applying a Rosgen (1996) type classification) appears insufficient in determining whether or not to apply a mobile versus fixed boundary model. Instead, evaluating local changes in stream width, stream slopes, and other local morphological features from section to section may provide insight to the overall local sedimentation processes.

As stated in Sections 4.2 and 4.3, a selected bridge length that had a Froude ratio (F_u / F_b) of less than unity correlated in over 90% of the case bridge lengths with the bridge exerting the dominating influence on the backwater curve. Along with the preferred physical attributes described in Section 5.2, the user should use this Froude ratio as a principle determining factor for whether or not the bridge is the dominating morphological influence at the proposed site. Table 5.4 presents the bridge domination process.

To summarize the above and Table 5.4, the user should first perform an overall morphological assessment of the site (i.e., perform Rosgen (1996) stream classification criteria and assessment). Second, the user should decide whether or not the site has comparable morphology and sediment attributes to those presented in Table 5.2. If not, then the site may require a mobile analysis to assess the associated bridge backwater. If the site does have physical attributes comparable to those presented in Table 5.2, then the user should compute the Froude ratio for the rigid or fixed boundary condition. If the value is greater than one, then the mobile boundary model may provide a superior backwater result to the fixed boundary model. If the Froude ratio is less than or equal to one, then the user should proceed to Section 5.5 for a cost analysis to determine the cost effectiveness of applying a mobile model to the proposed bridge site.

5.5 Cost Analysis

At this stage, the user has concluded that the proposed bridge layout dominates the morphological processes (i.e., scour, deposition) at the site. This section presents a process for selecting between a fixed and a mobile model for predicting the bridge backwater. Table 5.5 summarizes this process.

5.5.1 General Approach

For the fixed boundary analysis, the user has computed the bridge backwater value, h_{1R}^*(usually taken one bridge length upstream of the bridge crossing). As part of the overall bridge scour analysis, the user should have also computed the contraction scour, A_{SR}, and the total flow area, A, at the proposed bridge crossing (see Section 4.3). Using the computed A_{SR} / A ratio and Figure 4.1, the user selects an estimated h_{1M}^* / h_{1R}^* value (predicted), X_P.

Assuming the bridge site has the physical attributes described in Section 5.2, the user computes a new h_{1M}^* / h_{1R}^* (modeled) value, Y_M, using equation 4-1 and X_P. The estimated value h_{1M}^* for the selected bridge site becomes the product of Y_M and h_{1R}^*. With the h_{1M}^* value, the user estimates any potential savings in bridge costs, (SBC).

The SBC value consists of the present value difference in the life-cycle costs for the different bridge alternatives. For example, the fixed boundary model may produce backwater results requiring a certain bridge layout with specific life-cycle costs and SEE constraints. Based upon the estimated h_{1m}* value, the mobile model may allow for a bridge layout that still meets the SEE constraints but with a lower life-cycle cost. The difference in the present value of the two bridge layouts (fixed-based model vs. mobile-based model) is the SBC value.

In many instances, the SBC value will primarily consist of the difference in initial bridge construction costs between a fixed-based model layout versus a mobile-based model layout. As long as the bridge layout meets the backwater requirements for a given design flood, the user normally does not have to consider the economic or risk-based costs of the layout (i.e., life-cycle maintenance, property damage). For example, there is typically no economic advantage for exceeding the backwater criterion (FHWA, 1996-2000).

The user then estimates the additional engineering costs, (EC), for implementing a mobile model for the selected bridge site. For estimating EC, Section 5.6 presents the additional engineering items needed to use the mobile model. The user then compares the extra engineering costs, EC, to the potential savings in bridge costs, SBC, of applying the mobile model. If the SBC value exceeds the EC value, the user employs the mobile boundary model at the bridge crossing.

5.5.2 Case Example

The following example illustrates the process outlined in Table 5.5 (see Table 5.6 for a summary of the calculations). All the below costs are computed in present dollars (i.e., SBC, EC).

Using the Skagit River case study, we compare the h_{1R}^* values of 1.74' and 0.90' for the 300' and 315' long bridges, respectively (see Table 4.1). Using a maximum allowable backwater value of one foot, the fixed boundary analysis would require us to use the 315' bridge instead of the 300' option. Assuming a minimum bridge width of 32' and an approximate bridge construction cost of \$ 200 per square foot, the 315' bridge would cost about \$ 96,000 more than the 300' long bridge (\$200/ft^2 x 32 ft x (315 ft - 300 ft)).

The 300' and 315' bridges have substantially the same layout. The pier locations and sizes, and the abutment locations and sizes are essentially the same for both bridges as shown in Figure 3.18. Although the bridges have differences in their computed backwater values, the overall hydraulic performance is about the same for each alternative.

Given the comparable bridge layouts and hydraulic performances, it is important to note that the case example assumes negligible differences in the life-cycle costs other than the initial construction costs. While life-cycle costing methods are beyond the scope of this thesis, FHWA (1981) presents one approach for assessing and analyzing the capital costs and associated risks for the hydraulic design of bridge crossings. The potential life-cycle costs include such items as property damage, traffic interruptions, structural and roadway damage, environmental disturbances, and hazards to human life. Also, it is assumed that both layouts will meet the same socio-economic and environmental requirements (SEE). The major design and cost difference between the 300' and 315' bridge is the bridge length. The SBC value for this example becomes \$ 96,000, the initial construction cost difference in the two bridge lengths.

From Table 4.2, the 300' bridge section has a computed fixed boundary scour, A_{SR}, of 1049 ft^2, and fixed boundary flow area, A, of 4854 ft^2. The computed ratio, A_{SR} / A, is about 0.22. From Figure 4.1, this ratio yields a predicted h_{1M}^* / h_{1R}^* value, X_P, of about 0.7. Using equation 4-1, this yields a Y_M or expected model value of 0.69 for the h_{1M}^* / h_{1R}^* ratio. Multiplying this value times the h_{1R}^* value of 1.74' yields a h_{1M}^* of 1.20'. On average, the user would expect the 300' bridge using a mobile boundary for the computed backwater to still exceed the backwater limit of one foot. Using Figure 4.3, the lower average and individual confidence limits (90%) yields Y_M values of 0.65 and 0.45, respectively. These values yield respective h_{1M}^* values of 1.13 and 0.78 feet. Thus, there is some possibility that the mobile model could yield a backwater value equal to or less than one foot for the cheaper 300' bridge.

Still undecided about using a mobile boundary model, the user decides to estimate the additional time and money for implementing the model. Assuming a couple of extra days to gather additional data, develop the model input values, and perform the simulation runs as outlined in Section 5.6, the user estimates a total additional engineering cost of about \$2000 (\$ 100 per hour (billable rate) x 20 hours).

The user compares the potential savings in bridge costs (SBC) of \$ 96,000 to an additional engineering cost (EC) of \$ 2000 for implementing the mobile model. Since the SBC value exceeds the EC value, applying the mobile model appears a worthwhile investment. As Table 4.1 shows, the 300' bridge has an actual h_{1M}^* value of 0.96'. If the user does consider the mobility of the stream in the modeling process, the 300' bridge would, thus, meet the one foot maximum backwater design criterion.

5.5.3 Other Design Considerations

The above example focuses on the design relationship between bridge length and the associated backwater. As stated under Section 5.1.1, the engineer must also consider bridge height or vertical clearance. The user must, furthermore, evaluate the foundation depths for such design factors as scour.

From the above example, the 300' bridge with the one foot of backwater (mobile boundary model) would most likely have the same modeled vertical clearance for such items as floating debris and ice as the 315' bridge with about one foot of backwater for the fixed boundary model. As for data and model errors, the mobile model should have comparable errors to the fixed boundary model. The mobile model analyzes physical processes (sediment transport, morphologic changes) that the fixed boundary model does not analyze for a bridge site, and could thus possibly be more accurate.

Similarly for foundation depths (i.e., piers, abutments) the mobile model should provide more accurate depth and velocity estimates than the fixed model within the vicinity of the bridge. Again, this is due to its greater capacity to analyze the physical processes at a bridge crossing than a fixed model. This increased level of analysis should lead to a more accurate scour analysis for foundation purposes.

For the mobile 300' bridge condition, it is assumed that the foundation scour potential is no greater than the scour potential for the fixed 315' bridge. This is indirectly reflected in the comparable backwater values of about 1' for both conditions. A comparable backwater depth indicates a comparable bridge opening. Although the 300' bridge has less opening width, it has greater flow depth in the mobile condition than the fixed condition. This creates the potential for a lower bridge opening velocity and, thus, less foundation scour.

To re-state, the above cost analysis determines whether to accept the results of the fixed boundary water surface profile or proceed with a mobile boundary analysis. It is not a substitute for actually performing a mobile boundary analysis. If the cost analysis indicates that the user or engineer should perform a mobile boundary analysis, then the engineer should use the mobile boundary model to evaluate all bridge design aspects (length, depth, and height) for the given design floods and related criteria.

5.6 Mobile Boundary Analysis

Table 5.7 presents a flow chart for completing the mobile boundary analysis. Sections 2.5.2 and 2.5.4 present the theory and assumptions related to this analysis. Similar to the fixed boundary model, Section 2.4 presents the data required for the mobile model.

At this point, the user should have developed a fixed boundary model (FBM) per Section 5.3. Developing the mobile boundary model (MBM) consists of adding certain hydrology and sediment data and setting various operational parameters. The following summarizes this process as outlined in Table 5.7.

First, the user should develop a complete flood hydrograph for the site. USGS gage station data or a deterministic hydrology method (e.g., SCS method) should provide the source for developing a site specific hydrograph. As stated earlier, the hydrograph should have a minimum duration of one to two days.

With the flood or water hydrograph, the MBM needs an associated sediment inflow hydrograph. This hydrograph typically derives from field collected data or from a developed sediment rating curve (sediment discharge versus water discharge) using a sediment transport equation (i.e., Yang (1984), Parker (1982, 1990)). If the sediment inflow hydrograph does not exist for the site, then the user could add about five "dummy" stream cross-sections upstream of the study site at an approximate spacing of 1000'. The five dummy sections should replicate the last upstream cross-section of the selected study area with a constant stream slope (uniform sections and slope). In this case, the model will start with clear water scour at the dummy cross-section located farthest upstream and should eventually develop into a sedimentation equilibrium (sediment in equals sediment out) by the time the model computations reach the actual study area. This situation generally applies to only bed load motion type streams.

In addition to the upstream dummy sections, the user should add enough sections to the farthest downstream section of the study site to insure that the downstream boundary conditions will not adversely affect the study area. This also compensates for models like BRI-STARS that do not incorporate a transmissive boundary at the downstream end of the model and permits sediment to mathematically "flow-out" of the modeled reach.

The user also needs to input the sediment distribution (gradation curve) and water temperature data to the model. The MBM uses this data with physical and operational data to complete the sedimentation computations. These computations are the primary component for determining the stream section boundary.

After inputting the physical data for the FBM, the water and sediment hydrographs, and the sediment gradation and water temperature data, the user must input the required operational values. For BRI-STARS, these include hydrograph time steps, active layer thickness, sediment transport equation, stream tubes, time iterations, and roughness equation. The following recommended operation values derive from Section 4.4.

The user should select a time step anywhere from 2 to 60 minutes. From the case studies in Chapter 3, a 12-minute step should provide satisfactory results. Corresponding to the 12-minute time step, an active layer thickness of one times the geometric mean of the largest gradation size(one D (NF)) should work well for the MBM. The selected transport equation also interrelates to time step and active layer thickness in the sedimentation computations. From the literature, the user should select the transport equation most applicable to the study area. If doubt exists as to the proper equation for the site, the research used for this paper recommends the Yang equation for gravel beds.

For the case studies in Chapter 3, the number of stream tubes equaled five. This is generally enough to break the stream channel into three main sections. The remaining two tubes represent the left and right flood plains.

The number of suggested time iterations is simply the duration of the flood hydrograph (i.e., 40 hours = 1.67 days) divided to the time step duration (i.e., 12 minutes = 0.00833 days, which yields about 200 time steps). Finally, the case studies used Manning's equation for the hydraulic roughness equation.

After inputting all the above information into the MBM, the user then performs the first simulation run. The model should execute all the computational steps with out severe oscillations (i.e., excessive scour or deposition). If the model does experience severe oscillations, then the user should re-evaluate the operational parameters. In particular for BRI-STARS, active layer thickness in combination with the sediment transport equation will generally exert the most influence on the MBM's overall behavior.

Once completing a stable simulation for the MBM, then the user should evaluate the results for their reasonableness when compared to the actual physical evidence of the study site. Of course, this is a very subjective process (see Section 1.5). Such an evaluation may include comparisons to high water marks, comparing, if available, changes in stream cross-sections and aerial photographs over time, and comparing the model results (i.e., amount of scour, deposition) to the expected outcomes for the type of morphological system for the selected study site. If the MBM results do not appear satisfactory, then the user should reassess the operational parameters. The user should consider the full range of parameters (i.e., cross-section spacing, flood hydrograph, upstream and downstream boundary conditions) in adjusting the accuracy of the model.

5.7 Mobility of the Bridge Approaches

Previous chapters have presented the influence of the bridge layout (i.e., length) on backwater values and how they differ between the types of models (fixed vs. mobile). This chapter has shown the influence of backwater on selecting a potential bridge layout and the influence of the boundary model type on the selected bridge layout (i.e., Section 5.5 example). This section briefly discusses the mobility of the bridge approaches or bank and the selection of the optimum bridge.

So far, the research has emphasized the mobility of the stream bed in the mobile boundary model. The selected models lend themselves to analyzing the influence of the stream hydraulics on the stream bed. However, bridge approaches generally consist of materials (i.e., large boulders in the form of riprap) that may have the structural resistence to withstand major flood events such as a 100-year flood. Furthermore, high flood resistant materials such as riprap do not conform to the application of most sediment transport formulas or methods. All the case studies, thus, only permitted scour and deposition at the stream bed level.

The user does have a few choices in addressing the mobility of the bridge section banks or approaches. First, compute the resistance of the bridge approach to stream erosion for the design flood (i.e., 100-year flood). For example, "Design of Riprap Revetment, HEC-11" (FHWA, 1989) provides a method for determining the factor of safety for a given riprap design for a given set of flow conditions. The user should perform this analysis using the fixed boundary values and before starting the mobile boundary analysis. Federal, state, or local regulations may require the riprap design to withstand the proposed design flood. This case would resemble the case studies used in this paper. Thus, only the stream bed experiences scour and deposition, not the stream bank. This is the design approach that this paper highly recommends.

The other approach is more speculative. Assuming that the design criteria and regulations permit for an approach failure, the user has HEC-11 (FHWA, 1989) or similar methods to predict under which hydraulic and hydrologic conditions that the failure may occur. The user could adjust the fixed and possibly the mobile model at the point of failure to reflect the modified bridge section with the failed banks.

Unfortunately, the methods for estimating the conditions for riprap failure (i.e., incipient motion) generally do not present methods for estimating the quantity of failed material. Thus, the user would know when the approach failed but not the configuration of the failure. Furthermore, applying an adjusted bridge cross-section in the middle of a series of reiterative hydraulic/sediment computations in a mobile model does not consider the time-related changes that occur from the initial starting conditions till the point of approach failure. Based upon the case studies, it is these time and related spatial changes that occur in the mobile model computational process that does not allow the user to simply substitute the nonscoured fixed boundary cross-section with a contraction scour-based cross-section to estimate the mobile boundary profile. Finally, the time and spatial changes that occur over the duration of the flood hydrograph also at least partially explain the weak correlation between fixed boundary scour values (i.e., contraction scour) and the predicted backwater ratios (mobile/fixed) provided from equation 4-1.

5.8 Summary

This chapter has presented a detailed approach for applying mobile boundary models at bridge crossings. For background, Section 5.1.1 presents a brief and general discussion on the hydraulic design of bridges (Section 5.1.1). Section 5.1.2 and Table 5.1 summarize the overall processes for applying mobile boundary models at bridges sites.

Section 5.2 and Table 5.2 list the preferred physical attributes for identifying bridge sites applicable to the process presented in Table 5.1. These preferred physical attributes are based upon those attributes discussed in Section 2.3 and the case studies of Chapter 3. The physical attributes consist of the stream hydraulics, stream hydrology and morphology, sediment traits, and bridge hydraulics.

Section 5.3 and Table 5.3 summarize the requirements for performing a fixed boundary analysis at a given bridge site. The modeler must collect various field and hydrologic data, develop the natural water surface profile, and determine the bridge hydraulics. From this information, the modeler determines the bridge backwater value for the fixed boundary model, h_{1R}^*.

Section 5.4 and Table 5.4 present an approach for determining the relationship or dominance of the bridge layout relative to the natural morphology. If the natural morphology is the predominate influence on the water surface profile at the bridge site, then the mobile boundary model is the preferred model. If the bridge is the dominating morphological feature at the crossing, then the user should proceed with the cost analysis described in Section 5.5.

Section 5.5 and Table 5.5 provide an approach for comparing the cost of using a mobile vs. fixed boundary model and the potential economic benefits (e.g., reduced bridge costs). Without developing the mobile boundary model, the user estimates the mobile boundary backwater, h_{1M}^*, from equation 4-1 for the given bridge layouts. If the estimated h_{1M}^* allows for a less expensive bridge layout than the computed h_{1R}^*, then the user compares the difference or savings in bridge costs, SBC, to the estimated engineering costs, EC, of developing a mobile boundary model. If SBC exceeds EC, then the user implements the mobile boundary model for computing the actual h_{1M}^*. Table 5.6 presents a case example.

Section 5.6 and Table 5.7 present an approach for using the mobile boundary model (i.e., physical and operational parameters). This approach consists of collecting certain hydrology and sediment data and setting various operational data. The hydrologic data consists of the complete flood hydrograph, the sediment data includes stream bed gradations, and the operational parameters consist of active layer thickness, sediment transport equation, time step, and stream tubes.

Section 5.7 discusses the mobility of the bridge approaches or banks and their influence on the bridge backwater values and in selecting an optimum bridge length. This section emphasizes the speculative nature of estimating the mobility of bridge approaches. In particular, there currently are no accurate methods for estimating the erosion processes of riprap bridge approaches (e.g., estimating quantity of eroded materials such as riprap bank protection).

TABLE 5.1 Flow chart for applying mobile models at bridge crossings

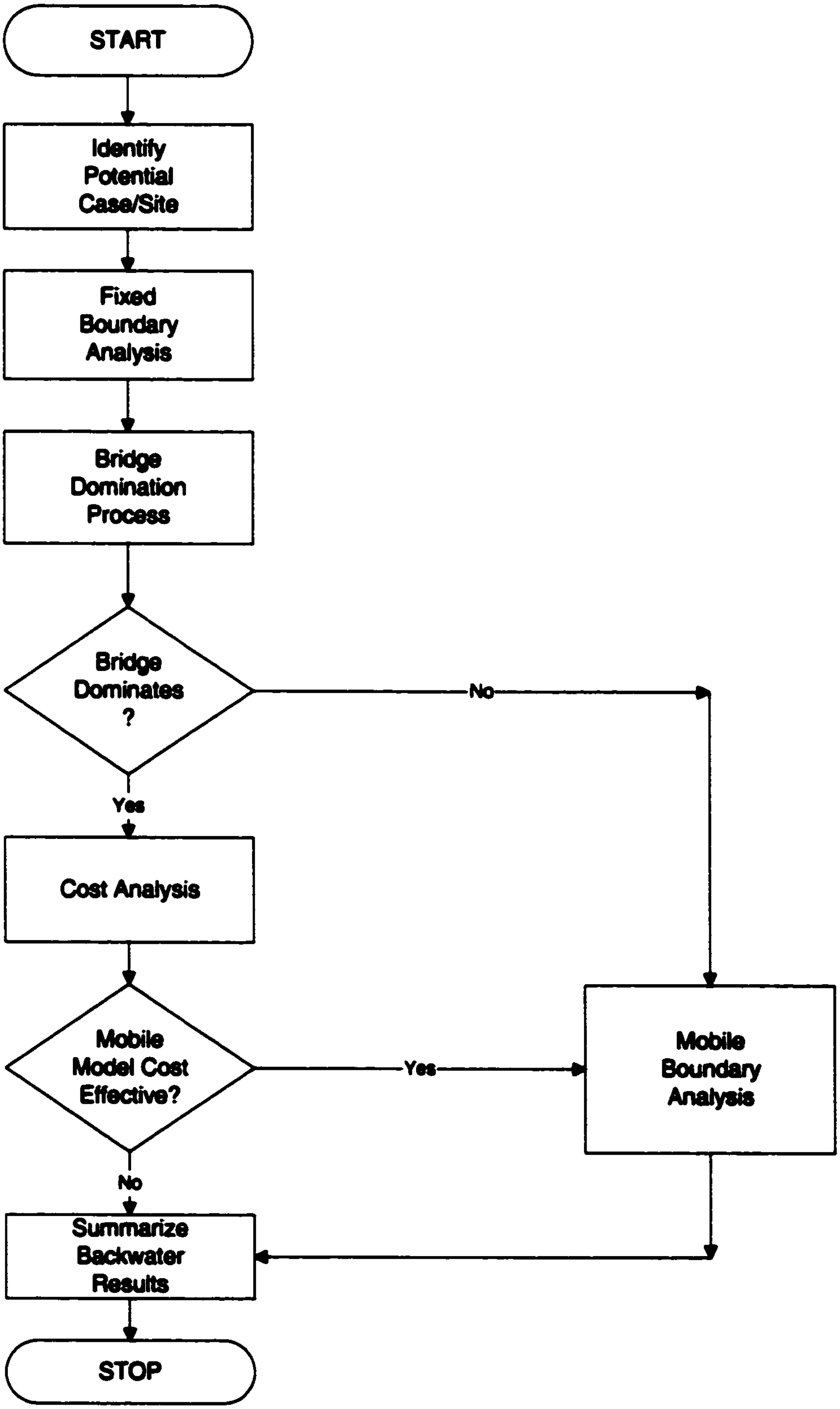

Table 5.2 Preferred physical attributes of potential bridge sites

Stream Hydraulics	Stream Hydrology and Morphology	Sediment Traits	Bridge Hydraulics
One-dimensional flow	Flood peaks: 2,500 cfs to 75,000 cfs	Gravel to cobble bed	Bridge opening dominant hydraulic feature of the bridge
Sub-critical, gradually varied conditions	Main flood hydrograph durations: 1 to 2 days	d_{50} range: 8 to 80 mm	Minimal bridge skew or eccentricity
	Main channel and flood plains: well-defined, stable, fairly uniform slopes and widths	Uniform to armored channel beds	Minimal pier influence
	Stream slopes: 0.1% to 3%	Sediment inflow comparable to sediment outflow	Subject to energy-based analysis (i.e. preferably no hydraulic jumps)
	Stream pattern and form: Moderate sinuosity, moderate entrenchment, and moderate bank width to depth ratios	Flood shear stresses exceed boundary shear stresses (i.e. sediment in transport during peak flood event)	

TABLE 5.3 Flow chart for fixed boundary analysis

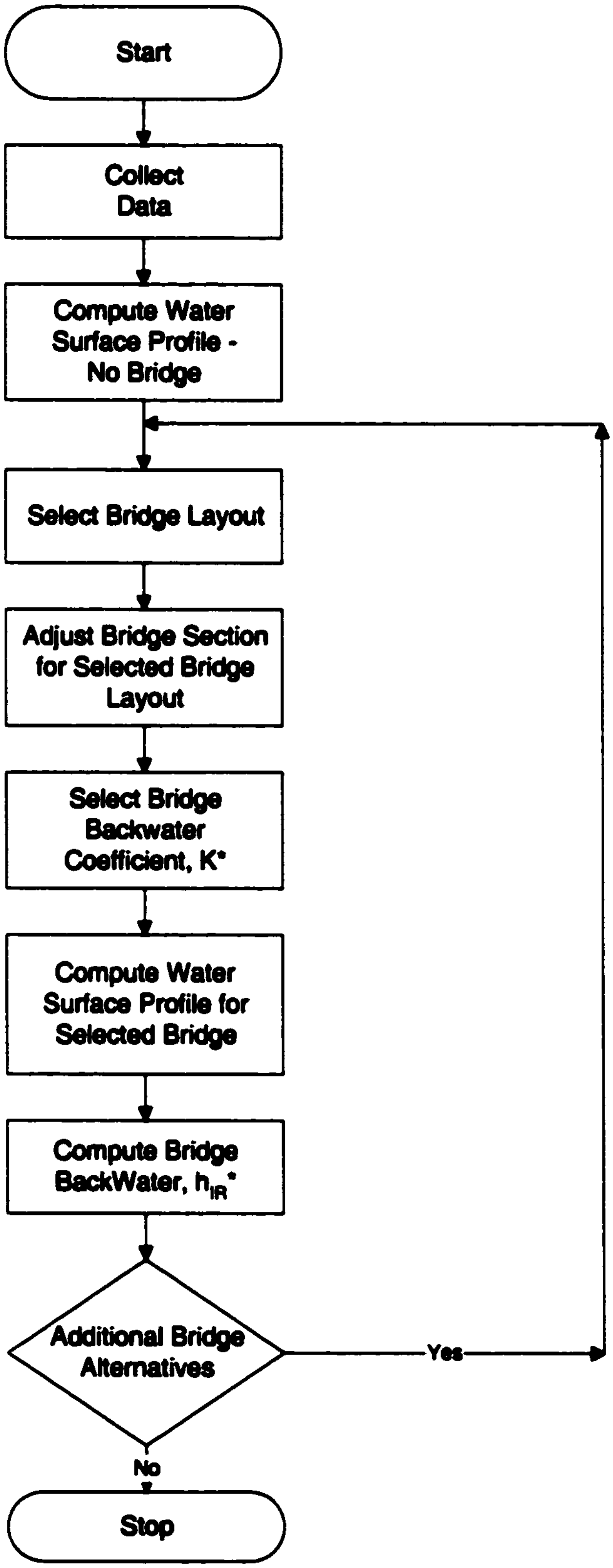

TABLE 5.4 Bridge domination process

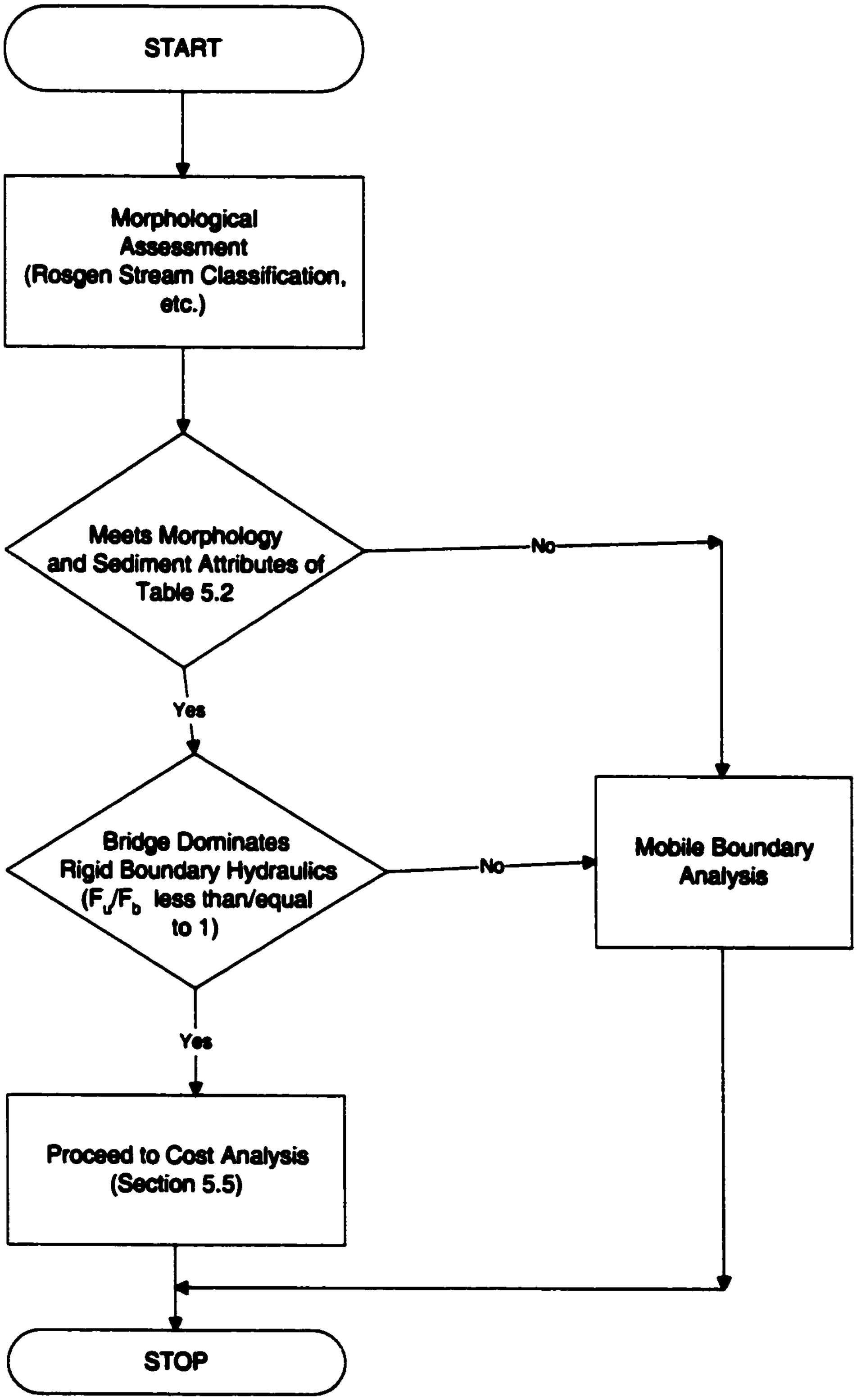

TABLE 5.5 Cost analysis

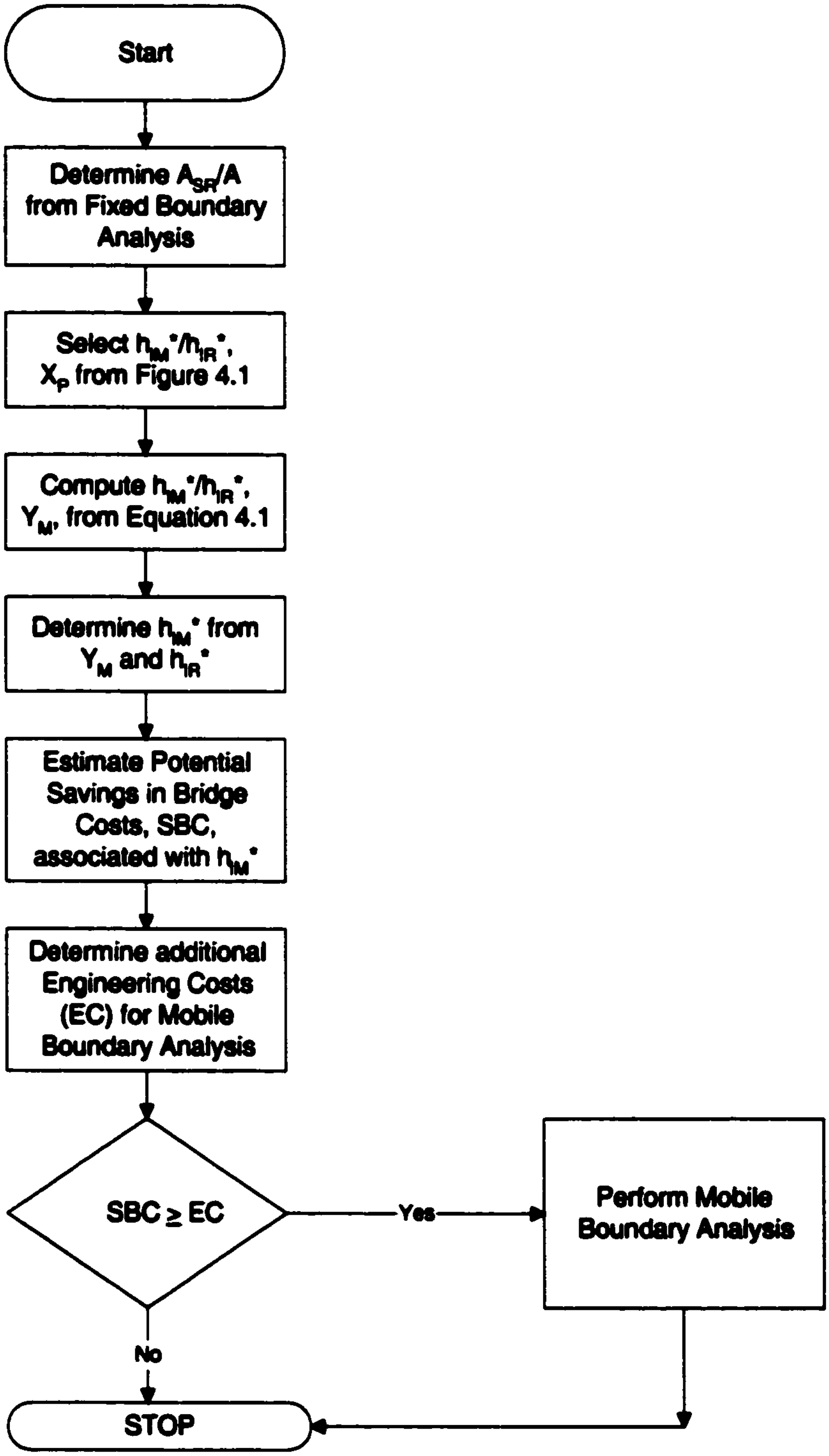

TABLE 5.6 Example cost analysis for Skagit River

From Table 4.1	$h_{1R}^* = 1.74$ ft and 0.90 feet for bridge lengths of 300 ft. and 315 ft., respectively.
For $h_{1(max)}$	= 1 ft., maximum allowable backwater, rigid model requires 315 ft. bridge length
From Table 4.2	$A_{SR} = 1049$ ft.^{2} and $A = 4854$ ft.^{2} for 300 ft. bridge length
From Figure 4.1	$\dfrac{h_{1R}*}{h_{1M}*} = X_p = 0.7$ for $\dfrac{A_{SR}}{A} = \dfrac{1049}{4854} = 0.22$
From Equation 4-1	$Y_M = 0.46145 + 0.323218\, X_p =$ expected model value $= \dfrac{h_{1R}*}{h_{1M}*}$
	$Y_M = 0.46145 + 0.323218\,(0.7) = 0.69$

Thus, expected average $h_{1M}^* = Y_M\, h_{1R}^* = (0.69)1.74$ ft. = 1.20 ft. for 300 ft. bridge

	$h_{1M}^* > h_{1(max)}$. Still need 315 foot bridge
From Figure 4.3,	Y = 0.65 and 0.45 for lower 90% confidence limits of average and individual expected model values, respectively
For 300 foot bridge	$h_{1M}^* = (0.65)(1.74) = 1.13$ ft, average lower limit
	$h_{1M}^* = (0.45)(1.74) = 0.78$ ft, individual lower limit

Based upon the above, possibly $h_{1M}^* \le h_{1(max)}$

Let	w = bridge width = 32 feet
	ΔL = difference in bridge length = 315' - 300' = 15 feet
	CC = \$ per unit bridge area = \$ 200 per ft.^{2}
	SBC = potential bridge cost savings = W x ΔL x CC
	$SBC = 32' \times 15' \times \dfrac{\$200}{ft^2} = \$\,96{,}000$

TABLE 5.6 Example cost analysis for Skagit River (continued)

Except for the differences in initial bridge construction costs, it is assumed that the two bridge lengths have negligible differences in life-cycle costs.

Estimate EC, additional engineering costs, for mobile model,

EC = B x CE, B = Billable engineering hours = 20 hours

CE = cost of engineering per hour = $ 100 per hour

EC = (20)(100) = $2,000

Since, SBC ≥ EC, then the engineer or modeler should consider using a mobile model to justify the shorter bridge length of 300 feet.

All the above costs - SBC and EC - are in present dollars

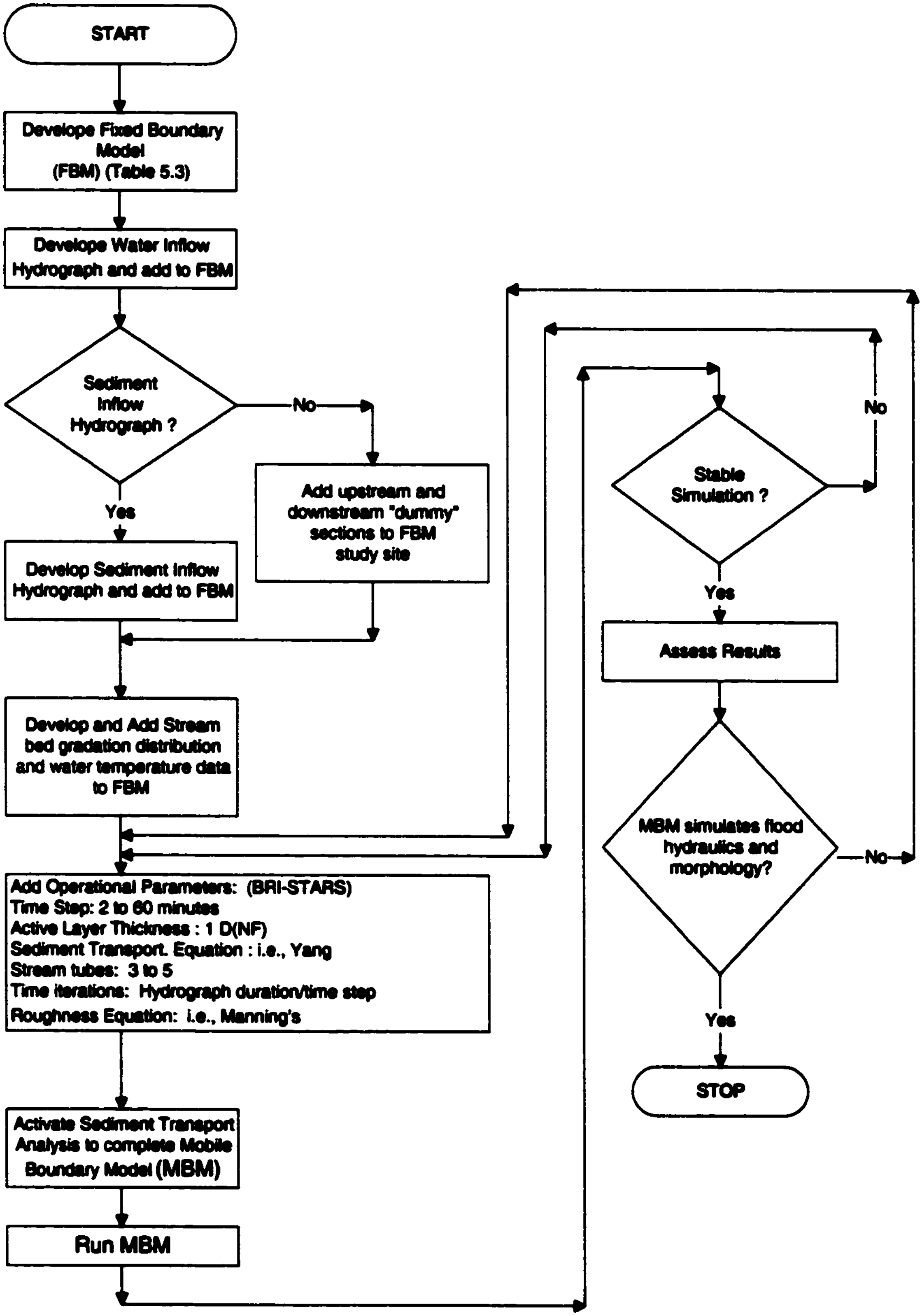
START
Develope Fixed Boundary Model (FBM) (Table 5.3)
Develope Water Inflow Hydrograph and add to FBM
Sediment Inflow Hydrograph ?
No
Yes
Add upstream and downstream "dummy" sections to FBM study site
Develop Sediment Inflow Hydrograph and add to FBM
Develop and Add Stream bed gradation distribution and water temperature data to FBM
Add Operational Parameters: (BRI-STARS)
Time Step: 2 to 60 minutes
Active Layer Thickness : 1 D(NF)
Sediment Transport. Equation : i.e., Yang
Stream tubes: 3 to 5
Time iterations: Hydrograph duration/time step
Roughness Equation: i.e., Manning's
Activate Sediment Transport Analysis to complete Mobile Boundary Model (MBM)
Run MBM
Stable Simulation ?
No
Yes
Assess Results
MBM simulates flood hydraulics and morphology?
No
Yes
STOP

CHAPTER 6: CISPUS AND SNAKE RIVER CASE COMPARISONS

6.1 Overview

This chapter presents two cases for testing the assumption that mobile models will provide more accurate bridge backwater elevations than fixed boundary models. The first case uses the Cispus River in Washington State. The second case uses the Snake River in Idaho.

6.2 Cispus River

This case study compares the water surface profiles generated with various computer models against surveyed high waters for the Tom Music bridge site. Assuming the high water marks represent an accurate estimate of the selected flood wave or profile, this case assesses how closely each computer model matches an actual flood wave. The models used for the comparisons are HEC-RAS (USACE, 1998), BRI-STARS (Molinas, 1994), FESWMS (FHWA, 1989), and HEC-6 (USACE, 1993).

The Tom Music bridge crosses the Cispus River in Gifford Pinchot National Forest, WA, the bridge lies about 8 miles south of Randle, WA., on Forest Development Road 29 (see Figure 6.1). On February 8, 1996, the bridge experienced a scour failure. The USGS estimates that this flood had a return frequency of about 100 years.

The following discusses the hydrology, hydraulics, sedimentation/ geomorphology, computer model traits, and resulting comparisons of the various models against the surveyed high water marks.

6.2.1 Hydrology

The Tom Music bridge lies just upstream of the confluence of Yellowjacket Creek with the Cispus River (see Figure 6.2). USGS gage station #14232500 lies just downstream from the confluence. Unfortunately, the February flood destroyed this Cispus gage. The USGS used high water marks to compute slope-area flood discharges at a Huffakre Bridge. The Huffakre bridge lies 9 miles downstream from gage #14232500.

The Huffakre bridge has a drainage area of 390 sq. mi. Gage #14232500 has a drainage area of 321 sq. mi. The USGS estimated a flood peak of 38400 cfs at Huffakre. Using a straight area ratio between the two sites, the USGS estimated a flood peak of 31,600 cfs for gage #14232500. This represents the flood of record for this gage (water years 1930 to 1996) with a return interval exceeding 100 years.

For the following computer models, the case study used 32,500 cfs below the Tom Music bridge and 25,500 cfs above the bridge. The 32,500 cfs derives from an area ratio of 321/390 raised to a suggested power contained in USGS report "Magnitude and Frequency of Floods in Washington", WRI 97-4277 (Sumioka, Kresch, and Kasnick, 1998). The 25,500 cfs derives from an area ratio of 249/390 raised to the suggested power. The difference in drainage areas/flood peaks below and above the bridge represents the exclusion of the Yellowjacket drainage area (about 72 sq. mi.) which flows into the Cispus just below the bridge.

For the rigid boundary models (i.e., HEC-RAS, FESWMS), the above flood peaks suffice for computing the estimated water-surface profiles. For the mobile models, however, the analysis requires at least part of the estimated flood hydrograph. The USGS estimated average daily floods through February 8 at gage #14232500. Using a ratio between the USGS estimated flood peak and average daily value for February 8, the mobile model starts with an estimated flood discharge based upon the February 8 ratio and the estimated February 7 average daily flow.

Assuming a 40-hour hydrograph, the mobile models assume the flood peak occurs at 20 hours. The models also assume that the flood discharges change uniformly at 12-minute intervals. Using the above flood peak to average daily flow ratios, February 7 had a starting peak discharge at 0 hours of about 16,000 cfs above the Tom Music bridge. This uniformly changed until it reached the flood peak of 25,500 cfs at 20 hours. Assuming a symmetrical flood wave, the peak discharges decline from 25,500 cfs to about 16,000 cfs during the next 20 hours. Figure 6.3 displays the complete hydrograph for the Cispus located above the Tom Music bridge.

6.2.2 Hydraulics

After the February 8,1996, flood, Gifford Pinchot National Forest elected to replace the Tom Music bridge instead of repairing it. As part of their preliminary engineering process, they requested the Federal Highway Administration to perform a hydraulic and scour analysis of the site. To do this work, FHWA hired WEST Consultants, Seattle, WA (WEST, 1997).

WEST used FESWMS and HEC-RAS to analyze the site. Except at the bridge site, their analysis showed that generally the Cispus flowed under subcritical conditions. At or near the bridge site, the flood peaks passed through critical flow. This is due to the natural constriction at the bridge site. For their analysis, WEST used flood peaks of 8110, 16300, 21200, 25500, 30000, and 42300 cfs. WEST used the same flood peaks upstream and downstream of the bridge location.

Since the design flood peaks (50-year, 100-year) pass through critical depth at the bridge site, the upstream bridge backwater curve is independent from the water surface profile downstream from the bridge. Within the vicinity of the bridge site, the water surface profiles ultimately reach super-critical flow conditions and then return to subcritical just downstream of the bridge. Thus, a hydraulic jump occurs near or at the bridge site.

6.2.3 Sedimentation/Geomorphology

The Cispus consists of a cobbly, gravel bed. Using pebble counts, the bed material has a d_{50} of about 30 to 35 mm. Figure 6.4 presents the sediment gradation for the bridge site.

Based upon aerial photographs from 1959 to 1993, the Cispus appears fairly stable since the original bridge construction in the 1950's. Some lateral migration has occurred over the years to the northern bank upstream of the bridge site. A spur dike constructed along the southern upstream bank in the 1970's may have contributed to this migration. However, the approaching valley to the bridge does have a general northerly direction. During higher flows, the natural constriction of the bridge site, furthermore, may cause some upstream deposition that contributes to the northerly migration of the Cispus. During the 1996 flood, the Cispus experienced further migration to the north of its main channel.

As previously mentioned, Yellowjacket Creek enters from the south into the Cispus just downstream of the bridge site. The Yellowjacket system enters the Cispus as a multiple channel/alluvial fan system. While some instability appears in the system, generally, it has heavily-wooded, flood plains interspersed with distinct gravel/cobble stream beds. Figure 6.2 shows the confluence of the Yellowjacket with the Cispus. Using the Rosgen classification system, the Cispus is generally a C4 stream type.

Despite some lateral instability and the potential for sediment influxes from such systems as the Yellowjacket, the Cispus site appears stable enough to use the computer models described below. The following will discuss some simplifying assumptions related to sedimentation processes at the site. The sedimentation assumptions primarily apply to the mobile models.

6.2.4 Computer Models

The case study used HEC-RAS, FESWMS, BRI-STARS (fixed and mobile), and HEC-6 (fixed and mobile). The study did not include FHWA's WSPRO (Shearman, 1990). Although HEC-RAS includes a WSPRO bridge analysis option, the USACE (1998) recommends the WSPRO option for only subcritical flows. As described above, mixed flow conditions (subcritical, critical, super critical) occur through the study reach.

Figures 6.5, 6.6, and 6.7 show the water surface and bed profiles for the following models. Table 6.1 at the end of this report presents the water surface and bed elevations for each profile relative to the river stationing.

HEC-RAS - This USACE model is a rigid boundary, one-dimensional, steady-state model. WEST consultants used the standard step/energy equation to compute the water surface profile through the bridge site. Their profile started about 800' feet downstream from the bridge site. The profile ended about 2300' upstream from the bridge for a total profile distance of about 3100'.

Both the original bridge and the proposed bridge have a length of about 170'. Both lie in nearly the same location. The original bridge, however, had a center pier that settled due to scour during the February 1996 flood. The proposed bridge will have no center pier.

The case study used the WEST HEC-RAS analysis with two modifications. First, the study increased the contraction and expansion coefficients from 0.3 and 0.5, respectively, to 0.6 and 0.8. Since the bridge lies in a location that severely restricts the flow, the study recommends the higher values rather than the standard values.

Second, the study used 32,500 cfs downstream of the bridge and 25,500 cfs through and upstream of the bridge. Since the flood peak passes through critical depth, however, the bridge backwater curve for 25,500 cfs is nearly identical for both the 25,500 cfs and 32,500 cfs downstream flow conditions.

Figures 6.5 and 6.6 present the WEST-based profile with the adjustments as described above.

FESWMS - This FHWA model provides a two-dimensional, rigid boundary profile. It uses a planimetric grid system (nodal system). It solves for the local water surface elevation and depth-averaged velocity using a finite element scheme. Figures 6.5 and 6.6 present the WEST-based profile without modification. FESWMS actually shows variation in the water surface elevations across each stream cross-section. The plotted profile, therefore, presents the best estimate of the water surface profile for 25,500 cfs along the thalweg of the stream (same peak discharge upstream and downstream of the bridge).

BRI-STARS (Rigid) - This FHWA model functions similar to the HEC-RAS model (one-dimensional, rigid boundary, steady state). To simulate the February 1996 flood, the rigid model uses a constant 25,500 cfs for the study reach. For the energy equation approach, the model uses a bridge loss coefficient, K^*, of 0.6. This value mainly represents the constriction of the flow at the bridge site. The loss coefficient derives from procedures outlined in FHWA's "Hydraulics of Bridge Waterways" (Bradley, 1978). Figures 6.5 and 6.6 show the profile results for this model.

BRI-STARS (Mobile) - This FHWA model uses the rigid boundary information plus the hydrograph and sediment data presented in figures 6.3 and 6.4, respectively. The analysis assumes that the study area is in a state of sediment equilibrium (sediment inflow equals sediment outflow). To insure this, the analysis extends the study area 6000 feet upstream and downstream by repeating the original boundary cross-sections. There is no incoming sediment at the start of the repeated cross-sections.

By the time the flow reaches the actual upstream boundary cross-section, the model has reached a sediment equilibrium condition. At the downstream end, the repeated cross-sections insure that artificial boundary conditions due not influence the actual study area (i.e, excessive deposition at the downstream end due to a non-transmissive boundary).

The mobile model uses a time step of 12 minutes and an active layer thickness of 362 mm. The Yang equation for gravel sizes computes the sediment loads for each time step and river reach. The model uses 5 stream tubes equally spaced by conveyance to distribute the sediment loads for each stream cross-section.

Figures 6.5 and 6.7 show the bed and water surface profiles resulting from the above analysis. Figures 6.8, 6.9, and 6.10 show the mobile cross-section at locations upstream of the bridge (STA 973), at the bridge (STA 848), and downstream of the bridge (STA 756), respectively.

Figures 6.8, 6.9 and 6.10 illustrate the computer-generated scour and deposition of the stream cross-sections within the vicinity of the bridge site. They show the time and spatial changes that occur during the 40-hour flood wave (i.e., beginning - 0 hours, peak - 20 hours, and at the end - 40 hours). In particular, these figures illustrate the influence of the mobile boundary on the computed water surface profile. For example, these mobile boundary figures show that the local bridge scour leads to a lower bridge backwater profile (Figures 6.5 and 6.7) compared to the rigid boundary results.

HEC-6 (Rigid) - This USACE model operates similarly to the one-dimensional, steady state BRI-STARS rigid water surface profile model. To simulate the February 1996 flood, the model uses a constant 25,500 cfs for the study reach. At the bridge site, the model uses contraction and expansion loss coefficients of 0.6 and 0.8, respectively. This value mainly represents the constriction of the flow at the site. These loss coefficients match those used for HEC-RAS. Figures 6.5 and 6.6 show the profile results for this model.

HEC-6 (Mobile) - This model operates similarly to the BRI-STARS mobile model. It uses the same 12-minute step hydrograph, bed gradation, and Yang (1984) sediment transport equation. It also assumes no incoming sediment at the upstream boundary (STA 9100).

Analytically, however, it uniformly distributes the sediment loads (scour, deposition) over the entire stream cross-section. BRI-STARS nonuniformly distributes these loads over the 5 user-selected, stream tubes. BRI-STARS also uses a user-selected, active layer thickness to limit scour for each time step (i.e., 362 mm for Cispus).

HEC-6, furthermore, computes an equilibrium scour depth for each time step (depth of scour at which transport ceases). HEC-6 also uses a pre-selected scour depth limitation (for the Cispus, a total depth of 10'). Figures 6.5 and 6.7 show the bed and water surface profiles for the HEC-6 mobile analysis.

To compare the above computed water surface and bed profiles, the study used surveyed high water marks. West and Exeltech (Olympia, WA.) consultants surveyed the high water marks after the February 1996 floods. Figures 6.5, 6.6, and 6.7 show the high water marks.

6.2.5 Summary of Results

Figures 6.5, 6.6, and Table 6.1 show that HEC-RAS, FESWMS, and BRI-STARS (Rigid) have backwater profiles within a few tenths of a foot of one another (using maximum depth, less than a 5% variance between models). Unfortunately, they are two to three feet higher than the surveyed high water marks. HEC-6 (Rigid) produces a slightly lower profile. Nevertheless, it also produces a profile about one and one-half to two feet higher than the high water marks.

For the bridge back water, BRI-STARS (Mobile) and HEC-6 (Mobile) match the high water marks within a couple of tenths of a foot. This is because the mobile boundary model accounts for the scour that occurred at and downstream of the bridge area during the February 1996 flood.

Downstream of the bridge, the profiles show more variability. This is probably due to the differences of the models in their approaches for computing super-critical flow conditions with hydraulic jumps. The analysis, thus, considers the downstream profiles of all the models to represent less reliable results. All the mobile boundary profiles, however, eventually begin to approach the surveyed high water marks at the beginning of the study area (as the flow returns to subcritical conditions).

Since the bridge backwater curve is the focus of this study, then the BRI-STARS (Mobile) and HEC-6 (Mobile) models appear to yield the most accurate results compared to the high water marks. As for scour at the bridge site, BRI-STARS develops a much lower bed profile for the flood peak than HEC-6 (see Figure 6.7). This is due to HEC-6 uniformly distributing the scour over the cross section compared to BRI-STARS non-uniform distribution system. For example, some stream tubes may actually experience deposition while others experience severe scour within the same cross-section for the same time step.

For comparison, the study used FHWA's HEC-18 to estimate the contraction scour at the bridge site. Using HEC-RAS hydraulic values for the flood peak, HEC-18 estimates a clear water contraction value of about 10 feet. At STA 848, BRI-STARS has a maximum scour depth of about 10 feet at the flood peak (25,500 cfs, see Figure 6.9). The average scour depth appears to be closer to six to seven feet.

For HEC-6, the scour depth averages about two to three feet at the bridge site. The HEC-6 model, however, does not experience deposition within the same cross-section. The average net cross-section scour of the two models, thus, is closer than the thalweg profiles indicate in Table 6.1 and Figures 6.5 and 6.7.

Overall, HEC-6 (Mobile) appears to most closely match the high water marks both upstream and downstream of the bridge. The model more uniformly distributes the scour at the bridge area, and, thus, produces a more stable bed and water surface profile. This is especially helpful just downstream of the bridge where super-critical flow and hydraulic jumps occur.

As for BRI-STARS, the greater scour for some tubes may cause instability of the model just downstream of bridge in hydraulic jump and super critical locations. During the computer analysis, the location of the hydraulic jump varied greatly from time step to time step. Nonetheless, BRI-STARS does provide a good match with the high marks upstream of the bridge and downstream from hydraulic jump and super-critical areas.

6.3 Snake River

This case study compares the water surface profiles generated with various computer models against surveyed high water marks for the Snake River near Blackfoot, Idaho. Assuming the high water marks represent an accurate estimate of the selected flood wave or profile, this case assesses how closely each computer model matches an actual flood wave. The models used for the comparisons include HEC-RAS and BRI-STARS. The HEC-RAS models derive from a consultant's hydraulic study of the Snake River. The consultant, CH2MHILL (1998), Boise, Idaho, performed the study for the Idaho Department of Transportation (IDOT) in 1998.

The case study focuses on three bridges (US 26, Railroad, Old County Road) that cross the Snake River (see Figure 6.11). During June 1997, the area experienced record flooding. The US Geological Survey (USGS) recorded a peak of about 43,200 cubic feet per second (cfs) on June 17. According to the CH2MHILL hydrologic analysis, this represented a nearly 100-year flood event. The combination of extreme flooding and bridge backwater influences resulted in the inundation of adjacent properties of the Blackfoot area.

The following sections discuss the hydrology, hydraulics, sedimentation/ geomorphology, computer model traits, and the resulting comparisons of the various models against the surveyed high water marks.

6.3.1 Hydrology

The USGS recorded the flood peak of 43,200 cfs at gage station #13062500 (USGS, 1997). This station lies just upstream from the Old County road bridge (sometimes referred to as the old Riverside Highway bridge) and just downstream from the Railroad and US 26 bridge crossings. The gage site represents a drainage area of about 9,950 square miles.

Several lakes and reservoirs regulate the flow to the site. These lakes and reservoirs include Jackson Lake, Palisades Reservoir, Henry's Lake, Island Park Reservoir, and Grassy Lake. Also, there are numerous upstream diversion channels for irrigation purposes.

For the water surface profile comparisons, the case study used 43,200 cfs for the flood peak. For the rigid boundary models (i.e., HEC-RAS, BRI-STARS (fixed- no sediment transport)), this flood peak suffices for computing the estimated water-surface profiles. For the BRI-STARS mobile model (sediment transport model), however, the analysis requires at least part of the estimated flood hydrograph.

Figure 6.12 presents the flood hydrograph for the USGS gage that occurred from June 10, to June 29, 1997. Assuming a 20-day or 480-hour hydrograph, the mobile model assumes the flood peak occurs at 192 hours or after 8 days from the beginning of the flood wave. The model also assumes that the flood discharges change at one hour intervals.

6.3.2 Hydraulics

As shown in Figure 6.11, the study area covers about 2 miles of a fairly straight section of the Snake River. The straightness of this area derives from levees constructed on both the east and west sides of the river. For the 43,200 cfs flood, the CH2MHILL/HEC-RAS analysis produces average channel velocities of 4 to 8 fps and maximum flow depths of 15 to 25 feet. Flow is subcritical with energy slopes ranging from 0.05% to 0.15%.

The Old County Road, Railroad, and US 26 bridges lie within 1500 linear feet of one another. Starting at the Old County bridge, these bridges collectively influence the Snake River water profile for an upstream distance of nearly one mile. At about 1000 feet upstream of the US 26 bridge, the HEC-RAS and BRI-STARS (fixed) models produce about 1.5 feet of elevated backwater attributable to the bridges.

6.3.3 Sedimentation/Geomorphology

The Snake consists of a sandy, gravel bed. Using pebble counts and IDOT gradation tests near the US 26 bridge, the bed material has a d_{50} of about 30 to 40 mm. Figure 6.13 presents the sediment gradation for the study area.

The Snake study area has fairly well-defined flood plains (i.e., grasslands with some heavy brush and trees) and generally stable banks. Within the main channel, gravel bar formations occur throughout the study reach. The main channel has flow widths up to 500 feet with the flood plain widths exceeding one-half of a mile.

As stated above, manmade levees and bridges clearly influence the hydraulics and, thus, the morphology of the Snake. Even in non-levee and non-bridged areas, the dams and diversion systems influence the hydrology and sedimentation processes. The non-levee areas normally exhibit a semi-braided, sinuous stream system. Using the Rosgen classification system, the Snake is generally a DA4 stream type.

6.3.4 Computer Models

As previously mentioned, the case study used HEC-RAS and BRI-STARS (fixed and mobile). Figure 6.14 presents the water surface and bed profiles for these models. Table 6.2 summarizes the water surface and bed elevations for each profile relative to the river stationing. The following discusses the assumptions and methods used for both models.

HEC-RAS - This US Corps of Engineers (USACE) model is a rigid boundary, one-dimensional, steady-state model. This model relies on the standard step/energy equation to compute the water surface profile through the study site. For this case, the profile starts about 400 feet downstream from the Old County Road bridge. The profile ends about 9500 feet upstream from the US 26 bridge for a total profile distance of about 11000 feet.

The Old County, Railroad, and US 26 bridges lie at stations 424, 705, and 1764, respectively. The bridges have an average length of about 475' with piers in the main channel. The HEC-RAS model adjusts for the influence of the bridges primarily by increasing the contraction and expansion coefficients from 0.1 and 0.3 to 0.5 and 0.8, respectively, with additional adjustments for the piers. The model uses Yarnell's, momentum, or an energy-based method to solve the water profile through the bridge site. In this case, the model selects the method yielding the highest profile. Due to the backwater from the Old County and Railroad bridges, the HEC-RAS model produces a profile under pressure flow at the US 26 bridge. At this site, the model uses the orifice equation to develop the bridge profile.

BRI-STARS (Rigid) - This FHWA model functions similar to the HEC-RAS model (one-dimensional, rigid boundary, steady state). To simulate the June 1997 flood, the rigid model uses a constant 43,200 cfs for the study reach. For the energy equation approach, the model uses loss coefficients, K^*, of 1.09, 0.50, and 1.00 for the Old County, Railroad, and

US 26 bridges, respectively. The model multiplies the loss coefficient by the respective velocity head to reflect the influence of each bridge upon the water surface profile. The loss coefficients derive from trial adjustments to approximate the HEC-RAS profile for the 43,200 cfs flood.

BRI-STARS (Mobile) - This FHWA model uses the rigid boundary information plus the hydrograph and sediment data presented in Figures 6.13 and 6.14, respectively. The analysis assumes that the study area is in a state of sediment equilibrium (sediment inflow equals sediment outflow). To insure this, the analysis extends the study area 5000 feet upstream (STA 12086 through STA 16086) and downstream (STA 1000 through STA 5000) by repeating the original boundary cross-sections (STA 11086 and STA 0). There is no incoming sediment at the start of the repeated cross-sections.

By the time the flow reaches the actual upstream boundary cross-section, the model has reached a sediment equilibrium condition. At the downstream end, the repeated cross-sections insure that artificial boundary conditions due not influence the actual study area (i.e., excessive deposition at the downstream due to a non-transmissive boundary).

The mobile model uses a time step of one hour and an active layer thickness of 90 mm. The Yang (1984) equation for gravel sizes computes the sediment loads for each time step and river reach. The model uses 5 stream tubes equally spaced by conveyance to distribute the sediment loads for each stream cross-section.

Figure 6.14 shows the bed and water surface profiles resulting from the above analysis. Figures 6.15, 6.16, and 6.17 show the stream cross-sections at the US 26 (STA 1764), Railroad (STA 705), and Old County (STA 424) bridges, respectively, for the mobile and fixed boundary analysis.

Figures 6.14 through 6.17 illustrate the computer-generated scour and deposition of the stream cross-sections throughout the study area. They show the time and spatial changes that occur during the 40-hour flood wave (i.e., beginning - 0 hours, peak - 192 hours, and at the end - 480 hours). In particular, these figures illustrate the influence of the mobile boundary on the computed water surface profile.

For example, Figures 6.14 through 6.17 show that the relatively large change in channel width and elevation from stream section to section results in several feet of respective scour and deposition. These figures show the channel deposition resulting from the bridge backwater curves of the Old County, Railroad, and US 26 bridge at STA 1764 (Figure 6.15). Finally, Figures 6.14 through 6.17 show the complex scour and deposition patterns of the stream cross-sections that generate the backwater curve from STA 424 to STA 5274.

6.3.5 Summary of Results

Table 6.2 and Figure 6.14 show that HEC-RAS and BRI-STARS (Rigid) have backwater profiles within a few tenths of a foot of one another. Using an average maximum depth of 20', the flow depths are within 3% of one another. The differences primarily derive from computational approaches (i.e., energy slopes based upon simple arithmetic versus conveyance-based averages) and cross-section modifications (BRI-STARS uses a maximum of 27 geometry points per cross-section).

The BRI-STARS (Mobile) model produces a consistently lower profile than the HEC-RAS and BRI-STARS (Rigid) model. The lower water surface profile derives from scour at the downstream cross-sections (i.e., STA 705 (Figure 6.16)) and scour in the deeper portions of the channel cross-section at higher velocity locations. Although much deposition occurs in several locations and some deposition and scour occurs within the same section (i.e., deposition on existing bars with scour in the deeper channel section), these locations do not control the overall water profile elevations. Including the bridge sections shown in Figures 6.15 (STA 1764), 6.16 (STA 705), and 6.17 (STA 424), the downstream sections determine the profile elevations proceeding upstream to about STA 5274. This is the bridge backwater curve from STA 424 to STA 5274. The mobile model, thus, produces a lower profile due to the scouring of these controlling downstream stations.

Table 6.2 and Figure 6.14 show water surface depths for the mobile model (WSM 192 HR) about 0.1' to 1.5' lower than for the rigid models. Using STA 2839 as a reference, this backwater location is only 0.5' or 2% less in depth than for the rigid condition. Using limited high water mark information, the data suggests an actual June 1997 flood elevation of about 4487.0 for this location. This elevation falls within the range of the flood elevations for the rigid models. From a qualitative perspective, the mobile model probably provides a more detailed and perhaps more accurate water surface profile for the area. Quantitatively, however, the results suggest no measurable or practical differences in the models. The results, thus, fall within the computational accuracies of the models.

6.4 Case Conclusions

The case studies generally support the assumption that mobile models will produce a more accurate bridge backwater profile when compared to rigid models. For the Cispus study, the water surface elevation differences between the two model types are clearly measurable differences (one and one-half to two feet). They also exceed the typical computational differences between models (greater than 10% difference in computed maximum depths between the mobile versus rigid model). Based upon the surveyed high water marks, the mobile model definitely produced a more accurate backwater profile because of its ability to consider scour and deposition processes within the bridge site.

For the Snake study, the mobile model does produce a more accurate profile than the rigid model. This is due to its ability to account for the complex scour and deposition processes within the vicinity of the multiple bridge crossings. However, the differences in the bridge backwater elevations for the two model types are within 2% of one another. For practical design applications, the mobile model is probably not significantly better than the rigid model in this case.

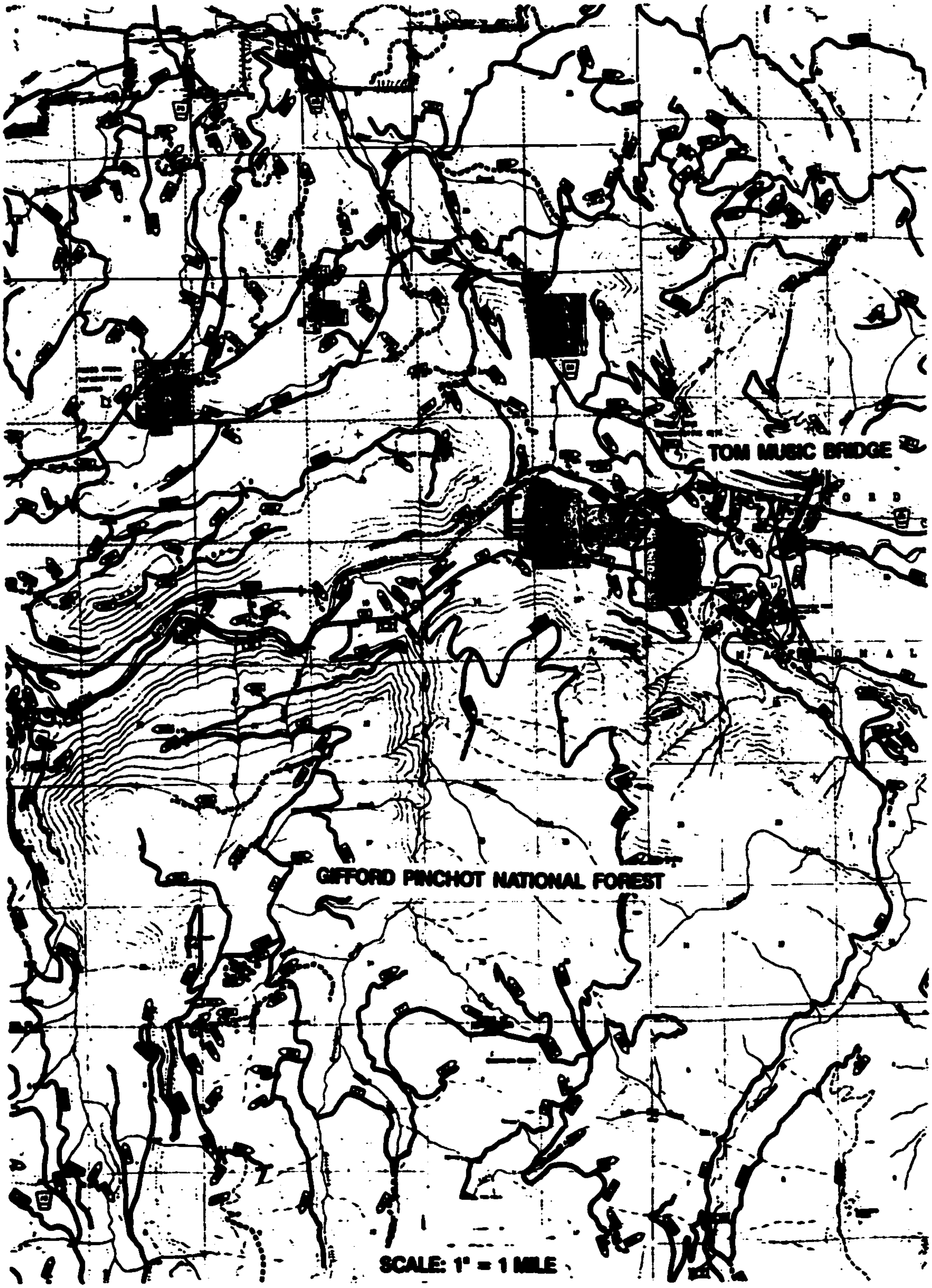

Figure 6.1 Cispus River location map

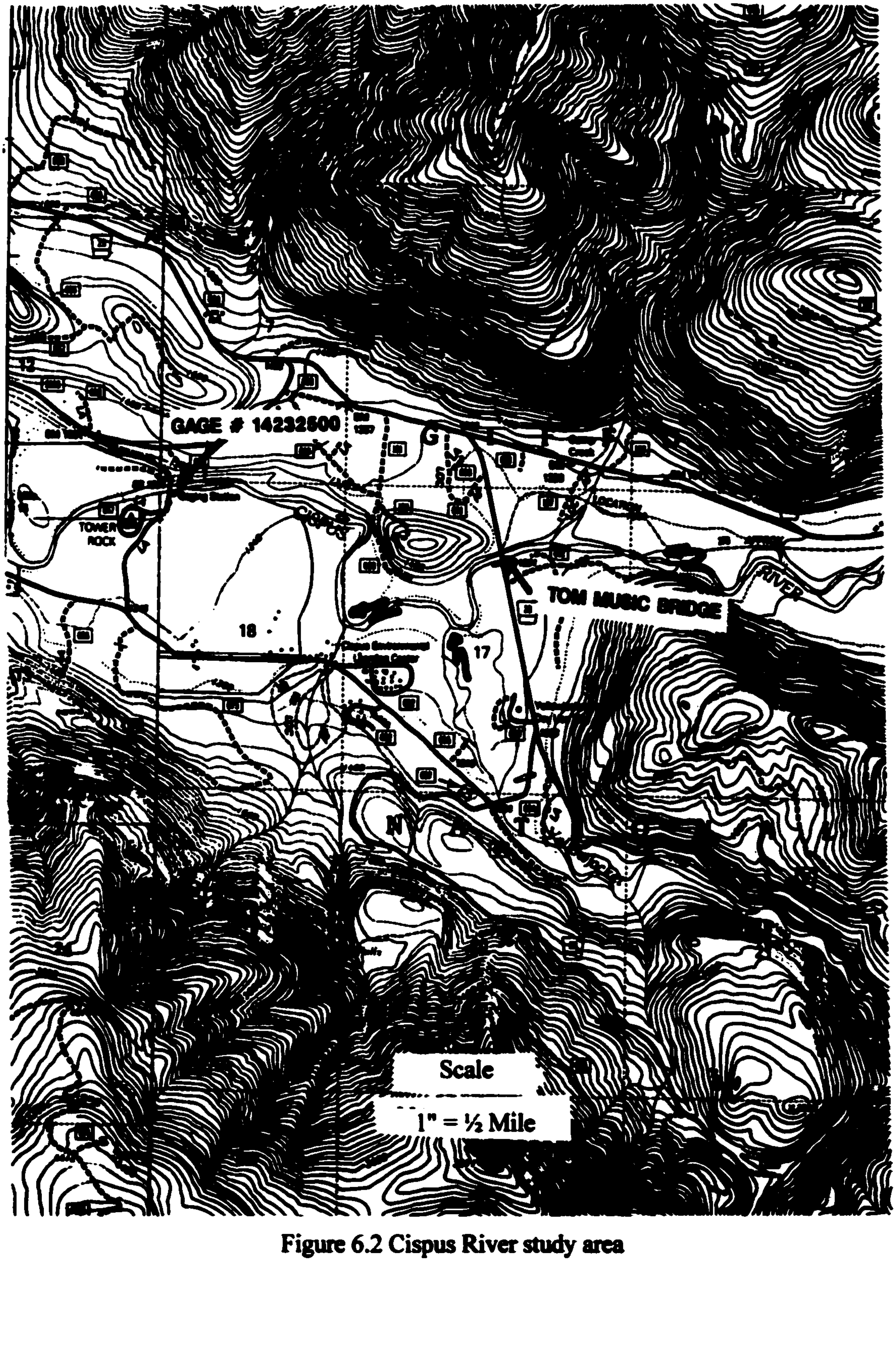

Figure 6.2 Cispus River study area

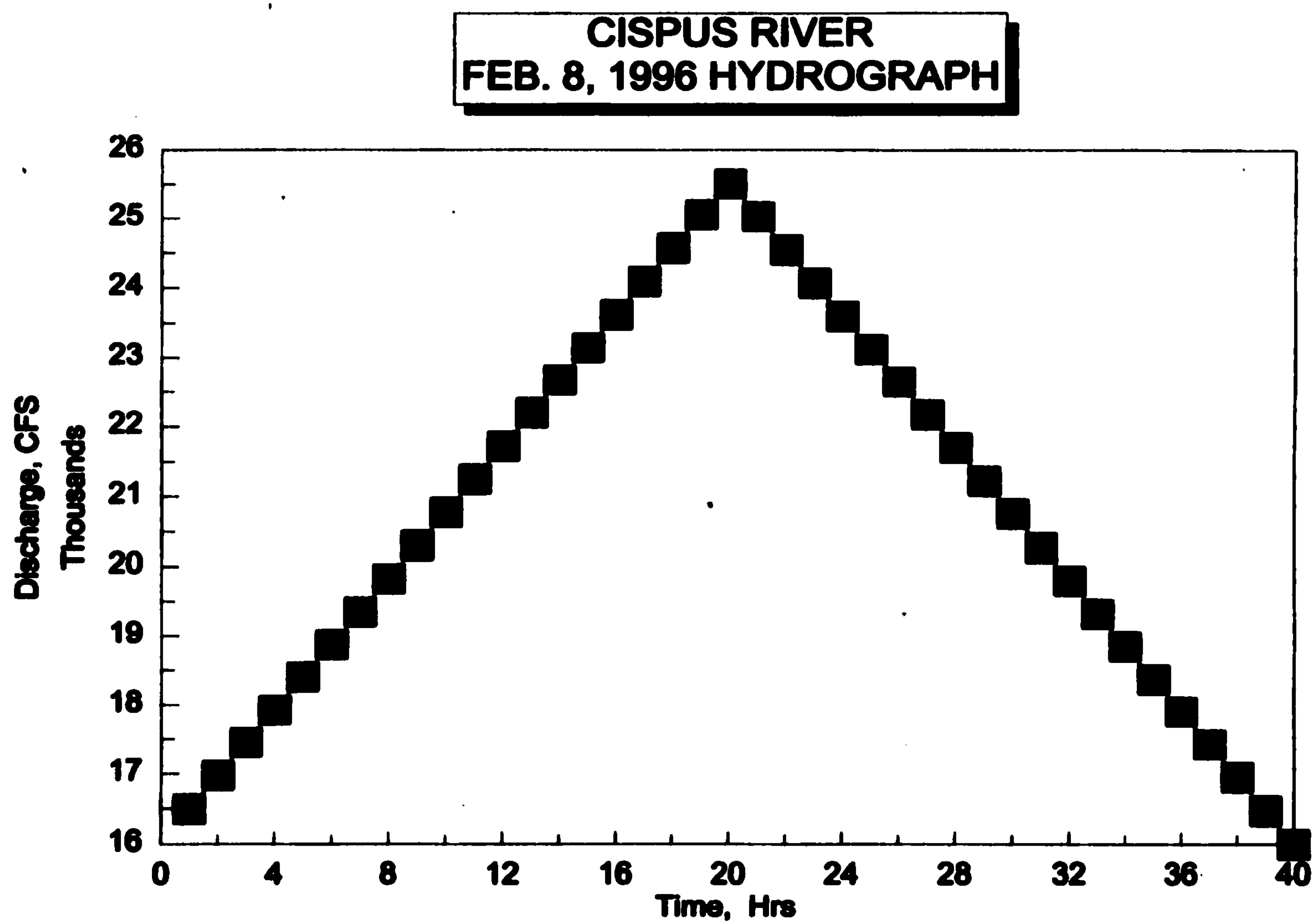

Figure 6.3 Cispus River hydrograph

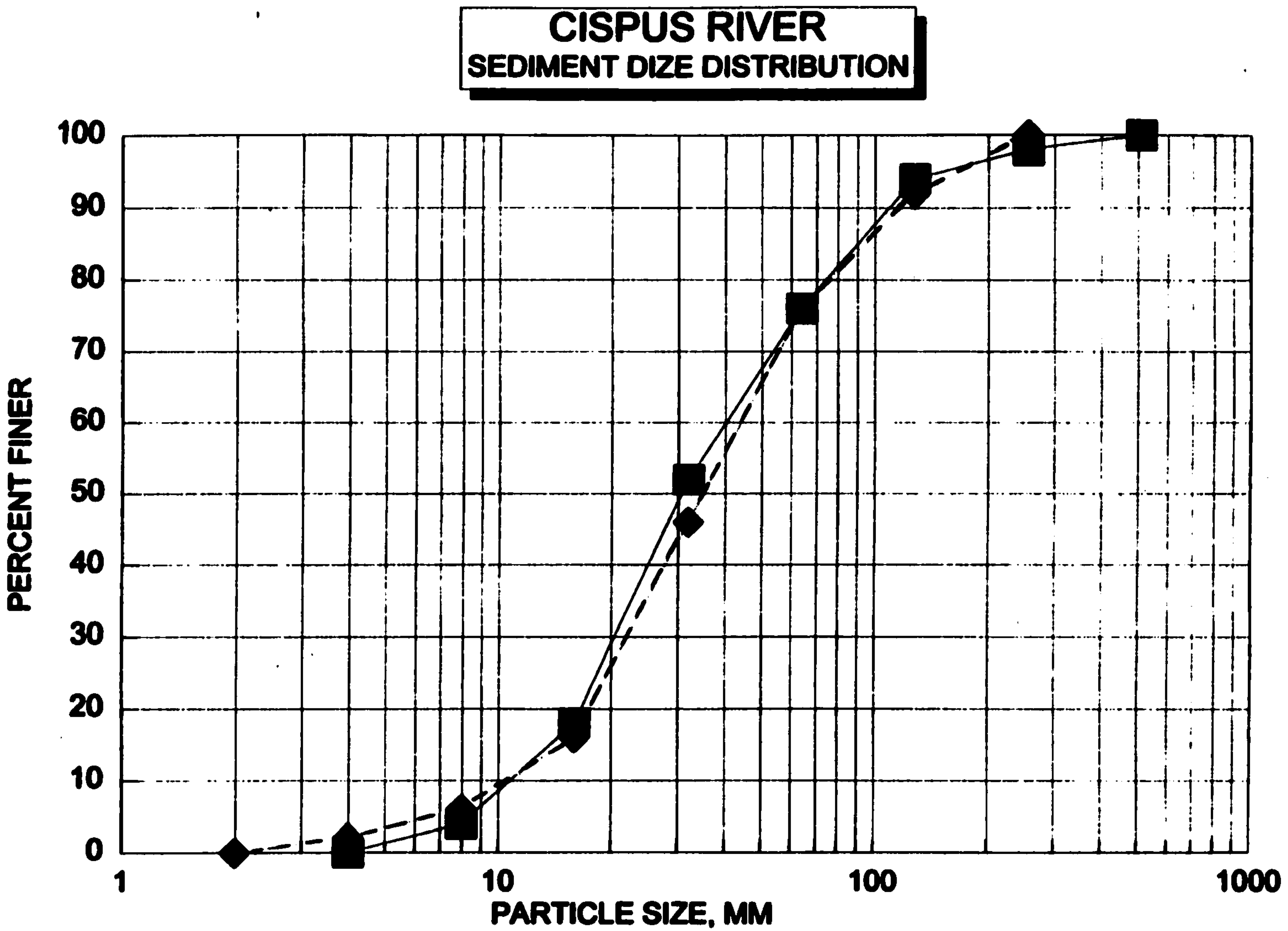

Figure 6.4 Cispus River sediment size distribution

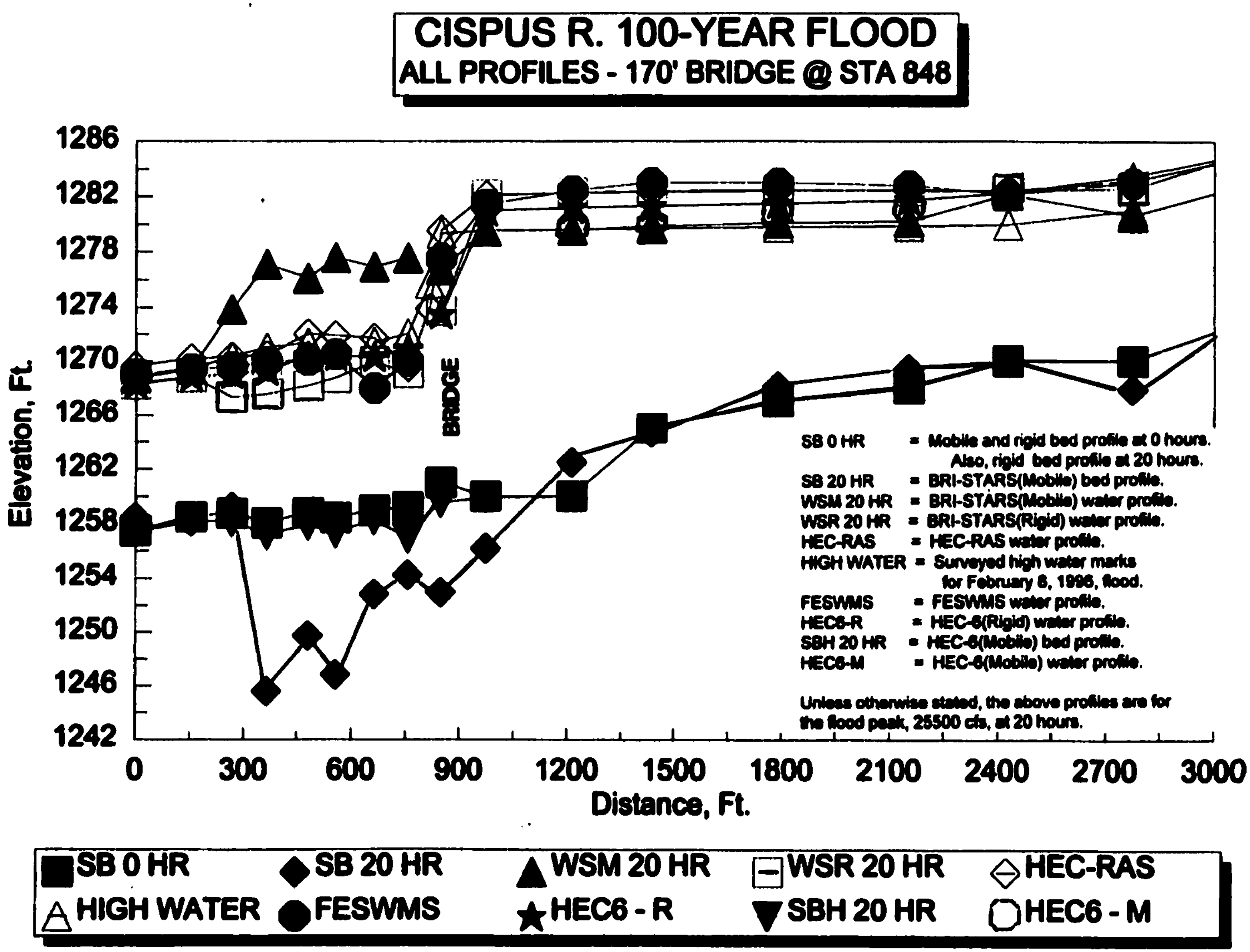

Figure 6.5 Cispus River, 100-year flood, all profiles

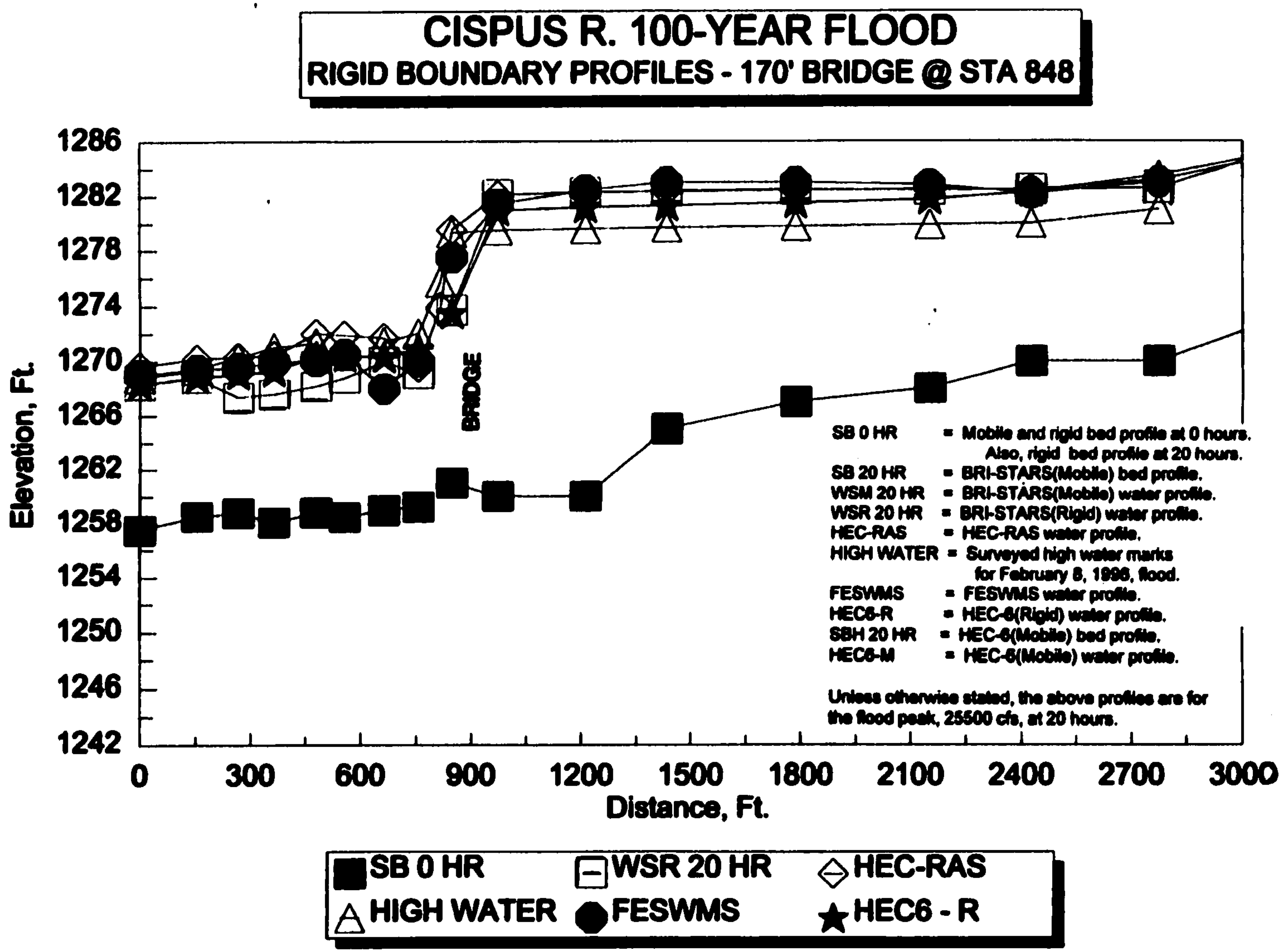

Figure 6.6 Cispus River, 100-year flood, rigid boundary profiles

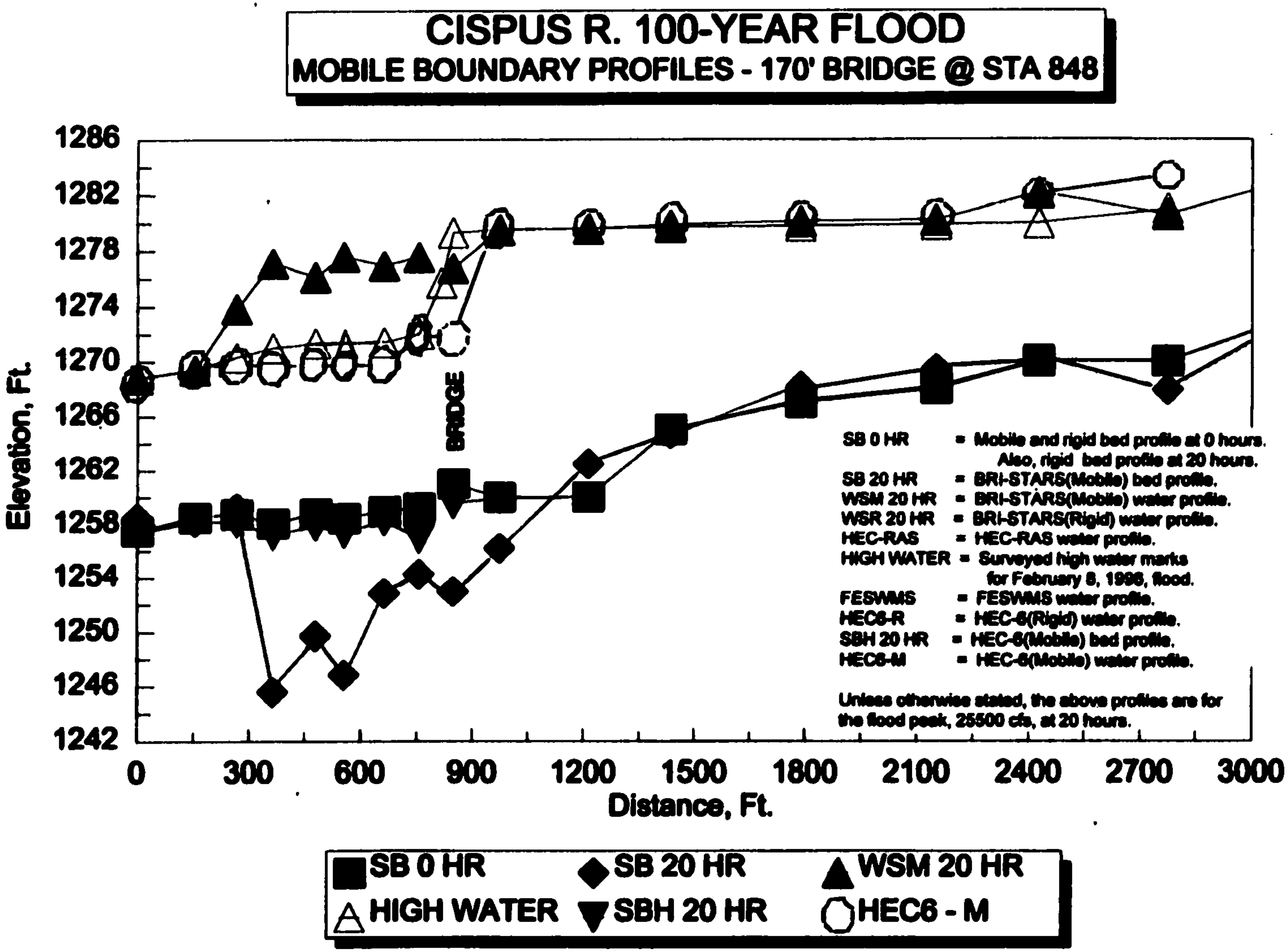

Figure 6.7 Cispus River, 100-year flood, mobile boundary profiles

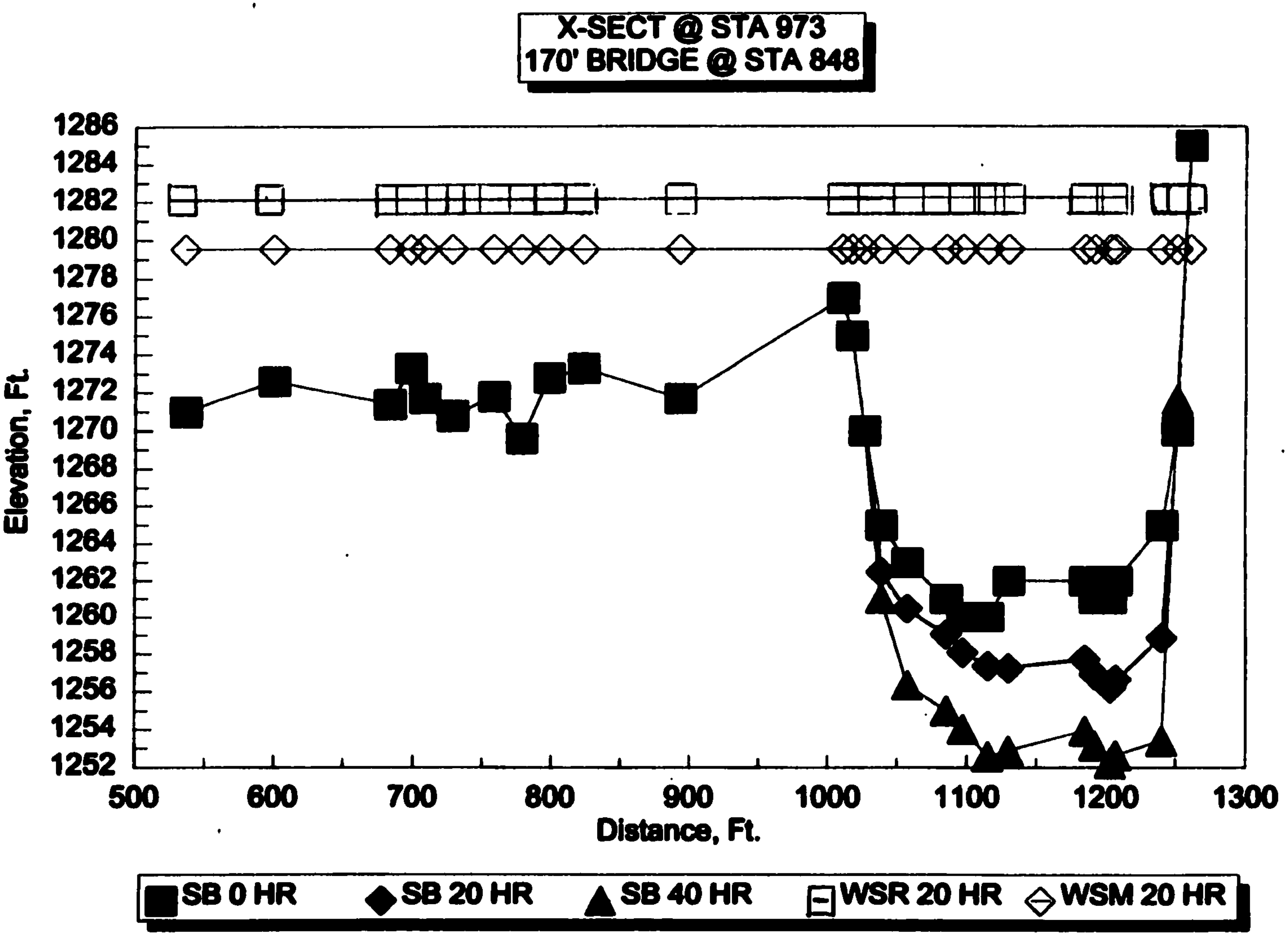

Figure 6.8 Cispus cross-section at STA 973
170' bridge

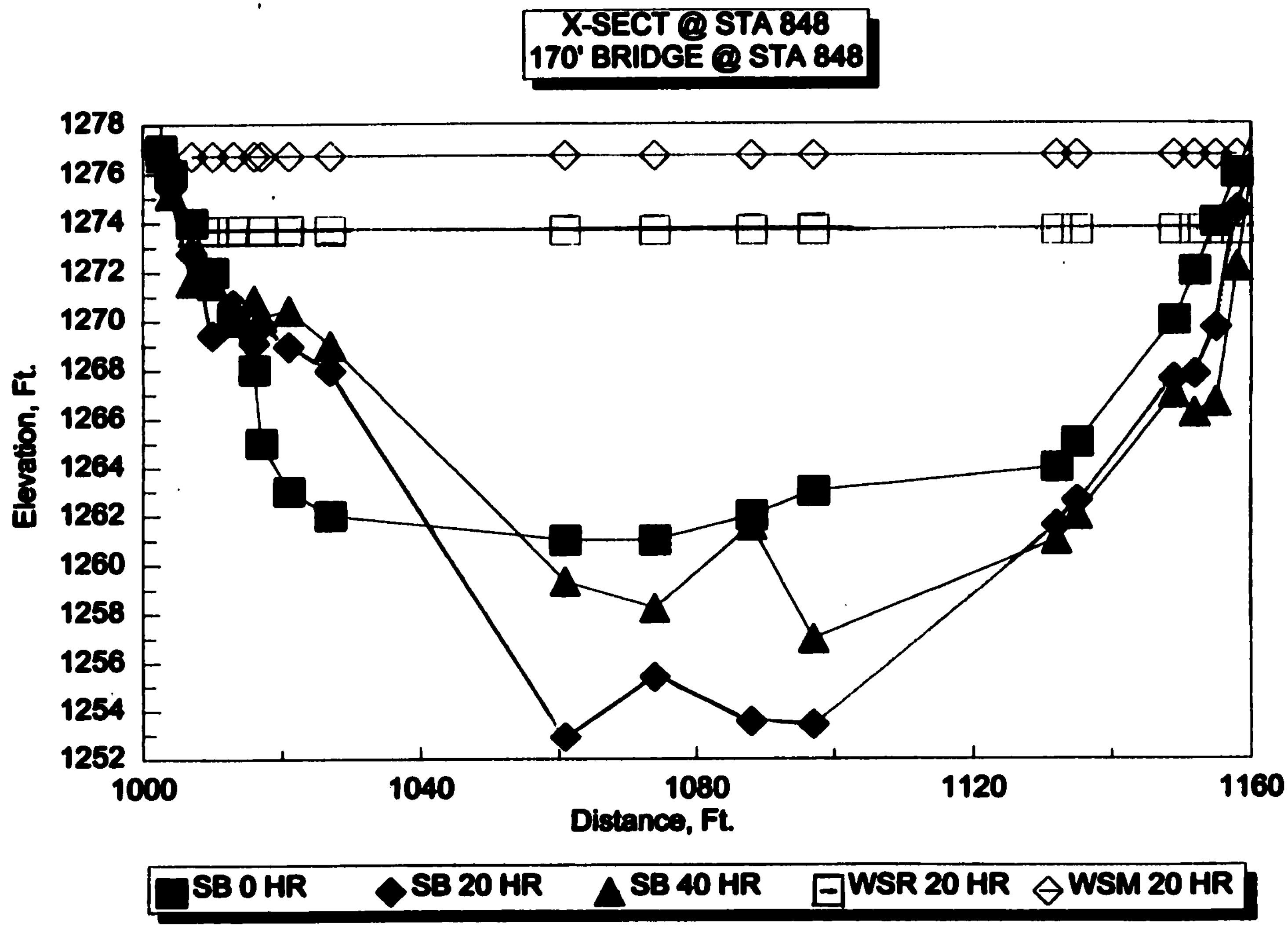

Figure 6.9 Cispus cross-section at STA 848
170' bridge

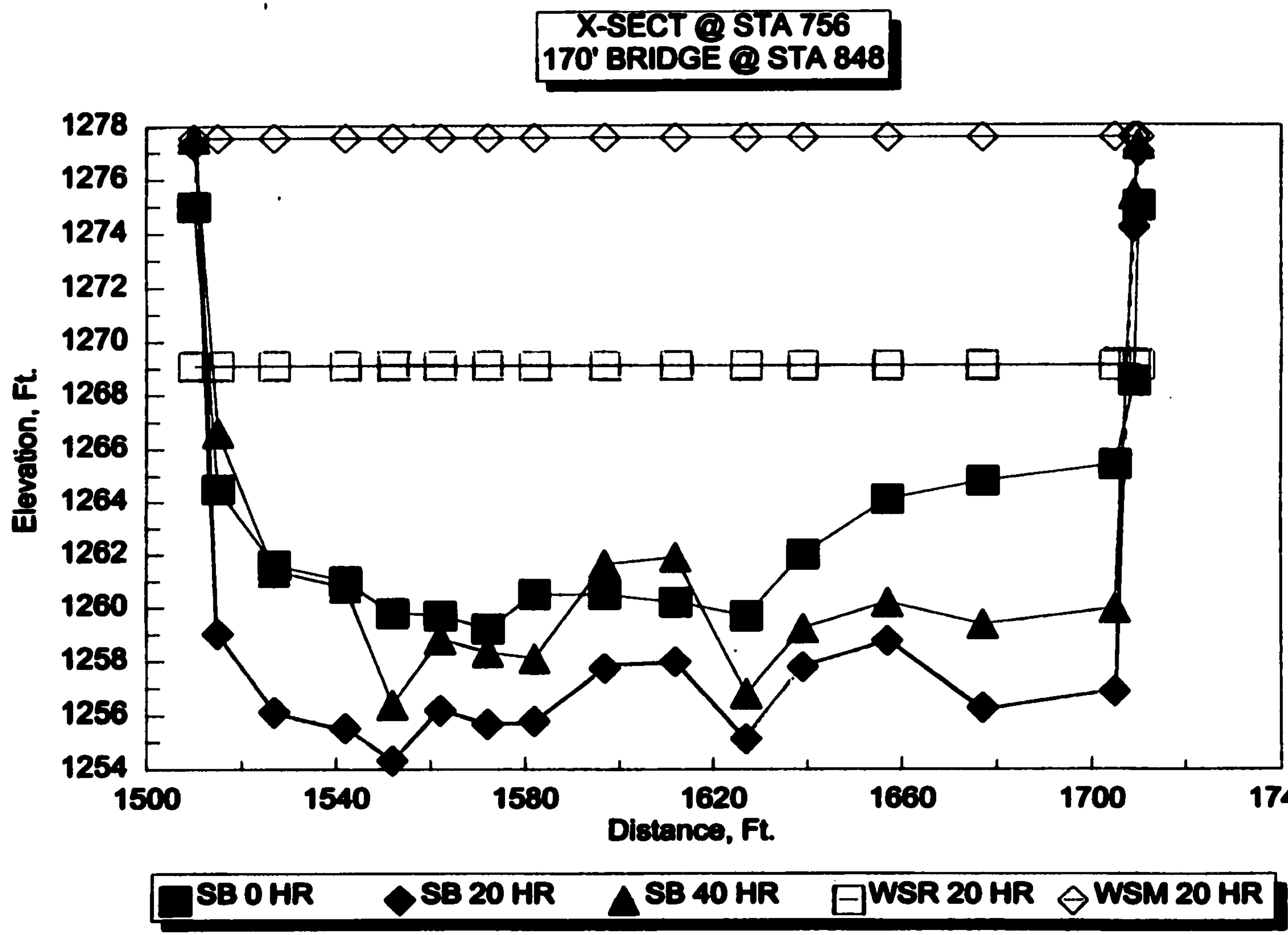

Figure 6.10 Cispus cross-section at STA 756
170' bridge

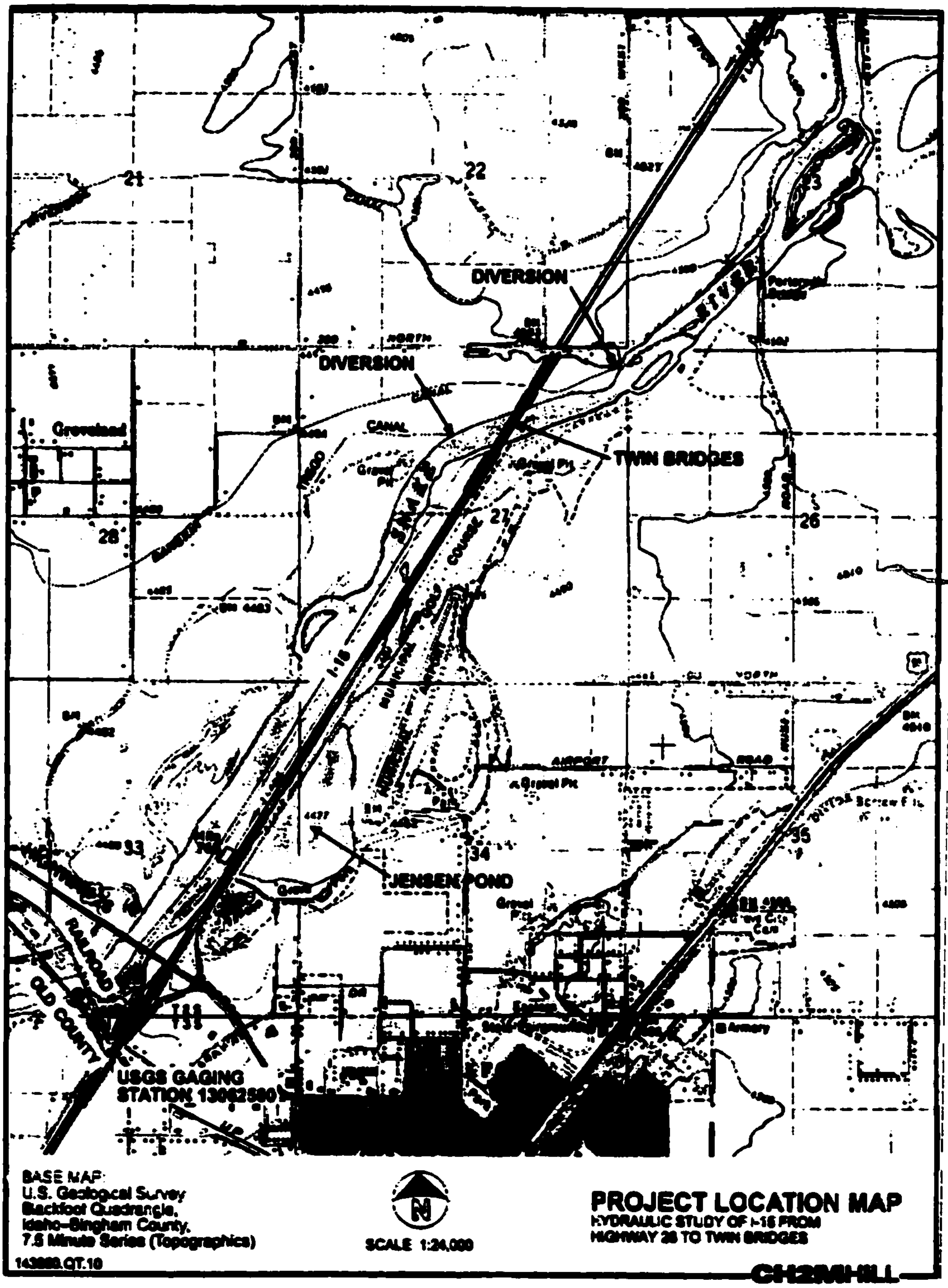

Figure 6.11 Snake River location map

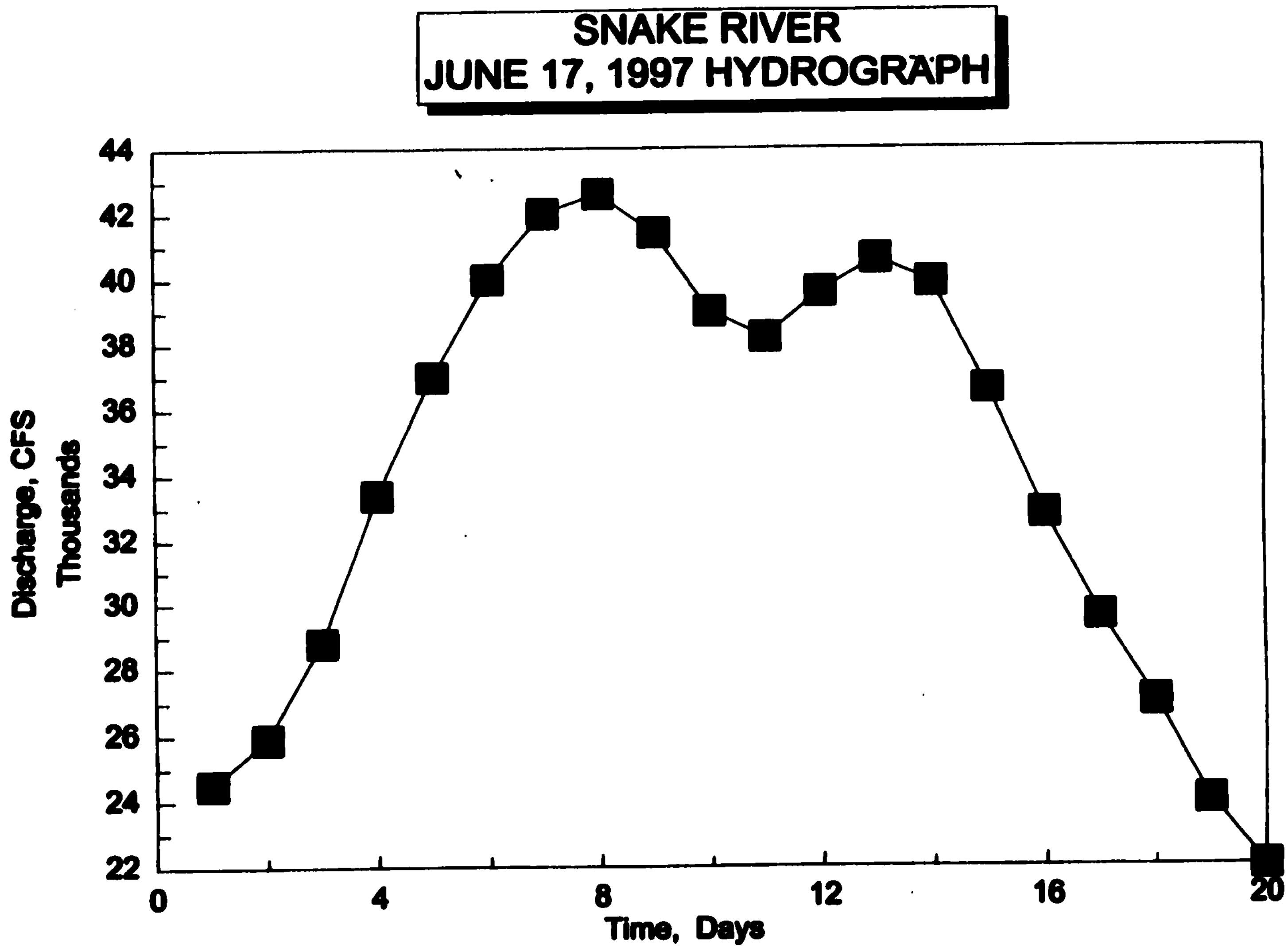

Figure 6.12 Snake River hydrograph

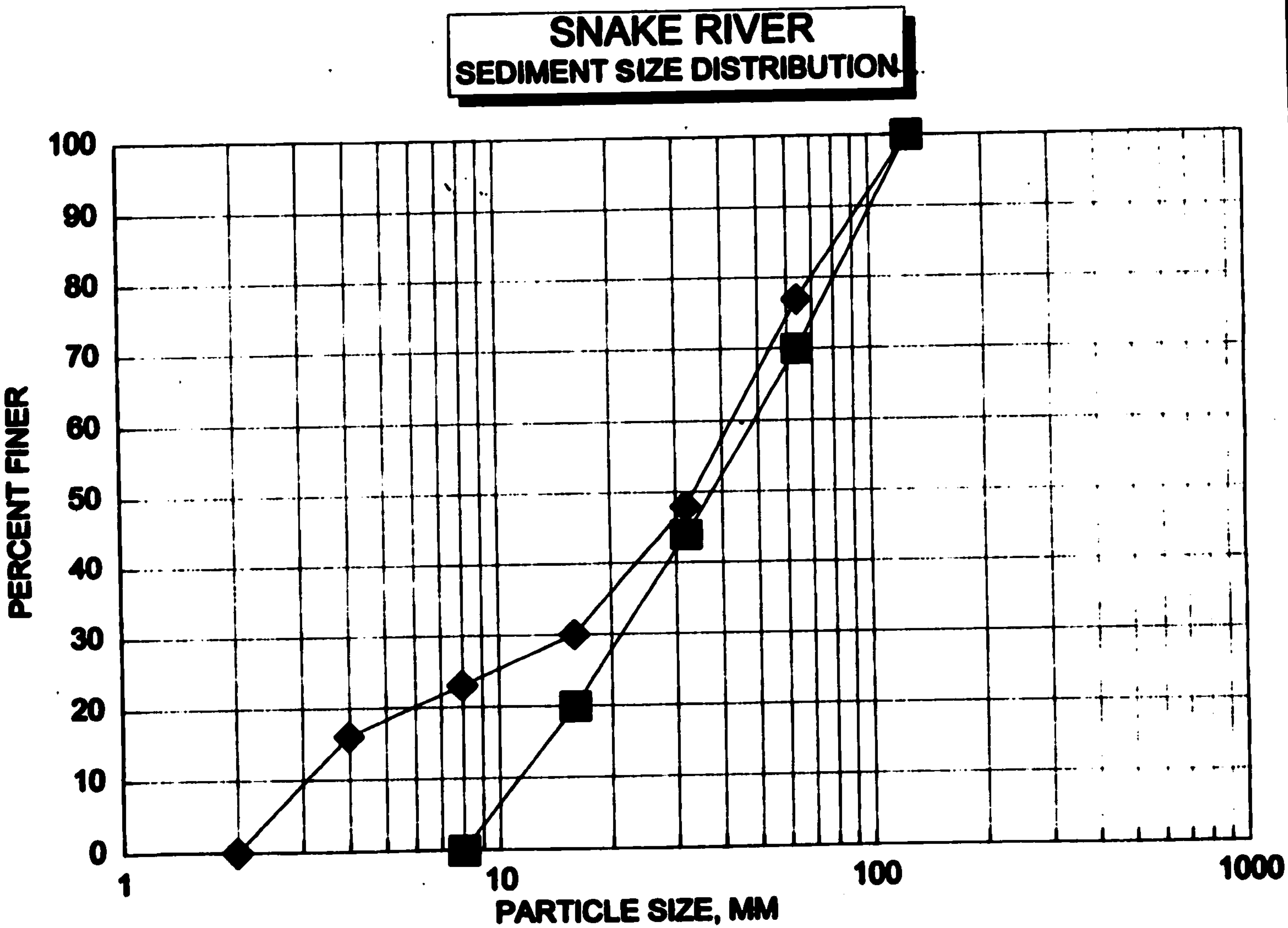

Figure 6.13 Snake River sediment size distribution

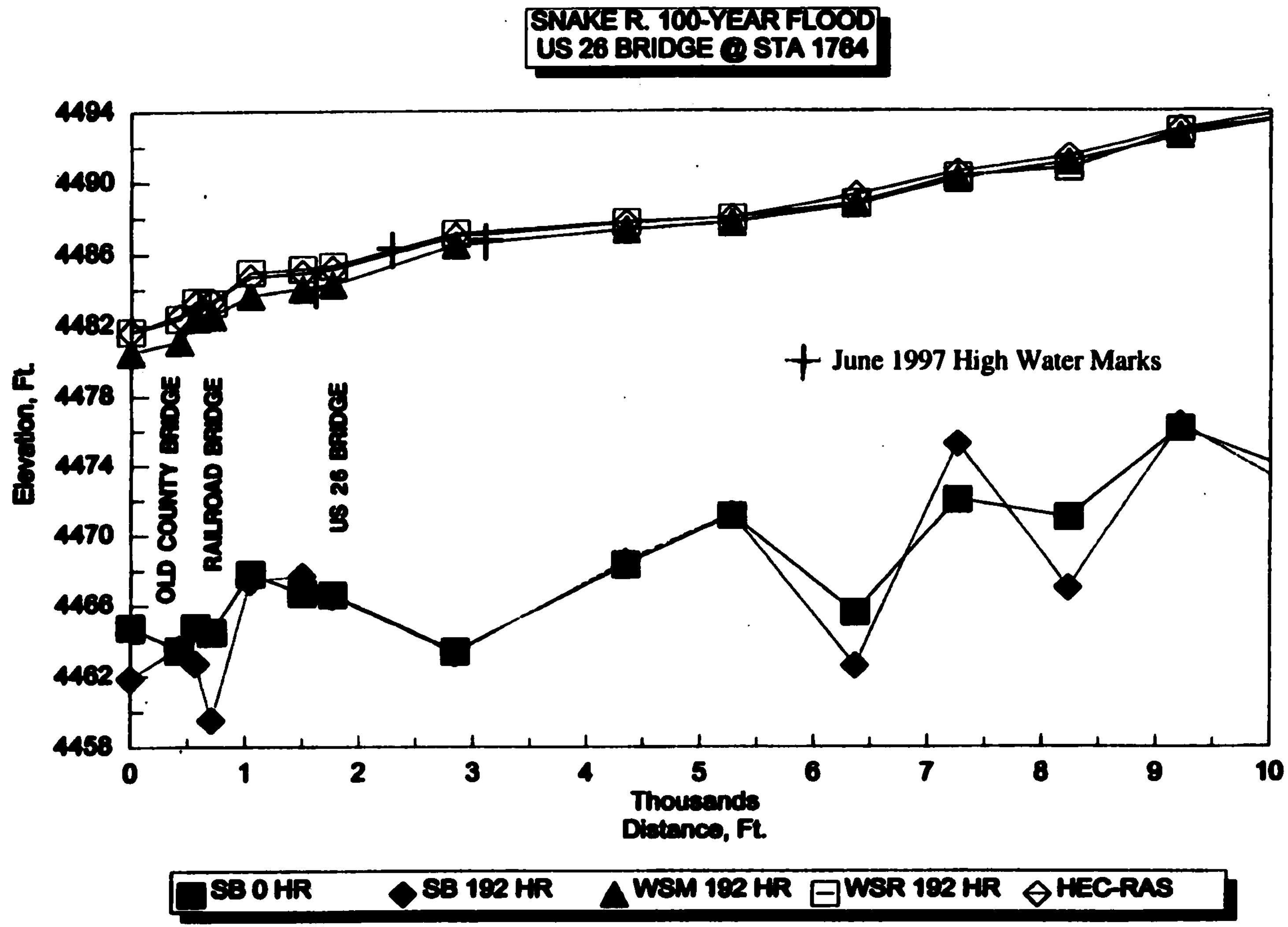

Figure 6.14 Snake River, 100-year flood, all profiles
(surveyed length)

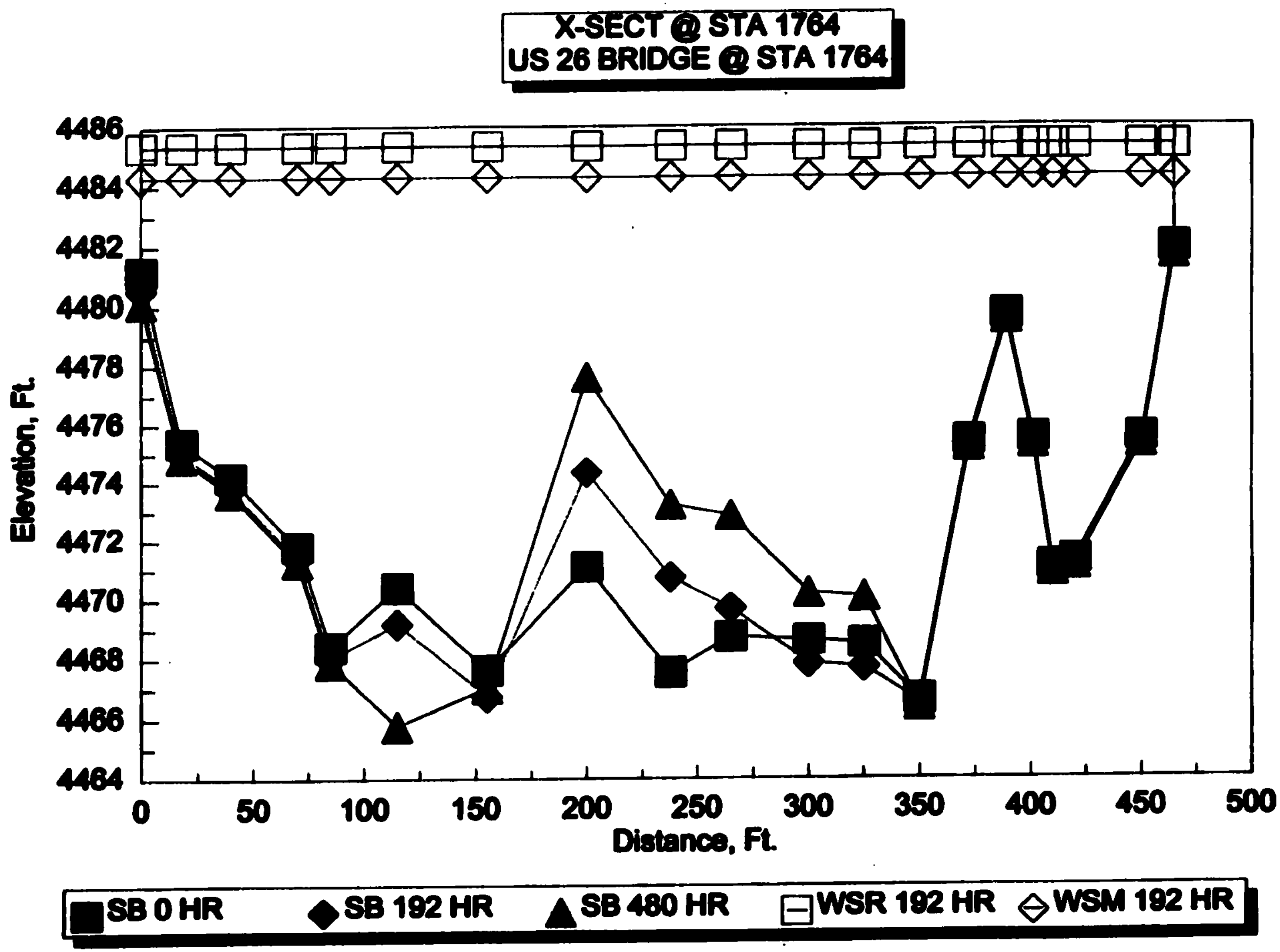

Figure 6.15 Snake cross-section at STA 1764

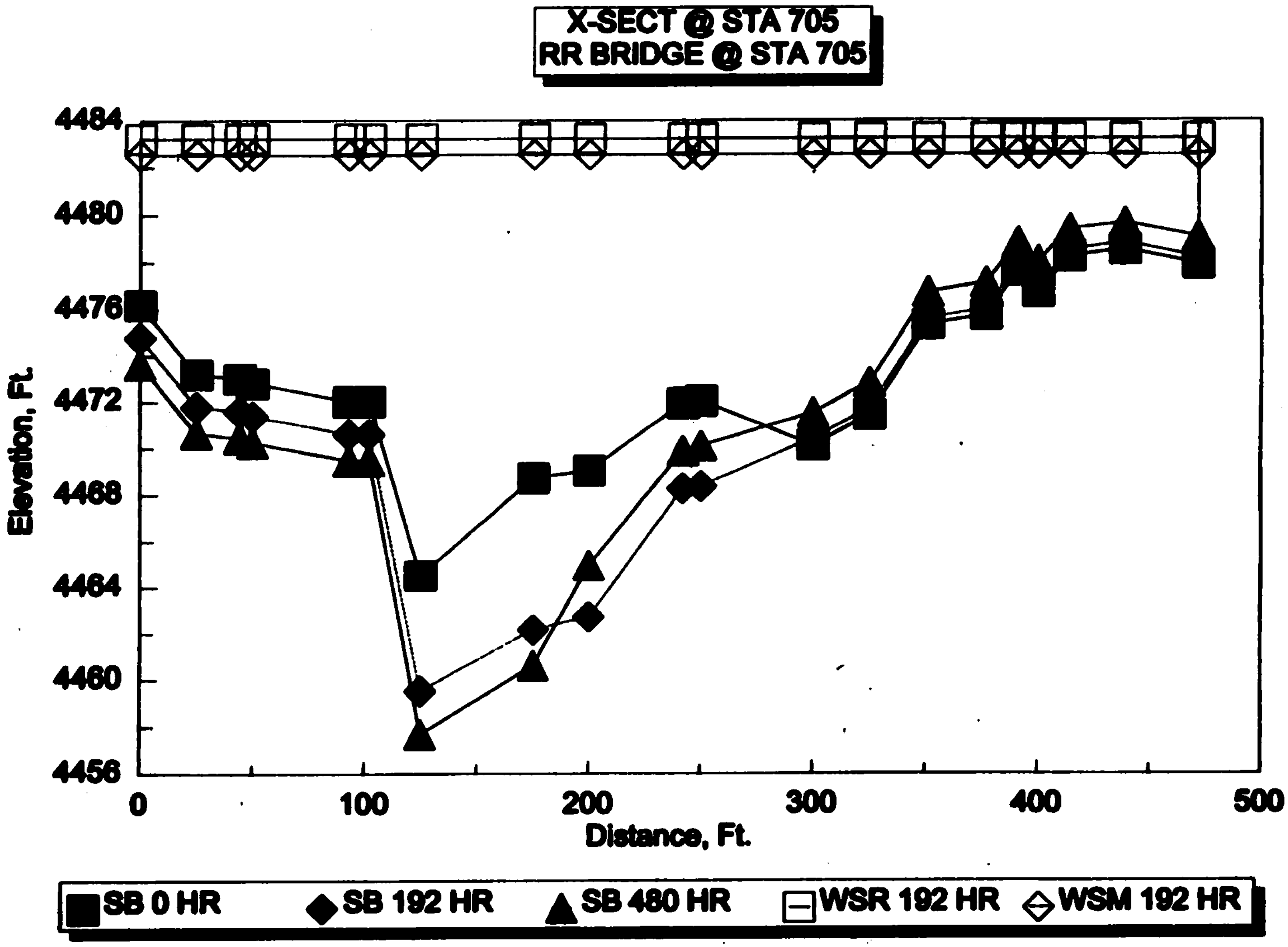

Figure 6.16 Snake cross-section at STA 705

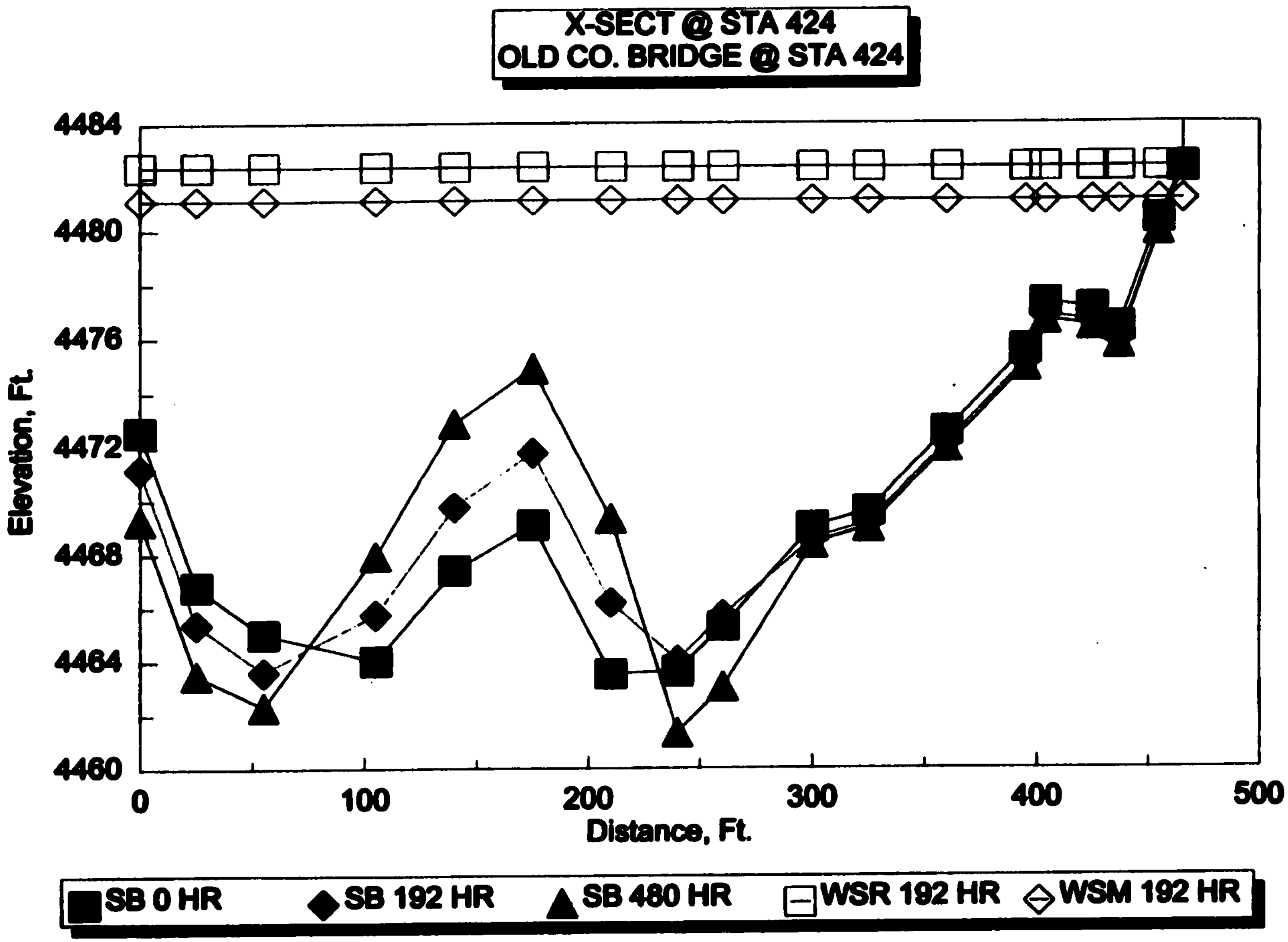

Figure 6.17 Snake cross-section at STA 424

Table 6.1 Cispsus River, 100-year flood, all profiles

ALL PROFILES - 170' BRIDGE @ STA 848

STATION	SB 0 HR	SB 20 HR	WSM 20 HR	WSR 20 HR	HEC-RAS	HIGH WATER	FESWMS	HEC6 - R	SBH 20 HR	HEC6 - M
9100	1309.60	1309.60	1319.74						1309.14	1320.14
8100	1303.50	1300.88	1312.86						1303.44	1314.45
7100	1297.40	1296.93	1307.78						1297.38	1308.45
6100	1291.30	1291.26	1301.78						1291.3	1302.24
5100	1285.20	1285.15	1296.74						1285.19	1296.37
4100	1279.10	1279.24	1290.14						1279.12	1289.87
3100	1273.00	1272.81	1283.01	1285.37	1284.97			1285.20	1273.09	1285.18
2774	1270.00	1267.88	1280.80	1282.54	1283.14	1281.00	1283.00	1283.48	1270.03	1283.33
2426	1270.00	1269.90	1282.16	1282.49	1282.40	1280.00	1282.20	1282.27	1270.07	1281.76
2151	1268.00	1269.44	1280.21	1282.43	1282.48	1279.90	1282.80	1281.75	1268.14	1280.79
1786	1267.00	1268.14	1280.14	1282.48	1282.42	1279.80	1283.00	1281.49	1267.13	1280.3
1436	1265.00	1264.72	1279.81	1282.35	1282.33	1279.70	1283.00	1281.29	1265.03	1279.98
1213	1260.00	1262.48	1279.68	1282.24	1282.24	1279.60	1282.40	1281.16	1260	1279.78
973	1260.00	1258.21	1279.63	1282.14	1282.07	1279.50	1281.40	1280.93	1259.88	1279.49
848	1261.00	1252.97	1278.73	1273.67	1279.56	1279.30	1277.50	1273.46	1250.53	1272.04
816					1273.83	1275.70				
756	1259.20	1254.27	1277.56	1269.09	1269.59	1272.00	1270.00	1270.88	1256.95	1272.12
683	1258.97	1252.86	1278.93	1269.93	1271.88	1271.40	1269.00	1270.33	1258.27	1269.81
566	1258.46	1246.86	1277.60	1268.78	1271.88		1270.50	1270.40	1257.34	1270.17
478	1258.80	1249.73	1276.10	1268.14	1272.00	1271.30	1270.10	1270.43	1257.89	1270.15
364	1258.06	1245.61	1277.10	1267.55	1270.42	1271.00	1269.90	1269.28	1257.2	1269.29
266	1258.75	1259.23	1273.83	1267.33	1270.31	1270.30	1269.53	1269.05	1258.14	1269.09
164	1258.50	1258.20	1269.42	1268.81	1270.18	1269.40	1269.42	1268.84	1258.18	1268.85
0	1257.50	1258.49	1268.75	1268.26	1269.63	1268.80	1269.02	1268.30	1257.39	1268.22
-1000	1254.00	1254.26	1264.85						1253.96	1264.72
-2000	1250.50	1250.80	1261.24						1250.48	1261.25
-3000	1247.00	1247.01	1257.72						1246.99	1257.76
-4000	1243.50	1243.50	1254.22						1243.5	1254.27
-5000	1240.00	1240.01	1250.74						1240	1250.77
-6000	1236.50	1236.53	1247.26						1236.5	1247.3

SB 0 HR = Mobile and rigid bed profile at 0 hours. Also, rigid bed profile at 20 hours.
SB 20 HR = BRI-STARS(Mobile) bed profile.
WSM 20 HR = BRI-STARS(Mobile) water profile.
WSR 20 HR = BRI-STARS(Rigid) water profile.
HEC-RAS = HEC-RAS water profile.
HIGH WATER = Surveyed high water marks for February 8, 1986, flood.
FESWMS = FESWMS water profile.
HEC6-R = HEC-6(Rigid) water profile.
SBH 20 HR = HEC-6(Mobile) bed profile.
HEC6-M = HEC-6(Mobile) water profile.

Unless otherwise stated, the above profiles are for the flood peak, 25600 cfs, at 20 hours.

Table 6.2 Snake River, 100-year flood, all profiles

SNAKE R. 100-YEAR FLOOD
US 26 BRIDGE @ STA 1764

	SB 0 HR	SB 192 HR	WSM 192 HR	WSR 192 HR	HEC-RAS
16066	4482.10	4482.10	4500.39		
15066	4480.60	4477.59	4499.55		
14066	4479.10	4477.80	4498.49		
13066	4477.60	4477.04	4497.30		
12066	4476.10	4475.99	4496.05		
11066	4474.60	4474.69	4494.80	4494.45	4494.94
10191	4473.70	4472.68	4493.70	4493.64	4493.98
9206	4476.10	4476.38	4492.61	4492.89	4493.00
8228	4471.00	4467.00	4491.11	4490.77	4491.44
7257	4472.00	4475.23	4490.17	4490.30	4490.53
6366	4465.60	4462.60	4488.72	4488.78	4489.25
5274	4471.10	4471.18	4487.70	4487.98	4487.98
4344	4468.30	4468.48	4487.35	4487.77	4487.70
2839	4463.40	4463.30	4486.48	4487.12	4486.99
1764	4466.60	4466.49	4484.30	4485.34	4485.16
1500	4466.70	4467.67	4484.04	4485.16	4484.95
1040	4467.80	4467.38	4483.65	4484.96	4484.74
705	4464.50	4459.54	4482.55	4483.23	4483.35
567	4464.80	4462.75	4482.44	4483.34	4483.28
424	4463.50	4463.60	4481.12	4482.39	4482.50
0	4464.80	4461.91	4480.48	4481.65	4481.65
-1000	4463.30	4462.29	4479.18		
-2000	4461.80	4461.63	4477.98		
-3000	4460.30	4460.49	4476.65		
-4000	4458.80	4459.07	4475.37		
-5000	4457.30	4457.72	4474.13		

SB 0 HR = Mobile and rigid bed profile at 0 hours.
Also, rigid bed profile at 192 hours.
SB 192 HR = BRI-STARS(Mobile) bed profile.
WSM 192 HR = BRI-STARS(Mobile) water profile.
WSR 192 HR = BRI-STARS(Rigid) water profile.
HEC-RAS = HEC-RAS water profile.

Unless otherwise stated, the above profiles are for the flood peak, 43200 cfs, at 192 hours.

For the June 1997 flood, the approximate high water mark elevations of 4485.0, 4486.7, and 4487.0 are just downstream of STA 1764, between STA 1764 and STA 2839, and near STA 2839, respectively. See Figure 6.14 for approximate location of high water marks.

CHAPTER 7: CONCLUSIONS AND FUTURE RESEARCH

7.1 Overview

This chapter presents the research constraints, conclusions, practical implications, and future research needs related to mobile boundary models. Specifically, Section 7.2 summarizes the research constraints for the conclusions discussed in this chapter. Section 7.3 discusses the conclusions from the research objectives as outlined under Section 1.2. Section 7.4 presents the practical implications of the presented research. Section 7.5 discusses some of the research deficiencies. Using these deficiencies, Section 7.5 also defines possible areas for future research.

7.2 Research Constraints

The following physical constraints apply to the conclusions below. They derive from Table 5.2:

- The stream hydraulics consist of one-dimensional, subcritical, and gradually varied flow conditions.
- The stream morphology consists of well-defined, relatively stable, and fairly uniform slopes and widths. Streams slopes range from 0.1% to 3%. The stream pattern and form have moderate sinuosity, moderate entrenchment, and moderate bank width to depth ratios as defined in Rosgen (1996).
- The sediment traits consist of gravel to cobble beds with uniform to armored beds. Sediment inflow (Q_{sin}) approximates the sediment outflow (Q_{sout}). The flood-related shear stress exceeds the sediment-laden boundary shear stress.
- The bridge hydraulics consist of the bridge opening or length as the dominating hydraulic bridge feature. The bridge piers, skew, and eccentricity have minimal influence on the bridge hydraulics. The bridge hydraulics are consistent with energy-based solution methods (i.e., preferably no hydraulic jumps).

7.3 Conclusions

Section 1.2 presents four main objectives or areas for analysis and development. First, the research tests the assumption that a mobile boundary model will produce lower water surface profiles upstream from a given bridge (backwater elevations) when compared to a fixed or rigid boundary model. Second, the research tests the assumption that a certain combination of fixed boundary hydraulic values will lead to an estimated value of the mobile bridge backwater elevations. Third, the thesis presents a cost-based approach for when and how to use a mobile model at coarse-bedded bridge crossings. Fourth, the research evaluates the assumption that mobile boundary models will produce more accurate water surface profiles than fixed boundary models.

7.3.1 Do Mobile Models Produce Lower Backwater Elevations Than Fixed Models?

When the hydraulics is dominated by the bridge opening, this first assumption proves to be true. Chapter 3 presents five case studies that support the assumption that the mobile model would produce lower bridge backwater elevations than fixed boundary models in locations of natural sediment equilibrium ($Q_{sin} \approx Q_{sout}$). As previously stated, there are a couple of exceptions to this premise. These exceptions occur when the natural morphology (i.e., naturally aggrading location) dominates the hydraulics of the site instead of the proposed bridge layout ($Q_{sin} \neq Q_{sout}$).

7.3.2 Can Fixed Boundary Parameters Predict Mobile Bridge Backwater Elevations?

The research produces no strong correlations between the fixed boundary hydraulic values and the mobile boundary bridge backwater elevations. Using the data from the Chapter 3 case studies, Section 4.2 evaluates various combinations of stream flow, bridge scour, Froude number, unit stream power, and shear stress as they correlate to the ratio of fixed backwater to mobile backwater, (h_{1M}^* / h_{1R}^*). No correlations are observed between these fixed boundary parameters and h_{1M}^* / h_{1R}^*.

Given the results presented in Section 4.2, the research incorporates the bridge backwater correction curve from HDS No.1 (Bradley, 1978) (Figure 4.1) with the computed bridge flow area, A, and scour area, A_{SR}, from the fixed boundary case studies of Chapter

3. This yields a weakly correlated but statistically significant relationship between the predicted h_{1M}^*/h_{1R}^* ratios using the rigid boundary ratio of A_{SR}/A from Figure 4.1 and the modeled h_{1M}^*/h_{1R}^* values from Chapter 3. From this correlation, Section 4.3 presents a relationship between the predicted h_{1M}^*/h_{1R}^* and the modeled h_{1M}^*/h_{1R}^* as shown in Figure 4.3 and equation 4-1. Although the research does not yield a strong quantitative relationship between fixed boundary hydraulic values and mobile boundary backwater elevations, the relationship is qualitatively strong enough for developing an approach for deciding when to consider a mobile model at coarse-bedded bridge crossings.

7.3.3 Applying Mobile Boundary Models at Bridge Sites

Based upon the presented research, the engineer should apply mobile models at bridge crossings under the following circumstances:

- The natural morphology dominates the bridge backwater conditions ($Q_{sin} \neq Q_{sout}$). In this case, severe aggrading or degrading of the natural stream bed will produce measurably different backwater values for mobile models versus fixed boundary models. For example, Nisqually River bridges at Sta 3120 and Sta 5605 produce large differences in water surface elevations (0.4' to 1.2') between the two model types when the natural morphology is the dominating feature at the bridge site.
- The bridge is the dominating morphologic feature at the site and the additional mobile model costs are less than the potential assessed savings in life cycle costs. For example, for every additional dollar expended in using a mobile model versus a rigid model, the user should have a minimum assessed, life-cycle cost savings of at least $ 1 for the proposed bridge design. To test for bridge dominance, the Froude value, F_u, upstream of the bridge site should not exceed the Froude value, F_b, at the bridge site. The natural (without bridge) stream should also have a sediment equilibrium condition ($Q_{sin} = Q_{sout}$).

To aid the reader, Chapter 5 presents seven tables and flow charts for applying mobile boundary models at bridge crossings. Tables 5.1 through 5.7 present the overall process for applying mobile models, the preferred physical attributes for the potential bridge sites, the required fixed boundary analysis, a bridge domination evaluation process, a mobile model cost analysis, an example for applying a mobile model cost analysis, and a flow chart for performing a mobile boundary analysis, respectively.

The presented mobile boundary analysis also includes recommended values for operational parameters discussed in Section 4.4. These parameters included time step, active layer thickness, sediment transport equations (Yang, 1984), and stream bed gradation (pebble counts, gradation tests). The recommended values derive from the Section 4.4 sensitivity analysis. Section 5.6 explains how to apply these parameters and other variables (sediment inflow conditions, hydrograph duration, boundary conditions, stream tubes, etc.) in using a mobile boundary model.

7.3.4 Do Mobile Models Produce More Accurate Water Profiles Than Fixed Models?

Consistent with the findings of Chapter 3, Chapter 6 presents the Cispus River bridge in which the mobile model produces not only a lower bridge backwater curve than the rigid models but also a profile more closely matching the high water marks for the modeled flood event. Also, from Chapter 6, the Snake River case study also produces a lower water surface profile for the mobile versus the rigid model. Given the accuracy of both models and the limited high water mark data in the Snake River case, it is difficult to argue that the mobile model necessarily produces a more accurate bridge backwater curve than the rigid model in terms of practical engineering design applications.

7.4 Practical Implications

The presented research has the following practical implications:

- Selection of more cost-effective bridge designs - The more accurate the computed bridge backwater profile, then the greater is the potential that the engineer will select a more efficient bridge layout (i.e., length) for the given hydraulic design constraints. Through the proper use of mobile models, the thesis provides methods that should aid the engineer in producing a more accurate backwater profile for coarse-bedded, bridge crossings. Chapter 5 presents the processes for developing the required bridge backwater profiles.

- Improvement of scour and bridge embankment protection measures - Most scour and embankment protection measures rely upon computed depth and velocities within the vicinity of the bridge crossing. When applicable, mobile boundary models should produce more accurate depths and velocities than those produced with a fixed boundary model. This is reflected in computing a more accurate bridge backwater profile with a model that incorporates the changes in the stream boundary. More accurate bridge depths and velocities should, thus, lead to better scour and embankment protection designs for the given bridge site.
- Improvement of the hydraulic design decision-making processes - This thesis provides a simple cost-based, decision-making process for deciding whether or not to use a mobile boundary model at a bridge crossing. The presented cost approach can be applied to most design situations. For example, the number of potential design activities frequently exceeds the engineering organization's resources for performing these potential activities. Using the presented cost approach, the engineer can select those design activities that have a minimum payback ratio of one compared to the potential assessed savings in life cycle costs (i.e., $ 1 additional savings in life cycle costs for every $ 1 in additional design engineering costs).
- Expansion of the current base of knowledge on the computer analysis of bridge backwater profiles - As compared to fixed boundary models, there is very little in the literature on the use of mobile models at bridge sites. This thesis presents seven case studies on the subject. These case studies include nine different bridge sites having up to 35 potential bridge lengths. Overall, the selected case studies represent a comprehensive base for performing future studies and analysis of mobile boundary models at bridge crossings.
- Improvement of the general understanding and application of the mobile boundary models to natural stream systems - The research shows that these models produce realistic results. Although the thesis uses simple assumptions such as natural sediment equilibrium and zero incoming sediment at upstream boundaries, this does

not deter the models from producing realistic water surface profiles at the given bridge sites. Through the many figures and tables contained in this thesis, the selected case studies also demonstrate the potential morphologic changes that could occur for various combinations of bridge layouts and stream types.

7.5 Future Research

There are numerous areas needing more research and information. This section discusses a few of them.

The sensitivity analysis of Section 4.4 shows that the sediment transport method, the active layer thickness, and their relationship to one another represent important areas for further research. In particular, different sediment transport equations generally produce widely different quantities of transported sediment for a given set of hydraulic and sediment conditions. These transport differences result in large differences in the computed bridge backwaters for the mobile models (see Sections 4.4.4 and 4.4.5 and Table 4.5). To stabilize the mobile models (i.e., prevent oscillations), the sensitivity analysis often requires the adjustment of the active layer thickness along with a change in the selected transport equation. While mobile models clearly need more accurate sediment transport equations, there is a need for more information on applying the selected transport equation with a correlated active layer thickness (i.e., supply of sediment available for transport).

In terms of field data, sediment transport data is very limited. None of the USGS gage stations used in the case studies have any sediment data (i.e., bed transported, suspended). Nationwide, there are very few sites with enough data to develop sediment rating curves (i.e., water flow versus sediment flow). This lack of data partly explains the previously discussed limited accuracy of sediment transport equations. While the sediment transport equations used in the case studies and sensitivity analysis have a theoretical basis, ultimately the final form(s) (i.e., empirical coefficients) derive from the actual field and lab sedimentation data.

Similarly, such figures as Figure 4.1 (bridge backwater versus scour area) derive from lab data. Again, more field data as it relates to scour and deposition in streams would prove most helpful in applying mobile models. This is especially true at bridge crossings.

As for computer model verification, large floods often occur at bridges without any accurate methods for determining the water surface profile elevations. Often the engineer and other professionals with interest in the bridge hydraulics are left with high water marks that may or may not represent the desired peak flood elevations. In some instances, various personnel (Federal agencies, private consultants, etc.) will collect hydraulic data such as velocity and depths at a bridge site but little information upstream or downstream from the bridge. As shown in the case studies, upstream and downstream changes during major flood events could alter the scour/deposition at the bridge site and, thus, the computed bridge backwater.

Finally, the engineer frequently selects the optimum bridge design based upon life-cycle costs. These costs include such items as property damage, traffic interruptions, structural and roadway damage, environmental disturbances, and hazards to human life. For a given flood event (i.e., Q_{100}), the engineer typically assigns a cost to that event. Accurately assigning an associated set of costs to a wide range of flood events is very subjective. For example, the dollar value of a human life may vary greatly between public and private entities. Furthermore, it is normally difficult to estimate the modes of failure for property and human life and the resulting costs associated with a major flood event. Thus, there is a need for additional research into assigning life-cycle costs to flood risks (Wacker, 1993).

The above briefly discusses just a few of the areas requiring improved equations and/or more data to improve model results. The previously discussed areas needing additional research also help explain the low to nonexistent correlation between the fixed boundary analysis and the computed mobile boundary results. The user can derive much hydraulic information from the fixed boundary model (i.e., velocities, depths, energy slopes). Combining this information with collected physical data (i.e., sediment gradation size) to produce methods for predicting sedimentation-derived results such as mobile boundary water profiles, however, may prove elusive. The engineer or scientist involved with the sedimentation process of rivers would greatly benefit from further research in the above areas.

REFERENCES

Ackers, P. and White, W.R. (1973). Sediment Transport: New Approach and Analysis. *Journal of Hydraulic Division, Proceedings of American Society of Engineers*, **Vol. 99, HY11**, 2041-2060.

Amein, M. and Fung, C.S. (1970). Implicit Flood Routing in Natural Channels. *Journal of the Hydraulics Division, Proceedings of the American Society of Civil Engineers*, **Vol. 96, HY12**, 2481-2500.

American Association of State Highway and Transportation Officials (AASHTO) (1999). Guidelines for Hydraulic Analysis for the Location and Design of Bridges. *Highway Drainage Guidelines*, **Volume VII**.

American Association of State Highway and Transportation Officials (AASHTO) (1999). Bridges. *Model Drainage Manual*, **Chapter 10.**

Anthony, D.J. (1992). *Bedload Transport and Sorting in Meander Bends, Fall River, Rocky Mountain National Park, Colorado*. Phd. Thesis, Colorado State University.

Bennett, J.S. and Nordin, C.F. (1977). Simulation of Sediment Transport and Armoring. *Hydrological Science Bulletin*, **Vol. 22, No. 4**, 1486-1503.

Bierman, H., Bonini, C.P., and Hausman, W.H. (1986). *Quantitative Analysis for Business Decisions, 7th Edition*. Richard D. Irwin, Inc.

Borah, D.K., Alonso, C.V., and Prasad, S.N. (1982). Routing Graded Sediments in Streams: Formulations. *Journal of the Hydraulics Division, Proceedings of the American Society of Civil Engineers*, **Vol. 108, HY12**, 1486-1503.

Bradley, J.N. (1978). *Hydraulics of Bridge Waterways, HDS-1, Federal Highway Administration.*

Buffington, J.M. and Montgomery, D.R. (1996). *A Systematic Analysis of Eight Decades of Incipient Motion Studies, with Special Reference to Gravel-Bedded Rivers.* Dept. of Geological Sciences, University of Washington, Seattle, Wa.

Canali, G.E. (1992). *The Impact of Watershed Dynamics and Homogeneity on Sedimentation.* Phd. Thesis, Colorado State University.

CH2MHILL (1998). *Hydraulic Study: I-5 US26 to the Twin Bridges Blackfoot, Idaho, Project ER-15-2 (060) 96.* Boise, Id.

Chang, H.H. (1980). Geometry of Gravel Streams. *Journal of the Hydraulics Division, Proceedings of the American Society of Civil Engineers*, Vol. 106, No. HY9.

Chang, H.H. (1994). Selection of Gravel-Transport Formula for Stream Modeling. *Journal of Hydraulic Engineering*, Vol. 120, No. 5, 646-651.

Chang, H.H. (1998). *Fluvial Processes in River Engineering.* John Wiley & Sons, Inc.

Chang, H.H. and Hill, J.C. (1982). Modeling River-Channel Changes Using Energy Approach. *Applying Hydraulic Research, River Channel Modeling, Proceedings of American Society of Civil Engineers*, 454-465.

Chang, H.H., Swanson, M.L., and Kondolf, G.M. (1992). *An Investigation of the Causes of Accelerated Channel Erosion and Development of Countermeasures for Bridge Stabilization on Stony Creek, Executive Summary.* Mitchell Swanson and Associates, Sacramento, Ca.

Chen, Y.H. (1979). Water and Sediment Routing in Rivers. *Modeling of Rivers*. John Wiley & Sons, Inc.

Chow, J.T. (1959). *Open-Channel Hydraulics*. McGraw-Hill Book Co.

Cummons, J.E., Collings, M.R., and Nassar, E.G. (1975). *Magnitude and Frequency of Floods in Washington, OFR 74-336, United States Geological Survey.*

Cunge, J.A., Holly, Jr. F.M., and Verwey A. (1980). *Practical Aspects of Computational River Hydraulics*. Pitman Publishing Limited, London.

Davidian, J.D (1984). *Computation of Water-Surface Profiles in Open Channels, United States Geological Survey,* **Book 3, Chapter A15**.

Engelund, F., and Hansen, E. (1967). A Monograph on Sediment Transport in Alluvial Streams. *Teknish Forlag*, Copenhagen, Denmark.

Federal Highway Administration (FHWA) (1981). *Design of Encroachments on Floodplains Using Risk Analysis, HEC-17.*

Federal Highway Administration (FHWA) (1986). *Bridge Waterways Analysis Model: Research Report, FHWA/RD -86/106.*

Federal Highway Administration (FHWA) (1989). *Design of Riprap Revetment, HEC-11.*

Federal Highway Administration (FHWA) (1989). *Finite Element Surface-Water Modeling System: Two-Dimensional Flow in a Horizontal Plane, FESWMS-2DH, User's Manual.*

Federal Highway Administration (FHWA) (1989). *Two-Dimensional Finite-Element Hydraulic Modeling of Bridge Crossings, Research Report.*

Federal Highway Administration (FHWA) (1990). *Highways in the River Environment.*

Federal Highway Administration (FHWA) (1995). *Evaluating Scour at Bridges, HEC-18, Third Edition.*

Federal Highway Administration (FHWA) (1995). *Stream Stability at Highway Structures, HEC-20, Second Edition.*

Federal Highway Administration (FHWA) (1996). *PHT Business Measures, Federal Lands Highway.*

Federal Highway Administration (FHWA) (1996-2000). *Hydrology/ Hydraulics, Project Development Design Manual, Federal Lands Highway.* **Chapter 7.**

Fischer, H.B., List, E.J., Koh, R.C.Y., Imberger, J., and N.H. Brooks (1979). *Mixing in Inland and Coastal Waters*. Academic Press Inc.

Gomez, B. and Church, M. (1989). An Assessment of Bed Load Sediment Transport Formula for Gravel Bed Rivers. *Water Resources Research*, **Vol. 25, No. 6**, 1161-1186.

Habib, M. (1994). *Sediment Transport Estimation Methods in River Systems.* Phd. Thesis, University of Wollonyong.

Haschenburger, J.K. (1996). *Scour and Filling Gravel-Bed Channel: Observations and Stochastic Models*. Phd. Thesis, University of British Columbia.

Henderson, F.M. (1966). *Open Channel Flow*. Macmillan Publishing Co., Inc., New York.

Hsu, S.M. (1991). *An Assessment of Analytical and Numerical Prediction of One-Dimensional Mobile-Bed Dynamics*. Phd. Thesis, University of Iowa.

Huang, Cheng-Chang (1990). *Local Scour at Isolated Obstacles on River Beds*. Phd. Thesis, Oregon State University.

Ibbotson Associates (1998). *Stocks, Bonds, Bills, and Inflation 1998 Yearbook*.

Jarrett, R.D. (1984). Hydraulics of High-Gradient Streams. *Journal of Hydraulic Engineering*, **Vol. 110, No. 11**, 1519-1539.

Jarrett, R.D. (1990). Hydrologic and Hydraulic Research in Mountain Rivers. *Water Resources Bulletin*, **Vol. 26, No. 3**, 419-429.

Kaatz, K.J. and James, W.P.(1997). Analysis of Alternatives for Computing Backwater at Bridges. *Journal of Hydraulic Engineering* , **Vol. 123, No. 9, 784-792.**

Kessy, M.E. (1993). *Armoring and Pavement in Gravel-Bed Rivers: Numerical and Physical Analysis*. Phd. Thesis, University of Iowa.

Lee, H.Y. and Odgaard, A.J. (1986). Simulation of Bed Armoring in Alluvial Channels. *Journal of Hydraulic Engineering*, **Vol. 112, No. 9, 794-801.**

Leopold, L. B. (1994). *A View of the River*. Harvard University Press, Cambridge.

Liggett, J.A. and Cunge, J.A. (1975). Numerical Methods of the Solution of the Unsteady

Flow Equations. *Unsteady Flow in Open Channel, Water Resources Publications*, **Vol. 1, Chapter 4**. Fort Collins, Colorado.

Linsley, R.K. Jr., Kohler, M.A., and Paulhus, J.L.H. (1982). *Hydrology for Engineers*. McGraw-Hill.

Liu, H.K., Bradley, J.N., and Plate, E.J. (1957). *Backwater Effects of Piers and Abutments*. Colorado State University.

Lowham, H.W. (1988). *Stream Flows in Wyoming, WRI Report 88-4045, United States Geological Survey*.

Lyn, D.A. and Goodwin P. (1987). Stability of a General Preissmann Scheme. *Journal of Hydraulic Engineering*, **Vol. 113, No. 1**, 16-28.

Lyn, D.A. (1987). Unsteady Sediment-Transport Modeling. *Journal of Hydraulic Engineering*, **Vol. 113, No. 1**, 1-15.

Mansfield, W.A. (1988). *The Hydrogemorphological Effects of River Channel Crossings*. PH.D. Thesis, University of Southampton, Southampton, United Kingdom.

Meyer-Peter, E. and Muller, R. (1948). Formulas for Bed-Load Transport. *In Proc., 2nd Meeting Int. Association Hydr. Res.*, Pages 39-64, Stockholm, Sweden.

Miller, I. And Freund, J.E (1977). *Probability and Statistics for Engineers*. Prentice-Hall, Inc.

Misri, R.L., Garde, R.J., and Range Raju, K.G. (1984). Bed Load Transport of Coarse

Nonuniform Sediment. *Journal of Hydraulic Engineering*, Vol. 110, No. 3, 312-328.

Molinas, A. (1994). *User's Manual for BRI-STARS, National Cooperative Highway Research Program (NCHRP).*

Molinas, A. (1997). *BRI-STARS Card Descriptions, Federal Highway Administration.*

Molinas, A. (1997). *Lectures, Notes, Getting Started with BRI-STARS, Federal Highway Administration.*

Molinas, A. (1998). *User's Manual for BRI-STARS, Federal Highway Administration.*

Molinas, A. (2000). *User's Manual for BRI-STARS, Federal Highway Administration.*

Molinas, A. and Marcus, K.B. (1998). Choking in Water Supply Structures and Natural Channels. *Journal of Hydraulic Engineering.* Vol. 36, No. 4, 675-694.

Molinas, A. and Wu, B. (1997). *User's Primer for BRI-STARS, Federal Highway Administration.*

Molinas, A. and Wu, B. (1998). Effect of Size Gradation on Transport of Sediment Mixtures. *Journal of Hydraulic Engineering*, Vol. 124, No. 8, 786-793.

Molinas, A.M. and Yang, C.T. (1985). Generalized Water Surface Profile Computations. *Journal of Hydraulic Engineering.* Vol. III, No. 3, 381-397.

Morris, H.M. and Wiggert, J.M. (1972). *Applied Hydraulics in Engineering.* John Wiley & Sons, Inc.

Nakato, T. (1990). Tests of Selected Sediment-Transport Formulas. *Journal of Hydraulic Engineering*, **Vol. 116, No. 3**, 362-379.

Nelson, M.N. (1987). *Flood Characteristics for the Nisqually River and Susceptibility of Sunshine Point and Longmire Facilities to Flooding in Mount Rainier National Park, Washington, WRI Report 86-4179, United States Geological Survey.*

Office of the Federal Register (OFR) (1999). Subpart A - Location and Hydraulic Design of Encroachments on Flood Plains; Part 650-Bridges, Structures and Hydraulics; *Title 23, Part 1, Section 1*. U.S. Government Printing Office.

Omang, R.J. (1992). *Analysis of the Magnitude and Frequency of Floods and the Peak-Flow Gaging Network in Montana, WRI Report 92-4048, United States Geological Survey.*

Parker, G., Klingeman, P.C. and McLean, D.G. (1982). Bedland and Size Distribution in Paved Gravel-Bed Streams. *Journal of Hydraulics Division, Proceedings of the American Society of Civil Engineers*, **Vol. 108, No. HY4**, 544-571.

Parker, G. (1990). Surface-based Bedload Transport Relations for Gravel Rivers. *Journal of Hydraulic Research*, **Vol. 28, No. 4**, 417-436.

Parker, G. and Sutherland, A.J. (1991). Fluvial Armor. *Journal of Hydraulic Research*, **Vol. 28, No. 5**, 529-544.

Paulos, Y.K. (1999). *Intense Bedload Transport in Nonuniform Flow*. Phd. Thesis, University of British Columbia.

Potter, J.C.(1988). *Life Cycle Costs for Drainage Structures, GL-88-2, US Army Corps of*

Engineers.

Price, R.K. (1974). Comparison of Four Numerical Methods for Flood Routing. *Journal of the Hydraulics Division, Proceedings of the American Society of Civil Engineers*, **Vol. 100, HY7**, 879-899.

Rahuel, J.L., Holly, F.M., Chollet, J.P., Belleudy, P.J. and Yang, G. (1989). Modeling of Riverbed Evolution for Bedload Sediment Mixtures. *Journal of Hydraulic Engineering*, **Vol. 115, No. 11**, 1521-1542.

Raudkivi, A.J. (1990). *Loose Boundary Hydraulics, 3rd Edition.* Pergamon Press.

Richards, K. (1985). *Rivers, Form and Process in Alluvial Channels.* University Press, Cambridge.

Rosgen, D. (1996). *Applied River Morphology.* Wildland Hydrology.

Ross, S.A. and Westerfield, R.W. (1988). *Corporate Finance.* Times Mirror/Mosby College Publishing.

Samaga, B.R., Range Raju, K.G., and Garde, R.J. (1986). Bed Load Transport of Sediment Mixtures. *Journal of Hydraulic Engineering*, **Vol. 112, No. 11**, 1003-1018.

Schmeeckle, M.W. (1998). *The Mechanics of Bedload Sediment Transport.* Phd. Thesis, University of Colorado.

Scott, K.M. and Vallance, J.W. (1995). *Debris Flow, Debris Avalanche, and Flood Hazards at and Downstream from Mount Rainier, Washington, Hydrologic Investigations Atlas HA-729, United States Geological Survey.*

Scott, K.M., Vallance, J.W., and Pringle, P.T. (1995). *Sedimentology Behavior, and Hazards of Debris Flows at Mount Rainier Washington, United States Geological Professional Paper 1547.*

Shearman, J.O. (1990). *WSPRO User's Instructions, United States Geological Survey.*

Song, C.S. and Yang, C.T. (1980). Minimum Stream Power Theory. *Journal of the Hydraulics Division, Proceedings of the American Society of Civil Engineers*, **Vol. 106, No. HY9**, 1477-1487.

Song, C.S. and Yang, C.T. (1982). Minimum Energy and Energy Dissipation Rate. *Journal of Hydraulics Division, Proceedings of the American Society of Civil Engineers*, **Vol. 108, No. HY5**, 690-706.

Sumioka, S.S., Kresch, D.L., and Kasnick, K.D. (1998). *Magnitude and Frequency of Floods in Washington, WRI Report 97-4277, United States Geological Survey.*

Swanson, M.L. and Kondolf, G.M. (1991). *Geomorphic Study of Bed Degradation in Stony Creek, Glenn County, California.* Mitchell Swanson and Associates, Sacramento, California.

U.S. Army Corps of Engineers (USACE) (1986). *Accuracy of Computed Water Surface Profiles*, **Research Document 26.**

U.S. Army Corps of Engineers (USACE) (1990). *Water Surface Profiles, HEC-2, User's Manual.*

U.S. Army Corps of Engineers (USACE) (1993). *Scour and Deposition in Rivers and Reservoirs, HEC-6, User's Manual.*

U.S. Army Corps of Engineers (USACE) (1994). *Risk-Based Analysis for Evaluation of Hydrology/Hydraulics and Economics in Flood Damage Reduction Studies, EC 1105-2-205.*

U.S. Army Corps of Engineers (USACE) (1998). *Applications Guide, HEC-RAS River Analysis System, Version 2.2.*

U.S. Army Corps of Engineers (USACE) (1998). *User's Manual, HEC-RAS River Analysis System, Version 2.2.*

U.S. Army Corps of Engineers (USACE) (1998). *Hydraulics Reference Manual, HEC-RAS River Analysis System, Version 2.2.*

U.S. Geological Survey (USGS) (1953). *Computation of Peak Discharges of Contractions, Geological Survey Circular No. 284.*

U.S. Geological Survey (USGS) (1968). *Measurement of Peak Discharge at Width Contractions By Indirect Methods, Water Resources Investigation*, **Book 3, Chapter A4.**

U.S. Geological Survey (USGS) (1997). *Water Resources Data, Idaho, Water Year 1997*

Wacker, A. M. (1993). Rigorous and Routine Application of Least Total Economic Cost (LTEC) Analysis. *Southeastern FHWA Hydraulic Engineers Meeting.*

Walder, J.S. and Driedger, C.L. (1994). *Geomorphic Change Caused By Outburst Floods and Debris Flows at Mount Rainier, Washington, With Emphasis on Tahoma*

Creek Valley, WRI Report 93-4093, United States Geological Survey.

Walder, J.S. and Driedger, C.L. (1994). Rapid Geomorphic Change Caused by Glacial Outburst Floods and Debris Flows Along Tahoma Creek, Mount Rainier, Washington, U.S.A. *Arctic and Alpine Research*, **Vol. 26, No. 4**, 319-327.

Walder, J.S. and Driedger, C.L. (1995). Frequent Outburst Floods From South Tahoma Glacier; Mount Rainier, U.S.A.: Relation to Debris Flows, Meteorological Origin and Implications for Subglacial Hydrology. *Journal of Glaciology*. **Vol. 41, No. 137**, 1-10.

Wargadalam, J. (1993). *Hydraulic Geometry Equations of Alluvial Channels*. Phd. Thesis, Colorado State University.

WEST Consultants, Inc. (WEST) (1997). *Bridge Hydraulics and Scour Assessment for Tom Music Bridge, Cispus River.* Seattle, Wa.

White, W.R., Bettess, R., and Paris, E. (1982). Analytical Approach to River Regime. *Journal of Hydraulics Division, Proceedings of the American Society of Civil Engineers*, **Vol. 108, No. HY10**, 1179-1193.

Yang, C.T. (1973). Incipient Motion and Sediment Transport. *Journal of Hydraulics Division, Proceedings of the American Society of Civil Engineers*, **Vol. 99, No. HY10**, 1679-1704

Yang, C.T. and Molinas, A. (1982). Sediment Transport and Unit Stream Power Function. *Journal of Hydraulics Division, Proceedings of the American Society of Civil Engineers*, **Vol. 108, No. HY6**, 774-793.

Yang, C.T. (1984). Unit Stream Power Equation for Gravel. *Journal of Hydraulic Engineering*, **Vol. 110, No. 12**, 1783-1797.

VITA

Mark Clayton Browning was born on September 3, 1955, in Covington, Kentucky. He received his Bachelor of Science in Civil Engineering from the University of Kentucky in 1979. He received his Masters in Business Administration from the University of Portland in 1989. He received his Master of Science in Civil Engineering from Oregon State University in 1990. Since 1979, he has worked as a highway/hydraulics engineer with the Federal Highway Administration. He is also a professionally licensed civil engineer in Washington (1984) and Oregon (1990).